INVESTIGATION INTO THE GROUNDWATER INTERACTION BETWEEN A DEEP COAL MINE AND A DEEPER LYING GOLD MINE

by

Morne Burger

Submitted in fulfillment of the requirements for the degree **Magister Scientiae** in the Faculty of Natural Sciences and Agriculture, Department of Geohydrology, University of the Free State, Bloemfontein, South Africa

Supervisor: Dr. P.D. Vermeulen

November 2010

DECLARATION

November 2010

I, Morne Burger, declare that the dissertation hereby submitted by me for the Master of Science degree at the University of the Free State, is my own independent work and has not previously been submitted by me at another University/Faculty. I further cede copyright of the thesis in favour of the University of the Free State.

_____

Morne Burger

ACKNOWLEDGEMENTS

This project was only possible with the co-operation of many individuals and institutions. I wish to record my sincere thanks to the following:

- My faithful Father in heaven who has always answered my prayers.
- Sasol Secunda and Harmony Evander for their co-operation in this study.
- Prof. G. van Tonder and Dr. S. R. Dennis for their assistance and time.
- Mr. Eelco Lucas for his time and patience in WISH.
- The personnel and fellow students at the Institute for Groundwater Studies for their support.
- My girlfriend Salumé for motivation and love.
- My parents and family, which includes the Calitz family, you have given me the strength which I can call my own.
- Prof. Teuns Verschoor for believing in me when others did not.
- Most importantly, to Dr. Danie Vermeulen, for whom I have the utmost respect, you have influenced me far more than the boundaries of this project.

TABLE OF CONTENTS

LIST OF FIGURES

LIST OF TABLES

LIST OF ABBREVIATIONS

A	Area
ABA	Acid Base Accounting
AP	Acid Potential
ARD	Acid Rock Drainage
BP	Board and Pillar
DWAF	Department of Water Affairs and Forrestry
DME	Department of Mines and Energy
EC	Electrical Conductivity
EIA	Environmental Impact Assessment
EPA	Environmental Planning and Assessment
EMP	Environmental Management Programme
EMPR	Environmental Management Program Report
GIS	Geographic Information System
GMWL	Global Mean Water Line
GPS	Global Positioning System
HE	High Extraction
i	Gradient
IGS	Institute for Groundwater Studies
K-value	Hydraulic conductivity
MAR	Mean Annual Run-off
NNP	Net Neutralisation Potential
NP	Neutralisation Potential

NWA	National Water Act
Rr	Reference standard
Rs	Reference sample
S	Storage coefficient
SMOW	Standard Mean Ocean Water
S_y	Specific yield
TSF	Tailings Storage Facility
TDS	Total Dissolved Solids
WISH	Windows Interpretation System for Hydrogeologist
Q	Rate of inflow

Chapter One: Introduction

1.1 Background Information

Coal and gold mining in South Africa and more specifically the Mpumalanga Province have been in existence for more than a century. Due to the scale of these operations in area and the time period of operation, these activities have significantly altered the geohydrological environment of the area. These alterations or impacts are not only limited to the operational life of the mines, but are expected to continue for an indefinite number of years after mining has ceased. As such, an understanding of the groundwater interaction between the coal and gold mines are to be exercised in area where these two mining activities affect each other hydrogeologically.

One of the key areas of concern is the phenomenon of intermine flow existing between the different mines. This has been studied by previous researchers, such as Grobbelaar (2001) and Havenga (2002). After the closure of mines, it is expected that water in the mined-out areas will flow along preferred pathways and accumulate in lower-lying areas (Grobbelaar, 2001). Over time, these man-made voids will fill up with water and hydraulic gradients will be exerted onto peripheral areas within mines, resulting in groundwater flow between mines and possibly to the surface. This flow is referred to as intermine flow (Grobbelaar, 2001). Due to the potential long-term impact of intermine flow in terms of water quantities and qualities, the Department of Water Affairs and Forestry regards intermine flow as one of the most important challenges in the mining industry.

In order to address these issues, individual mining houses undertake periodic and ongoing research into water quantity and quality issues. Through the collaborative contribution of **Sasol Coal Mining (Pty) Limited, Secunda** and **Harmony Gold Mining (Pty) Limited, Evander** this research project was launched to address certain issues to provide a more quantitive solution to these problems. This research project was done to determine the potential groundwater interaction between Sasol Coal Mining's Middelbult (Block 8) Colliery, which extracts the coal above the Harmony Evander Gold Mining Operations extracting the underlying gold deposits.

1.2 Scope of Work

Impacts have to be assessed in terms of the potential environmental liabilities of each mining operation and the impact on closure costs.

- It is appropriate that each party accepts and acknowledges its legal responsibility for decanting or management of its seepage water into the activities or areas within the jurisdiction of the other party. Each party has the responsibility to exercise a "duty of care" to prevent any pollution/degradation or harm that may arise from their activities. This "duty of care" entails taking reasonable steps to prevent the pollution/degradation from occurring continuing and/or to minimise and remediate the effects as far as is practicably possible.
- It is therefore necessary to determine that whoever creates the risk remains responsible for managing that risk and is liable for the impact or consequences of that risk.

The main aim of the proposed work is to determine the potential groundwater interaction between Sasol Mining's Middelbult (Block 8) and Harmony Evander Operations including the combined impacts on the environment. The impacts have to be assessed in terms of the potential environmental liabilities of each mining operation and the impact on closure costs.

To determine the potential water groundwater interaction between the mines, the following issues need to be addressed:

- Understand the hydrological interaction, if any, between Middelbult and Harmony Evander Operations.
  - Is there any influence between the coal and gold mines during the operational phase?
  - Is there any influence between the coal and gold mines during the decommissioning phase and post closure?
  - Determine the influence pre-operational phase (exploration done by both parties before mining commenced).
  - Identify preferred pathways that has been created by industry, which includes exploration boreholes (pre- and during mining), shafts, boreholes, etc.
- Determine (model) if decanting will occur:
  - Will Middelbult decant?
  - Will Harmony decant?
- If decanting is going to occur, determine (model) the following:
  - Qualities to be expected?
  - Quantities to be expected?

- Will seepage occur as a result of the coal and gold mining?
- Identify where seepage is taking place and what is the cause.

1.3 Approach to Research

The first step towards achieving these aims was the collection and collation of available data. This included large quantities of data from the different mines in different forms (documents, Excel files, GIS files, etc.). Review the available literature on topics related to the research. This information was combined into databases and formatted to be compatible with GIS systems, such as the SURFER surface mapping system and Windows Interpretation System for Hydrogeologist (WISH) software packages.

Samplings were done at strategic points on the surface as well as underground in each individual mine. These samples were then submitted to laboratories for hydro-chemical and isotope analysis and interpreted to "fingerprint" each specific sample's origin.

1.4 Regional Setting

1.4.1 Magisterial District and Regional Services Council

The study area/interaction area is situated in the Mpumalanga Province north-northwest of the town of Secunda (Figure 1). This area is part of the Highveld Coal Field (Havenga, 2002). It is located in the Block 8 coal reserves owned by Sasol Mining (Pty) Limited which overlies the deeper Harmony Evander (Pty) Limited gold mining operations. The study area falls within the Highveld East Magisterial District and Govan Mbeki Regional Services Council.

1.4.2 Direction and Distance to Nearest Towns

Kinross lies to the north-northeast, approximately 12 km from the northern study area boundary, whilst Embalenhle is situated on the southern boundary. Secunda is located to the southeast, approximately 8 km from the southern study area boundary. Evander is located approximately in the centre of the study area. The co-ordinates (Transverse Mercator: LO 29) of the investigated study area are -20000 to 25000 East and -2920000 to -2945000 South (Figure 1).

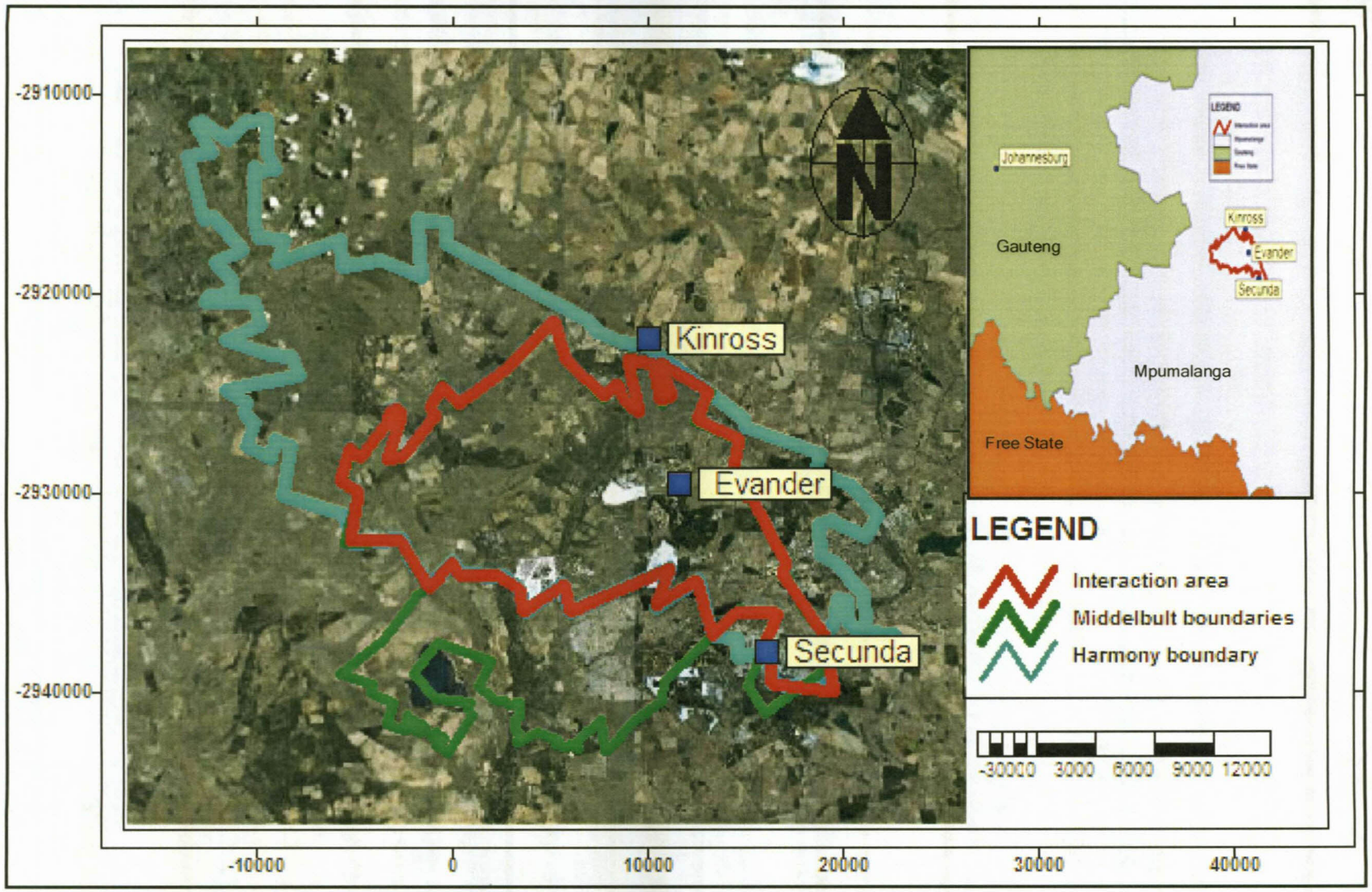

Figure 1: Location of the study area/interaction area with its surrounding towns.

1.4.3 Surface Infrastructure

1.4.3.1 Roads

Several roads cross the study area, ranging in magnitude from national freeways such as the N17 [(previously R29) and arterial routes (Leandra-Standerton Road (R50)] to secondary and farm roads (Middelbult Mine Block Expansion EMPR, 2003).

1.4.3.2 Power lines

A number of Eskom power lines cross the surface of the area (Middelbult Mine Block Expansion EMPR, 2003).

1.4.3.3 Railway lines

The Springs-Trichardt-Bethal railway line passes over the northern extent of the study area. The railway line links to the Witbank-Richards Bay railway line (Middelbult Mine Block Expansion EMPR, 2003).

1.4.3.4 Pipelines

A number of Rand Water and gold mine water and slurry pipelines cross over the surface of the area (Middelbult Mine Block Expansion EMPR, 2003).

1.4.3.5 Servitudes

A number of servitudes exist in the area for:

- District roads;
- Pipelines;
- Eskom overhead electrical power distribution lines;
- Telkom telephone lines;

1.4.3.6 Land Tenure and Use

The land adjacent to mining activities is utilised for agricultural purposes, mixed residential, commercial, and industrial uses. Summer crops such as maize and sunflower are cultivated. The rest of the land is utilised for sheep/cattle grazing and for game farming (Middelbult Mine Block Expansion EMPR, 2003).

1.4.3.7 Catchment in which the study area is situated

The study area is located in the quaternary sub-catchments C24D, C23G and C23H of the Waterval River Catchment drainage region as shown in Figure 2. Grootspruit, Winkelhaakspruit,

and Trichardtspruit drain over the area and join the Waterval River upstream of the confluence (Vermeulen & Dennis, 2009).

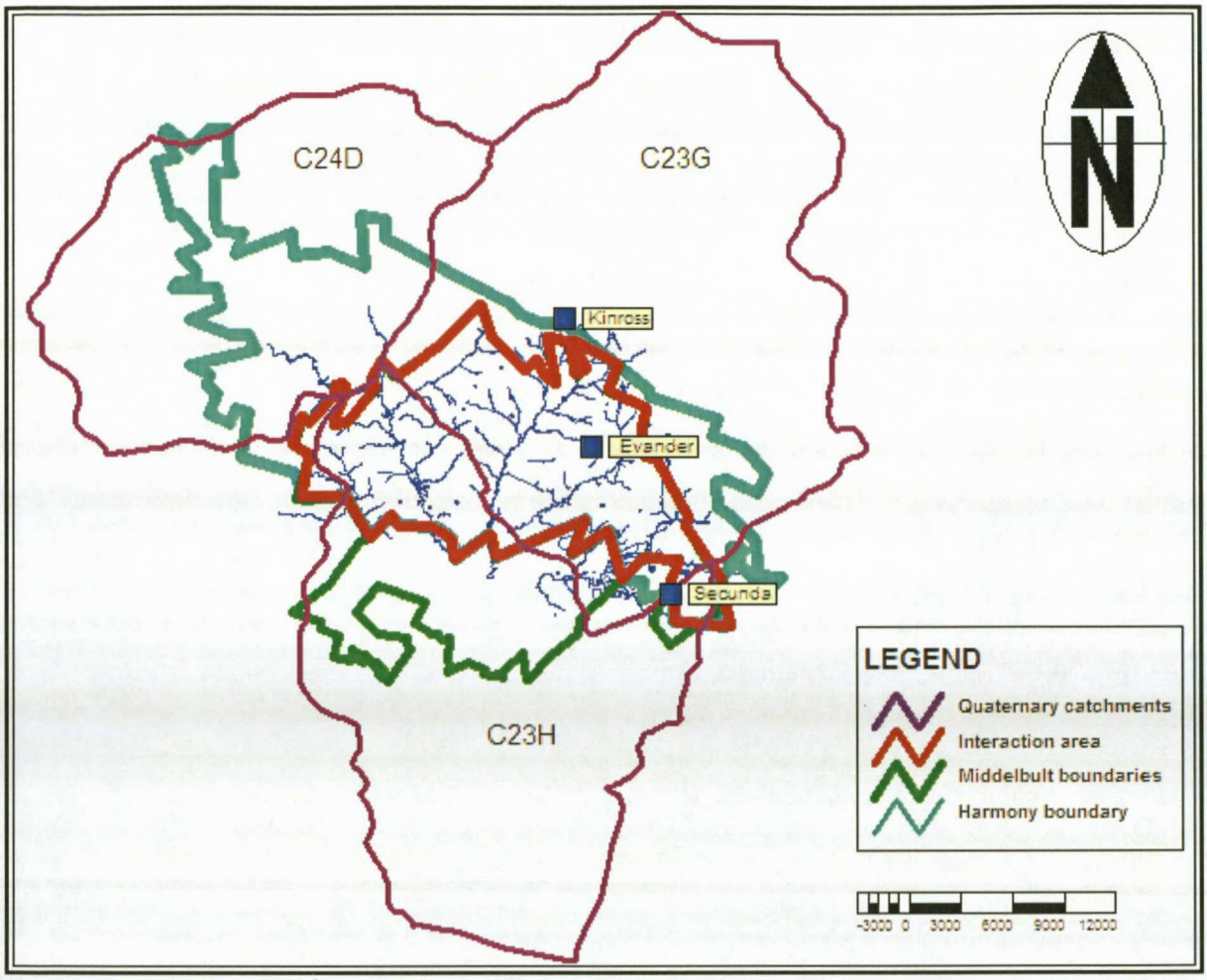

Figure 2: Location of the study area and with quaternary catchments C24D, C23G and C23H.

1.5 Physiographic Conditions

1.5.1 Data collection

Climatic data for the study area was obtained from the South African Weather Service for the Secunda weather station (Secunda, 04783303) which has accurate records of weather conditions for more than 20 years.

1.5.2 Climate

The monthly distribution of average daily maximum temperatures shows that the average midday temperatures for Secunda range from 16.4°C in June to 25.8°C in January (South African Weather Service). The region is coldest during the month of June, when the mercury drops to 0°C on average during the night (Figure 3).

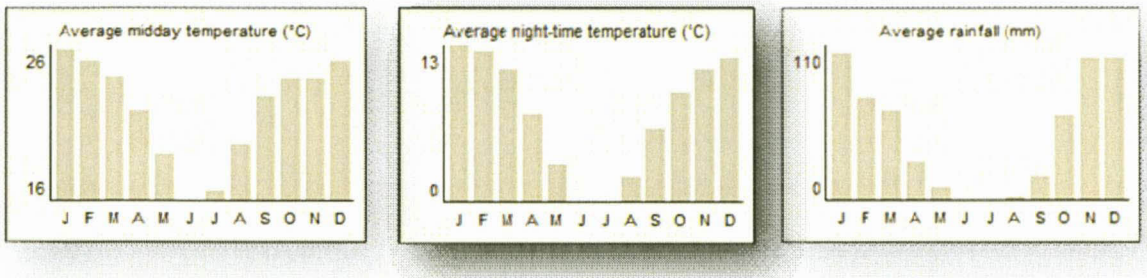

Figure 3: Climate data for Secunda weather station (Secunda Weather Station, 04783303).

1.5.3 Rainfall

Secunda normally receives about 560 mm of rain per year, with most rainfall occurring during the summer. It receives its lowest rainfall (0 mm) in June and the highest (105 mm) in January as shown in Figure 4 (Secunda Weather Station, 04783303).

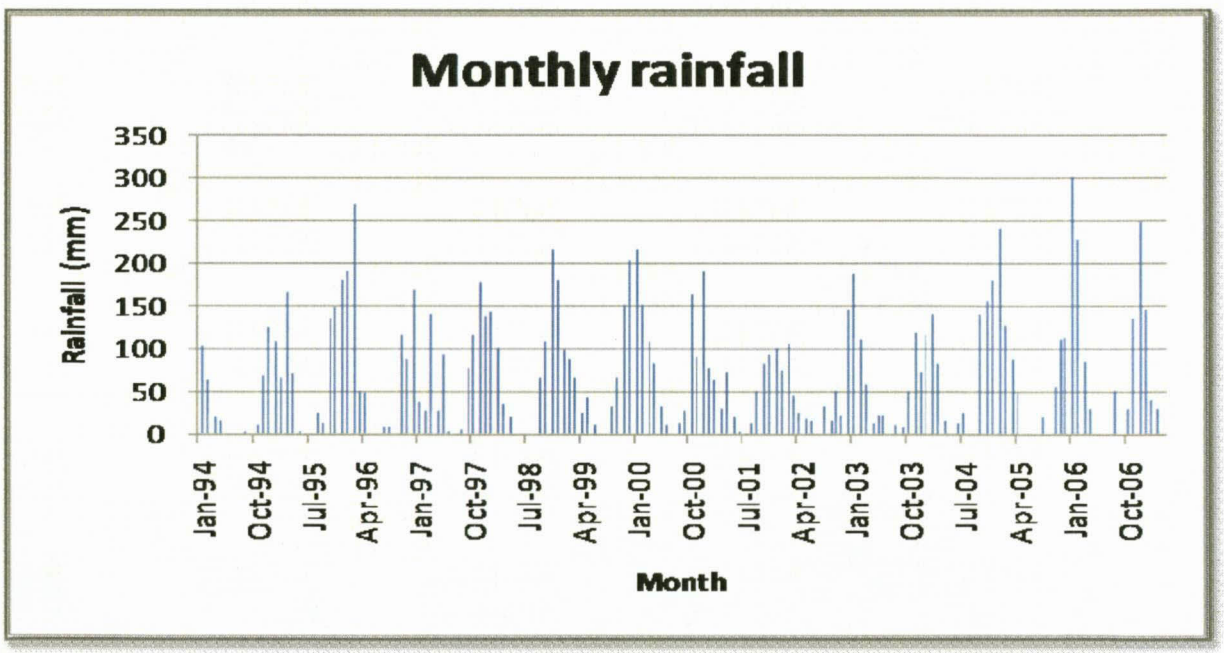

Figure 4: Monthly rainfall data for the Secunda weather station (Secunda Weather Station, 04783303).

1.5.4 Topography and Drainage

The topography of the study area is shown in Figure 5 . The surface elevation varies from 1560 to 1695 m.a.m.s.l. The topography dips towards the rivers. According to Midgley *et al.*, (1994), the mean annual runoff (MAR) varies between 30 to 73 mm/a for the study area. The groundwater contribution to base flow is estimated at approximately 4 to 7 mm/a (Midgley *et al.*, 1994).

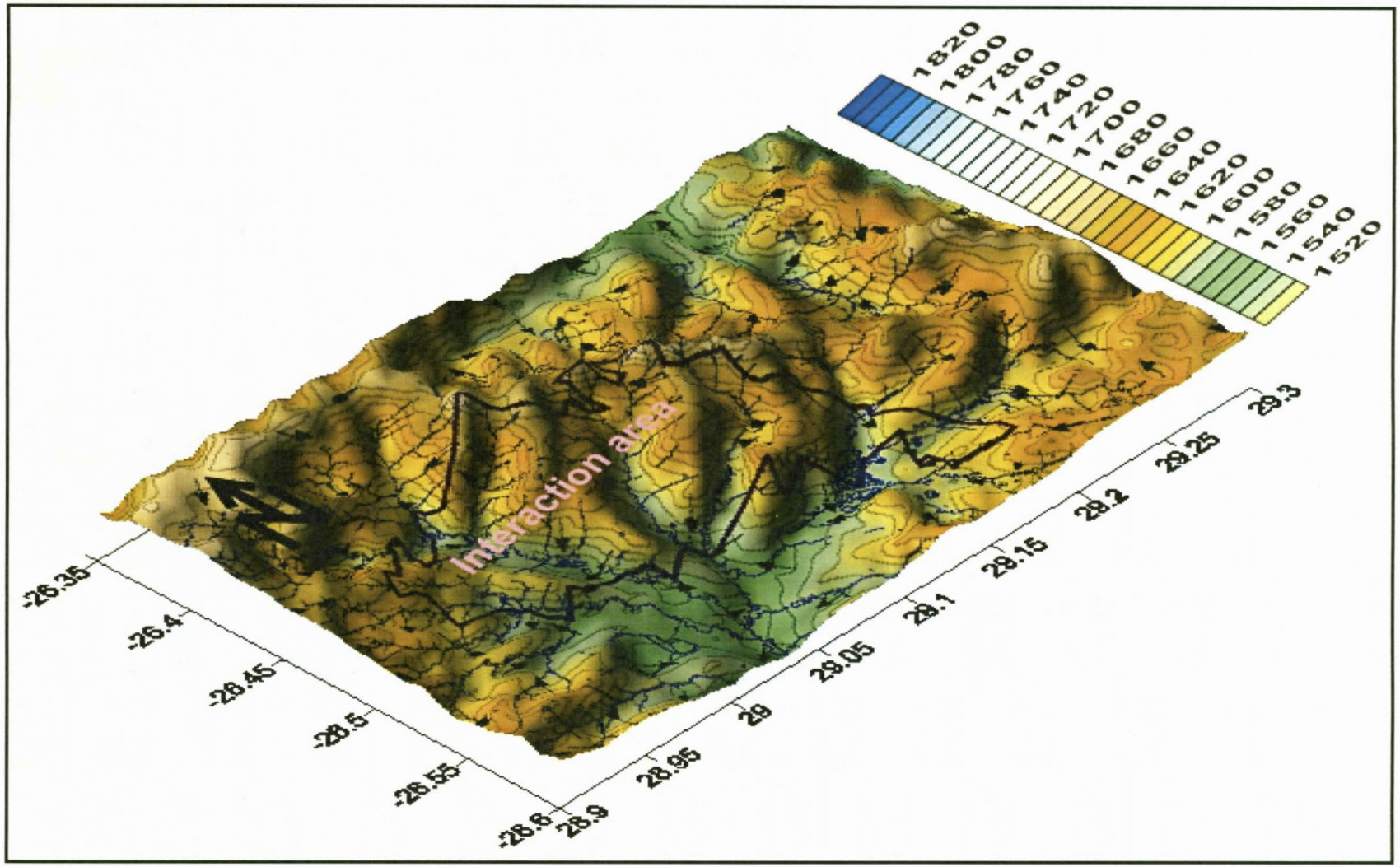

Figure 5: Topography of the study area and surface drainage directions.

Chapter Two: Literature Study

2.1 Introduction

The literature study involved a review of all relevant available information, including Harmony Gold Mining Evander and Sasol Coal Mining Secunda groundwater databases, all relevant geological databases, previous sampling surveys, hydro-census, remote sensing data and a literature survey. It also involved the application of environmental isotopes and hydro-chemistry in hydrogeological aquifer conceptualisation.

A comprehensive literature search was carried out on the following:

- The geology of the study area;
- The hydrogeology of the study area, which included water levels;
- The application of environmental isotopes and hydro-chemistry in hydrogeological aquifer conceptualisation.

The major findings of the literature study are incorporated in the text, where appropriate, throughout this report.

2.2 Previous work undertaken in the Study Area

Harmony Gold Mining Evander and Sasol Coal Mining Secunda operations respectively, both have underground mining operations as well as surface infrastructure in the study area. Both have in the past affected the environment and in future will affect the environment through underground as well as surface mining activities.

Over the past two decades, a number of environmental as well as mining related studies have been done on both mines. These studies have been done to assess and quantify the impact that historical, current, and future mining activities have had or will have on the environment and more specifically the groundwater environment of the study area.

2.3 Harmony Gold Mining Evander Operations

The Winkelhaak mines were formed in 1955, being the first gold-mining company in the Evander Basin. The first gold was poured in 1958. In 1959, Bracken and Leslie mines were incorporated, and poured their first gold in 1962. Kinross mine was formed in 1966, pouring its first gold the

following year. In 1996, the four mines were combined to form Evander Gold Mines and in 1997 were bought by Harmony Gold Mining Company Products (Harmony Evander Servitudes, 2008).

Previous studies done on Harmony Gold Mining Evander operations and used in this study are:

- [GCS] Groundwater Consulting Services (2002). Harmony gold mining company Evander operations water quality status report. Project nr 2002-11-338.
- [GCS] Groundwater Consulting Services (1998). Evander goldmines hydrogeological investigation final report, Johnstone, A. C. and Jansen H.C.
- Harmony Gold Mining Company (1994). "Kinross Mines Limited, Environmental Management Programme Report."
- Harmony Gold Mining Company (1994). "Leslie Gold Mines Limited, Environmental Management Programme Report."
- McKnight Geotechnical Consulting, C. Oliver, D. and De Bruyn, I. (2002). Evander Mine Poplar Gold Project, Mpumalanga. A Review of the Geological Structural Model and Assessment of possible Groundwater Ingress for Mining of Kimberley Reef. Internal Report prepared for Rison Groundwater Consulting.
- Pritchard-Davies, E.W.D. (1962). Bulletin No. 77. "Sub- Karoo water table." Addendums 1-7.
- Rison Groundwater Consulting (2002). Harmony Gold Mining Limited- Evander operations: Hydrogeological assessment of the potential risk of groundwater inflow into the Rolspruit Project. Rison Groundwater Consulting, M.
- Rison Groundwater Consulting (2007). Harmony Gold Mining Limited - Evander operations: Hydrogeological assessment of the groundwater table in Evander no. 6 shaft. Rison Groundwater Consulting, M.
- Rison Groundwater Consulting (2003). Harmony Gold Mining Limited - Evander operations: Hydrogeological assessment of the potential risk of groundwater inflow into the Poplar Project. Rison Groundwater Consulting, M.
- Tweedie, E.B. (1986): The Evander Goldfield. In: Mineral Deposits of Southern Africa 1, Anhaeusser C.R. & Maske, S. (eds.). Geological Society of South Africa, Johannesburg, South Africa.
- Harmony Gold Mining Company (1988). "Winkelhaak Mines Limited, Environmental Management Programme Report."

2.4 Harmony Gold Mining Evander: Geology

The following section is a summary of the geology as found by previous investigations, especially the work done by Tweedie *et al.* (1986) into the Evander Basin. Sediments of the Witwatersrand Supergroup unconformably overlie the Archaean Basement. These Witwatersrand sediments are then overlain by rocks of the Ventersdorp Supergroup and the Transvaal and Karoo Supergroups (Tweedie *et al.*, 1986).

2.4.1 Witwatersrand Supergroup

The Witwatersrand Supergroup, as compiled from exploration boreholes done by Harmony, has a total estimated thickness of approximately 1500 m in the Evander Basin (Winkelhaak Mine EMPR, 1994). The Kimberley reef as described by Tweedie *et al.,* (1986) represents the distal facies of a fluvial placer that was deposited by a system of braided streams which flowed down a north-easterly dipping palaeoslope, as the sequence is divided into the basal West Rand Group and the overlying Central Rand Group, which contains the auriferous gold deposits. The Central Rand Group is subdivided into the lower Johannesburg Subgroup and the overlying Turfontein Subgroup (Tweedie *et al.*, 1986). These formations consist predominantly of quartzite with subordinate lava, shale and conglomerate. The Kimberley Shale separates the two units and is marked by a basal unconformity. Immediately above this unconformity is a conglomerate layer known as the Kimberley Reef. The primary focus for gold exploration in this area has been the thinly developed Kimberley Reef conglomerate (Tweedie *et al.*, 1986). The Kimberley Reef Horizon is situated at variable depths below surface. This variable depth is partly due to faulting, but also due to sub-outcropping of the strata against the overlying Black Reef Formation. The Witwatersrand stratigraphy overlying the Kimberley Reef has an average thickness of approximately 261 m (Rison Groundwater Consulting, 2007). This becomes significantly less towards the west (Rolspruit Project area), where the Kimberley Reef sub-outcrops against the base of the Transvaal strata (Rison Groundwater Consulting, 2007).

2.4.2 Ventersdorp Supergroup

Overlying the Witwatersrand strata is a thick Supergroup of andesite (lava) of the Klipriviersberg Group, Ventersdorp Supergroup. The Klipriviersberg Group thickness of 0 to approximately 1036 m thick is represented in the Evander Basin by a succession of superimposed flows of greenish-grey, andesitic lavas (Tweedie *et al.*, 1986). Amygdaloidal, non-amygdaloidal and porphyritic varieties are present, together with thin zones of greenish grey pyroclastic rocks. Two well defined porphyritic units are present near the base of the Group. The contact between the lavas of the Klipriviersberg Group and the underlying Witwatersrand sediments appears to

be conformable in the Evander Basin (Tweedie *et al.*, 1986). The Supergroup, which consists of numerous lava flows, attains a maximum thickness of approximately 1430 m between the Black Reef unconformity and the Witwatersrand strata. The Ventersdorp lava package appears to be thinning towards the southwest, where a minimum thickness of approximately 400 m was recorded in exploration boreholes (Rison Groundwater Consulting, 2007).

The variable thickness of the Ventersdorp lava is partly attributed to the faulting in the area. It is important to note that for the current mining area the Ventersdorp Supergroup mantles the Witwatersrand Supergroup (Rison Groundwater Consulting, 2007). ***This is a very important observation made from a groundwater point of view as it effectively means that the Ventersdorp lavas form an impermeable barrier between the overlying (shallower) Karoo aquifers and the underlying (deeper) Witwatersrand aquifer.***

2.4.3 Transvaal Supergroup

The Transvaal sediments overlie the Ventersdorp Supergroup and dip to the north and north-east at 8° to 10°. The Transvaal Supergroup consists of a thin, basal quartzite and conglomerate package belonging to the Black Reef Formation. The latter grades conformably upwards into manganiferous, chert-poor dolomite of the Malmani Subgroup, Chuniespoort Group (Rison Groundwater Consulting, 2007). According to McKnight Geotechnical Consulting Geotechnical Consulting (2002), above the Chuniespoort Group is the Pretoria Group which consist of a basal breccia-conglomerate unit known as the Bevets Conglomerate Formation and overlying the ferruginous shale of the Timeball Hill Formation (Rison Groundwater Consulting, 2007). Overlying the shale is a volcanic unit of andesite that belongs to the Hekpoort Formation. Several diabase sills intrude the Transvaal Supergroup. There are two main sills that formed lensoid intrusions into the shale of the Timeball Hill Formation. It is, however, unclear if these features are continuous along dip and strike (Tweedie *et al.*, 1986). The Transvaal Supergroup rests unconformably on the Ventersdorp Supergroup and the strike orientation differs 90° to that of the underlying strata (Rison Groundwater Consulting, 2007). During previous investigations of the Rolspruit and Poplar Project areas situated to the north-northwest of the study area, McKnight Geotechnical Consulting Geotechnical Consulting (2002) concluded that there are ***no major displacements in the unconformity below the Black Reef Formation.***

2.4.4 Karoo Supergroup

Directly overlying the Transvaal Supergroup are the glacial and deltaic sediments of the Karoo Supergroup. The Supergroup is typically 150 m to 330 m thick (Rison Groundwater Consulting,

2007). An important feature that was highlighted by the McKnight Geotechnical Consulting (2002) investigation is the presence of a paleo-glacial valley. The ice sheet of the Dwyka glaciations was grounded in the study area and subsequently carved out broad "U" shaped valleys. ***This event stripped out any old regolith developed on the underlying formation and in particular it removed the karstification within the dolomite***. The karstification forms the main aquifer in dolomitic formations. ***Other than the paleo-glacial valley, the Karoo unconformity is not disrupted by any major faults*** (Rison Groundwater Consulting, 2007).

In the study area, the sediments of the Vryheid Formation were invaded by doleritic magma that formed thick sills and dykes. A prominent sill (known as the B4 sill) is present in the Evander Basin, forming the general outcrop geology for the region. It is possible that the dykes and sills within the dolomites are part of the same intrusion event, but there is not enough evidence to suggest that these dykes are groundwater compartment forming such as is found in the West and Far West Rand (Rison Groundwater Consulting, 2007).

2.4.5 Structural Geology

In assessing the groundwater occurrences during mining of the Kimberley Reef it is important to understand the nature of faulting and in particular the age limits of such events. McKnight Geotechnical Consulting (2002) concluded that both early compression tectonics and later extensional tectonics affected both the Witwatersrand and Ventersdorp Supergroups in the Evander Basin, but pre-dated the deposition of the Transvaal Supergroup (i.e. >2500 Ma). ***No evidence of major post-Transvaal faulting was found that could potentially link the gold mine underground workings with the overlying (shallower) Karoo aquifers*** (Rison Groundwater Consulting, 2007).

2.4.6 Faulting

Faulting is the most common form of deformation and both primary and secondary fault features are recognised. The secondary faults are generally antithetic and throw down to the south. They divide the gold mine into discrete structural blocks. Most common are south-downthrown normal faults striking essentially northeast-southwest. Large losses of ground are associated with this type of faulting (Tweedie *et al.*, 1986).

2.4.7 Intrusives

The incidence and frequency of intrusives in the Witwatersrand sediments of the Evander Goldfield are low (Tweedie *et al.*, 1986).

2.5 Harmony Gold Mining Evander: Hydrogeology

Previous hydrogeological studies undertaken by McKnight Geotechnical Consulting (2002), Rison Groundwater Consulting: Rolspruit Project (2002) Rison Groundwater Consulting: Poplar Project (2003) and Rison Groundwater Consulting No. 6 shaft (2007) in the Evander Basin suggest that there are potentially two significant aquifers that may affect mining. These are as described by Rison Groundwater Consulting (2007):

- A perched aquifer situated in the weathered Karoo strata. This aquifer is restricted to a zone of approximately 60 m below surface. This aquifer was classified as semi-confined, due to the underlying impermeable base formations and is recharged by rainfall. The Karoo aquifer is the main water supply to farmers in the region and the groundwater quality is generally good. The current understanding of the hydrogeology of the region clearly indicates that this aquifer poses no threat to the underground coal mine workings as hydraulic connections between the aquifer and the coal mine are limited to selected dolerite dykes (Rison Groundwater Consulting, 2007).
- A deeper Witwatersrand aquifer. Gold mining in the region has shown that groundwater is still encountered underground. This water may be derived from the overlying formations or it could have been trapped in the sediments during deposition. The latter would be referred to as connate water (Rison Groundwater Consulting, 2007).

Both aquifers are discussed and described by Rison Groundwater Consulting in Rison Groundwater Consulting: Rolspruit Project (2002) Rison Groundwater Consulting: Poplar Project (2003) and Rison Groundwater Consulting N0.6 shaft (2007). It should be noted that no reference is made to the dolomite aquifer. This is due to the geological investigation done by McKnight Geotechnical Consulting (2002) at the Rolspruit and Poplar Project areas, which has shown that no significant dolomite aquifer has been preserved. The possibility of encountering large volumes of dolomite water is therefore considered negligible. The McKnight Geotechnical Consulting (2002) investigation has also shown that the Karoo aquifer is not connected to the gold mine workings (Rison Groundwater Consulting, 2007).

2.5.1 Karoo Aquifer

Sasol undertook a very detailed hydrogeological investigation during its EMPR studies for the Middelbult Colliery Block 8 expansion. During this study, 30 hydrogeological boreholes were drilled and a detailed hydro census of some 170 privately owned boreholes was completed (Rison Groundwater Consulting, 2007).

The drilling confirmed the presence of at least two phases of dolerite intrusions. The oldest intrusive is typically a massive (B4) sill mostly restricted to the surface with a maximum thickness of 49 m Jasper Muller Associates cc (2002) . A second intrusion is a porphyritic dolerite (B8) sill that ranges in thickness from very thin to a maximum thickness of 18 m. This dolerite sill features near vertical dykes, where it transfers from one horizontal plane to another. This resulted in extensive geological/hydrogeological compartmentalisation Jasper Muller Associates cc (2002) . Twenty-three dolerite intersections were recorded in twenty of the newly drilled hydrogeological boreholes. Thirteen water strikes, associated with the host rock contacts as well as the contacts between the weathered and fresh dolerite, were recorded along these intersections. These water intersections constitute the two aquifers typically encountered within the Karoo strata. The first aquifer is classified as a shallow, weathered aquifer in which the primary water intersections are found on the weathered - fresh bedrock interface. The second aquifer is classified as a deeper, fractured aquifer in which fracture flow dominates. The contacts between dolerite intrusions and the host rock are the primary target for the drilling area in this deeper aquifer. The two aquifers may or may not be hydraulically connected (Rison Groundwater Consulting, 2007).

The groundwater levels in the shallow, weathered Karoo aquifer varied between artesian and 11.04 m below surface, with a mean of 3.9 m below surface. The groundwater levels in the deeper, fractured Karoo aquifer vary between 0.26 m below surface and 73.86 m below surface, with a mean of 14.42 m below surface (Rison Groundwater Consulting, 2007).

Rison Groundwater Consulting: Poplar Project (2003) stated that the Karoo aquifers have not been affected by the past 50 years of gold mining in the region, although large volumes of water have been pumped from the underlying gold mines. This serves as a good indication of the poor hydraulic connectivity of the Karoo aquifers to the gold mine workings (Rison Groundwater Consulting, 2003).

2.5.2 Witwatersrand Aquifer

Despite the deep geological setting of up to 2.5 km, groundwater is encountered in Harmony Evander's gold mine workings. The McKnight Geotechnical Consulting (2002) report highlighted the potential reasons for this.

- McKnight Geotechnical Consulting (2002) established that the spacing of the exploration boreholes and the subsequent geological interpretation do not allow for the detection of smaller, potentially younger faults and joints. The presence of joints and fractures is

important in the sense that due to the fact that no displacement is associated with them they go undetected, but they may still be water-bearing. If such features are present they may tap water from the overlying Karoo aquifer. If they were major fractures they would have caused the subsequent dewatering of the overlying Karoo aquifer. McKnight Geotechnical Consulting (2002) also concluded that there is no evidence of this anywhere in the study area and hence they stated that ***there are no major fractures or faults connecting the gold mine workings with the overlying Karoo aquifer*** (McKnight Geotechnical Consulting *et al.*, 2002).

- A second theory is that connate water may be trapped in the Witwatersrand sediments as is the case in the Free State Goldfields (Rison Groundwater Consulting, 2007). Significant groundwater intersections have been recorded in this type of environment and Oryx Mine was at one stage dewatering at a rate of 60 mega litres per day (Rison Groundwater Consulting, 2007).

Post-Karoo tectonic events along fracture planes and igneous intrusions of post-Karoo age could form conduits for leakage from the Karoo aquifer to the deep Witwatersrand aquifer. Rison Groundwater Consulting (2007) concluded that the deep Witwatersrand aquifer recharge from surface is a negligible quantity and that the Karoo aquifer is unaffected by any dewatering of the deeper gold mining in the Witwatersrand aquifer. Rison Groundwater Consulting (2007) also concluded that the deeper Witwatersrand aquifer can then be regarded as a confined aquifer that is not recharged by rainfall and/or near surface aquifers (Rison Groundwater Consulting, 2007).

2.6 Harmony Gold Mining Evander: No. 6 shaft's water level

Evander No. 6 shaft is located on the eastern boundary of the mining area, *Rison Groundwater Consulting* (2007) conclude that No. 6 shaft it is totally isolated in the sense that there are no connections to the rest of the mining areas and the groundwater table, and has remained at a constant water level for the past few years. This assumption made by *Rison Groundwater Consulting* (2007) is based that there is no direct connection to other mining activities. *Rison Groundwater Consulting* (2007) also made the assumption that the No. 6 shaft could be hydraulically connected to other parts of the gold mine workings, but they state the fact that the groundwater table does not fluctuate indicates that there is no effect from neighboring mining activities (Rison Groundwater Consulting, 2007). This suggests that this portion of the mine void either does not receive any recharge or the recharge is equal to the loss through seepage (possibly horizontal flow to neighboring mine voids?). ***The groundwater elevation in the shaft is***

at approximately 925 m above mean sea level or 707 m below surface (Rison Groundwater Consulting, 2007). Based on the Middelbult Mine: Block 8 Expansion EMPR, 2003 (2003) the coal seam varies in elevation between 1363 m.a.m.s.l to 1577 m.a.m.s.l or 55 m below surface to 269 m below surface (Middelbult Mine: Block 8 Expansion EMPR, 2003), thus the water level in No.6 shaft has not reached the coal mining level as the minimum difference between the coal mining and the water level is currently at 438 m.

Rison Groundwater Consulting (2007) stated that the groundwater levels have changed very little since 1969. It is important to note that their interpolated groundwater level in the vicinity of Evander No. 6 Shaft was in the region of 929 m.a.m.s.l at the end of 1969. It is currently at an elevation of 925 m.a.m.s.l. Based on this observation, Rison Groundwater Consulting (2007) concluded that ***the groundwater level in Evander No. 6 Shaft has remained static for the past 35 years*** (Rison Groundwater Consulting, 2007).

Rison Groundwater Consulting (2007) stated that the fact that the Evander No. 6 Shaft is situated close to the eastern extremity of the Witwatersrand aquifer suggests that this groundwater elevation represents the edge of the dewatering cone and that the shaft can in fact be representative of the final water level within the basin.

The groundwater levels measured by Rison Groundwater Consulting: Poplar Project (2003) at the Poplar Project, situated at the opposite western extremity of the Witwatersrand aquifer, show water levels varying between 1400 m.a.m.s.l and 1600 m.a.m.s.l or between 232 m below surface and 32 m below surface. This part of the basin has remained unaffected by mining and these elevations roughly equate to the original water levels encountered at the start of mining in the Evander area (1533 m.a.m.s.l or 99 m below surface) as listed by Pritchard-Davies (1962). This indicates that the dewatering at Evander has had no influence on the groundwater levels in the Poplar area, suggesting some compartmentalisation within the Witwatersrand aquifer that might be due to the major northeast-southwest trending faults between the two areas. These faults form impermeable barriers and allows for selected parts of the basin to be dewatered independently (Rison Groundwater Consulting, 2007).

Rison Groundwater Consulting (2007) were therefore of the opinion that the groundwater level in Evander No. 6 Shaft is representative of the final groundwater table of the Witwatersrand aquifer within the study area (Rison Groundwater Consulting, 2007).

2.7 Sasol Coal Mining Secunda

The development of new collieries at Secunda was commissioned in 1975. From 1975 to the present, numerous mining and environmental studies have been conducted on the mining area. Previous studies and data used in this study include the following:

- Grobbelaar, R. (2001). "Quantification and management of intermine flow in the western Witbank Coalfield: Implication for mine water volumes and quality." Unpublished M.Sc thesis, Institute for Groundwater Studies, University of the Free State.
- Jasper Muller Associates cc. Van der Berg, J. (2002). "Compilation of geology and groundwater inputs for the Middelbult block 8 EMPR - SASOL coal volume I and II - text and appendices." Report prepared for Sasol Mining (Pty) Limited.
- Middelbult Mine: Block 8 Addendum Volume 1. (2003). "Environmental Management Programme Report for the Middelbult Mine: Block 8 Expansion." Prepared for Sasol Mining (Pty) Limited. Oryx Environmental. nr.OE63.
- Vermeulen, P.D., Dennis I. (2009). "Numerical Decant Models for Sasol Mining Colleries, Secunda." Institute for Groundwater Studies. University of the Free State.

2.8 Sasol Coal Mining Secunda: Geology

Jasper Muller Associates cc (2002) describe the Sasol Secunda Coal Mines as being located in the Vryheid Formation of the Ecca Group, Karoo Supergroup. These rocks consist primarily of sandstones, shales and coal beds and are extensively intruded by dolerites of Jurassic age. The coal seams in the Highveld Coalfield are mainly flat to gently undulating, with a very gentle regional dip to the south (Grobbelaar, 2001). On the northern and western margins of the coalfield, however, coal seam topography and distribution are commonly controlled by pre-Karoo topography. Steeper dips are encountered where seams are situated against pre-Karoo hills. The dolerites occur both as sills and linear dyke structures that may extend over tens of kilometres. A large sill-like dolerite structure covers most of the study area. Apart from the displacement of the sedimentary succession caused by intrusive dolerite sills, the Karoo strata are not significantly faulted. Small faults (of less than one metre displacement) are present, but rare. Larger faults have not as yet been identified, except for an east-west striking graben structure with a down-throw of 22 m bisecting the south of the southern boundary of the study area. Locally, the general lithological profile, up to and including the deepest mine-able coal seam, comprises of:

- Soft overburden
- Hard overburden

- No. 5 coal seam
- Inter burden
- No. 4L coal seam

Dolerite dykes and sills also appear over the study area Jasper Muller Associates cc (2002) .

2.8.1 Dolerite Intrusions

Jasper Muller Associates cc (2002) stated that the Karoo sediments were invaded by two phases of post-Karoo dolerite intrusions. The oldest intrusive, namely the B4, being a fine to medium crystalline dolerite and is typically a massive sill that is mostly restricted to the surface, with a maximum thickness of approximately 49 m Jasper Muller Associates cc (2002) . This sill is eroded away in the lower lying areas. Locally, the B4 is not only surface bound, but transgresses the coal seams in a trough-like fashion to effectively compartmentalise these portions of the reserve on the mining horizon. The B6, is a porphyritic dolerite, usually 3 m thick, and intersects the coal seams less frequently than the B8 dolerite. Out of 615 exploration boreholes, only one intersection was noted Jasper Muller Associates cc (2002) . The B8 dolerite (a fine grained porphyritic dolerite) intruded later than the B4, along semi-planar features, with the result that it is mainly exposed as dykes, i.e. almost vertical intrusives. The B8 ranges in thickness from very thin to a maximum of 18 m. The prominent, east-west striking dyke or sub-vertical sill, separating most of the Block 8 reserve from Middelbult Colliery, can be seen to range in thickness between 7 m and 15 m. The B8 sill dolerite, approximately 18m in thickness, features near vertical off-shoots (dykes), where it transfers from one horizontal plane to another. These features occur predominantly along the planes of transference Jasper Muller Associates cc (2002) .

Jasper Muller Associates cc (2002) describes the B12 as a light grey, fine grained porphyritic dolerite with large needle-like phenocrysts, roughly ranging in thickness between 0, 12 m and 0, 75 m. Twenty-three dolerite intersections were recorded in twenty of the newly drilled geohydrological boreholes. Thirteen water strikes, associated with host rock contacts as well as the contact between weathered and fresh dolerite, were recorded along these intersections Jasper Muller Associates cc (2002) .

2.9 Sasol Coal Mining Secunda: Hydrogeology

Previous hydrogeological studies done by Jasper Muller Associates cc (2002) in the study area suggest that there is only one aquifer that may affect coal mining.

This aquifer is situated in the weathered or fractured Karoo strata. This aquifer is restricted to a zone of approximately 60 m below surface. This aquifer is classified as semi-confined, due to the underlying impermeable base formations and is recharged by rainfall. The Karoo aquifer is the main water supply to farmers in the region and the groundwater quality is generally good Jasper Muller Associates cc (2002) .

According to Jasper Muller Associates cc (2002), the displacement of the coal seams caused by dolerite intrusion is seen to range from no displacement to not much more than the coal seam thickness itself. The Block 8 underground reserve is largely separated from the existing Middelbult Colliery, compartmentalised and sub-compartmentalised by a ± 15 m thick B8 dolerite sill roughly southwest-northeast in orientation Jasper Muller Associates cc (2002) . The sill underlies the Middelbult Colliery close to the floor of the Karoo sediments before bending upwards to vertical again, transgressing the coal seams before surfacing. To both the east and the west, this sill has numerous sub-vertical split-offs that join up and split off again to compartmentalise and sub-compartmentalise the Block 8 reserve Jasper Muller Associates cc (2002) .

The larger Middelbult Colliery compartment is of particular significance, as a sizable portion of the proposed Block 8 mine layout falls within this compartment. Jasper Muller Associates cc (2002) state that of significance is the fact that both the Leslie and the Winkelhaak slimes dams are located in this area. Some existing high extraction mining panels occur as close as 20-50 m to the west of the southwestern corner of the slimes dam and 80-100 m to the east of the Winkelhaak slimes dam, as seen in Figure 6. Manifested impacts relating to the de-watering of the shallow weathered zone aquifer(s) over some of Middelbult Colliery's high extraction panels are likely and have already been observed by Jasper Muller Associates cc (2002) in some of the drilled monitoring boreholes.

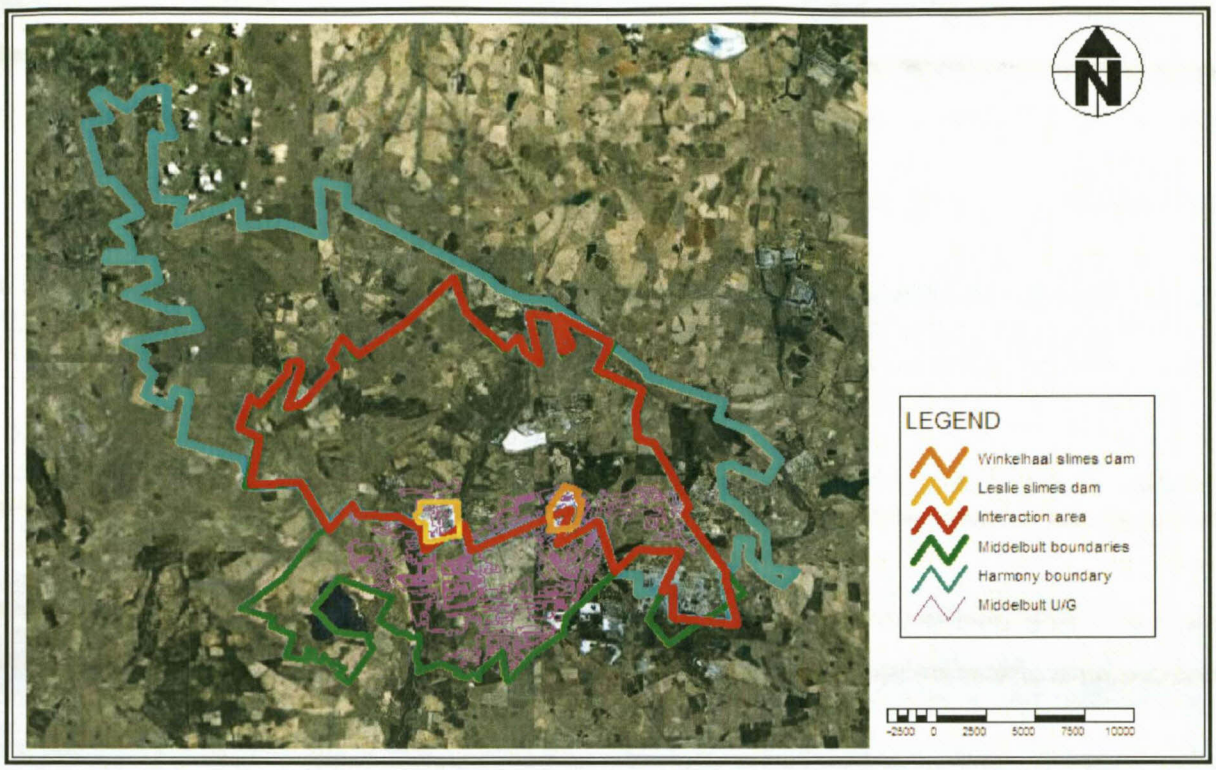

Figure 6: High extraction mining panels occurring close to the Leslie and Winkelhaak slimes dams.

During the geohydrological investigation undertaken by Jasper Muller Associates cc (2002), a total of 30 boreholes were drilled specifically for geohydrological purposes. Two boreholes were drilled per site, one shallow borehole 30 m deep to investigate the shallow weathered zone aquifer(s), and one deep borehole ranging in depth between 80 and 150 m, to investigate the deep fractured aquifer(s). The data of these boreholes is available in Jasper Muller Associates cc (RSA) (2002) Compilation of geology and groundwater inputs for the Middelbult block 8 EMPR - SASOL coal volume I and II - text and appendices. Van der Berg, J.

The following observations made in the Jasper Muller Associates cc (2002) report are important:

- The depth to water level observed, varied between 0 m and 74 m, with a mean of 6.16 m (Figure 7).
- The depth to water level observed in the newly drilled shallow weathered zone boreholes, varied between 0.27 m and 11.04 m, with a mean of 4.77 m (Figure 8).
- The depth to water level observed in the newly drilled deep Karoo aquifer boreholes, varied between 0.26 m and 73.86 m, with a mean of 14.42 m (Figure 9).

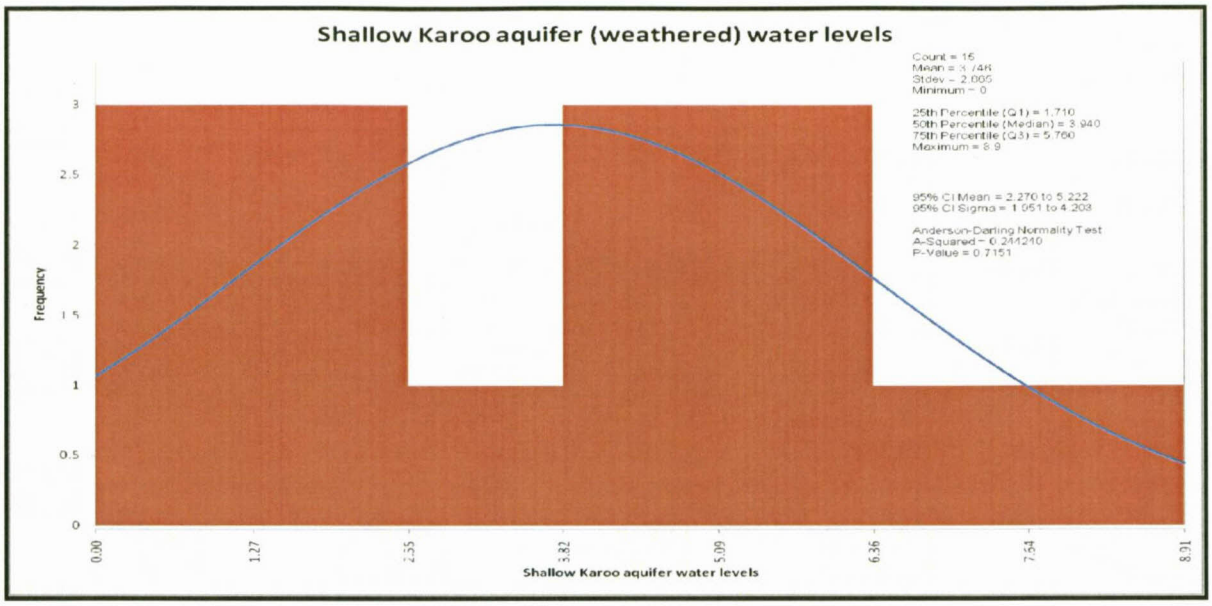

Figure 7: Histogram of the shallow (drilled 0-30m) Karoo aquifer's water levels.

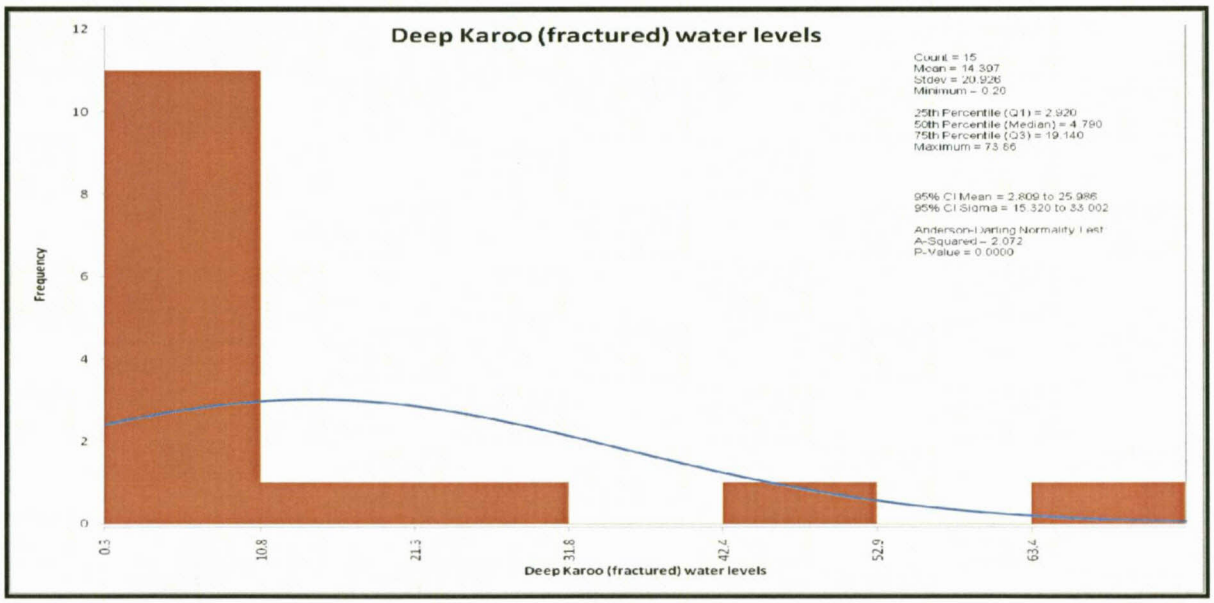

Figure 8: Histogram of the deep (drilled 80-150m) Karoo aquifer's water levels.

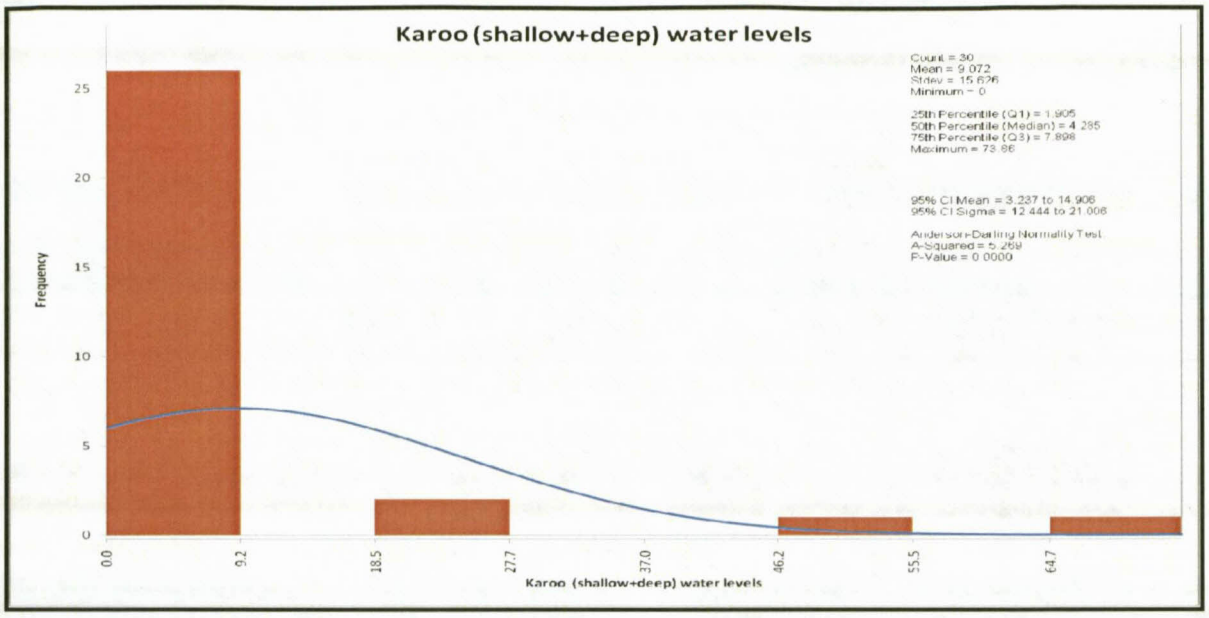

Figure 9: Histogram of the deep & shallow (drilled 0-150m) Karoo aquifer's water levels.

2.10 Stable Environmental Isotopes

A detailed discussion on the application of stable environmental isotopes in hydrogeology is available in Verhagen (1991, 1997 and 2000), Gat (1996) and Fritz *et al.*, (1980). A literature survey was done of the following:

- Fritz, P., Fontes, J., C.H., Elsevier, A. (1980). "Handbook of Environmental Isotope Geochemistry, Volume 1, The Terrestrial Environment." New York. USA. p. 21-29, 283-321, 473-495.
- Gat, J.R. (1996). "Oxygen and hydrogen isotopes in the hydrologic cycle." Unpublished paper, Department of Environmental Sciences and Energy Research, Weizmann Institute of Science, 76100 Rehovot, Israel.
- Verhagen, B. Th., Geyh, M.A., Fröhlich, K. and Wirth, K. (1991). "Isotope hydrological methods for the quantitative evaluation of groundwater resources in arid and semi-arid areas." Research Report, Fed. Ministry for Econ. Coop. of the Fed, Republic of Germany.
- Verhagen, B. Th. (1997). "Use of environmental isotopes in the characterisation of the Table Mountain Sandstone Aquifer, South Africa." Progress Report to the International Atomic Energy Agency, Research Contract 8983/RO/Regular Budget Fund.
- Verhagen, B. Th. (2000). "Environmental isotope hydrology: Principles and application to the geohydrology of the Karoo Basin." Karoo Aquifer Handbook, WRC, in preparation.

- Verhagen, B.Th. and Butler, M.J. (2004). "Isotope hydrology - An African Experience." Geoscience Africa, Extended Abstracts, Vol. 2. Geological Society of South Africa, Johannesburg. p. 671-672.
- Weaver, J.M.C., Talma A.S. and Cavé L.C. (1999). "Geochemistry and Isotopes for Resource Evaluation in the Fractured Rock Aquifers of the Table Mountain Group. Report No. 481/1/99, Water Research Commission, Pretoria.

2.10.1 General applications of stable environmental isotopes in hydrogeology

Stable isotopes ^{18}O and ^{2}H are unique for the investigation of hydrogeological processes. Isotopes act as naturally occurring tracers in groundwater (commonly referred to as environmental tracers) which can provide valuable information to the hydrogeologist about aquifer characteristics and groundwater flow paths that would otherwise be difficult, if not impossible, to establish (Verhagen *et al.*, 1991).

2.10.2 Fractionation

Molecules differ in mass, as the isotopes of the elements making up molecules differ in mass. These mass differences influence factors such as vapour pressure, diffusivity, etc. During phase processes, such as evaporation, condensation and exchange reactions, the abundance ratios of the isotopes of individual elements change, or undergo fractionation (Verhagen, 2000). Such processes usually take place at the interface of different phases or compounds containing the same elements, such as vapour in contact with a liquid, a liquid in contact with a solid, etc. These changes in abundance can be traced through natural and other systems (Verhagen, 2000).

The unit fractionation factor α is defined as: $\alpha = RA / RB$, where RA and RB are the abundance ratios of the rare (heavier) isotope to the more abundant (light) isotope in phases A and B respectively. α Is temperature dependent.

As isotopic abundances and changes in these abundances are generally small, it is customary to express these changes as fractional differences δ in per mille with reference to the value of a reference standard:

$$\delta = [(Rs / Rr) - 1] \times 1000 \text{ (‰)}$$ (Verhagen, 2000).

where the measured ratios for the heavy to the light isotope are Rs for the sample and Rr for the reference standard, respectively.

2.10.3 Application of stable isotopes ^{18}O and ^{2}H

The changes of ^{18}O and ^{2}H concentrations along groundwater flow paths is an effective tool to determine the altitude of groundwater recharge, estimation of mixing proportions of different sources or component flows and the relationships between groundwater and surface water (Gat, 1996).

^{18}O and ^{2}H are present in water in isotopic abundances (or ratios, R) of about $^{18}O/^{16}O$ = 0.2 % and $^{2}H/^{1}H$ = 0.015 %. In various combinations, these isotopes make up water molecules, principally of masses 18, 19 and 20 (Verhagen, 2000).

Stable isotope abundance is normally expressed in terms of a ratio to the abundant isotope of the same element or as positive or negative deviations of these isotope ratios from a standard, similar to that of the radioactive isotopes (Verhagen, 2000).

The most important physical process resulting in variations in isotopic compositions of natural water is vapour-liquid fractionation process during evaporation and condensation (Weaver *et al.*, 1996). The basic principle is that enrichment of the lighter isotope (^{16}O) occurs in the vapour during evaporation, as opposed to loss of the heavy isotope (^{18}O) from the vapour first during condensation (Weaver *et al.*, 1996). These small changes can be expressed as a fractional deviation δ from a standard called SMOW (standard mean ocean water).

Values of δ can be diagnostic of water from different recharge altitudes. Water vapour rising from the ocean is depleted in the heavy isotopes (Weaver *et al.*, 1996). Vapour masses moving inland are subject to equilibrium isotopic exchange processes, with the continued depletion in heavy isotopes in vapour travelling inland as a result of rainout. Consequently, the stable isotopic content of meteoric water lies on a regression line:

$\delta^2H = s\,\delta 18O + d$ (Weaver *et al.*, 1996).

(*where* ***s*** *is the slope, and the intercept* ***d*** *on the* δ^2H *axis the deuterium excess*).

The line with **s** = 8 and **d** = +10 is called the global meteoric water line (Figure 10). The ^{2}H - excess is controlled by the deuterium in the vapour source region and the slope by evaporation during rainfall and seasonal variations in precipitation. The position of any pair of δ^2H and $\delta^{18}O$ values on this line for rainwater worldwide will depend on local climatological conditions (temperature, latitude, altitude, and rainfall amount effects).

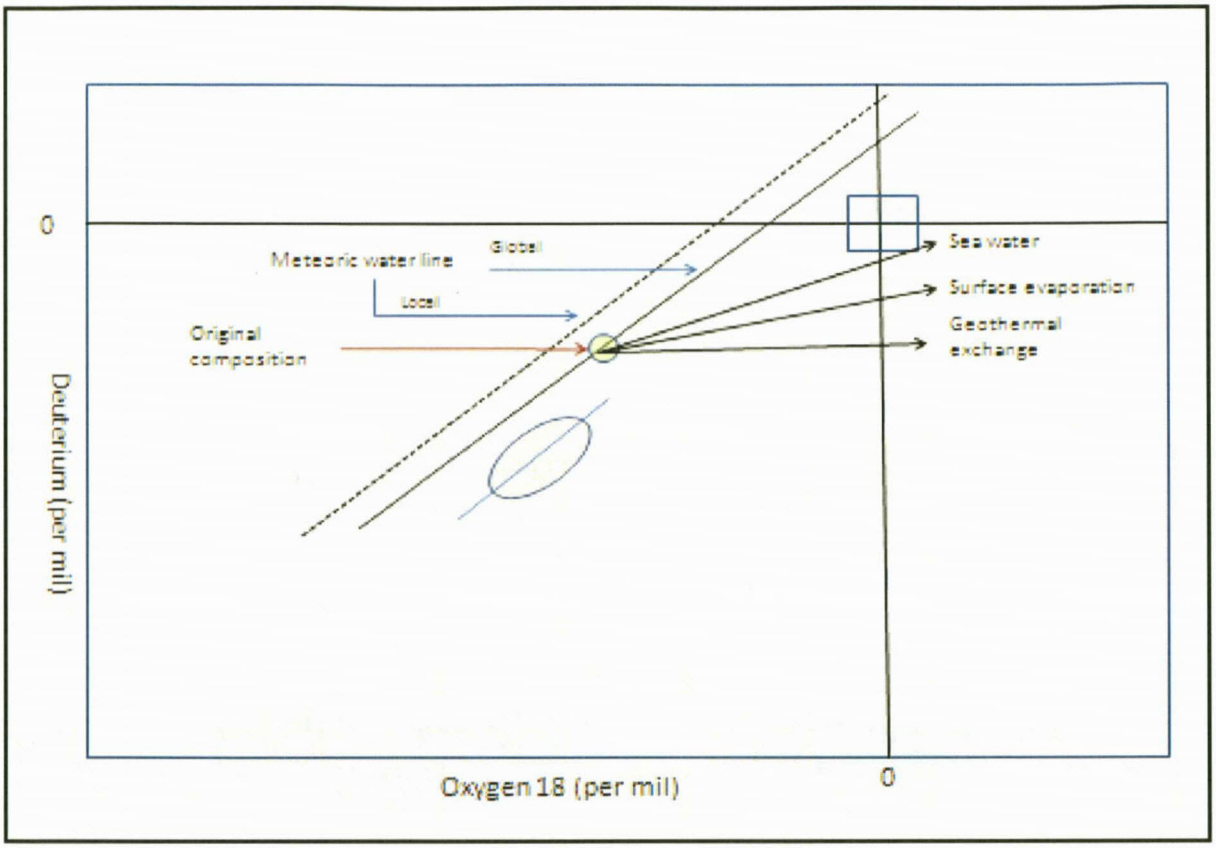

Figure 10: Meteoric water lines (Adapted from Gat, 1996).

Surface water bodies, such as dams, lakes and pans are enriched in the heavy isotope content during evaporation. Light isotopes are preferentially transferred to the vapour phase (Weaver *et al.*, 1996). The resulting surficial layer enriched in the heavy isotope is then readily mixed into the bulk of the water body through convective processes. This evolutionary enrichment produces δ^2H and $\delta^{18}O$ values which lie to the right of the meteoric water line, and plot on an evaporation line of lesser slope **s** (usually 4 to 5) and lower **d** than the GMWL (Figure 10). Groundwater derived through infiltration from such water bodies will carry this distinctive evaporative isotopic signal (Verhagen, 1997).

Evapo-transpiration losses from soil and groundwater generally occur under isotopic equilibrium, i.e. without fractionation. In semi-arid environments such as the Klein Karoo, isotopic values of groundwater derived directly from rain will therefore lie on or close to the GMWL. However, it will tend to be displaced to more negative (or "lighter") δ values than the weighted mean in rain, due to the process of rainfall selectivity (Verhagen, 1997). Major rainfall events, which produce isotopically lighter precipitation i.e. with more negative δ values, may contribute proportionately

more to recharge. It is possible to distinguish different processes of rainfall recharge by different stable isotope ranges on the GMWL (Gat, 1996).

Chapter Three: Mining Activities and Methods

3.1 Sasol Secunda Coal Mining Complex

Sasol Secunda Middelbult Mine Block 8 extracts coal from the economically viable No. 4L coal seam situated at varying depths (Figure 11) throughout the study area (Table 1). The underground workings of the Secunda Mining Complex consist of various layouts and configurations. These configurations are a function of mine planning and method, and can broadly be classified under board-and-pillar (BP) and high extraction (HE) methods (Middelbult Mine: Block 8 Expansion EMPR, 2003). Shaft entrances, haulages to active sections and ventilation channels can all be classified as types of board-and-pillar sections (Middelbult Mine: Block 8 Expansion EMPR, 2003).

In board-and-pillar mining, coal pillars are left as support, although they may be extracted at a later stage, resulting in high extraction mining. Middelbult has a mining height of approximately 3.5 m from the mining roof to the mining floor (Middelbult Mine: Block 8 Expansion EMPR, 2003). The mining layout of the Middelbult Block 8 area is shown in Figure 11.

Table 1: No. 4L coal seam elevations throughout Middelbult Block 8.

No. 4L coal seam elevations (m.a.m.s.l)			
Seam	**Minimum**	**Maximum**	**Average**
Roof	1450	1521	1490
Floor	1450	1520	1487
Surface	1560	1695	1600

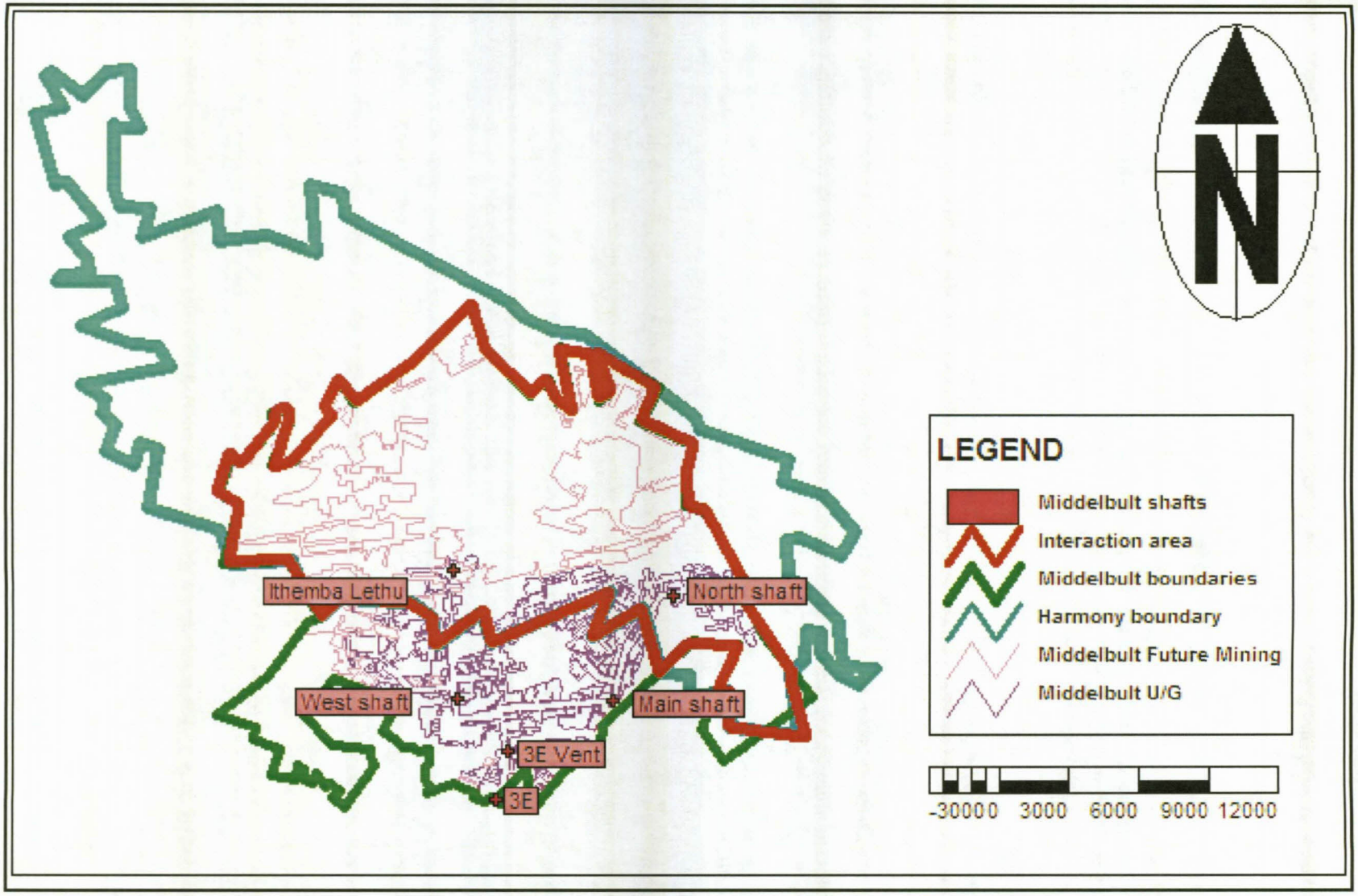

Figure 11: Middelbult layout of current and future mining.

3.2 Coal mining methods and their impact on groundwater quality and quantity

The common characteristic of board-and-pillar and more specifically high extraction coal mining methods is that the removal of the coal seam results in the caving of the overlying strata into the mined void. This disruption of the overlying rock mass may have a significant effect on the hydrogeology, especially where high extraction has been done, resulting in subsidence (Vermeulen & Usher, 2006). High extraction is when the board-and-pillar development is followed by pillar extraction using a coal-cutting machine.

For shallow mines (<200-300 m), the collapse usually propagates to the surface and establishes a direct connection between shallow groundwater aquifers and the underlying mine workings (Vermeulen & Usher, 2006). Although the specific technique used for high extraction does not significantly influence the extent of the impact on the groundwater regime.

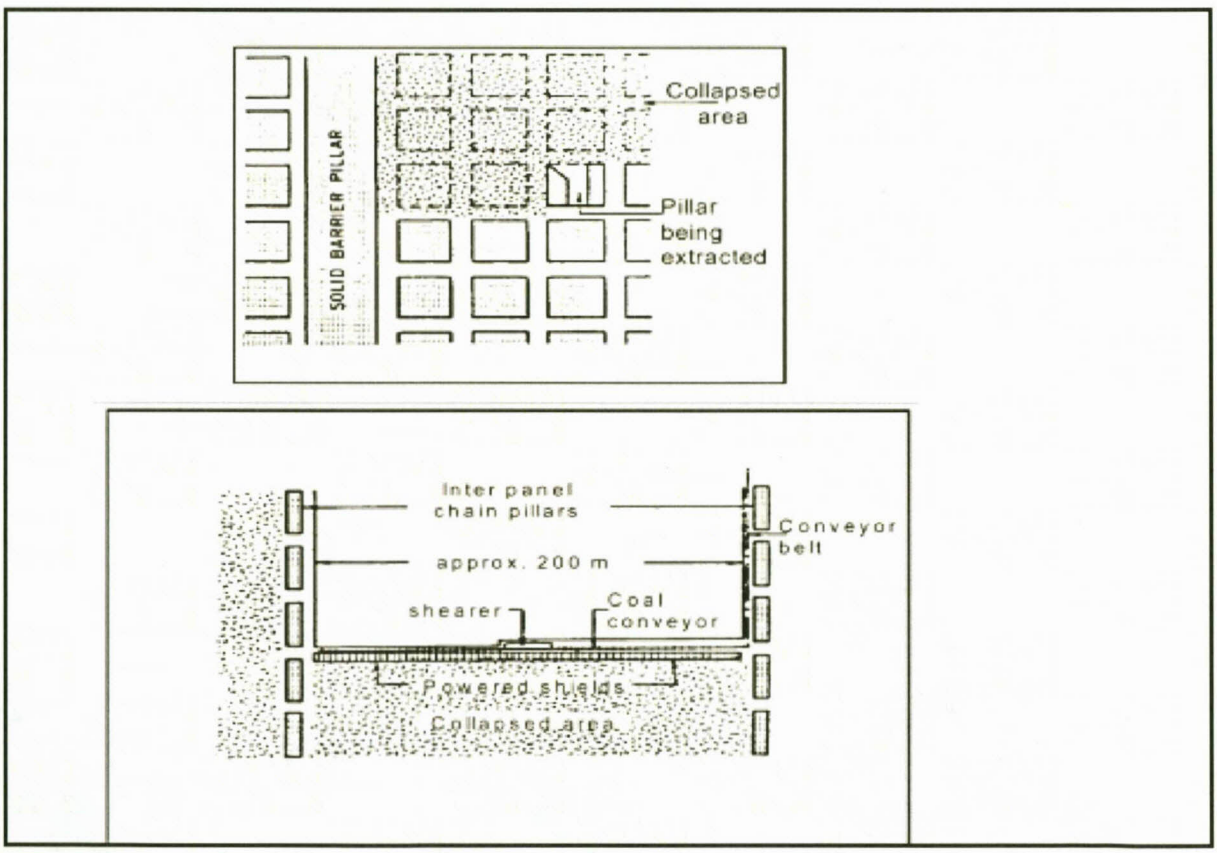

Figure 12: Board-and-pillar mining followed by high extraction (Vermeulen & Usher, 2006).

3.2.1 Board-and-pillar (BP) mining

Recharge into board-and-pillar mining compartments is generally lower when compared to high extraction compartments, due to the roof being kept intact through pillar support. This will result in slower fill rates, allowing the build-up of oxidation products during the filling period on reactive coal particle surfaces. Oxidation of pyrite is kinetically driven and, although it decreases over time if no flushing takes place, it can generate significant amounts of oxidation products (Vermeulen & Usher, 2006).

The Neutralisation Potential (NP) of a BP compartment is lower in comparison with a HE compartment, since it is only the NP in the exposed coal that can actively participate in the neutralisation of acidity released from pyrite oxidation. The lower recharge rates mean that the rate of alkalinity added to the underground workings from the recharge water is also slower. This means that BP compartments are not suitable for active flushing scenarios during the closure phase (Vermeulen & Usher, 2006). Fracturing of the coal by board-and pillar methods immediately results in an increased reactive surface area, which can significantly increase the mass of acidity produced by Acid Rock Drainage (ARD) processes (Vermeulen & Usher, 2006). BP compartments often await high extraction, allowing oxidation products to build up over time. BP compartments can be turned into compartment dams, which will allow for the inundation of compartment reactive surfaces, as well as make storage space available for water management/reticulation purposes (Vermeulen & Usher, 2006).

3.2.2 High extraction (HE) Mining

Recharge into HE compartments is generally higher when compared to BP compartments due to the fracturing of the overlying geology during goafing. This allows for higher recharge rates and hence faster filling rates, reducing the time for oxidation product build-up. Where goafing results in higher rainfall recharge, the alkalinity mobilised in the overlying geology can contribute to the overall NP of the HE compartment. Neutralisation Potential (NP) associated with overlying rocks is introduced in the compartment due to goafing. This NP can significantly contribute to the alkalinity already present in the coal, as well as that associated with the recharge water (Vermeulen & Usher, 2006).

Conversely, due to the presence of Karoo Supergroup marine sedimentary rocks in the roof, one would expect a higher pyrite content, which will in turn become active once goafing results in the exposure of fresh pyrite surfaces to oxygen. HE compartments can be sealed off and rapidly filled with water to reduce the potential rate of pyrite oxidation to insignificant levels. During

filling, the NP associated with roof material will become available for the neutralisation of water acidity in the compartment (Vermeulen & Usher, 2006).

Acid Base Accounting (ABA) and various leaching tests were performed on 20 samples, using the Modified Sobek (Lawrence) Method Jasper Muller Associates cc (2002) . The following conclusions were made by Jasper Muller Associates cc (2002) with regard to the overall acid generating potential of the overburden (Figure 22) above the No.4L coal seam:

- Paste pH levels measured indicate the presence of either excess base or acid material in the overburden for the current (in-situ) situation. None of the samples had paste (initial) pH-levels of lower than 7.77. This is an indication of the excess base material present in the overburden at this stage. Groundwater draining initially into the underground workings will display the effects of this excess base material, in the form of elevated alkalinity values Jasper Muller Associates cc (2002) .
- A total S % calculation usually gives an indication of the sum-total of all sulphur species present in the rock. This figure might include an entire range of sulphate species, sulfide species, and organic sulphur species, some of which are only partly or not oxidised at all. The total S calculated for Middelbult Block 8 does not give an overestimation of the material available for oxidation, since only the reactive components were measured. The range in total S % of all of the lithologies is relatively big (0.001 %-2.271 %), with an average value of 0.370 %. This is an indication of the heterogeneity in terms of pyrite mineralisation and distribution in the different overburdens Jasper Muller Associates cc (2002) .
- The Acid Generation Potential (AP) gives an indication of the gross potential for acidification per volume material. The range in AP is between 0.031 kg/t CaCO3 and 70.969 kg/t CaCO3, with an average value of 11.573 kg/t CaCO3. A number of 5 samples (25 %) showed elevated values above the average Jasper Muller Associates cc (2002) .
- The Neutralisation Potential (NP) gives an indication of the total base potential available to neutralise acidification. The range in NP is between 5.5 kg/t CaCO3 and 62.5 kg/t CaCO3, with an average value of 18.3 kg/t CaCO3. A number of 8 samples (40 %) showed elevated values above the average. The average value for all the samples is higher than the values recorded for the Acid Generation Potential (AP) Jasper Muller Associates cc (2002) .

- The Nett Neutralisation Potential (NNP) is the total of NP - AP. A positive value means excess base potential, a negative value excess acid potential. The range in NNP is between -58.5 kg/t CaCO3 and 62.5 kg/t CaCO3, with an average value of 6.8 kg/t CaCO3. Overall, a positive NNP is present. The very large range in NNP indicates the heterogeneity in the different stratigraphic (geochemical) units Jasper Muller Associates cc (2002) .

3.3 Water Compartments

Middelbult Block is subdivided into water compartments shown Figure 13. In general, the water in smaller compartments is easier to manage. Larger compartments create the risk that, when filled to the decant elevation; certain areas of the compartment could be above the water level due to the coal-seam topography. This will result in the active production of acidity in those areas. Smaller compartments reduce the risk of failure, since smaller water volumes are retained (Vermeulen & Dennis, 2009).

Smaller compartments, located in areas of high recharge, produce smaller volumes of water to be managed in order to prevent an excessive build-up of head. If a compartment needs to be emptied for whatever reason, smaller compartments will have smaller volumes to manage. The negative aspect of smaller compartments is that they will have a higher cost of sealing implication compared to larger compartments, due to the need for more seals (Vermeulen & Dennis, 2009).

3.3.1 No water storage zones

A Minsim W analysis was done to determine the effect of gold mining on the coal horizon where a small middling (>100 m) exists (Harmony/Sasol Working Group, 2005). Particular attention was given to the tensile effect above the old gold workings. Results of the analysis show a small area above the sub-outcrop of the gold workings has a tensile effect that extends into the coal workings as shown in Figure 13. This zone has small horizontal stress change that can be expected on the coal horizon in areas where the middling to the gold workings is less than 100 m. In this zone no water should be stored to prevent any possible groundwater interaction from the coal mine workings into the gold mine workings (Figure 13).

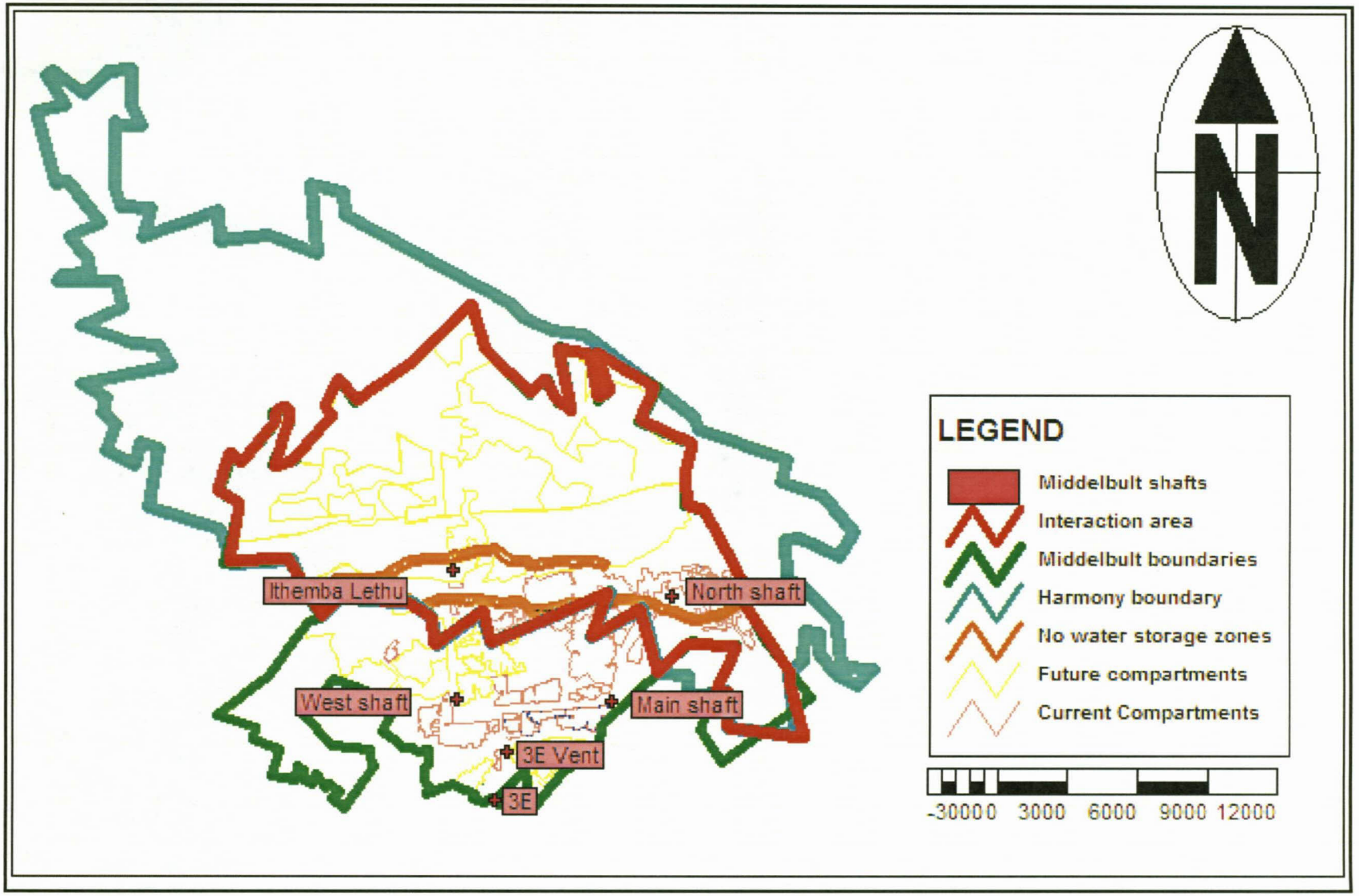

Figure 13: Coal mine water compartments and no water storage zones.

3.4 Harmony Evander Gold Mining Operations

Harmony Evander is a deep-level gold mine which currently and in future will extract gold from the economically viable Kimberley reef situated at variable depths underground. It is important to note that the gold mine has no opencast or shallow workings (< 200 m below surface). The underground workings of Harmony Evander gold mining operations consist of various layouts and configurations. These configurations are a function of mine planning and method, and can broadly be classified under conventional mechanised face and strike gully stoping methods with haulages, cross-cuts and ore passes (Leslie Gold Mines (EMPR), 1994).

The different depths of the gold mine are expected to have different effects on the quality of the ground water. The extent to which the mining affects the quality of ground water must be determined according to the different mining phases, the current status of the current mining area and the way in which water is managed within the mining area.

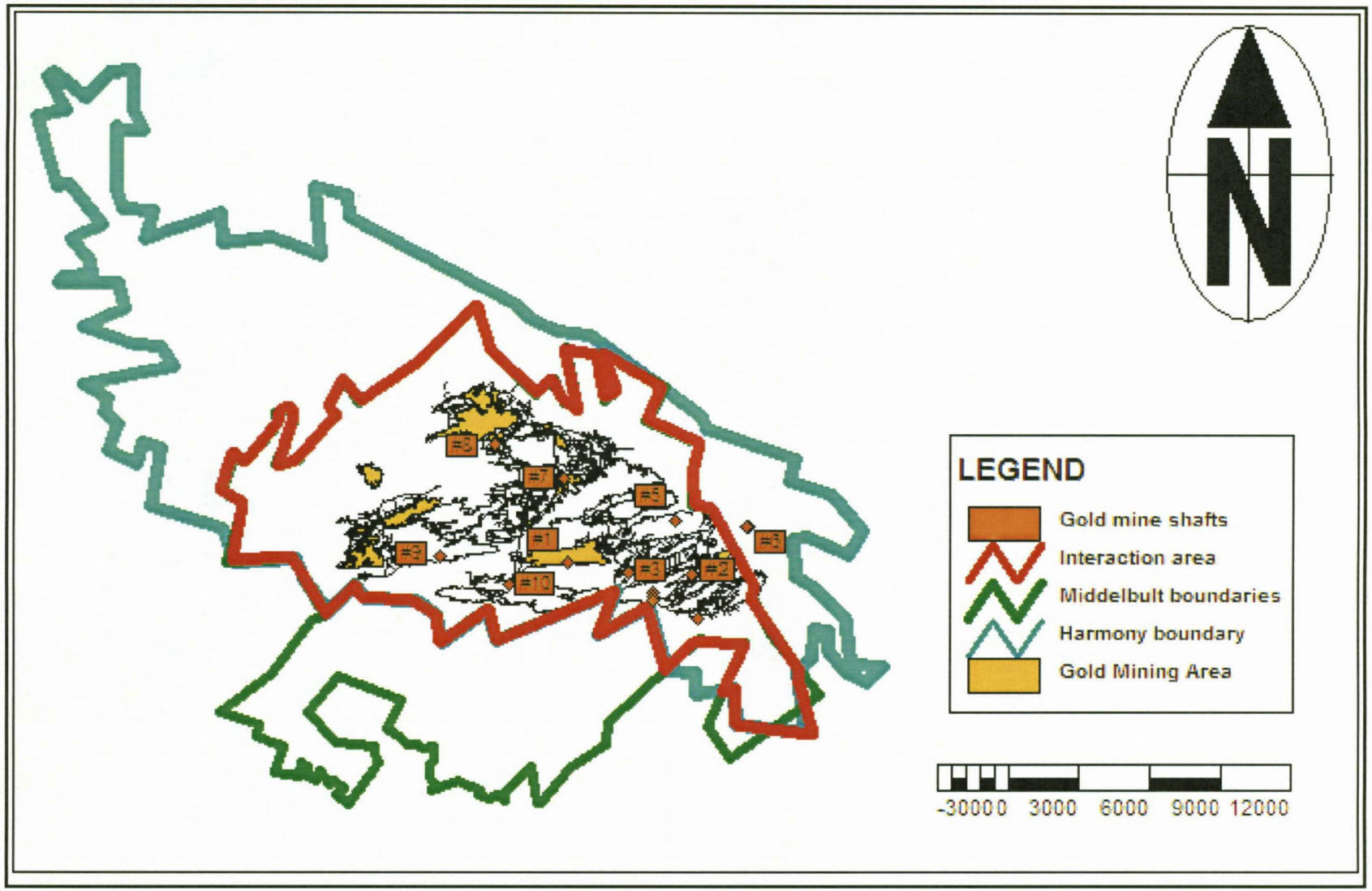

Figure 14: Gold mining area with shafts and ventilation shafts.

3.4.1 Gold Mining methods and their impact on groundwater

Gold mining operations in the study area take place at depths from approximately 250 to 2500 m below surface, using conventional mechanised face and gully stoping methods; the development is down the footwall of the Kimberly Reef (Winkelhaak Mine EMPR, 1988).

Stoping takes place on the economically viable Kimberly Reef, where ore from underground workings is then transported by overhead trolley lines from underground to the Metallurgical Plant situated on the surface (Winkelhaak Mine EMPR, 1988).

Figure 15: Gold mining stope from which ore containing gold is extracted from the Kimberley reef.

3.4.2 Causes and effects of gold mining methods

The gold mining area is at a far greater depth than the coal and therefore no subsidence is envisaged (Winkelhaak Mine EMPR, 1988). It is expected that over time pressure from the overlying rock will compress the stope or even close the stope completely as shown in Figure 15 where the effect can be seen on the wooden stacks supporting the overlying rock mass.

Acid Rock Drainage (ARD) usually happens after deep gold mines have been abandoned. The reason is deep sub-surface mines, when operational will have to keep pumping the groundwater out of the mine (Figure 16). Once abandoned, however, the pumping stops and the mine floods.

This flooding is the initial step of ARD. Acidity is generated when metal sulfides are oxidised after being exposed to air and water. Bacteria and archaeade microbes compose the metal-ions faster. These microbes are found naturally in the rock, but their numbers are usually low in deep gold mines due to limited oxygen and water (Freeze & Cherry, 1979). However, once they are in an environment with an abundance of water and oxygen, they flourish (Freeze & Cherry, 1979).

Figure 16: Groundwater flowing into the gold mine via exploration borehole in a gold mine shoots.

Sulfide-bearing minerals, of which pyrite (FeS_2) is the most abundant, will react with water in an oxidising environment to form sulphuric acid (H_2SO_4), Detailed reactions from Freeze & Cherry (1979).

Equation 1
(1) $FeS_2 + 7/2\ O_2 + H_2O \Rightarrow Fe^{2+} + 2SO_4^{2-} + 2H^+$

Equation 2
(2) $Fe^{2+} + 1/4O_2 + H+ \Rightarrow Fe^{3+} + 1/2\ H_2O$

Equation 3
(3) $Fe^{3+} + 3H_2O \Rightarrow Fe(OH)_3$ (yellow boy) $+ 3H^+$

Equation 4
(4) $FeS_2 + 14Fe^{3+} + 8H_2O \Rightarrow 15Fe^{2+} + 2SO_4^{2-} + 16H^+$

The geochemistry of the geological regime dictates the degree and significance of impact on the environment. The potential to generate acid rock drainage is largely determined by the presence of sulphide minerals. However, acid drainage will not occur if either the sulphides are non-reactive or sufficient alkaline materials are present to neutralise the acid (Vermeulen & Usher, 2006).

Static acid base accounting tests were conducted on samples of dust on rocks obtained from mined strata in order to provide a qualitative predication of the net acidity, a function of the relative content of acid generating minerals (sulphides) and acid consuming or neutralising minerals (carbonates) (Winkelhaak Gold Mines (EMPR), 1988).When acid generating capability exceeds acid consuming capacity, the pH of the water decreases with the consequent mobilisation of sulphates and heavy metals, resulting in acid rock drainage (Winkelhaak Mine EMPR, 1988).

Acid base accounting yielded a marginal negative (-0.10 kg/ton $CaCO_3$) net neutralising potential (NNP), indicating a slight potential for acidity over the short term. Rain would wash the rocks clean over the medium and long term. It was found that the rock rubble is hard and does not weather over the medium to long term (110 years) (Winkelhaak Mine EMPR, 1988).

3.4.3 Prevention of possible groundwater interaction between Harmony Evander gold mining operations and Sasol Secunda Middelbult (Block 8)

The two mines have specific regulations in place to prevent groundwater interaction between the mines. These regulations are listed below and in their respective Environmental Management Programmes.

- Barrier pillars of 100 m are left between all adjacent mining sections, to prevent the migration of groundwater to low-lying areas and associated mining and safety problems (Middelbult Mine; Block 8 Expansion EMPR, 2003).
- No mining activities will take place directly underneath the gold mine tailings storage facilities (Middelbult Mine; Block 8 Expansion EMPR, 2003).
- The minimum distance that high extraction activities will take place from the perimeter of the gold mine slimes dams is given as 300 m (Middelbult Mine; Block 8 Expansion EMPR, 2003).

- Coal mining activities will keep a barrier pillar of 50 to 100 m from vertical gold mine shafts (Middelbult Mine; Block 8 Expansion EMPR, 2003).
- All gold mine exploration boreholes will be sealed off with a non-reactive material to prevent the drainage of poor quality, low pH groundwater from the coal mine to the gold mine (Middelbult Mine; Block 8 Expansion EMPR, 2003).
- The gold mine shafts will be sealed using design and methods specified by a competent professional Civil Engineer (Leslie Mine EMPR, 1994).
- Any other excavations caused by mining operations will be back filled or graded to a safe condition and rainfall run-off control measure in these areas will be implemented (Leslie Mine EMPR, 1994).
- No water storage zones - In these zones no water should be stored to prevent any possible groundwater interaction from the coal mine workings into the gold mine workings. (Sasol/Harmony Working Group, 2005).

Chapter Four: Geology of the Study Area

4.1 Introduction

An important aspect of this investigation is the geology of the study area (Figure 17). It is the major contributor in defining the various aquifers present within the different geological lithologies. Geological processes also create preferential flow paths such as cracks, fissures, joints and faults which allow for the rapid movement of groundwater in the subsurface (Cook, 2003). As the study area is situated in the well known Evander Basin, a detailed description of the geology of the Evander Basin is included.

In the major part of the Basin sediments of the Witwatersrand Supergroup unconformably overlie the Archaean Basement. These Witwatersrand sediments are in turn overlain by rocks of the Ventersdorp Supergroup, Transvaal and Karoo Supergroups as shown in Table 2.

Three ages of intrusives are present in the Evander Basin, namely Bushveld, Ventersdorp and Karoo. These intrusives are present as both dykes and sills across the study area. The Evander Basin has undergone extensive structural dislocation and faulting is the most common form of deformation, with both primary and secondary fault-features being observed in the study area (Tweedie *et al.*, 1986).

The following section describes the geology of the study area. The geology is described according to the various Supergroups encountered in the study area from surface (Karoo Supergroup) to deepest (Archaean Basement). Most of the geological description was based on exploration borehole logs provided by Harmony and by work done by Tweedie *et al.*, (1986). The position of the exploration boreholes are shown in Figure 18 with a typical borehole log shown in Figure 19.

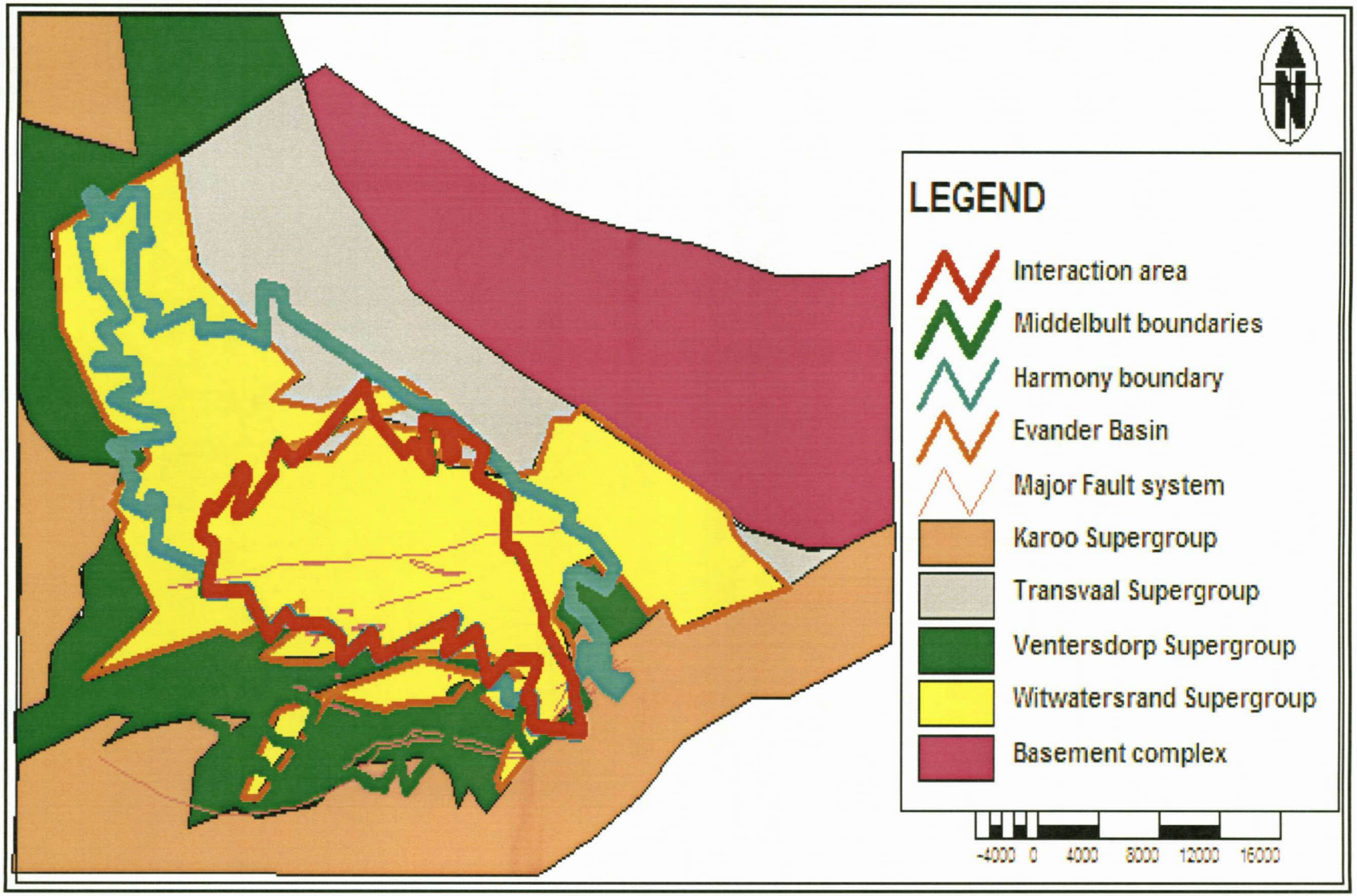

Figure 17: Geological map of the Evander Basin.

Table 2: Generalised Stratigraphy of the Study Area.

PLEISTONE TO RECENT	SUPERGROUP	SUBGROUP	SOIL AND ALLUVIUM	
Precambrian ca. 2000 x 10^6 years	Karoo Supergroup 183 - 22 m	Ecca Group Dwyka Group	Sandstones, carbonaceous shales and coal seams Tillite	Unconformably
Precambrian ca. 2300 x 10^6 years	Transvaal Supergroup up to 1100 m	Pretoria Group Olifants River Group Black Reef formation	Argilliccous quartzites, black shales, and tillites, with intercalated pyroclastic lava flows. Magnesium limestone, with chert bands. Quartzites and carbonaceous shales, with a poorly developed basal conglomerate.	Unconformably Unconformably
Precambrian ca 2600 x 10^6 years	Ventersdorp Supergroup up to 1324 m	Klipriviersberg Group	Grey-green pyroclastics and amygdaloidal andesitie lavas	Conformably
Precambrian ca 3100 x 10^6 years	Witwatersrand Supergroup up to 1500 m	Central Rand Group West Rand Group	Quartzites, amygdaloidal lava, shales, and conglomerates, including the Kimberley Reef Greywackes, quartzites, and magnetic shales	Unconformably
	Archaean basement		Shists, metasediments, and gneissose granites	Unconformably

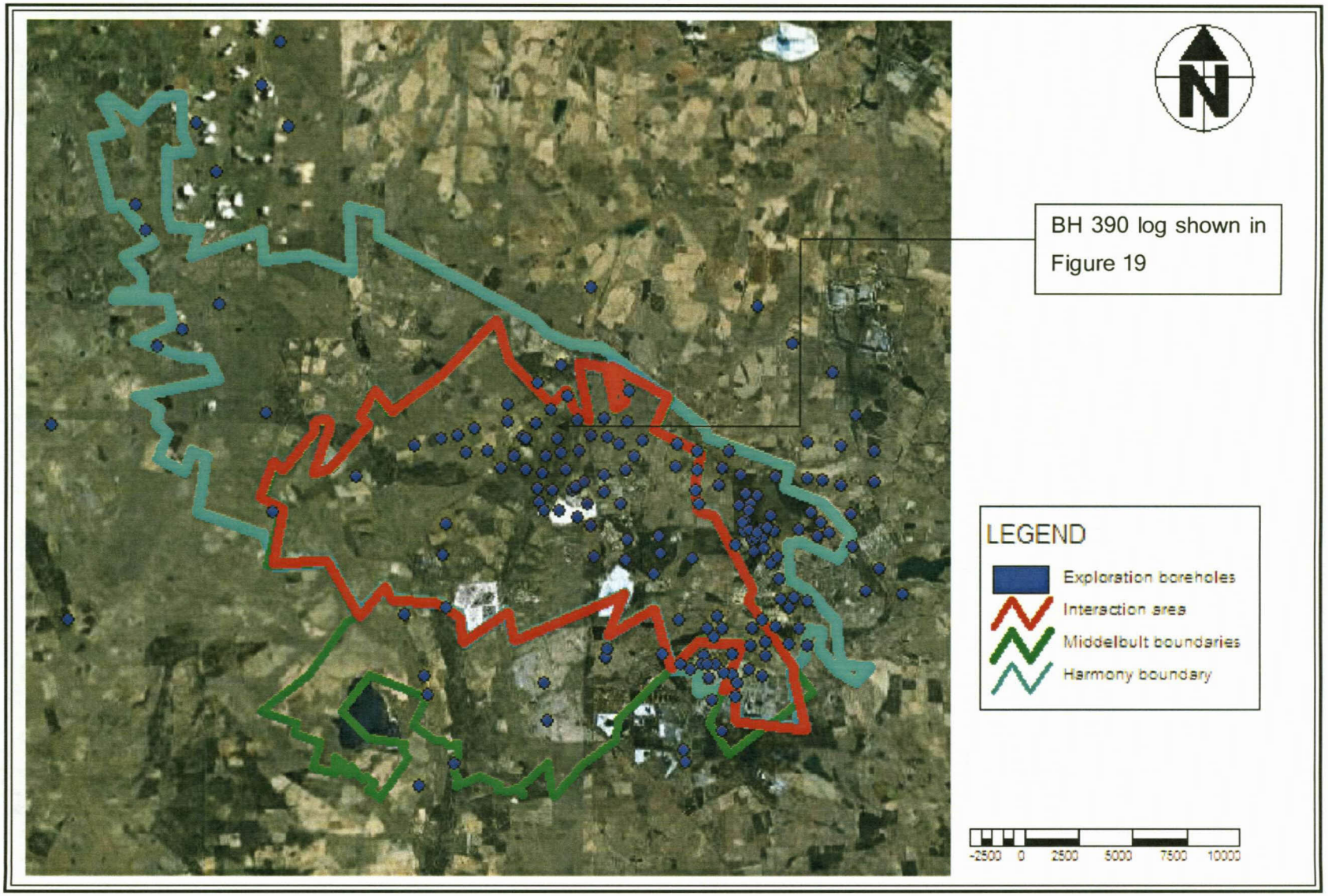

Figure 18: Exploration borehole positions within the study area.

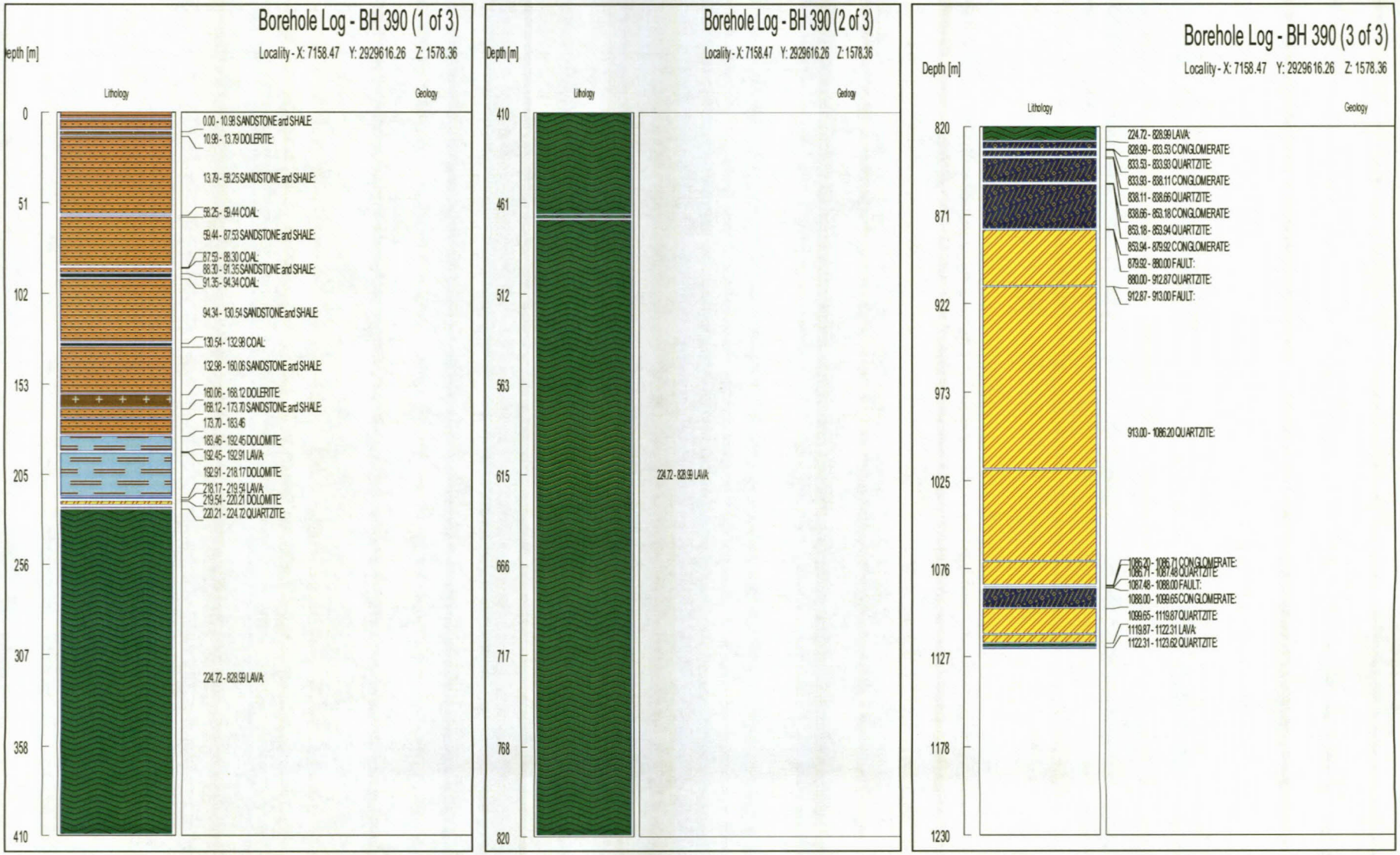

Figure 19: Geological log for exploration BH 390 (0-1129m).

4.2 Karoo Supergroup

The Karoo Supergroup is a relatively thick and extensive group of rocks that was deposited on the land and in fresh water, almost continuously from the Late Carboniferous to late Triassic age. The Karoo Supergroup hosts all the South African coal deposits. The coal deposits were formed in the great Gondwana basin (Tweedie *et al.*, 1986).

The study area is located on the north-eastern limit of the Main Karoo Basin, in which the sediments were not horizontally disposed but dip to the south-west at a very low angle (Tweedie *et al.*, 1986).

The Karoo Supergroup, with glacial and deltaic sediments in some places, directly overlies the Transvaal, Ventersdorp and Witwatersrand Supergroup with a range of 50 m to 300 m at an average of 210 m across the study area using the interpolated exploration boreholes (Figure 21). The lithology comprises of sedimentary rocks of the Dwyka Formation and Vryheid Formation of the Ecca Group formed by erosion during and before the deposition of the Dwyka Group of the Karoo Supergroup. These formations were deposited on an undulating glaciations period. These rocks primarily consist of sandstones, shales and coal beds and are extensively intruded by dolerites of Jurassic age. Figure 20 shows the sedimentary rocks encountered in the Karoo Supergroup within the study area.

Figure 20: Photographs of typical sedimentary rocks found in Karoo Supergroup of the study area.

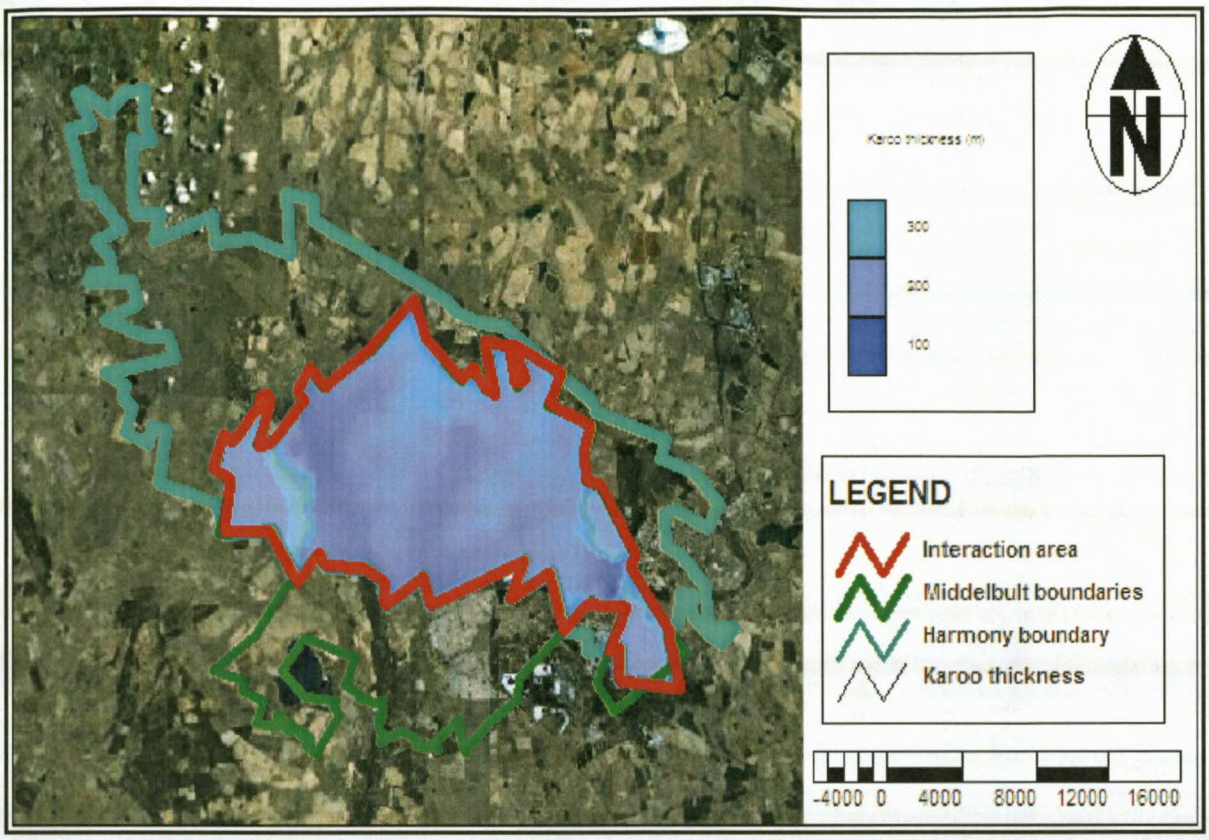

Figure 21: Interpolated thickness of the Karoo Supergroup in the study area.

The stratigraphic column consists of typical products of the Dwyka continental glaciation process, represented by deposits of diamictite, glacio-lacustrine varved siltstone, pebbly mudstones and fluvio-glacial gravels and conglomerates. Clastic sediments and coal overlie these rocks. The sediments were deposited in shallow marine and fluvio-deltaic environments and the coal accumulated as peat in swamps and marshes associated within these sedimentary environments (Tweedie *et al.*, 1986).

In general, three phases of sedimentation are recognised in the sedimentary of the Karoo Supergroup of the study area by Tweedie *et al.*, (1986):

- The lower delta-dominated phase;
- A fluvial dominated coal zone and an upper deltaic succession;
- The lower succession commonly comprises one or more upward coarsening cycles of dark micaceous siltstone.

The fluvial dominated coal zone is about 75 m thick. In the study area there are only two coal seams of significance as compared to the five coal seams of the Witbank Coalfield Jasper Muller Associates cc (2002) . The two coal seams of significance are the No. 4L coal seam and the No. 5L coal seam. Currently only the No. 4L coal seam is economically viable and is mined by Sasol Coal Mining Secunda (Pty) Limited (Middelbult Mine: Block 8 Expansion EMPR, 2003).

The coal seams are usually separated by course-grained sandstone, fining to siltstone or shale at the top. Glauconite sandstone, indicative of transgressive marine periods, is present above the No. 4 Upper Coal Seam and forms useful stratigraphic markers. The approximate thickness of the mainly sandstone overburden above the No. 4L coal seam is shown in Figure 22. Locally, the general lithological profile, up to and including the deepest mine-able coal seam, comprises of:

- Soft overburden;
- Hard overburden;
- No.5 coal seam;
- Inter burden;
- No.4L coal seam.

Dolerite dykes and sills also appear over the study area Jasper Muller Associates cc (2002).

The coal seams are mainly flat to gently undulating, with a very gentle regional dip to the south. The No. 4L coal seam has a maximum thickness of 6.60 m and a minimum of 4.14 m with an average value of 5.69 m Jasper Muller Associates cc (2002) .

Table 3: Thickness information of the different coal seams (adapted from JMA, 2002, Report No: JW98/02/8068).

Values in (m)	No. 5L coal seam (m)	No. 4L coal seam (m)
Minimum	0.08	4.14
Maximum	5.32	6.6
Average	1.38	5.69

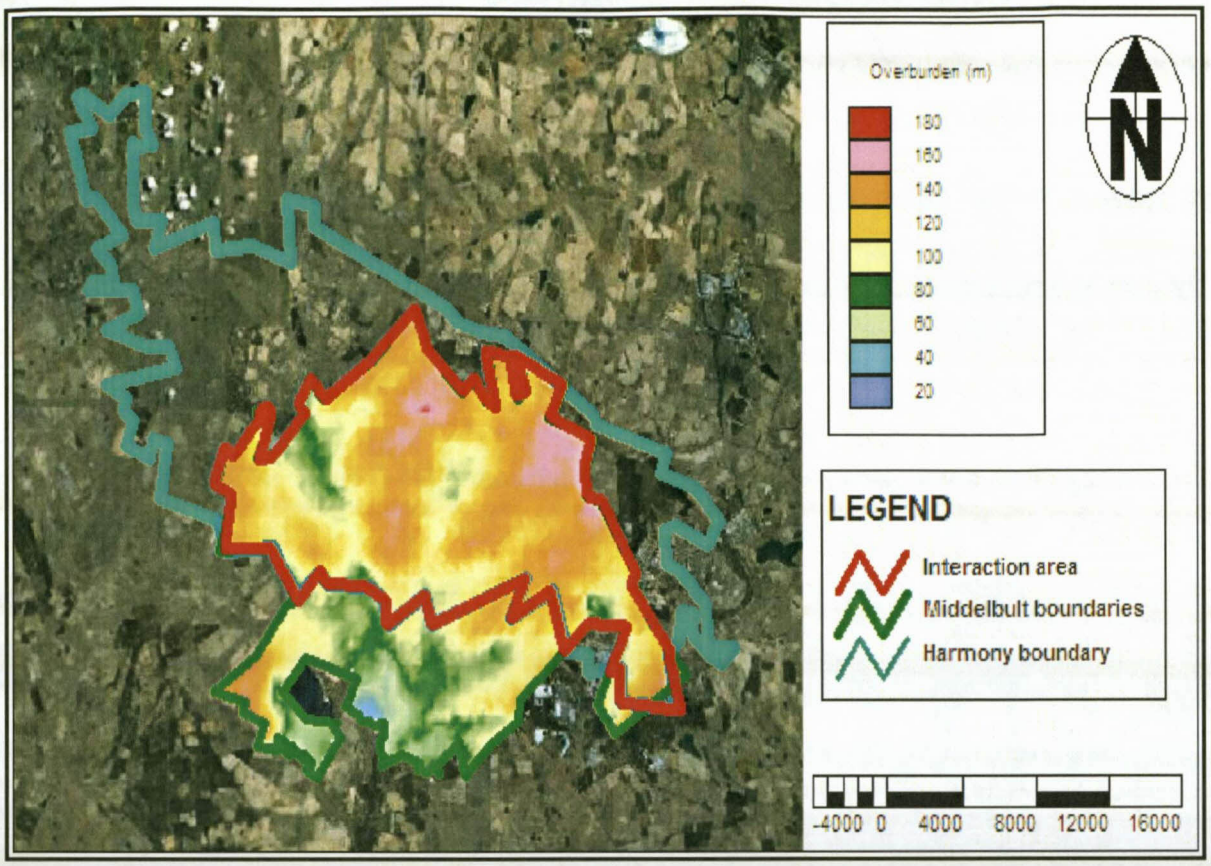

Figure 22: Interpolated overburden thickness in m above the No. 4L coal seam roof of the Middelbult Block 8 area.

Apart from displacement of the sedimentary succession caused by intrusive dolerite sills, the Karoo strata are not significantly faulted. Small faults - <1 m displacement - are present, but larger faults have not as yet been identified in the study area. Jasper Muller Associates cc (2002) . Intrusives are represented by dolerite, which covers large areas of the study area (Figure 34). The intrusives are in the form of sills and dykes. The sills are present over large portions of the study area as shown in Figure 23 and Figure 24. The sills are both conformable and transgressive with respect to the sedimentary rocks, and are of the non-porphyritic types. The intrusives are discussed in detail in Section 3.8.

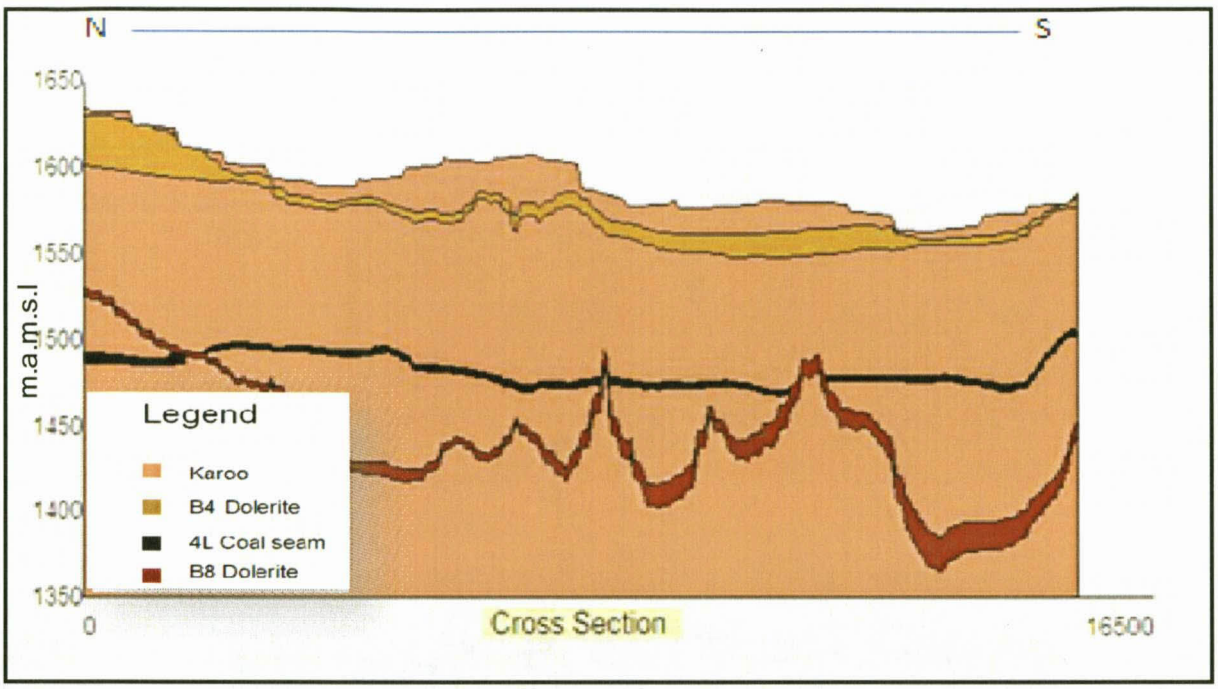

Figure 23: North-south cross section illustrating the No. 4L coal seam and the B4 and B8 dolerite sills.

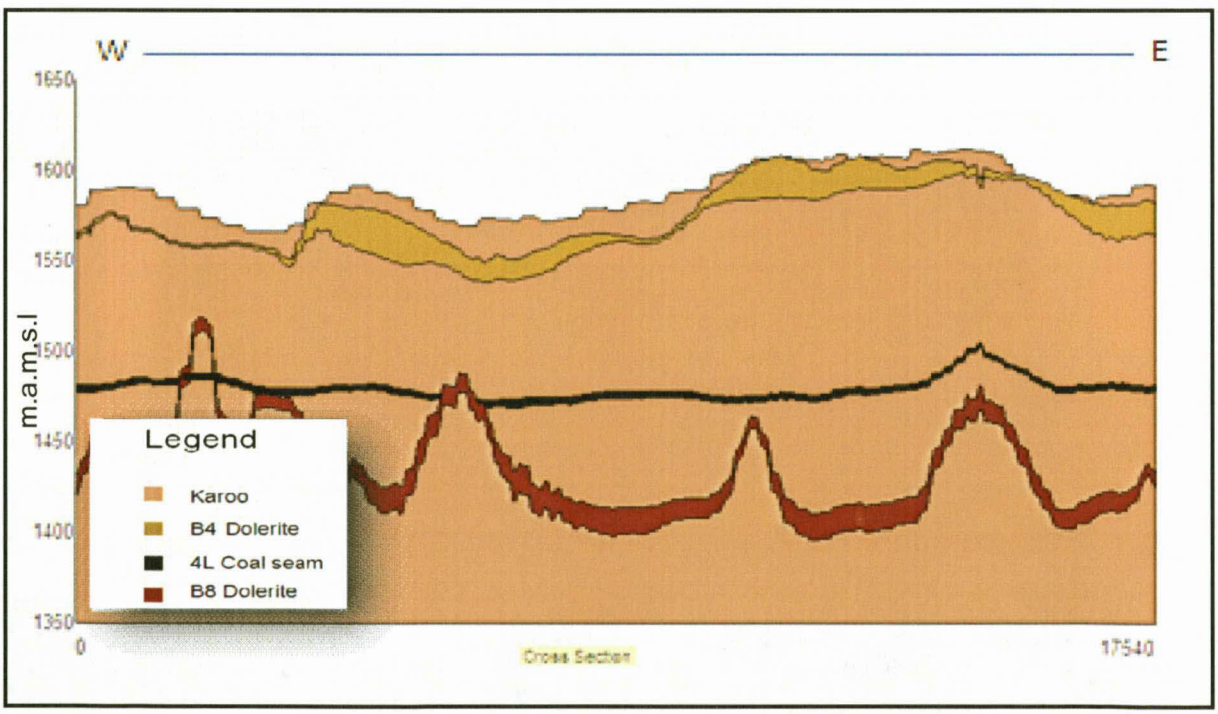

Figure 24: West-east cross section illustrating the No 4L coal seam and the B4 and B8 dolerite sills.

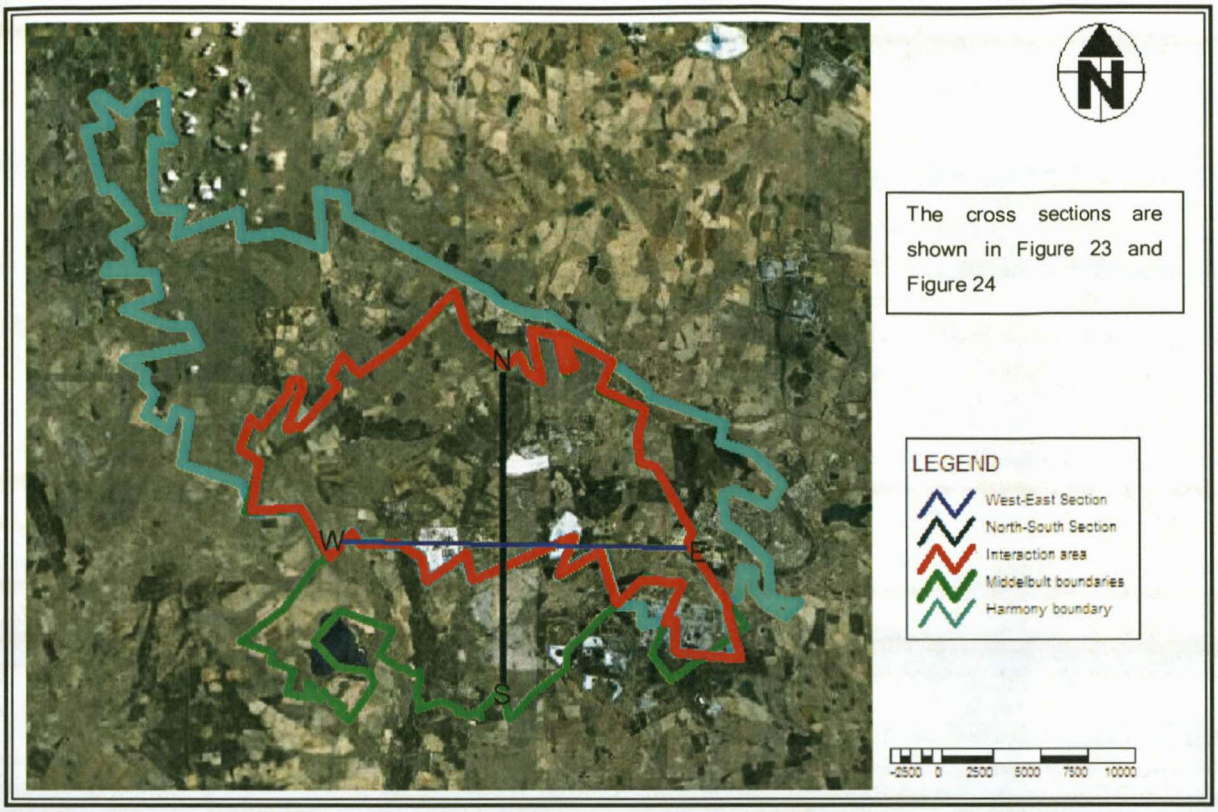

Figure 25: Surface view of the cross sections.

An important feature of the Karoo Supergroup is the presence of a paleo-glacial valley. This event stripped out any old regolith developed on the underlying formation and in particular it removed the karstification within the dolomite (Tweedie *et al.*, 1986). The latter forms the main aquifer in dolomitic formations. Other than the paleo-glacial valley, the Karoo unconformity is not disrupted by any major faults (Tweedie *et al.*, 1986).

4.2.1 Coal seam sedimentary processes

In general, coal seams formed during periods of low sedimentary deposition when plant growth and peat accumulation occurs at the same rate as the substrate. Such periods separate depositional events. At the study area, these depositional Supergroups took place in a deep, rapidly subsiding portion of the main Karoo Basin (Falcon, 1986).

According to Falcon (1986) the coal-forming environments are subdivided into two types.

- The paraglacial and the;
- epicontinental environments.

The paraglacial environment is a basin edge phenomenon that developed around the northwest and northern side of the basin as a result of the accumulation of glacia-lacustrine and glacio-fluvial sediments on the marine-covered surfaces of the Kaapvaal Craton (Falcon, 1986). These sediments were deposited at the close of the Dwyka continental glaciation. The distribution of the coal seams in this environment was controlled by post-Karoo topography, with peat accumulation predominantly occurring in low-lying land protected from active sedimentation. These coals are freshwater marsh in origin, with characteristically low sulphur content (Falcon, 1986).

The epicontinental coal forming environment is related to the major development of sediments across the north-eastern stable shelf area of the Karoo Basin, and overlies the older paraglacial sediments to the north (Falcon, 1986). This environment was locally subjected to marine or brackish water inundation during delta switching, resulting in a variety of geochemical (pH, salinity and Eh) environments. Such factors affect coal quality as well as the resultant sulphur content of the coal considerably.

Within each coal seam, a range of local conditions controls the development of the coal type and facies, such as topographical controls, the local paleo-environment, type of plant community, rate of accumulation and nature and rate of plant degradation, or biochemical coalification (Falcon, 1986).

The conditions for the formation of different coal facies varies with paleo-ecological environments. The in-situ inertinic coals are found predominately in relatively dry environments, viz. on high ground of valley flanks, levees of rivers, upper delta, and alluvial plane swamps. Drift forms occur in reworked organic detritus pieces usually transported by water and deposited on river banks, or as flooded deposits in deltaic or lacustrine environments (Falcon, 1986).

The vitrinite rich coals found at Secunda are usually associated with permanently wet or water-logged conditions, as may be found on sea shores, or in fluviatile, lacustrine, or lower deltaic/paralic back swamps (Falcon, 1986). Shallow open water, distal environments, lagoons, ponds, and distal deltaic settings typically accumulate very fine wind- and water-borne organic and inorganic matter - particularly algae, spores and pollens (Falcon 1986). Known as exinite, these components impart high hydrogen and volatile matter content to the host sediment.

4.2.2 Coal seam contours

The No.4L coal seam slopes downward from a roof elevation ranging between 1488 m.a.m.s.l and 1510 m.a.m.s.l along the northern and eastern bounds of the Block 8 reserve, to a floor

elevation ranging between 1460 m.a.m.s.l and 1465 m.a.m.s.l along the central southern boundary between the Block 8 reserve and Middelbult Colliery as shown in Figure 26 Jasper Muller Associates cc (2002) .

The No.4 seam slopes downwards from the central southern boundary between the Block 8 reserve and Middelbult Colliery to a floor elevation of 1450 m.a.m.s.l in the far south-western portion of the reserve on Leeuwpan (Figure 26). From here is a rise up to 1475 m.a.m.s.l along the central western extent of Middelbult Colliery, towards a high of 1520 m.a.m.s.l a little further to the south-southwest (Figure 26).

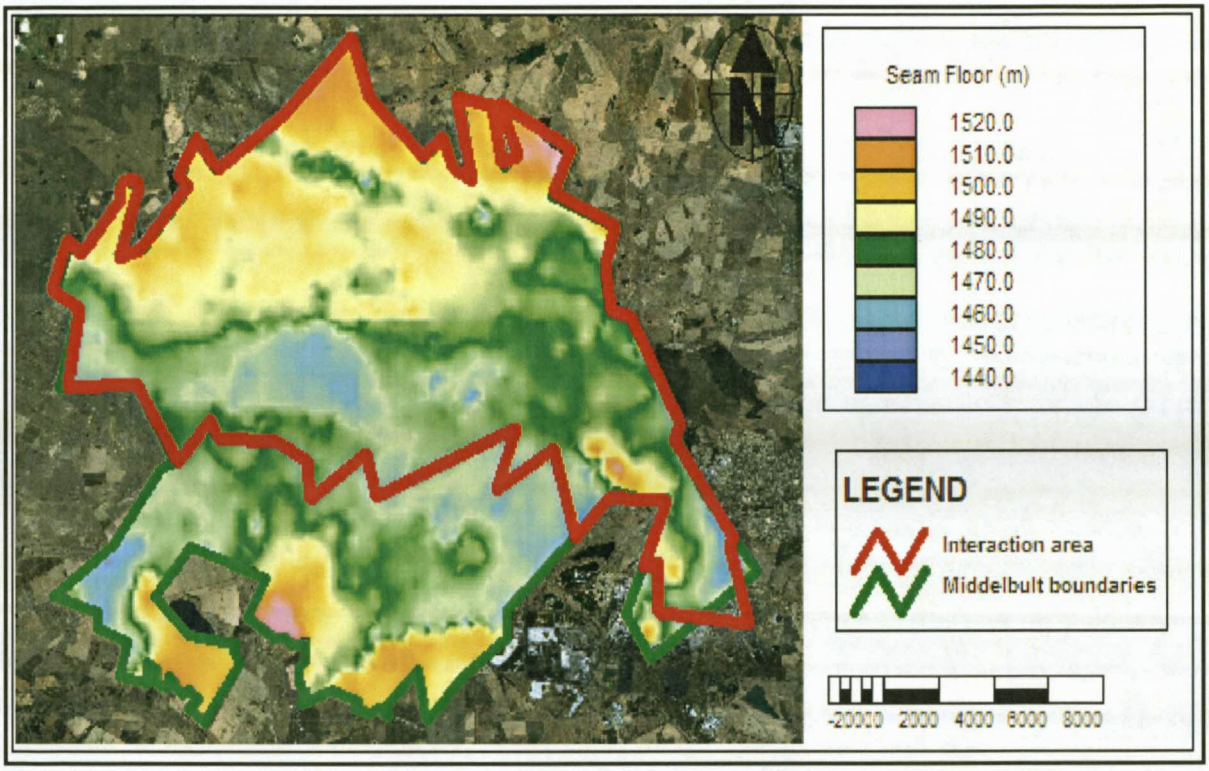

Figure 26: Interpolated elevations of the No. 4L coal seam floor in m.a.m.s.l.

4.3 Transvaal Supergroup

The Transvaal Supergroup is mostly present in the northern portions of the study area and has been intersected both in surface boreholes and in gold mine shafts (Leslie Mine EMPR, 1994). In the south-southeast of the study area, the sediments have been removed by pre-Karoo erosion, as shown in Figure 27 and Figure 28. The sequence consists of a thin, basal quartzite and conglomerate package belonging to the Black Reef Formation. The latter grades

conformably upwards into the manganiferous, chert-poor dolomite Malmani Subgroup of the Chuniespoort Group (Tweedie *et al.*, 1986). Above the Chuniespoort Group is the Pretoria Group, which consists of a basal breccia-conglomerate unit known as the Bevets Conglomerate Formation, overlying ferruginous shale of the Timeball Hill Formation. Overlying the shale is a volcanic unit of andesite that belongs to the Hekpoort Formation (Tweedie *et al.*, 1986).

Several diabase sills intruded the Transvaal Supergroup. There are two main sills that formed lensoid intrusions into the shale of the Timeball Hill Formation. It is, however, unclear if these features are continuous along dip and strike. The Transvaal Supergroup rests unconformably on the Ventersdorp Supergroup and the strike orientation differs by 90° to that of the underlying strata (Tweedie *et al.*, 1986).

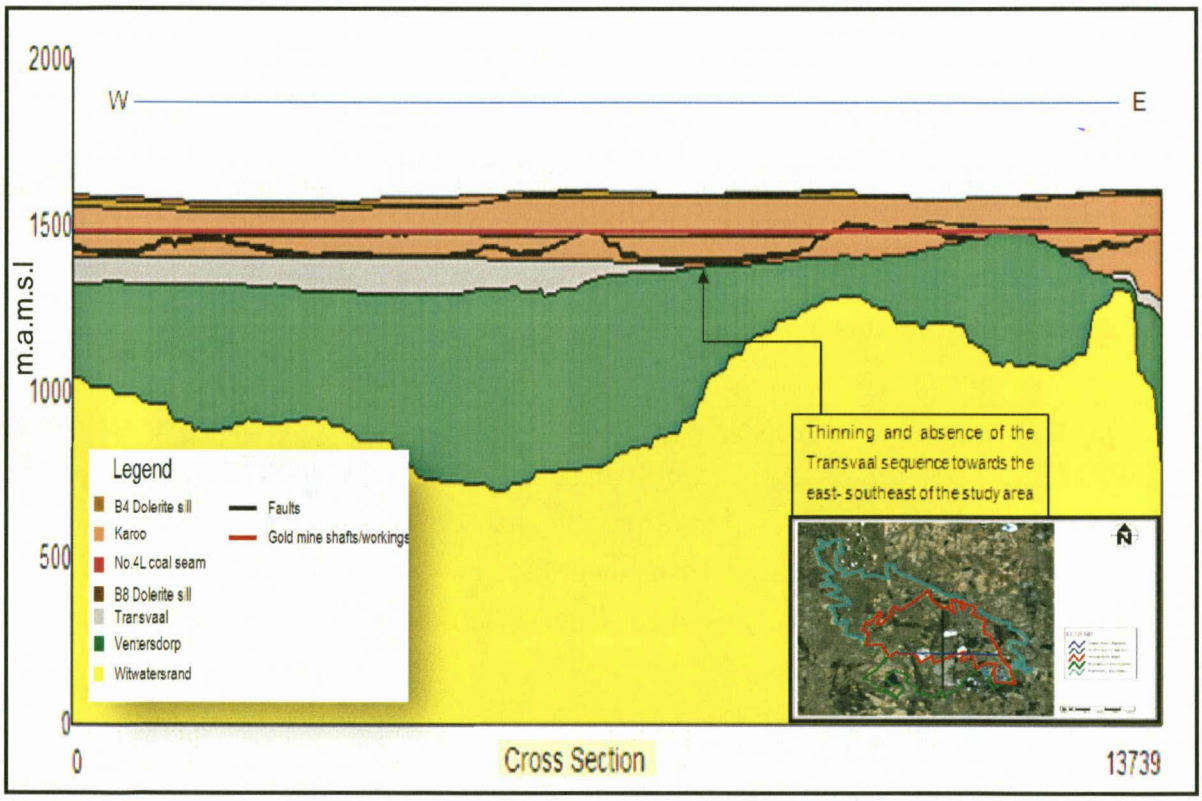

Figure 27: Thinning and absence of the Transvaal Supergroup towards the east-southeast of the study area.

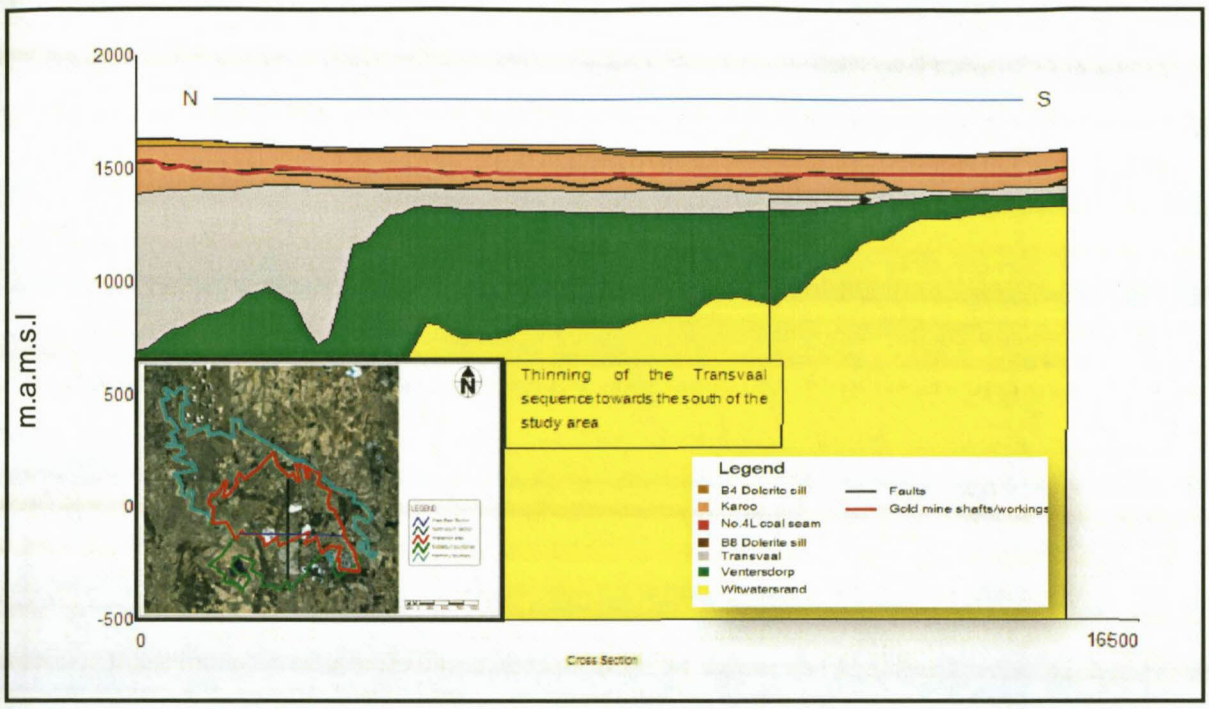

Figure 28: Thinning of the Transvaal Supergroup north to south across the study area.

4.3.1 Black Reef Formation

The Black Reef Formation is poorly developed in the study area and compromises a composite sequence of quartzites and intercalated carbonaceous shale with a basal conglomerate (Tweedie *et al.*, 1986). The sediments, which attain a maximum thickness of 24 m, dip to the north and northeast at 10° and appear to unconformably overlie the andesitic lavas of the Ventersdorp Supergroup. Because of its northerly dip, the Black Reef Formation has been truncated by the Karoo Supergroup and is only developed over the northeastern portion of the basin (Tweedie *et al.*, 1986).

The stratigraphic thickness of the formation is highly variable, suggesting a highly dissected Ventersdorp topography. As most of the faulting is pre-Transvaal in age, a certain amount of relief in the Ventersdorp topography should be expected (Tweedie *et al.*, 1986).

4.3.2 Olifants River Group

4.3.2.1 Malmani Dolomite

The Malmani Dolomite is the only member of the Olifants River Group found in the study area and dips to the north and northeast portion of the basin. The dolomite is generally massive, very

fine grained and varies in color from light grey to medium-dark grey (Tweedie *et al.*, 1986). A number of Karoo-age dykes and sills are present in the upper dolomite. Most of the major faulting is pre-Transvaal in age and therefore most of the major faults carry relatively little water (Tweedie *et al.*, 1986).

4.3.3 Pretoria Group

The Pretoria Group sediments are northerly dipping and underlie the northern portions of the study area (Tweedie *et al.*, 1986). There are three marker horizons that can be recognised:

- Bevet's Conglomerate,
- Daspoort Tillite,
- Ongeluk Volcanics.

The sediments of the Pretoria Group, as observed, are characterised by the lack of coarse-clastic rock types and comprise a sequence of interbedded, light grey, banded siltstones, shales and very occasional, micaceous, friable quartzites (Tweedie *et al.*, 1986).

4.4 Ventersdorp Supergroup

Overlying the Witwatersrand strata is a thick sequence of andesite (lava) of the Klipriviersberg Group (Tweedie *et al.*, 1986).

4.4.1 The Klipriviersberg Group

The Klipriviersberg Group of up to approximately 1324 m (Figure 29) thick is represented in the study area by a succession of superimposed flows of greenish-grey, andesitic lavas (Tweedie *et al.*, 1986). Amygdaloidal, non-amygdaloidal, and porphyritic varieties are present, together with thin zones of greenish-grey pyroclastic rocks (Tweedie *et al.*, 1986). Two well-defined porphyritic units, developed near the base of the Group, constitute good marker horizons. The contact between the lavas of the Klipriviersberg Group and the underlying Witwatersrand sediments appear to be conformable in the study area. The variable thickness of the Ventersdorp lava is partly attributed to the faulting in the area, but it is important to note that for most of the study area the Ventersdorp Supergroup mantles the Witwatersrand Supergroup (Tweedie *et al.*, 1986). The exception is in the east-southeast of the study area where the Group is very thin and in some areas sub-outcrops against the Karoo Supergroup as shown in Figure 30. In general, the Ventersdorp Supergroup thins from north to south in the study area, as shown in Figure 31.

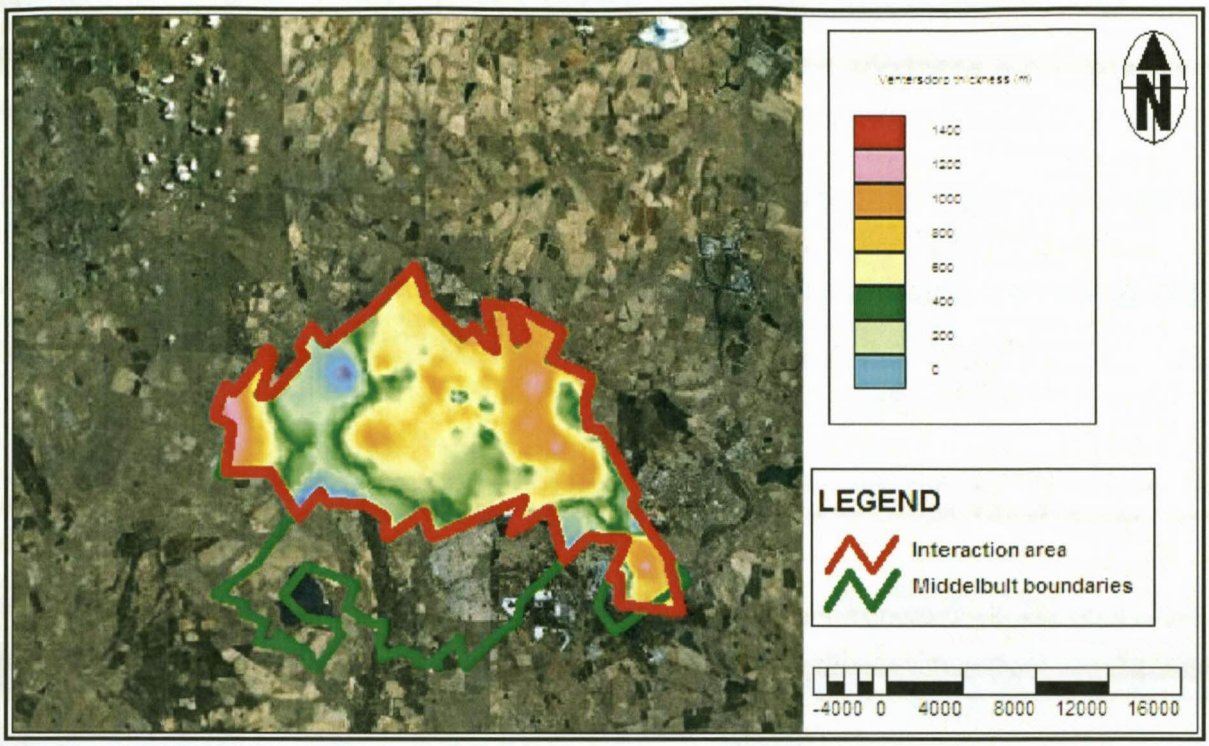

Figure 29: Interpolated thickness of the Ventersdorp Supergroup.

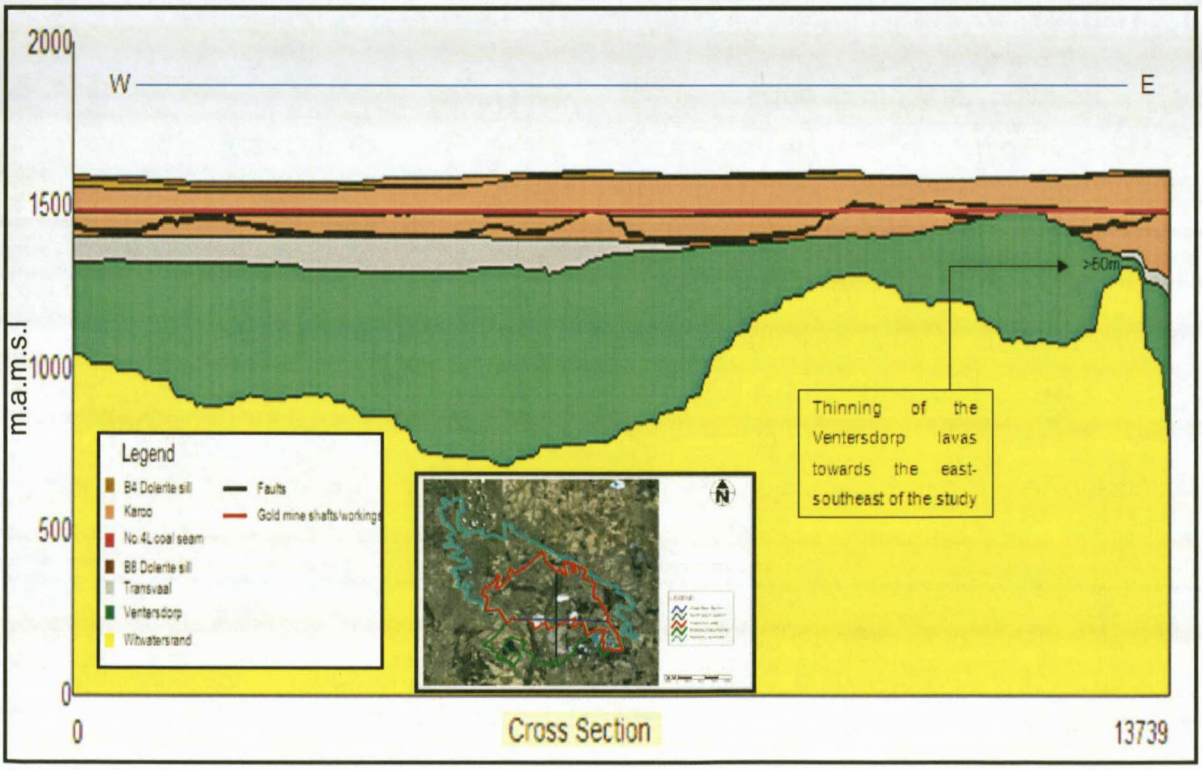

Figure 30: Thinning of the Kliprivierberg Group lavas towards the east-southeast of the study area.

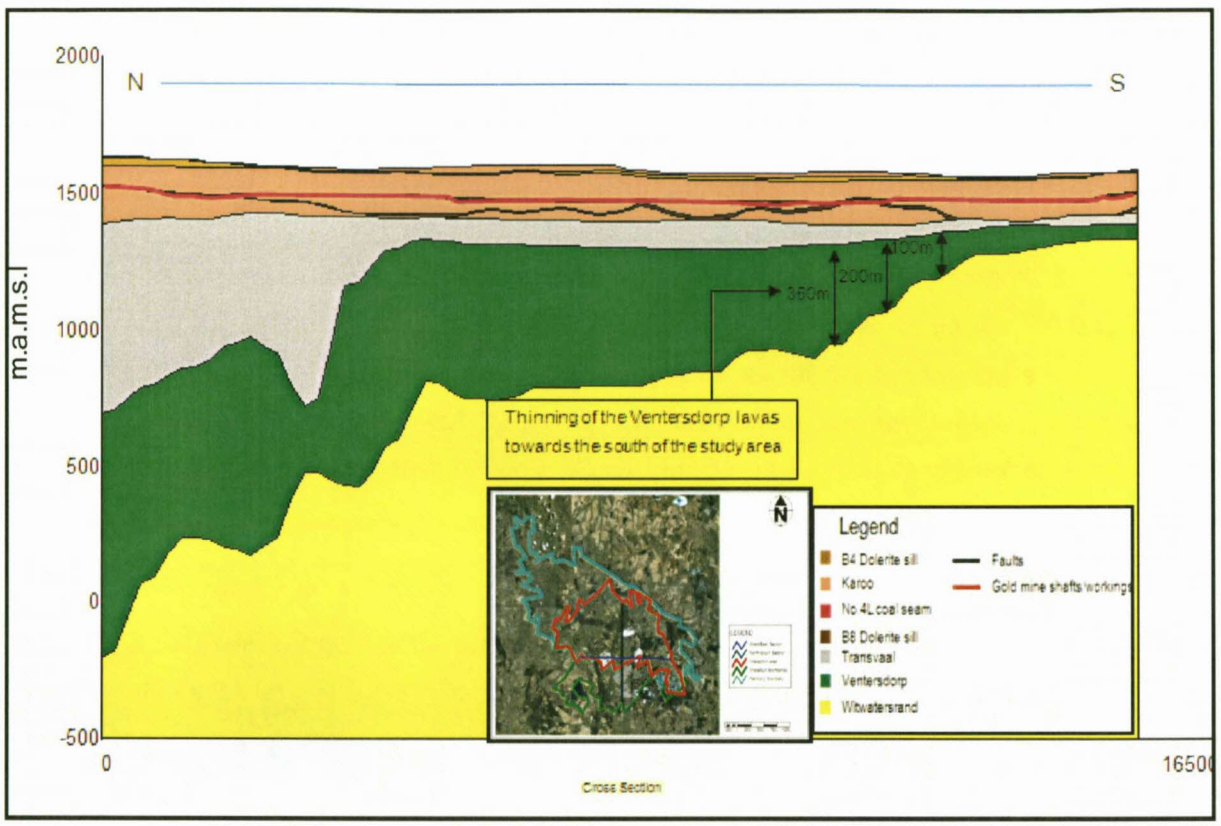

Figure 31: Thinning of the Kliprivierberg Group lavas towards the south of the study area.

4.5 Witwatersrand Supergroup

The Witwatersrand Supergroup is divided into the basal West Rand Group and the overlying Central Rand Group, which contains the auriferous gold deposits (Tweedie *et al.*, 1986). The Central Rand Group is subdivided into the lower Johannesburg Subgroup and the overlying Turfontein Subgroup. These formations predominantly consist of quartzite with subordinate lava, shale and conglomerate. The Kimberley Shale separates the two units and is marked by a basal unconformity. Immediately above this unconformity is a conglomerate layer known as the Kimberley Reef (Tweedie *et al.*, 1986).

Although the sediments of the West rand Group in the study area are poorly documented, the Jeppestown Subgroup is deemed to be missing due to the absence of the Crown Lava Formation and the polymitic greywacke development in places at the top of the Government Subgroup which appears to be very similar in lithological composition and stratigraphic position to the "Blue Grit" of the Heidelberg-Balfour area (Tweedie *et al.*, 1986).

The Central Rand Group in the Evander Goldfield comprises a composite sequence of interbedded conglomerate and non-conglomerate quartzites that averages 650 m in thickness (Tweedie *et al.*, 1986).

The Witwatersrand Supergroup is very thin by comparison with the Central Rand, a thinning of approximately 3:1 having taken place in the Evander Basin (Tweedie *et al.*, 1986). Interbedded within this sedimentary pile are two andesitic lava units, and the Kimberley shale is the only argillite present. Many of the units occurring below the Kimberley Reef are lithologically very similar to those occurring at a similar stratigraphic position in the East Rand Basin. However, above the Kimberley Reef, sediments from the Evander Basin bear no resemblance to their counterparts in the East Rand Basin. This is possibly related to their respective transport directions and provenance (Tweedie *et al.*, 1986).

4.5.1 Hospital Hill Subgroup

The Hospital Hill Subgroup is characterised by interbedded shales and quartzites. Shales are inter-grained, faintly to strongly banded and vary in color from greenish-black to maroon. Magnetic and non-magnetic varieties are present. By contrast, the quartzites are generally sub-siliceous, with fuchsite partings (Tweedie *et al.*, 1986).

4.5.2 Government Subgroup

The Government Subgroup has interbedded sequences of shales, siltstones, quartzites and polymitic greywacke. Shales are similar to those of the Hospital Hill Subgroup, but are generally less magnetic and seldom exhibit maroon colouration. The quartzites are highly variable in composition and are more argillaceous than their Hospital Hill counterparts (Tweedie *et al.*, 1986).

4.5.3 Turffontein Subgroup

The Turffontein Subgroup consists predominantly of quartzite with subordinate lava, shale and conglomerate. The Turffontein Subgroup also contains the thinly developed Kimberley Reef conglomerate, which is the primary focus for gold exploration in the area (Tweedie *et al.*, 1986

4.5.4 Johannesburg Subgroup

The Johannesburg Subgroup consists predominantly of quartzite with subordinate lava, shale and conglomerate (Tweedie *et al.*, 1986).

4.6 Basement Complex

The Complex consists mainly of Basement Schists and Basement Granites (Tweedie *et al.*, 1986). The Basement Complex was not considered in this study area as it has a great depth below the Witwatersrand and no data was available for interpretation.

4.7 Structural Geology

The Evander Basin appears to be arcuate in shape. Minor folding occurs along the eastern and western limbs of the basin. Folding in conjunction with faulting has resulted in the local overturning of the Witwatersrand sediments in some places in the study area (Tweedie *et al.*, 1986). Peripheral faults are encountered across the study area, together with an associated horst, graben and north-westerly plunging syncline to the south of the study area. The degree of faulting and structural dislocation within the study area is extremely high (Tweedie *et al.*, 1986).

A number of different fault types have been recognised by Tweedie *et al.* (1986) and these can be broadly classified as being either primary or secondary. The former are presented by the western and southern peripheral fault zones. The secondary faults comprise mostly normal faults, mainly throwing down to the south-east. Early compression tectonics and later extensional tectonics affected both the Witwatersrand and Ventersdorp Supergroups in the Evander Basin, but pre-dated the deposition of the Transvaal Supergroup and hence the Karoo Supergroup (i.e. >2500 Ma) (Tweedie *et al.*, 1986). The major faults covering the study area are shown in Figure 32.

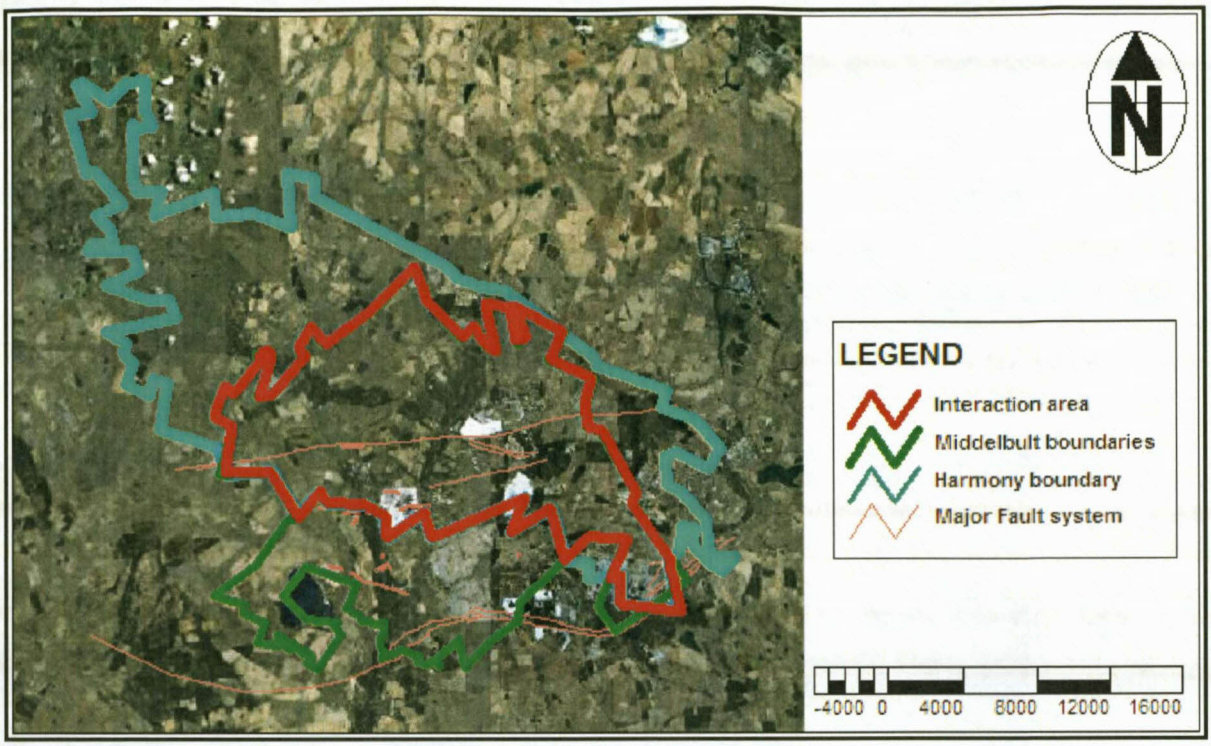

Figure 32: Major faults in the study area.

4.8 Intrusives

According to Tweedie *et al.*, (1986) the incidence and frequency of intrusives in the Witwatersrand sediments are low. This can be attributed to the following:

- Most of the faulting is of Ventersdorp age;
- A thick wedge of Ventersdorp lavas overlies much of the Witwatersrand Supergroup within the Evander Basin;
- The proximity of the Bushveld Complex;
- The degree of structural dislocation exhibited by the Witwatersrand sediments;
- The abundance of dolerite sills of Karoo age.

Three different ages of intrusives are recognised in the Evander Basin (Tweedie *et al.*, 1986):

- Karoo age intrusives;
- Ventersdorp age intrusives;
- Bushveld age intrusives.

4.8.1 Karoo age intrusives

The Karoo Supergroup sediments were invaded by two phases of post-Karoo dolerite intrusions. The oldest intrusive, namely the B4, a fine to medium crystalline dolerite, is typically a massive sill, mostly restricted to the surface, with a thickness range of 49 m to 0 m at an average of 12 m as shown in Figure 33. This sill is eroded in the lower-lying areas. The overburden thickness covering the B4 dolerite sill is shown in Figure 33.

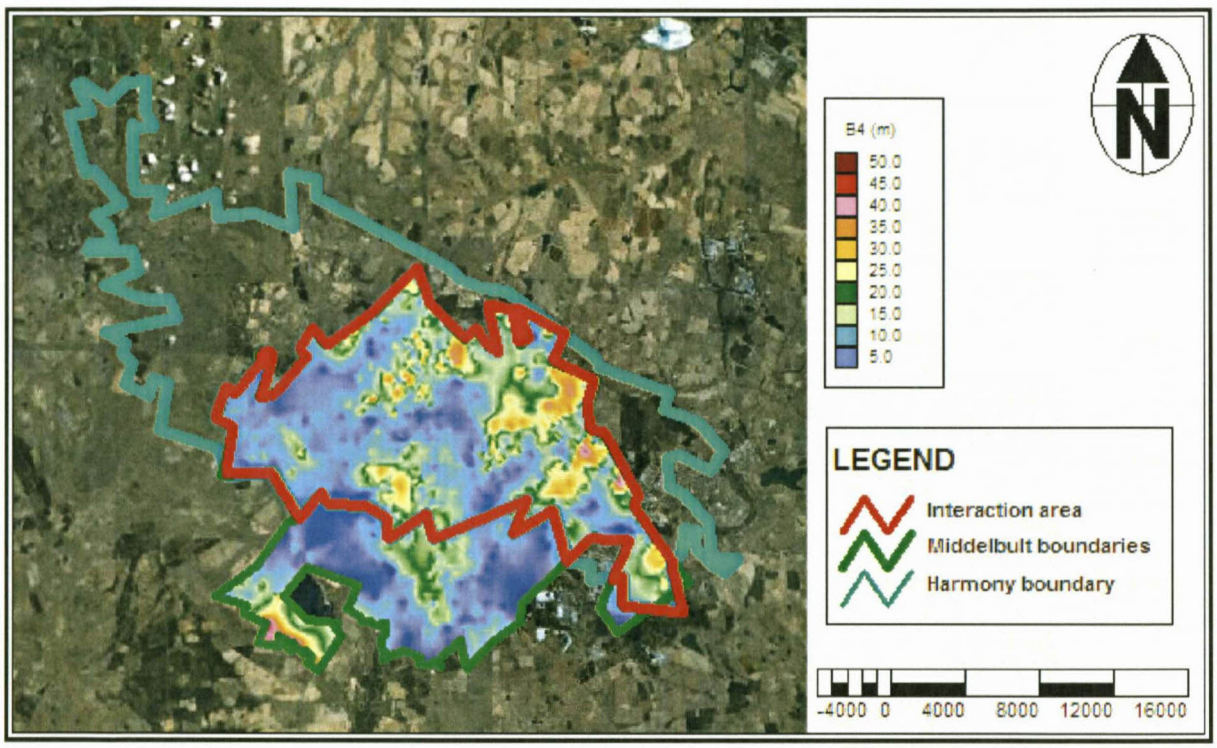

Figure 33: Interpolated thickness of the B4 dolerite sill covering the study area.

Locally, the B4 is not only surface-bound, but also transgresses the coal seams in a trough-like fashion to effectively compartmentalise these portions of the reserve on the mining horizon Jasper Muller Associates cc (2002) . Refer to Figure 23 and Figure 24.

The B8 dolerite (a fine-grained porphyritic dolerite) intruded later than the B4, along semi-planar features, with the result that it is mainly exposed as dykes, i.e. almost vertically intrusive. The B8 ranges in thickness from very thin to a maximum of 18 m. The prominent, east-west striking dyke or sub-vertical sill, separating most of the Block 8 reserve from Middelbult Colliery, can be seen to range in thickness between 7 m and 15 m Jasper Muller Associates cc (2002) . The dolerites dykes across the study area are shown in Figure 34.

The B8 sill dolerite, approximately 18 m in thickness, features near vertical off-shoots (dykes), where it transfers from one horizontal plane to another. These features occur predominantly along the planes of transference. This phenomenon results in extensive geological/ geohydrological compartmentalisation (Figure 23 and Figure 24).

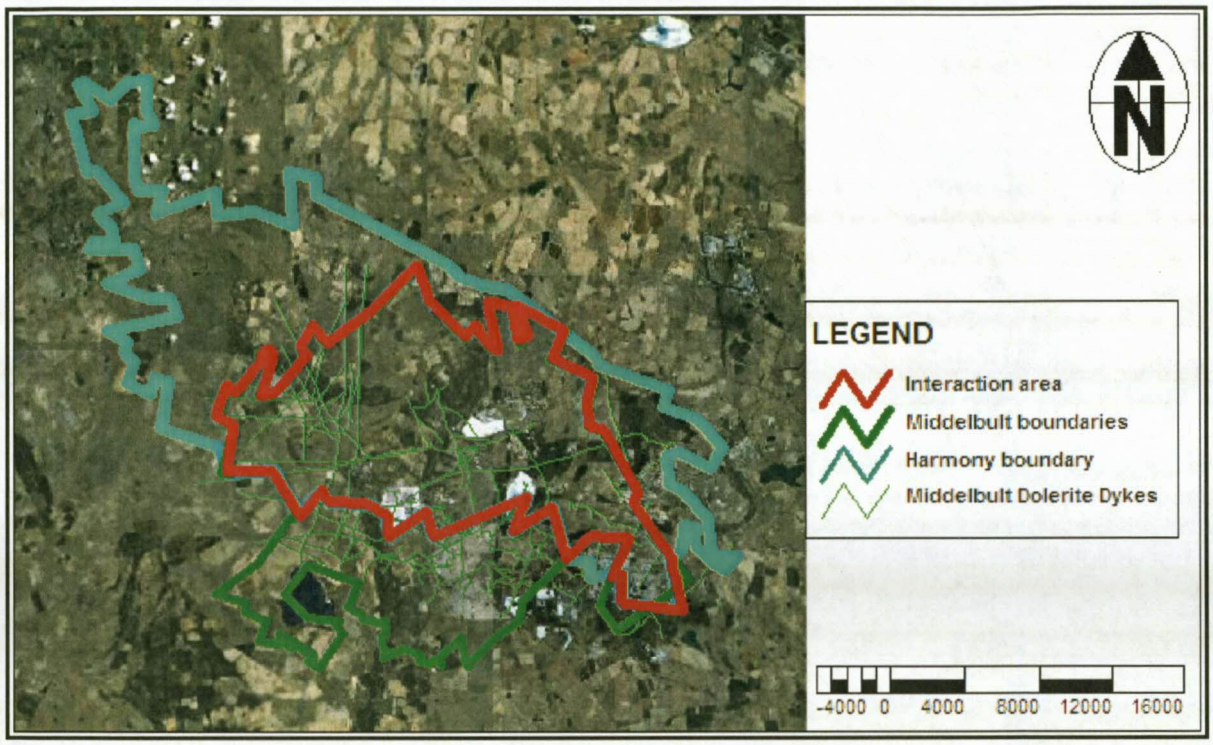

Figure 34: Surface view of the dolerite dykes in the study area.

4.9 Conceptual Model of Geology

A conceptual model of the geology was constructed using data from previous studies as well as data from the 195 exploration borehole logs received from Harmony Gold Mining (Ltd) Evander operations. The borehole logs were gathered in one Excel file and refined to be compatible with WISH (Windows Interpretation System for Hydrogeologists). WISH interpolates the Excel data by the distance weighting method to give an indication of the sub-surface geology across the study area. Through the use of cross sections the conceptual model is displayed in Figure 35. The cross sections were drawn to dissect the gold mine shafts were possible. The WISH program does not allow for the interpolation of faults and therefore they were drawn in by hand.

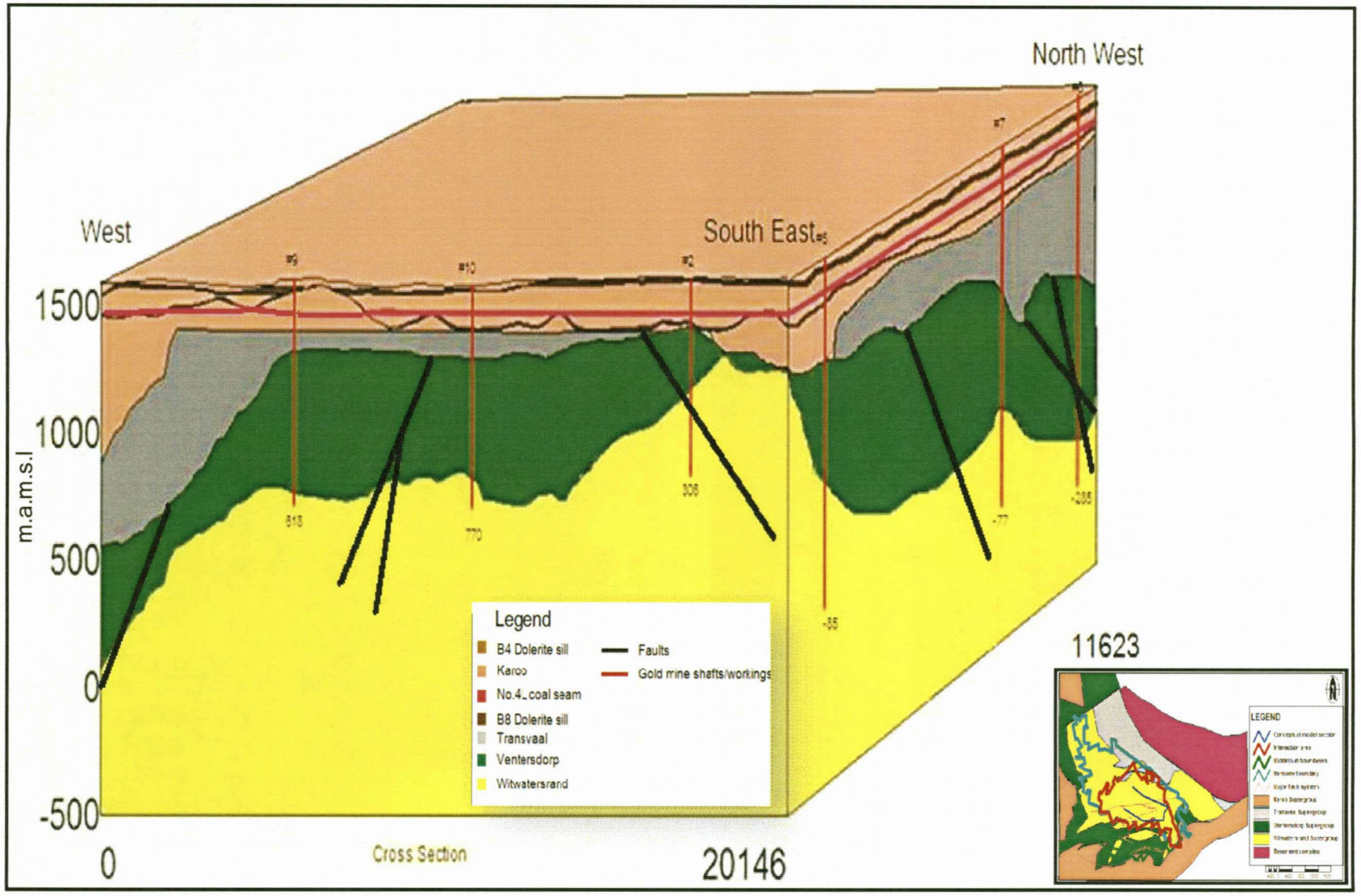

Figure 35: Conceptual model of the geology of the study area.

Chapter Five: Hydrogeology of the Study Area

5.1 Introduction

Sasol Middelbult Mine (Block 8) overlies Harmony Evander gold mining operations. There are different geological formations of different ages as discussed in Chapter 0 dividing the two mines from each other. In some of these geological formations (e.g. Karoo Supergroup), aquifer systems have developed due to their geological structure while other geological formations (e.g. Ventersdorp Supergroup) have resulted in aquiclude or impermeable layers.

Currently, there are seven different aquifer types within the study area:

- shallow perched Karoo aquifers (unconfined);
- shallow weathered zone Karoo aquifers (semi-confined);
- deep Karoo fractured aquifers (zone below the weathered zone & confined);
- coal mine artificial aquifer (confined);
- Transvaal dolomitic aquifer (confined);
- gold mine artificial aquifer (confined);
- deep Witwatersrand aquifer (confined).

Conceptually, the aquifers are displayed in Figure 36. Over the medium to long term, as mining continues, it is expected that the artificial aquifers created by coal and coal mining will expand and will cover a much larger area than currently exists.

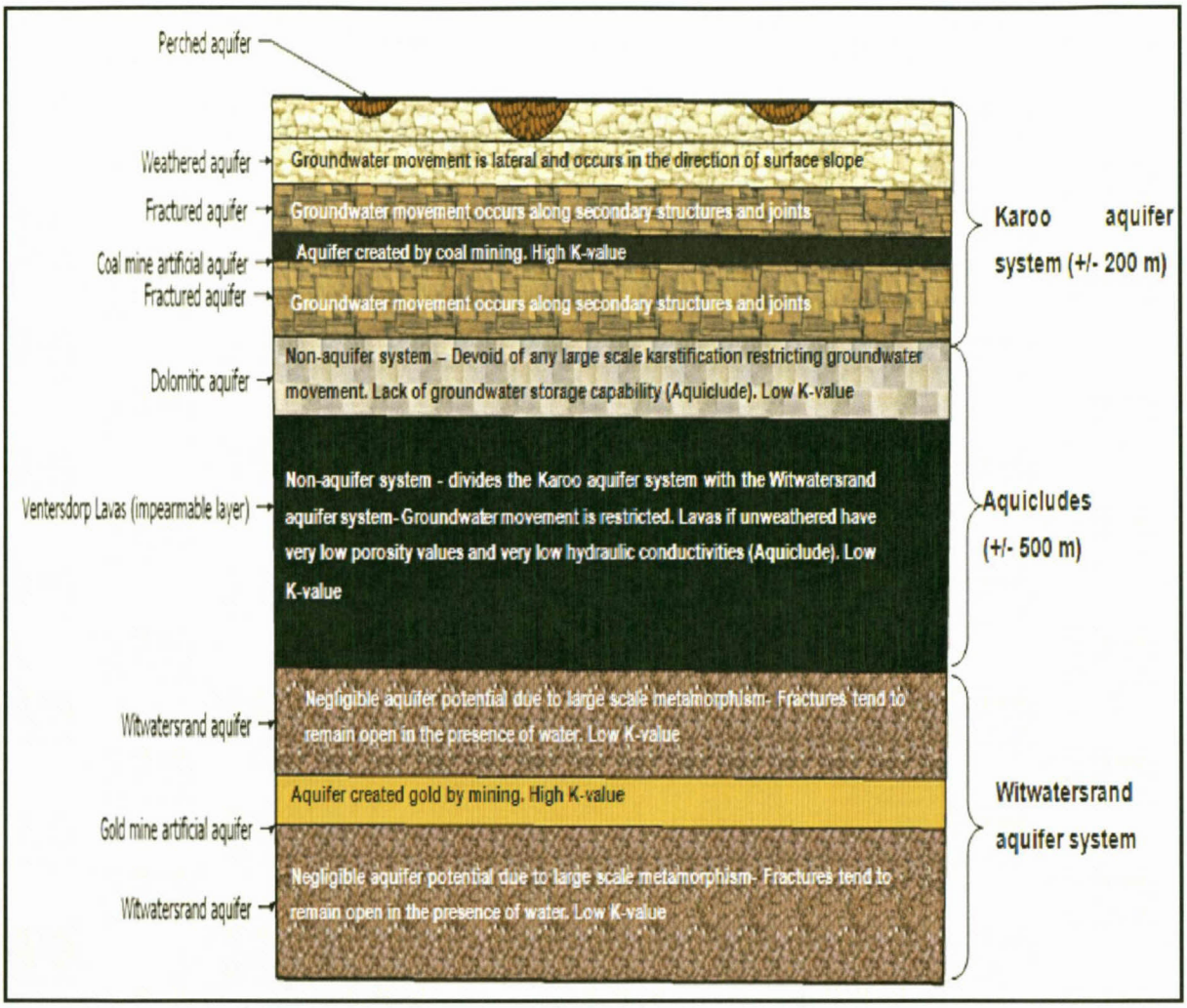

Figure 36: Conceptual model of the different aquifers in the study area (not to scale).

5.2 Aquifer Types

5.2.1 Shallow perched aquifer (unconfined)

The aquifer is characteristic of clay, colluvium alluvium and weathered sandstone. Within this unconfined (water table) aquifer, perched groundwater conditions often occur. These shallow perched aquifers are essentially restricted to the soil (soft overburden) horizon within the study area Jasper Muller Associates cc (2002) . The hydraulic conductivity value for the aquifer is estimated at $1x10^{-5}$ m/d to 0.10 m/d with an average of 0.02 m/d (Vermeulen & Dennis, 2009).

5.2.2 Shallow weathered zone Karoo aquifers (confined)

This aquifer comprises of white arenaceous sandstones located below the dolerite sheet but above the coal seam horizon. The Ecca sediments are weathered to depths between 5 to 12 m

below surface throughout the area Jasper Muller Associates cc (2002) . The upper aquifer is associated with this weathered zone and water is often found within a few metres of the surface. The hydraulic conductivity value for the aquifer is estimated at $1x10^{-6}$ m/d to $5x10^{-4}$ m/d with an average of $4x10^{-4}$ m/d (Vermeulen & Dennis, 2009).

5.2.2.1 Recharge into the shallow weathered Karoo aquifer

The main source of recharge into the shallow aquifer is rainfall that infiltrates the aquifer through the overlying unsaturated zone. Rainfall that manifests as surface run-off and drains to streams may also subsequently enter the shallow aquifer by infiltrating the stream bed (Grobbelaar, 2001). Water impoundments and features such as tailings dams may constitute additional recharge sources in certain areas.

The rainfall ultimately recharging the shallow aquifer is estimated at 3-5 % (Vermeulen & Dennis, 2009). A higher proportion of infiltration may occur in areas where the natural permeability is increased, such as the increased fracturing associated with high extraction mining. Generally accepted values for recharge in high extraction areas are between 5 % and 7 % (Vermeulen & Dennis, 2009).

5.2.3 Deeper fractured Karoo aquifers (confined)

The pores within the Karoo and more specifically the Ecca sediments are too well-cemented to allow any significant flow of water. All groundwater movement therefore occurs along secondary structures, such as fractures and joints in the sediments. These structures are better developed in competent rocks, such as sandstone, hence the better water-yielding properties of the latter rock type (Hodgson *et al.*, 1998).

It should be emphasised, however, that not all secondary structures are water-bearing. Many of these structures are constricted because of compression forces that act within the earth's crust (Hodgson *et al.*, 1998). The chances of intersecting a water-bearing fracture by drilling decrease rapidly with depth. At depths of more than 30 m, water-bearing fractures with significant yield were observed to be spaced at 100 m or greater.

Dwyka Tillite occurs at the base of the aquifer. Packer testing of the Dwyka Tillite done by Hodgson (1998) had a hydraulic conductivity distribution as indicated in Table 4 .

Table 4: Statistics for results on packer hydraulic conductivity testing of the Dwyka Tillite (Hodgson et al., 1998).

Statistics	Dwyka Permeability
Mean (m/d)	0,0034
Median (m/d)	0,0024
Standard Deviation (m/d)	0,0034
Minimum (m/d)	0,0002
Maximum (m/d)	0,0148
Number of tests	21

Due to its low hydraulic conductivity (Table 4), the Dwyka Tillite forms a hydraulic barrier (impermeable layer) between the overlying mining activities and the basal floor of the Karoo Supergroup (Hodgson *et al.*, 1998). The hydraulic conductivity value for the aquifer is estimated at $1x10^{-5}$ m/d to 0.10 m/d with an average of 0.02 m/d (Vermeulen & Dennis, 2009).The thickness of the deep aquifer depends on the depth of development of permeable zones and permeable fracture systems in relation to the water level and can extend deeper than the coal mine workings.

5.2.3.1 Recharge into the deeper Karoo fractured aquifer

Recharge of the deep Karoo aquifer occurs from the shallow Karoo aquifer through permeable fracture systems that link the two aquifers. The natural distribution of such fracture systems is highly variable, and the recharge of the deep aquifer is expected to be some orders of magnitude lower than for the shallow aquifer. However, induced fracturing associated with mining can extend from the deep aquifer up to the surface and provides a relatively direct and highly permeable recharge route. The magnitude of recharge by this route depends on the extent of mining and the nature of the induced fracture pattern (Vermeulen & Dennis, 2009).

5.2.4 Coal mine artificial aquifer (confined)

The artificial mine groundwater system associated with surrounding mined areas- the void zones where mining has taken place either by board-and-pillar, high extraction and/or long wall mining as well as subsided areas.

5.2.5 Effective Porosities/ Storage of the Karoo aquifer(s)

Twenty samples from the main sandstone unit in the Block 8 area at Middelbult were submitted for porosity testing by Jasper Muller Associates (2002) Jasper Muller Associates cc (2002) .

The results are shown in Table 5. The large range in porosity for the fine- and medium-grained sandstone is a function of the degree of pore-cementation. It also depends on the extent (depth)

of weathering. The difference in porosity between the different grain sizes of sandstone can be seen in Table 5. The storativity of the Karoo aquifer(s) was calculated at a minimum of 0.005 and a maximum of 0.07.

Table 5: Total porosity for samples taken at Block 8 Jasper Muller Associates cc (2002).

Lithological unit	Minimum (%)	Maximum (%)	Average (%)
Fine grained sandstone	0.3	9.9	4.1
Medium to coarse grained sandstone	7.7	14.4	10.1
Average for total	0.3	14.4	5.8

5.2.6 Hydraulic conductivity of the Karoo aquifer(s)

Slug tests were performed by Jasper Muller Associates (2002) in 13 of the 30 m deep shallow boreholes and 14 of the deep boreholes, ranging in depth between 80 and 150 m, to determine the hydraulic conductivity distribution within the saturated Karoo aquifers Jasper Muller Associates cc (2002) .

Statistical analyses of packer tests, conducted at different depths in three of the deep boreholes yielded the following results Jasper Muller Associates cc (2002) :

- A mean hydraulic conductivity of 4.3×10^{-3} m/d was calculated for fresh sandstone/siltstone intervals.
- A hydraulic conductivity of 1.56×10^{-2} m/d was calculated for the 4 m fresh to slightly jointed B4 dolerite test section (30-34 m).
- A hydraulic conductivity of 0.573 m/d was calculated for the 4 m (fine-grained sandstone) test section (60-64 m) across a water intersection.

Statistical assessment of hydraulic conductivities in South African hard rock aquifers indicate the actual K-values to be somewhere between the geometric and harmonic mean Jasper Muller Associates cc (2002) . A K-value of 0.02 m/d is therefore proposed as realistic for the shallow weathered Karoo aquifers at Block 8, while a value of 5×10^{-4} m/d is proposed for the deeper fractured Karoo aquifers Jasper Muller Associates cc (2002).

5.2.7 Transvaal dolomitic aquifer (confined)

The Transvaal dolomitic aquifer is an aquifer that comprises the dolomitic formation that underlies the Karoo rocks. The Karoo Supergroup has acted as a buffer to absorb weathering events, and this prevented the development of any large scale karstification in the study area's dolomites and its associated groundwater storage capacity. Furthermore, pre-Karoo glaciations stripped out old karst scenery (Tweedie *et al.*, 1986). As there is no or very little karstification in the dolomites, the porosity and hydraulic conductivity values of the aquifer are very low (Figure

37 and Figure 38). Kruseman & De Ridder (1994) estimated that the Transvaal dolomitic aquifer without karstification would have an effective porosity value of between 0 and 10 % and a hydraulic conductivity value of 10 x 10^{-5} m/s to 10 x 10^{-10} m/s (Figure 37 and Figure 38) and Table 6 (Kruseman & De Ridder, 1994).

Few of the local farmers, if any, tap water from the aquifer beneath the Dwyka Formation Jasper Muller Associates cc (2002) . The reasons for this, as stated by Van der Berg (2002) are:

- The great depth;
- Low-yielding character of the fractures;
- Inferior water quality, with high levels of fluoride, associated with granitic rocks;
- Low recharge characteristics of this aquifer because of the overlying impermeable Dwyka Tillite.

The weathered zone near the surface of the dolomitic members of the Olifants River Group has the highest groundwater potential in the area. However this is limited in extent (McKnight Geotechnical Consulting, 2002). Previous studies have shown that the level of karstification is negligible in the study area and as a result the hydraulic conductivity of the dolomite is greatly reduced (Tweedie *et al.*, 1986) Therefore, this aquifer can be regarded as insignificant as an aquifer system in this specific study area. It is more likely to act as an aquiclude.

5.2.8 Gold mine artificial aquifer (confined)

The aquifer is overlain by the thick Ventersdorp Supergroup with its very low hydraulic conductivity value resulting in it confining the Witwatersrand aquifer (Figure 29). Extensive footwall development (haulages, cross-cuts, ore passes) for ore collection has allowed for an artificial aquifer being created within the Witwatersrand that has a much higher hydraulic conductivity value than the naturally occurring Witwatersrand aquifer surrounding it.

5.2.9 Deep Witwatersrand aquifer (confined)

The Witwatersrand aquifer occurs in siliceous sediments at the base of a thick, clastic sedimentary sequence. The primary porosities of the sandstone sediments have been destroyed by metamorphism, with the effect that the resultant quartzites are essentially impermeable due to the precipitation of secondary quartz. However, the arenaceous members of the Supergroup are structurally competent and fractures tend to remain open in the presence of water (McKnight Geotechnical Consulting *et al.*, 2002). The aquifer is overlain by the thick Ventersdorp

Supergroup (aquiclude) with its very low hydraulic conductivity value resulting in it confining the Witwatersrand aquifer (Figure 29).

5.2.9.1 Recharge into the deep Witwatersrand aquifer

Groundwater is encountered within the gold mine workings of the Witwatersrand Supergroup, the origin of which is thought to be a mixture of paleo-meteoric water, 2.0-2.3 (Ga) hydrothermal fluid, connate water trapped in the Witwatersrand sediments during their deposition (Onstott *et al.*, 2006) and influx from shallower aquifers. The paleo-meteoric water and 2.0-2.3 (Ga) hydrothermal fluid of the Witwatersrand is thought to be finite within the Evander Basin and therefore it could be exhausted (Rison Groundwater Consulting, 2007).

Recharge into the gold mine workings is thus influx from the shallow Karoo aquifer through permeable fracture systems that link the two aquifers from the base of the Karoo aquifer into the Witwatersrand aquifer where the Witwatersrand sub-outcrops against Karoo Supergroup or where preferential paths through the Ventersdorp Supergroup intersect the gold mine. The natural distribution of the fracture systems and preferential flow paths is highly variable, and the recharge of the deep aquifer is expected to be lower than for the shallower Karoo aquifer (1-3 %) or (5-7%) where subsidence has induced fractures (Vermeulen & Dennis, 2009). However, induced fracturing or preferential flow paths associated with mining can extend from the deep Witwatersrand aquifer up to the Karoo aquifer and provide a relatively direct and highly permeable recharge route (Cook, 2003). The magnitude of recharge by this route depends on the extent of mining and the nature of the induced fracture or preferential flow paths. Both of these are the exception rather than the norm in the study area. The rate of recharge is therefore estimated at less than 1 % of annual precipitation. The rate of recharge calculated from the rate of inflow in the Witwatersrand aquifer (Table 15) was calculated at 0.5 % if the Evander Basin's surface extent is used as the recharge area (Figure 17).

5.2.10 Effective porosities/ storage of the Witwatersrand aquifer(s)

Based on work done by Kruseman & De Ridder (1994) the effective porosities of the Witwatersrand quartzites are a minimum of 0 to 5 %. The storativity value of the Witwatersrand aquifer was calculated at 1.3×10^{-6} (Du Preez *et al.*, 2007).

5.2.11 Hydraulic Conductivity for the Witwatersrand aquifer

The hydraulic conductivity value for the Witwatersrand aquifer is very low due to metamorphism of sedimentary rocks, which is estimated at 1×10^{-14} m/s to 1×10^{-11} m/s (Kruseman & De Ridder, 1994).

5.2.12 Summary of aquifers

There is dynamic interaction between the aquifers situated in the upper Karoo Supergroup as there is a direct link with recharge from precipitation into the shallow perched aquifer and the shallow weathered aquifer. This water then flows through preferential pathways (fractures) from these aquifers into the deeper artificial coal mine aquifer and fractured Karoo aquifer. Therefore the deeper Karoo aquifer is not directly recharged by precipitation but by influx from shallower Karoo aquifers through preferential pathways naturally at a rate of 1 to 3% or by induced fracturing resulting from subsidence at a rate of 5 to 7% of recharge. The water is prevented from moving further downward at the base of the Karoo Supergroup by the Dwyka Tillite, and further down by the Transvaal dolomites and the Ventersdorp Supergroup lavas that separate the Karoo aquifer affected by coal mining from the Witwatersrand aquifer affected by gold mining. The reason for the groundwater is due to the named layers low very low hydraulic conductivities (Kruseman & De Ridder, 1994).

Therefore, recharge into the Witwatersrand aquifer can only occur where the Witwatersrand aquifer sub-outcrops against the Karoo Supergroup and if preferential pathways exist connecting the Witwatersrand aquifer with the Karoo aquifer through the Ventersdorp Supergroup and Transvaal Supergroup. Some of the water in Witwatersrand aquifer could be a mixture of paleo-meteoric water and 2.0-2.3 (Ga) hydrothermal fluid or connate water trapped in the Witwatersrand sediments during their deposition (Onstott *et al.*, 2006). The source of this water is thought to be finite within the Evander Basin and it could therefore be exhausted (Rison Groundwater Consulting, 2007).

All recharge into the Witwatersrand aquifer is thus flux from preferential pathways connecting the shallower lying Karoo aquifers, as no direct precipitation will recharge the Witwatersrand aquifer or paleo-meteoric water from the Witwatersrand sediments. If no direct preferential pathways exist, the influx will be relatively slow through the sub-surface and will be much less than the recharge of 1-3 % in the Karoo aquifer and will be expected to be less than 1 % of annual precipitation.

For the purposes of this study, the Karoo aquifers were regarded as one significant aquifer situated above the Ventersdorp Supergroup and the deeper Witwatersrand aquifer situated below the Ventersdorp Supergroup (refer to Figure 36).

Thus there are two major aquifers dominating the geohydrology of the study area namely:

- the Karoo aquifer (unconfined to confined),

- the deeper Witwatersrand aquifer (confined).

The shallower Karoo aquifer is regarded as an unconfined to confined aquifer and its recharge can be linked directly to recharge by precipitation (1-3 % of annual precipitation and 5-7 % where high extraction mining has occurred). The deeper Witwatersrand aquifer is regarded as a confined aquifer that has no direct link of recharge to precipitation and has a very low flux from shallower Karoo aquifers though preferential pathways or where the Witwatersrand Supergroup sub-outcrops against the base of the Karoo Supergroup (>1 % of annual precipitation).

Table 6: Summary of the aquifer parameters within the study area (Vermeulen & Dennis, 2009; Kruseman & De Ridder, 1994).

Supergroup	Aquifer	Recharge %	Hydraulic conductivity (m/d)		Effective Porosity %(n)		Storativity (Ss)	
Karoo Supergroup			Min.	Max.	Min.	Max.	Min.	Max.
	Perched aquifer)	5	$1x10^{-5}$	$5x10^{-4}$	0.3	9.9	0.01	0.07
	Weathered aquifer/ Fractured aquifer	3-5	$1x10^{-6}$	0.1	7.7	14.4	0	0.005
	Goaf	< 5	0.5	5				
	Coal Seam (Before mined)	3-5	$1x10^{-6}$	$1x10^{-4}$	0	10	0.001	0.01
			Hydraulic conductivity (m/s)					
Transvaal Supergroup	Dolomites (Aquiclude)	3	$1x10^{-6}$	$1x10^{-0.5}$	0	50	0	$1x10^{-6}$
Ventersdorp Supergroup	Ventersdorp lavas (Aquiclude)	>1	$1x10^{-11}$	$1x10^{-6}$	0	0	0.1	$1x10^{-6}$
Witwatersrand Supergroup	Witwatersrand aquifer	>1	$1x10^{-14}$	$1x10^{-11}$	0	5	0	$1.3x10^{-6}$

5.3 Aquicludes/Impermeable layers

5.3.1 Karoo Supergroup (Aquicludes)

The thick shale successions within the Karoo Supergroup, the dolerite sills (K-value: 8.64 x 10^{-10} m/d) that are extensive over the area and the Dwyka Tillite (K-value: 0.0034 m/d) are all low hydraulic conductivity to impermeable zones that may reduce the recharge to the underlying aquifers (Hodgson *et al.*, 1998).

5.3.2 Transvaal Supergroup (Aquiclude)

The Karoo Supergroup has acted as a buffer to absorb weathering events; this prevented the development of any large-scale karstification in the study area's dolomites and its associated groundwater storage capacity. Furthermore, pre-Karoo glaciations have stripped out the old

karst scenery (Tweedie *et al.*, 1986). As there is little or no karstification in the dolomites, the porosity and hydraulic conductivity values of the aquifer are very low (Figure 37 and Figure 38). Kruseman & De Ridder, (1994) estimated that the Transvaal dolomitic aquifer without karstification will have an effective porosity value of between 0 and 10 and a hydraulic conductivity value of 10×10^{-5} to 10×10^{-10} m/s, as shown in Figure 37, Figure 38 and Table 6.

5.3.3 Ventersdorp Supergroup (Aquiclude)

The Ventersdorp lava in the study area is part of the Klipriviersberg lavas that were deposited as a flood basalt seqeunce (Tweedie *et al.*, 1986). Basalts if unweathered, as in the case of the study area, have very low porosity values and very low hydraulic conductivity values, as shown in Figure 37 and Figure 38 (Kruseman & De Ridder, 1994). Through the geological logs interpreted, it does not appear as if the Ventersdorp Supergroup is permeable (weathered or extensively fractured) and therefore the hydraulic conductivity value for the Ventersdorp lavas of the study area can be regarded as 1×10^{-7} to 1×10^{-8} m/s (Kruseman & De Ridder, 1994).

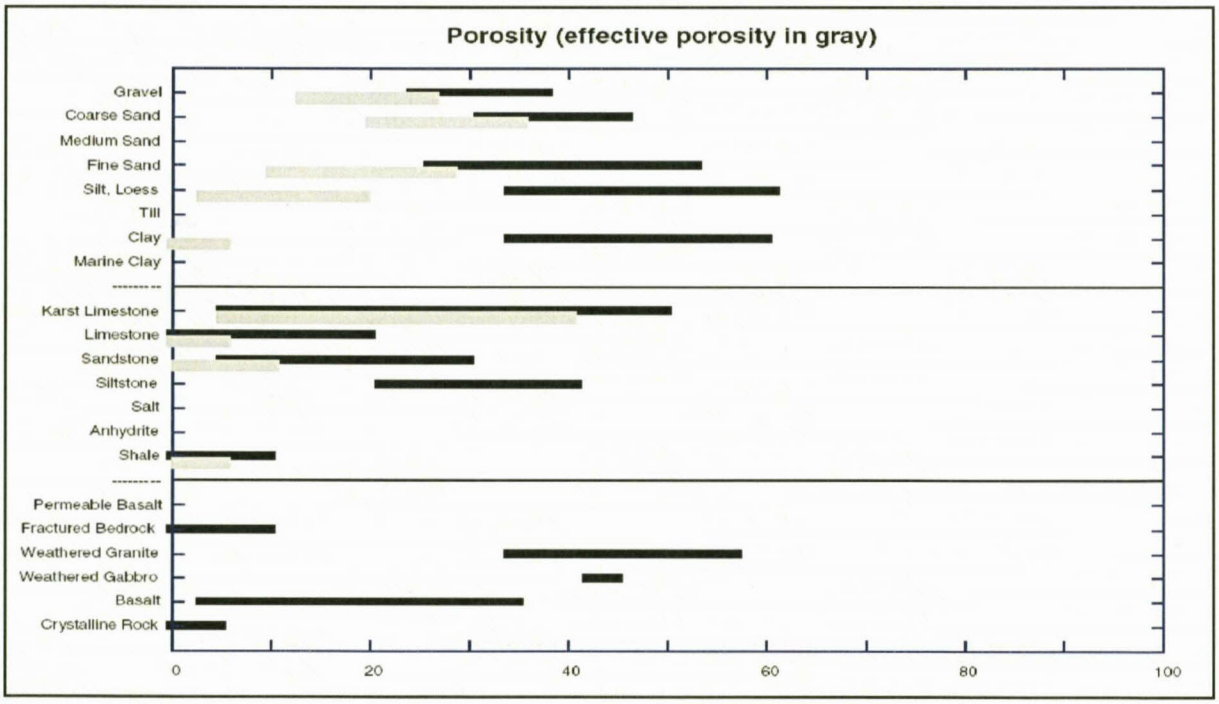

Figure 37: Porosity values of selected rock types (Kruseman & De Ridder, 1994).

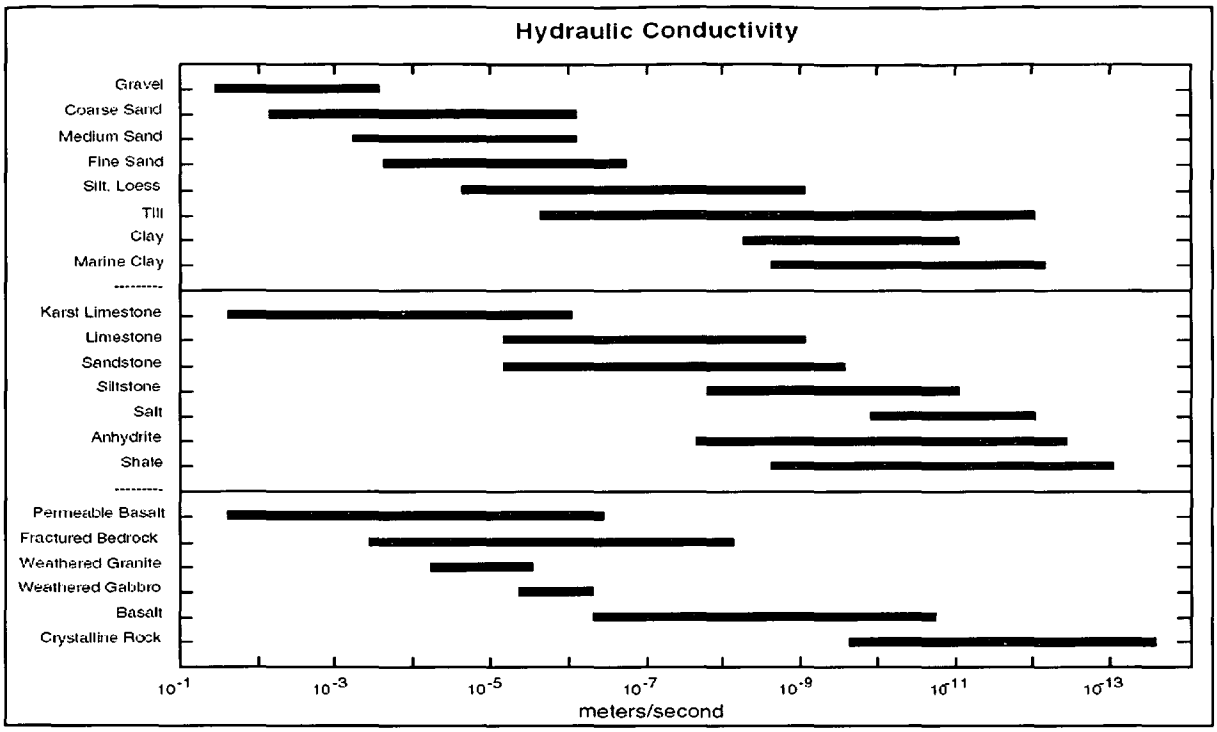

Figure 38: Hydraulic conductivity values of selected rock types (Kruseman & De Ridder, 1994).

The presence of the Ventersdorp lava is a critical issue, since it was found at other, similar mines in the West rand Basin that groundwater inflow from the overlying aquifers is more pronounced in areas where the lava is absent (Rison Groundwater Consulting, 2007).

Throughout the study area, the Ventersdorp lavas have a variable thickness (Figure 39), which is partly attributed to the faulting in the area (Tweedie *et al.*, 1986). Important to note is that for most of the study area the Ventersdorp Supergroup mantles the Witwatersrand Supergroup, with the exception of the south-southeastern boundary of the interaction area, where the Ventersdorp lavas are either very thin or non-existing (refer to Figure 30 and Figure 31). This effectively means that the Ventersdorp lavas in most parts of the study area form an aquiclude, restricting downward groundwater movement from the shallower Karoo aquifers towards the deeper Witwatersrand aquifer.

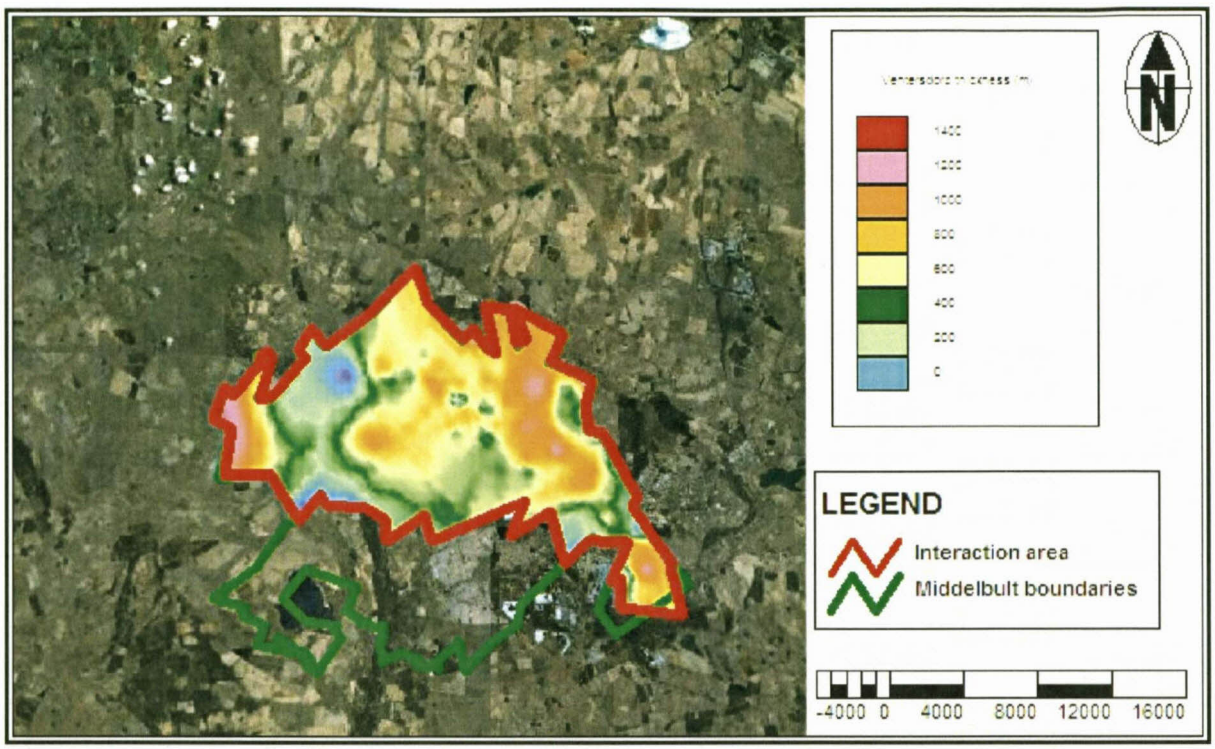

Figure 39: Ventersdorp thickness in the study area.

5.4 Preferential flow paths

5.4.1 Introduction

Preferential flow refers to the uneven and often rapid movement of water through subsurface media, giving rise to heterogeneous conditions. This occurs in both the unsaturated and saturated zones. Preferential flow paths can play a dominating role in the movement of water and contaminants in the sub-surface (Cook, 2003). Figure 40 shows the relationship of fracture aperture, fracture spacing and aquifer hydraulic conductivity, for an aquifer consisting of planar, parallel uniform fractures (Cook, 2003). It indicates the wider and more frequent the preferential pathways the higher the flow of water through a layer. As the coal mine lies above the gold mine, the preferential pathways connecting the two mines will allow for flow from the coal mine towards the deeper lying gold mine.

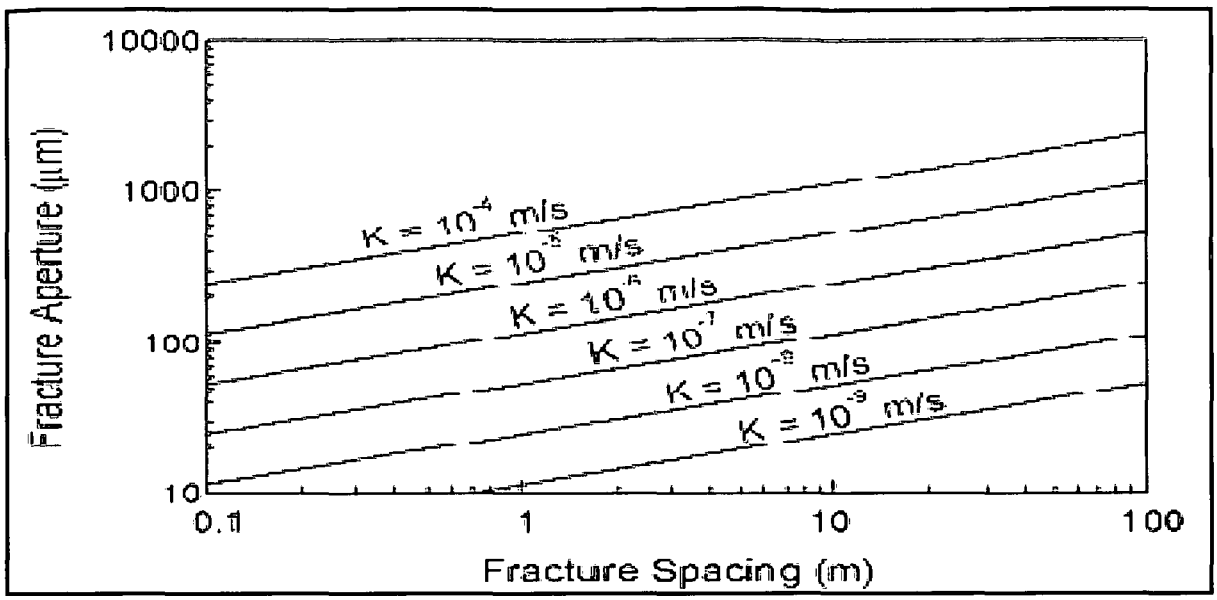

Figure 40: Relationship between fracture aperture, fracture spacing and aquifer hydraulic conductivity, for an aquifer consisting of planar, parallel uniform fractures (Cook, 2003).

In the study area some preferential flow are encountered. These flow paths may connect the shallow Karoo aquifer with the deeper Witwatersrand aquifer though the Ventersdorp Supergroup lavas. These pathways could have resulted from geological processes (faults/fractures) or from mining activities (shafts/exploration boreholes).

5.4.2 Geological preferential flow paths

5.4.2.1 Fissures/Joints and Fractures (cracks)

Fissures/joints and fractures are planes along which stress has caused partial loss of cohesion in the rock. Conventionally, a fracture or joint is defined as a plane where there is hardly any visible movement parallel to the surface of the fracture (Cook, 2003).

Dykes can either be barriers or conductors for groundwater flow. How the dykes act depends on their trends in relation to their hydraulic gradient and the density of the fracture system in the dykes (Cook, 2003). Due to thermal effects, dykes can also cause fracturing of adjacent to rock. Pumping tests indicate that dykes that are thicker than 10 m serve as groundwater barriers, but those of smaller width are permeable, as they develop cooling joints and fractures (Kruseman & De Ridder, 1994). Sills are nearly horizontal tabular bodies that commonly follow the bedding of enclosing sedimentary rocks or lava flows. Some of the sills are very thick and extend over large areas. Due to their low permeability, except when fractured, sills may support perched water bodies. Groundwater flow next to dykes is controlled by two kinds of fractures, namely, vertical

and sub-vertical fractures with recharge occurring along these vertical fractures (Kruseman & De Ridder, 1994).

In the study, only one water-bearing fracture in the gold mine (Table 7) next to a dyke was encountered at Evander No. 8 shaft, 11 level approximately 1340 m below surface, as shown in Figure 41. Early reports from the mines indicated that water- bearing fissures/fractures run dry rapidly, suggesting a poorly connected fracture system and a lack of recharge (Rison Groundwater Consulting, 2007).

The other water- bearing fractures (Table 7) were from the gold mine roof, which resulted from planes along which stress has occurred causing a partial loss of cohesion in the rock and allowing water to flow in these planes.

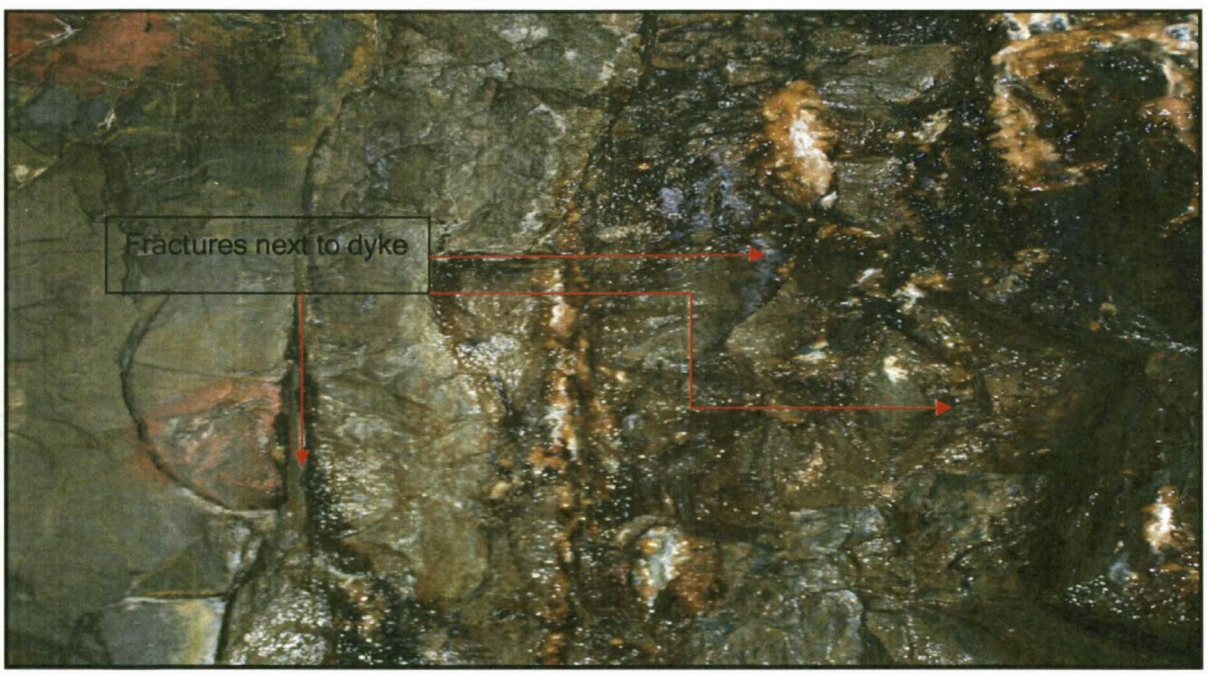

Figure 41: Fractures next to dyke with water at Harmony Evander No. 8 shaft 11 level (1340 m below surface).

5.4.2.2 Faults

Faulting affected both the Witwatersrand and the Ventersdorp Supergroups in the study area, but pre-dated the deposition of the Transvaal Supergroup (>2500 Ma) and the Karoo Supergroup (Tweedie *et al.,* 1986). This was also highlighted in previous investigations of the Rolspruit and Poplar Project areas (McKnight Geotechnical Consulting *et al.*, 2002). McKnight Geotechnical Consulting Geotechnical Consulting (2002) also concluded that there are no major displacements in the unconformity above the Black Reef Formation. In addition, McKnight

Geotechnical Consulting (2002) also concluded that the majority of the faults are under compression and tight, meaning that the faults are most likely not conduits for groundwater flow. In the study, two faults bearing water (Table 7) were encountered. They were at Evander No. 8 shaft, 11 level, 1340 m below surface (Figure 42) and at Evander No. 8 shaft, 18 level, 1830 m below surface.

Figure 42: Fault bearing water at Harmony Evander No. 8 shaft 11 level (1340 m below surface).

5.4.3 Mining activities

5.4.3.1 Shafts

The deep level gold mining shafts have been cemented to significant depths (Leslie Mine EMPR, 1994). If cracks occur within the cementation of the shafts, the shafts may act as preferential flow paths for groundwater flow, connecting the shallower Karoo aquifer affected by

coal mining to the deeper lying Witwatersrand aquifer affected by gold mining. The positions of the gold mine shafts are shown in Figure 43.

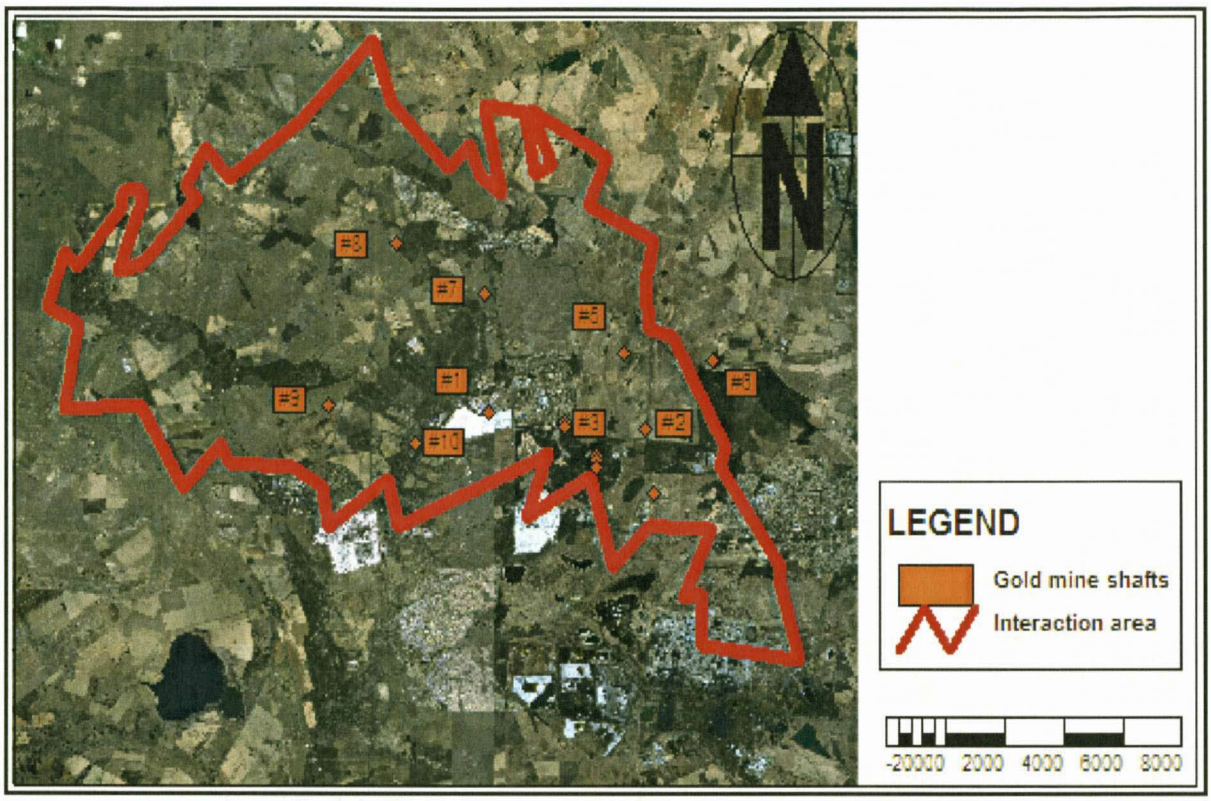

Figure 43: Gold mine shaft positions.

5.4.3.2 Exploration boreholes

Exploration boreholes intersecting the Karoo aquifer will act as preferential flow paths for groundwater flow to the Witwatersrand aquifer if left unsealed. There are numerous exploration boreholes covering the study area. The exploration boreholes with full geological logs are shown in Figure 18. In this study, one water-bearing exploration borehole was found at No. 8 shaft, 15 level, 1620 m below ground level (Table 7). The movement of water from the surface downward will be more rapid than in faults or fractures, as the exploration boreholes are drilled virtually vertically in to the sub-surface, whereas faults and fractures are at different angles.

Table 7: Preferential flow paths encountered in the study area.

Harmony samples	Depth in m below surface	Level	Shaft or position	Preferential flow paths encountered in study
H1	1340	11	8	Water from fault
H2	1340	11	8	Water next to dyke
H3	1620	15	8	Water from exploration borehole
H4	1830	18	8	Water from fault
H5	2152	24	8	Water dripping from roof stope
H6	282	1	9	Water dripping out of mine roof (minimal)
H7	282	1	9	Water dripping out of mine roof (minimal)
H10	634	8	2	Water dripping out of mine roof (minimal)
Sasol samples	**Depth in m below surface**	**Level**	**Shaft or position**	**Description**
S1	104	In coal mine	Near Main shaft	Borehole into mine workings
S2	113	In coal mine	Near North Shaft	Water dripping out of mine roof (minimal)
S3	105	In coal mine	Block 38	Fissure water from mine floor
S4	80	In coal mine	Near West shaft	Water dripping out of mine roof (minimal)
S5	55	In coal mine	Block 35	Water dripping out of mine roof (minimal)
All were physically located and verified. These are the only pathways found in this study				

5.5 Water levels

As there are different aquifers (unconfined to confined) in the study area, there are different water levels, with the unconfined to confined. When a confined aquifer is intersected by a borehole or a shaft, the water level in the borehole or shaft will rise and become a piezometric level. This level will always try to come into equilibrium with the atmosphere or the piezometric surface (piezometric surface = atmospheric pressure = 0). The piezometric surface is the hypothetical surface of the hydraulic head in a confined or semi-confined aquifer (Freeze & Cherry, 1979). The different water levels or piezometric levels within the aquifers will be discussed separately.

5.5.1 Karoo aquifer water levels

More than 240 shallow Karoo aquifer boreholes have been drilled across the study area in the vicinity of the mines. The positions of the boreholes are shown in Figure 44. The groundwater level is on average 3.9 m below surface, with a range of 0 to 69.6 m below surface.

In order to visualise the Karoo groundwater flow for the area, a water level contour map must be generated. Although groundwater does not occur across over the entire study area, it gives a good visualisation tool to interpret the general direction of groundwater flow and levels. An interpolation technique, using the available data, was used to simulate groundwater levels over the entire study area. The interpolation technique used is referred to as Bayesian interpolation,

where water levels are correlated with the surface topography. All available water levels were plotted against topography, shown in Figure 45. The results indicate a correlation of 97 % between the data sets. Therefore, Bayesian interpolation was valid and used to calculate water levels for the entire study area. The interpolated water levels are shown in Figure 46.

It is important to note that the Karoo aquifers have not been affected by the past 50 years of gold mining in the region, although large volumes of water have been pumped from the gold mines (Rison Groundwater Consulting, 2007). This suggests a poor hydraulic connectivity from the Karoo aquifer to the gold mine workings situated in the Witwatersrand aquifer, although some dewatering of the Karoo aquifer has been observed in the vicinity of the Middelbult Colliery high extraction panels, located to the south of the study area (Middelbult Mine: Block 8 Expansion EMPR, 2003). To some extent, dewatering of this aquifer has occurred because of the pumping in the gold mine. Here, the piezometric pressure in the deep Karoo aquifer is generally 10 to 50 m lower than that in the Karoo sediments (Hodgson *et al.*, 1998).

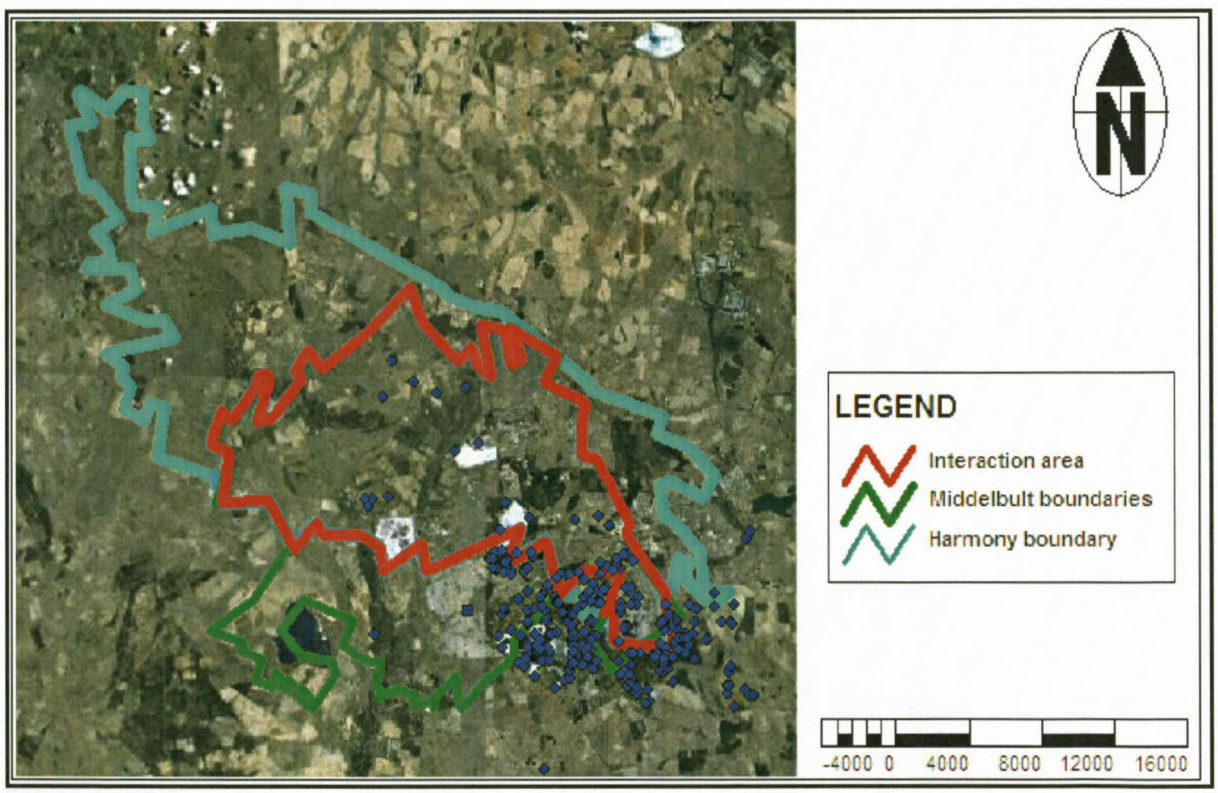

Figure 44: Karoo aquifer water levels.

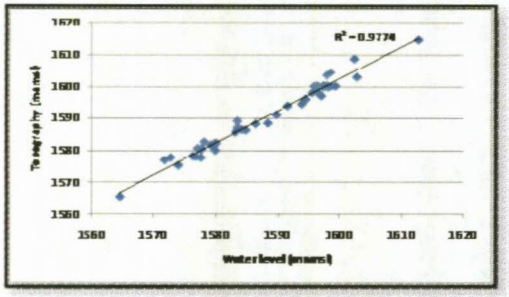

Figure 45: Correlation of the interpolated water levels with surface topography.

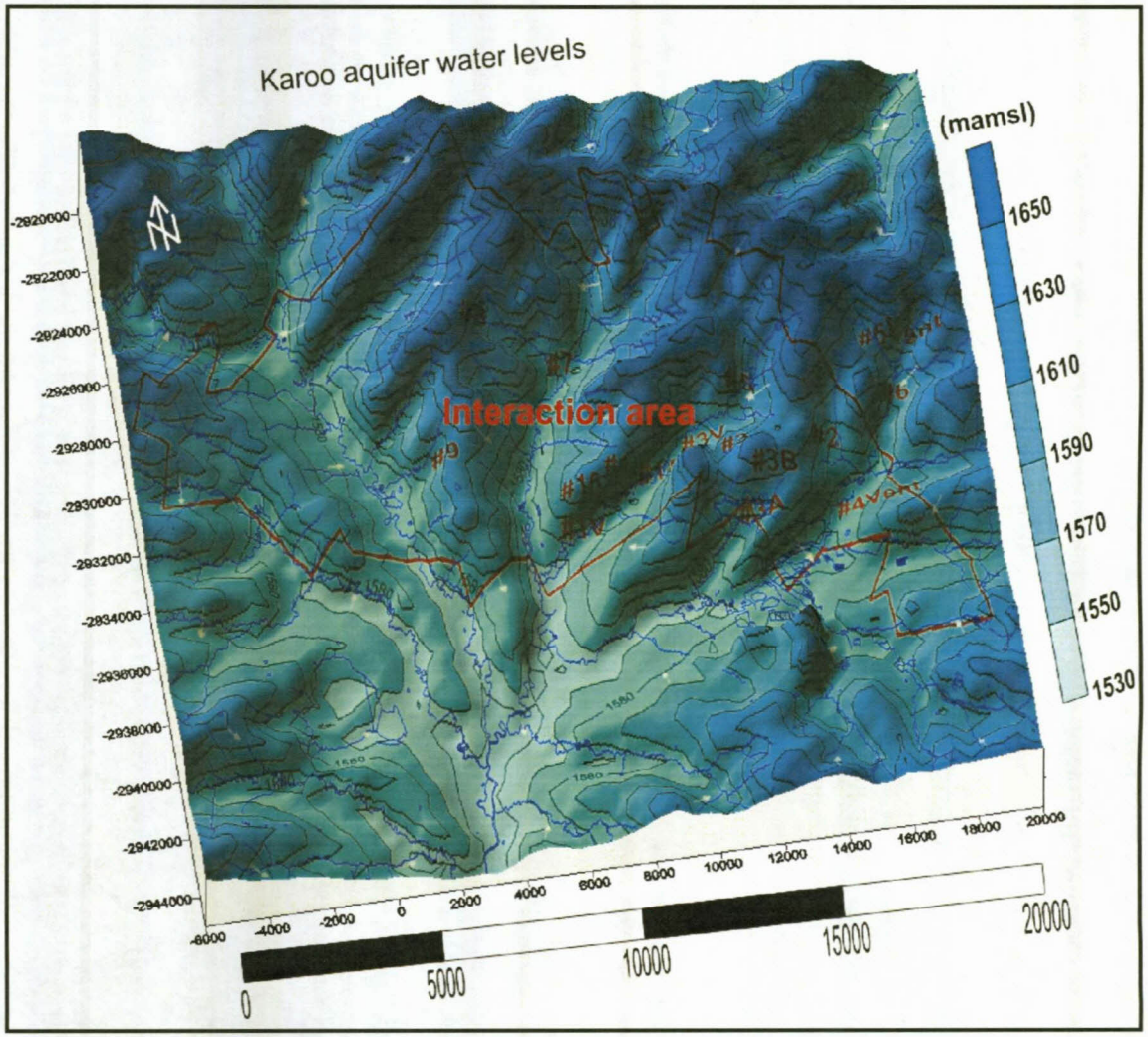

Figure 46: Interpolated groundwater elevation map for the Karoo aquifer water levels (Bayesian interpolation).

5.5.2 Witwatersrand aquifer groundwater levels

The Witwatersrand aquifer groundwater levels were found to be much more difficult to interpret compared to the Karoo aquifer water levels. The reasons for this are:

- The great depth of the Witwatersrand aquifer;
- The pumping of groundwater from the underground gold mine workings to the surface, lowering the water levels within the aquifer.

As no physical measurements of groundwater levels in the Witwatersrand aquifer were taken in this study, the interpretations were based on previous data and reports, and on communications with Harmony's environmental and geological department. The available groundwater levels are displayed in Table 8.

Table 8: Available water levels for the Witwatersrand aquifer.

Gold mine shaft name	Water levels		
	Shaft level	Metres above mean sea level	Metres below surface
Shaft No.1	not available	not available	not available
Shaft No.2	22	-143	1763
Shaft No.3	not available	not available	not available
Shaft No.5	22	-62	1682
Shaft No.6	9	925	701
Shaft No.7	22	-497	2101
Shaft No.8	22	-466	2070
Shaft No.9	not available	not available	not available
Shaft No.10	8	853	736

The first recorded Witwatersrand aquifer water level was measured at 1533 m.a.m.s.l. by Pritchard-Davies (1962). Important to note is that this water level elevation is within the Karoo

Supergroup formation, just above the No. 4L coal seam roof, which ranges from 1450 m.a.m.s.l. to 1521 m.a.m.s.l, at an average of 1490 m.a.m.s.l.

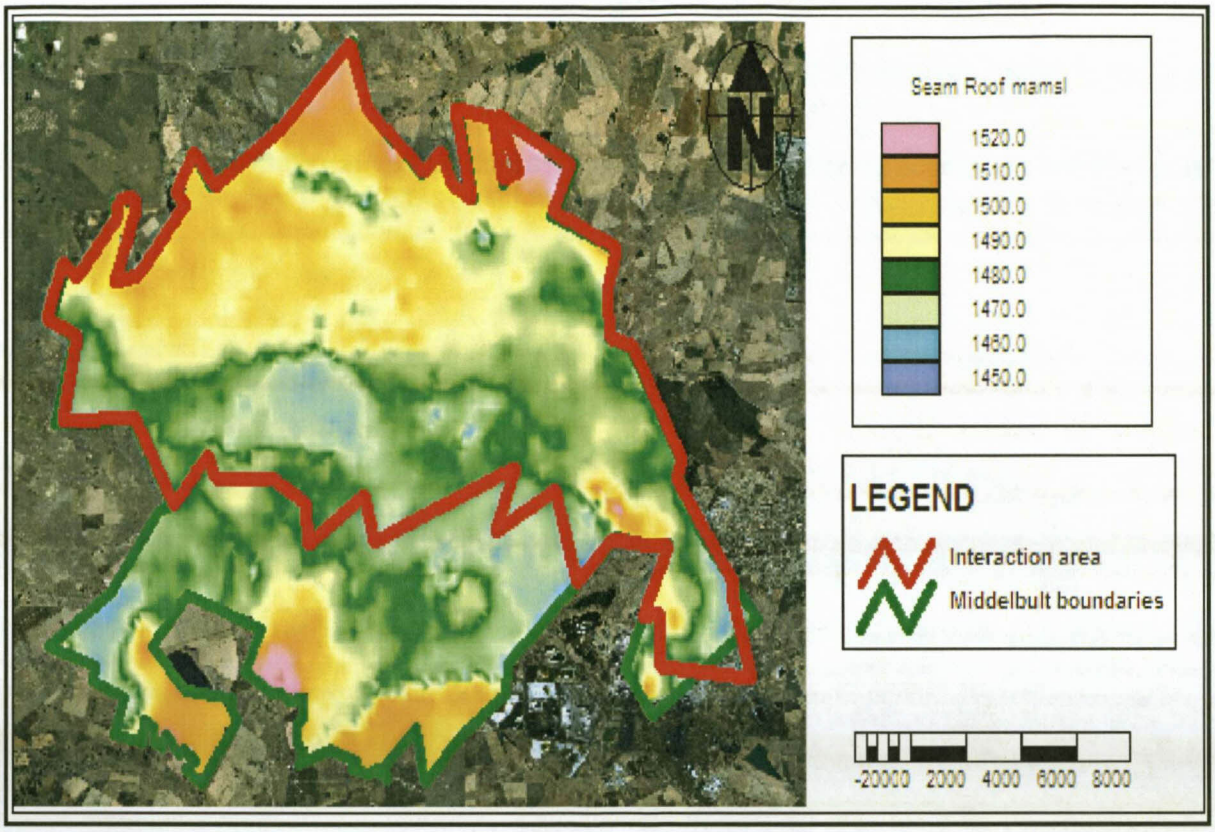

Figure 47: Interpolated elevations for the No. 4L coal seam roof.

The Witwatersrand Supergroup does not outcrop on the surface of the study area and is overlain by the Ventersdorp, Transvaal and Karoo Supergroups (Tweedie *et al.*, 1986). The average interpolated thickness of the overburden ranges from 2550 m to 254 m at an average of 1400 m. This indicates that the original water level measured by Pritchard-Davies (1962) is not a water level but a piezometric level, as there are aquiclude(s) confining the Witwatersrand aquifer, which results in the piezometric level of 1533 m.a.m.s.l. in the exploration borehole.

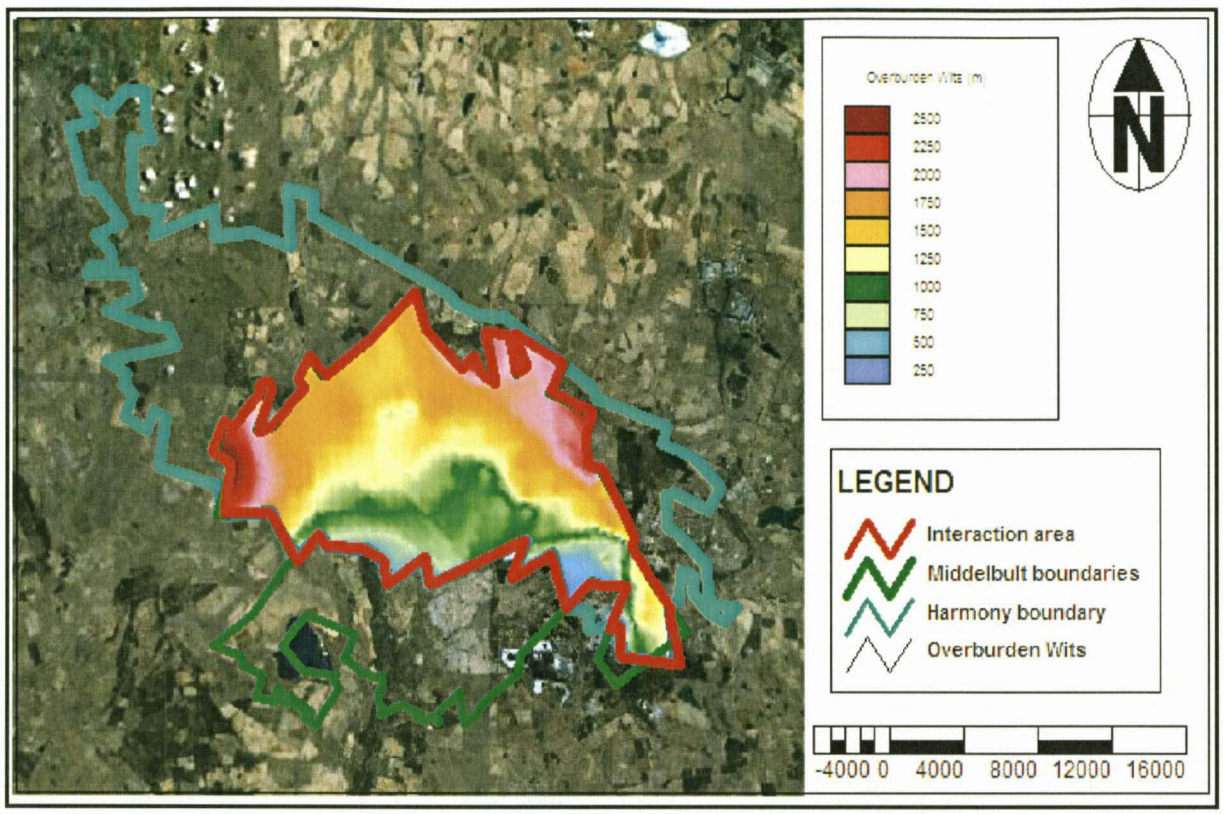

Figure 48: Interpolated thickness of the overburden above the Witwatersrand Supergroup.

During the period 1956 to 1969, a dewatering cone developed around the mine workings and the groundwater level was lowered to a deepest point of 1100 m below datum or 728 m.a.m.s.l. (Rison Groundwater Consulting, 2007). Pumping in one mine affected the water levels in adjacent mines. Groundwater drawdown therefore occurred at variable rates at the different mines. The water level in Winkelhaak dropped by 305 m between August 1956 and July 1962. The water level in Bracken dropped by 190 m between February 1961 and July 1962 and the water level in Leslie dropped by 170 m between February 1961 and July 1962 (Pritchard-Davies, 1962).

The values in Table 8 along with the top of the Witwatersrand Supergroup were used as the current water levels around the gold mine shafts, shown in Figure 49. The top of the Witwatersrand was derived from the exploration boreholes covering the study area and discussed in the geological section. The top of the Witwatersrand was used as a water level, as the base of the Ventersdorp Supergroup (aquiclude) confines the water level within the Witwatersrand aquifer.

Interpolation with the available data was used to simulate the Witwatersrand aquifer's water levels over the entire study area. The interpolation technique used was the inverse distance weighting method, which is deemed best for data with a large spatial variation. In Figure 49, the effect of pumping on the Witwatersrand aquifer can be seen around the gold mine shafts.

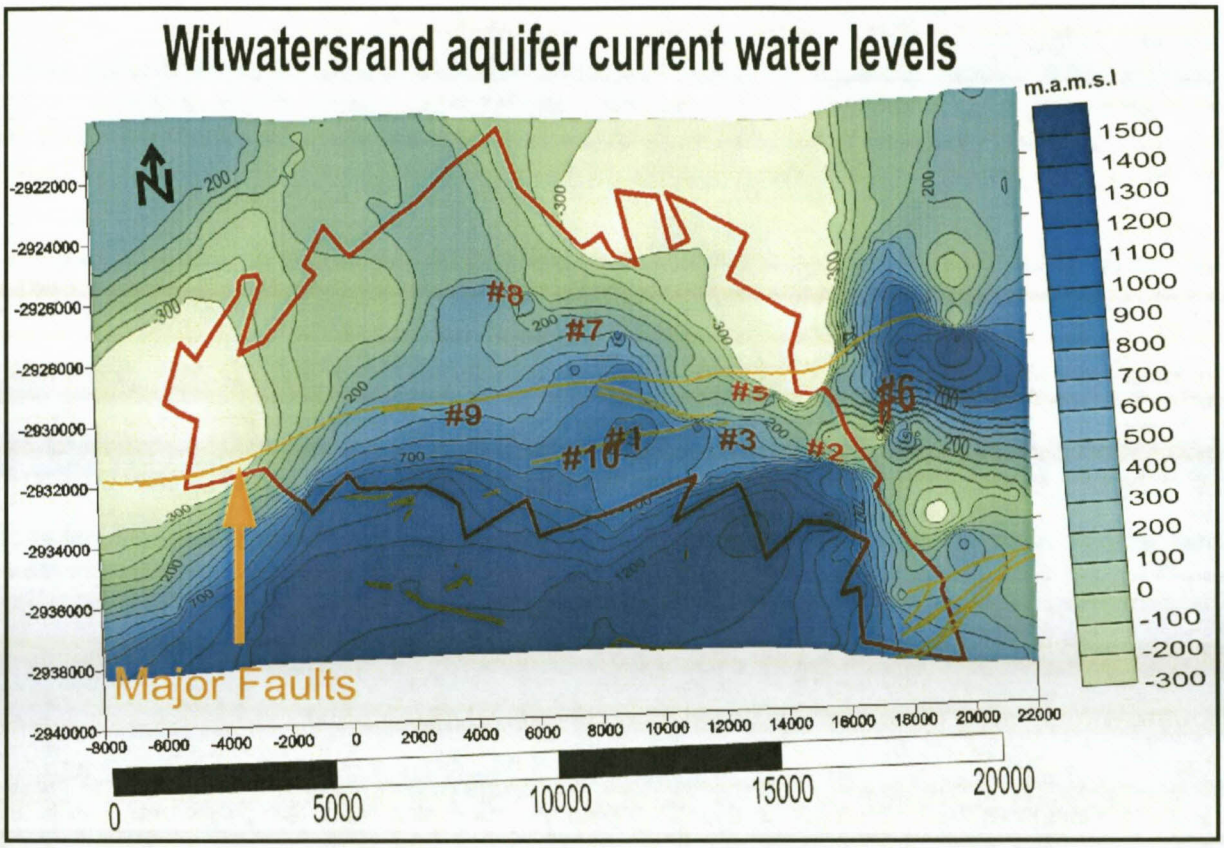

Figure 49: Interpolated groundwater levels around the gold mine shafts (Inverse distance weighting method).

5.5.3 Groundwater pumping stations and their effect on the Witwatersrand aquifer's water level

In the gold mine, excess water accumulating in the mine workings is pumped to the surface through a series of pumping stations. Currently, only two pumping stations are in operation: they are the pumping station in No. 8 shaft and the pumping station in No. 7 shaft. No. 7 shaft's pumping station is also the main pumping station within the gold mine. A summary of the gold mine pumping stations is included in Table 9.

Table 9: Shaft's and pumping stations of the gold mine.

Shaft name	Shaft status	Water pump stations	Pump Station depths		
			Metres below datum (1828.797	Metres below surface	Metres above mean sea level
Winkelhaak No. 1 shaft	Decommissioned (mothballed)	Water flows from 1 shaft towards 2 shaft where it is pumped out to surface	652	444	1177
Winkelhaak No. 3 shaft	Decommissioned (mothballed)	Water flows from 3 shaft towards 2 shaft where it is pumped out to surface	698	437	1179
Winkelhaak No. 5 shaft	Decommissioned (mothballed)	Water flows from 5 shaft towards 2 shaft where it is pumped out to surface	1849	1640	-20
Winkelhaak No. 2 shaft	Decommissioned (mothballed)	Water from 1, 3 and 5 shaft flows to 2 shafts from where it is pumped to surface. Pump decommissioned in April 2010. Water from 1, 2, 3 and 5 shaft is flowing towards 7 shafts from where it will be pumped to surface.	1471	1235	385
Winkelhaak No. 6 shaft	Decommissioned (mothballed)	Pump decommissioned in 1998	1471	1274	358
Kinross No. 7 shaft	Decommissioned in December 2009.	Water from 7, 9 and 10 is currently being pumped to surface. It is expected that water from 2 shaft will reach 7 shaft by 2011. 7 shaft is the main pumping station	1857	1823	-219
Kinross No. 8 shaft	In production	Water pumped to surface	2048	1855	-219
Leslie No. 9 shaft	Decommissioned (mothballed)	Pump decommissioned in October 2001. Excess water flows to 7 shaft	unknown	unknown	unknown
Bracken No. 10 shaft	Decommissioned	Pump decommissioned in 1994	1002	762	827

The shafts and the pumping stations are affecting the naturally occurring Witwatersrand aquifer groundwater level either by lowering the groundwater level surrounding the shafts where pumping stations are in operation or by creating piezometric levels in the shafts above the Witwatersrand aquifer, where the pumping stations have been decommissioned for more than

10 years, as shown in Figure 52. The concept of a piezometric levels is shown in Figure 50 below.

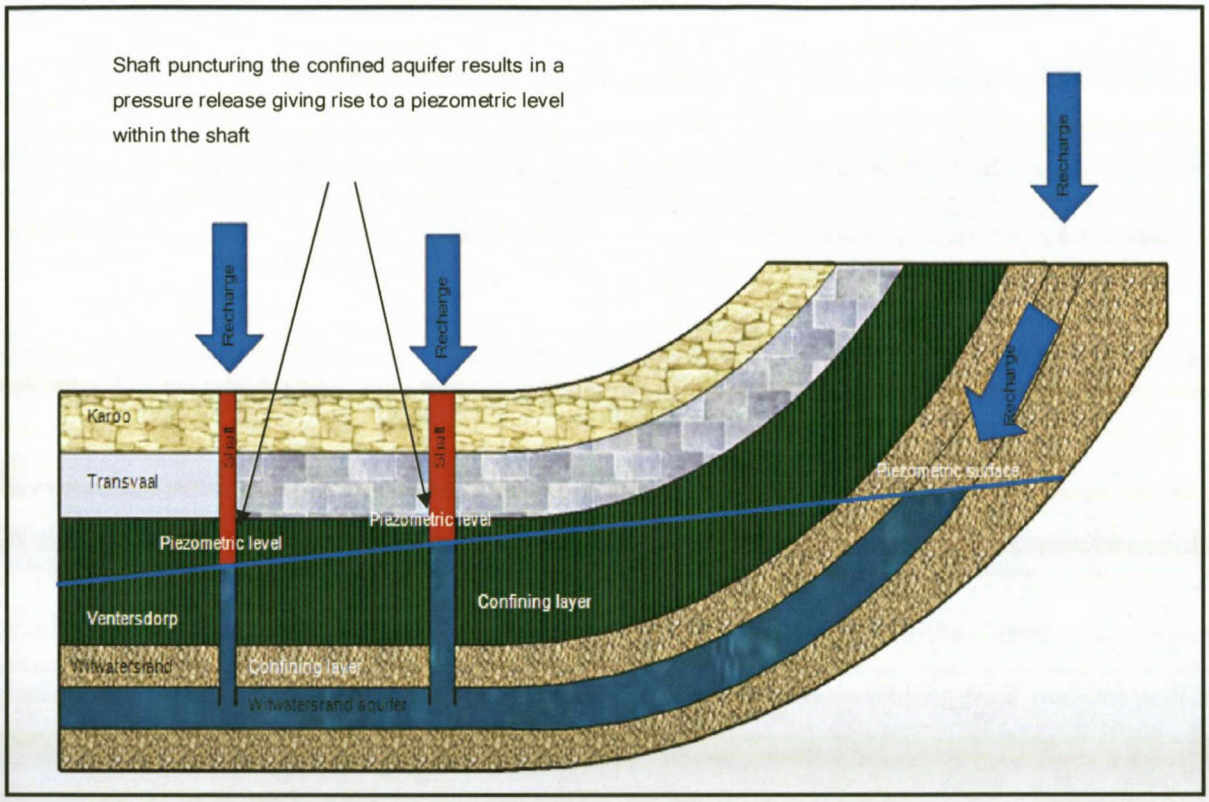

Figure 50: Conceptual model of piezometric levels within a confined aquifer.

The effect of the piezometric surface can also be seen in the conceptual model of the interpolated groundwater levels in Figure 51. Both No. 6 and No. 10 shafts have been decommissioned for over 10 years, which has resulted in the piezometric level in the confined Witwatersrand aquifer rising above the confined water level within the aquifer. It will continue to rise within the shafts until it reaches equilibrium below 1533 m.a.m.s.l. (Pritchard-Davies, 1962), which is expected to be the maximum the Witwatersrand water level can reach. Important to note is that the 1533 m.a.m.s.l recorded by Pritchard-Davies (1962) was before extensive mining in the Witwatersrand Supergroup took place and that the Witwatersrand aquifer (confined) was therefore under more pressure than currently exists due to the extensive voids created by mining activities, which have decreased the pressure within the aquifer.

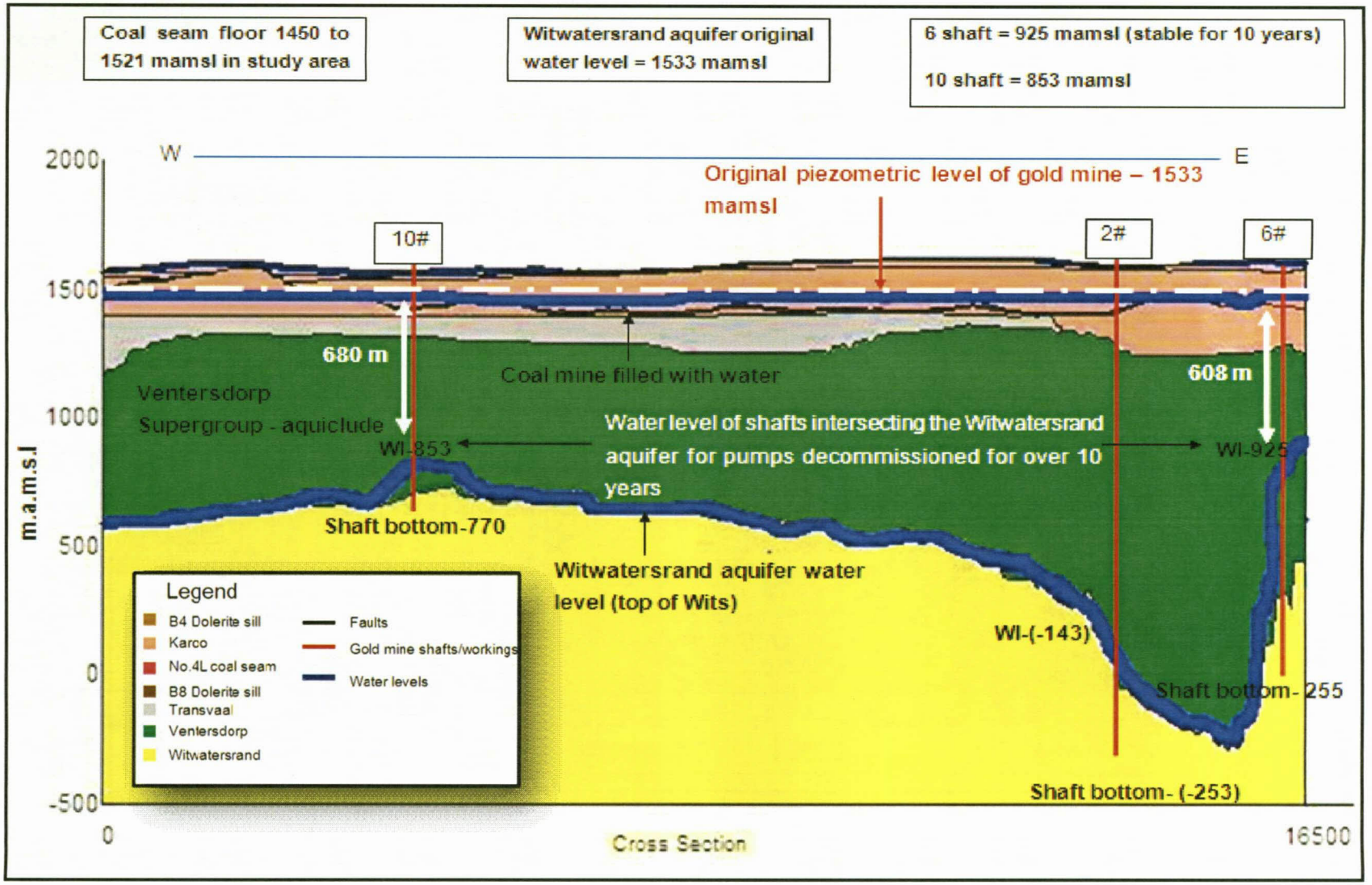

Figure 51: Conceptual model of the water levels in the Witwatersrand aquifer where pumping stations have been decommissioned.

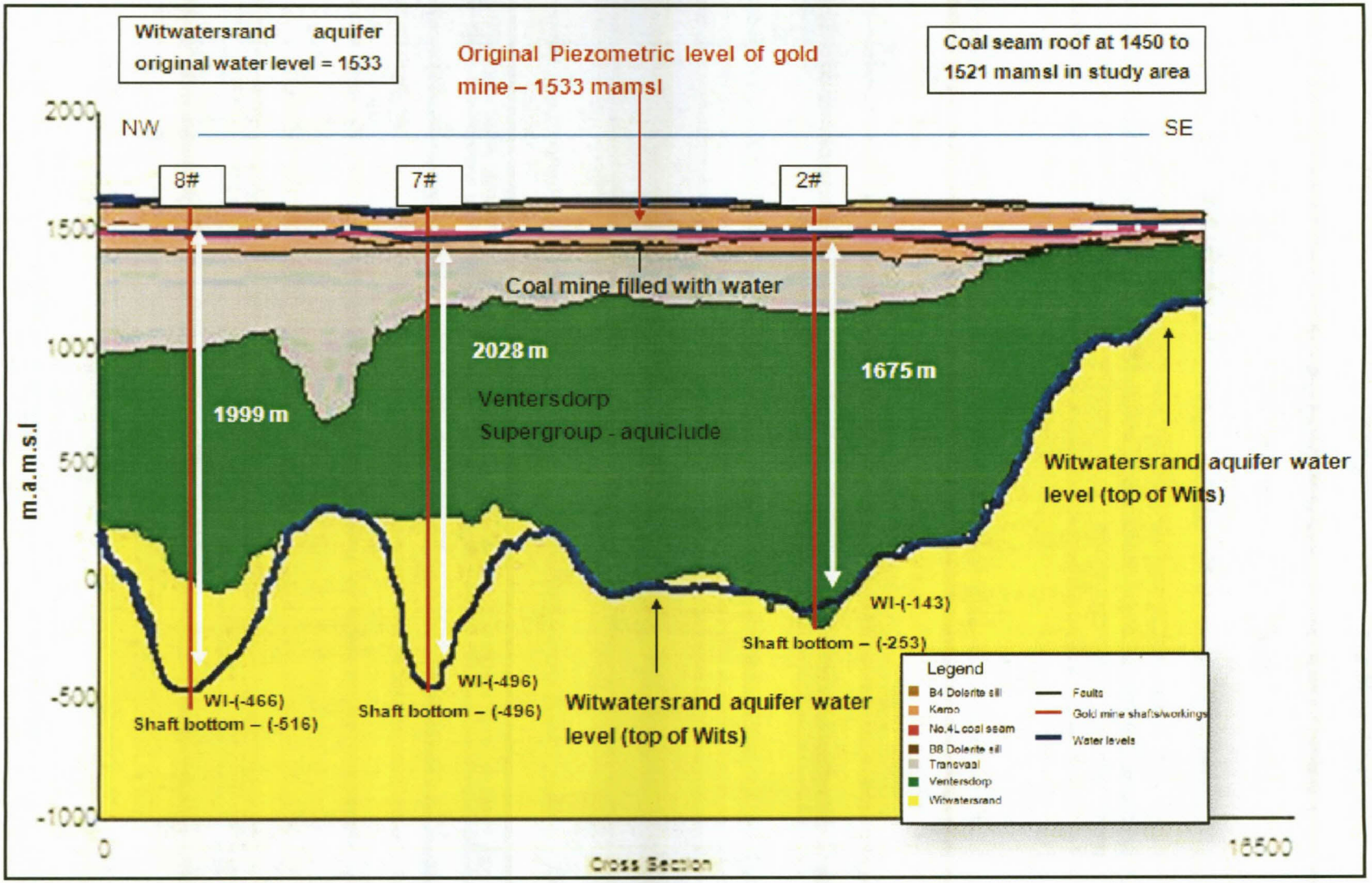

Figure 52: Conceptual model of the water levels in the Witwatersrand aquifer where pumping stations are in operation.

Chapter Six: Possible interaction areas within the study area

The possible areas of interaction are where Sasol Mining's Middelbult (Block 8) Colliery is currently and where it will in future extract coal from the No. 4L coal seam, overlying Harmony Evander gold mining operations that mine the underlying gold-bearing Kimberley reef (Figure 53).

Sasol coal mining will expand its existing Middelbult Colliery into the Block 8 reserves to the west and north of its current mining operations (Figure 53). The initial expansion will be to the west from the existing underground coal mining, as shown Figure 53 (Middelbult Mine: Block 8 Expansion EMPR, 2003).

There is a potential risk that the coal mining will damage the geohydrological barriers (aquicludes) that currently exist between the shallow Karoo aquifer where Sasol coal mining takes place and the deeper Witwatersrand aquifer where Harmony gold mining operates. Damage to these geohydrological barriers could result in an increase of groundwater influx from surface (gold mine slimes dams) as well as the shallower Karoo aquifer affected by coal mining into the deeper Witwatersrand aquifer affected by gold mining. This could affect both the quality and quantity of groundwater in the study area.

In some areas, the potential risk for groundwater interaction is much higher than in others. The potential risk for groundwater interaction is a function of the following:

- depth and areas of mining;
- tailings storage facilities (TSF);
- geology;
- preferential pathways.

If the above factors are considered, certain high risk areas for potential interaction can be identified.

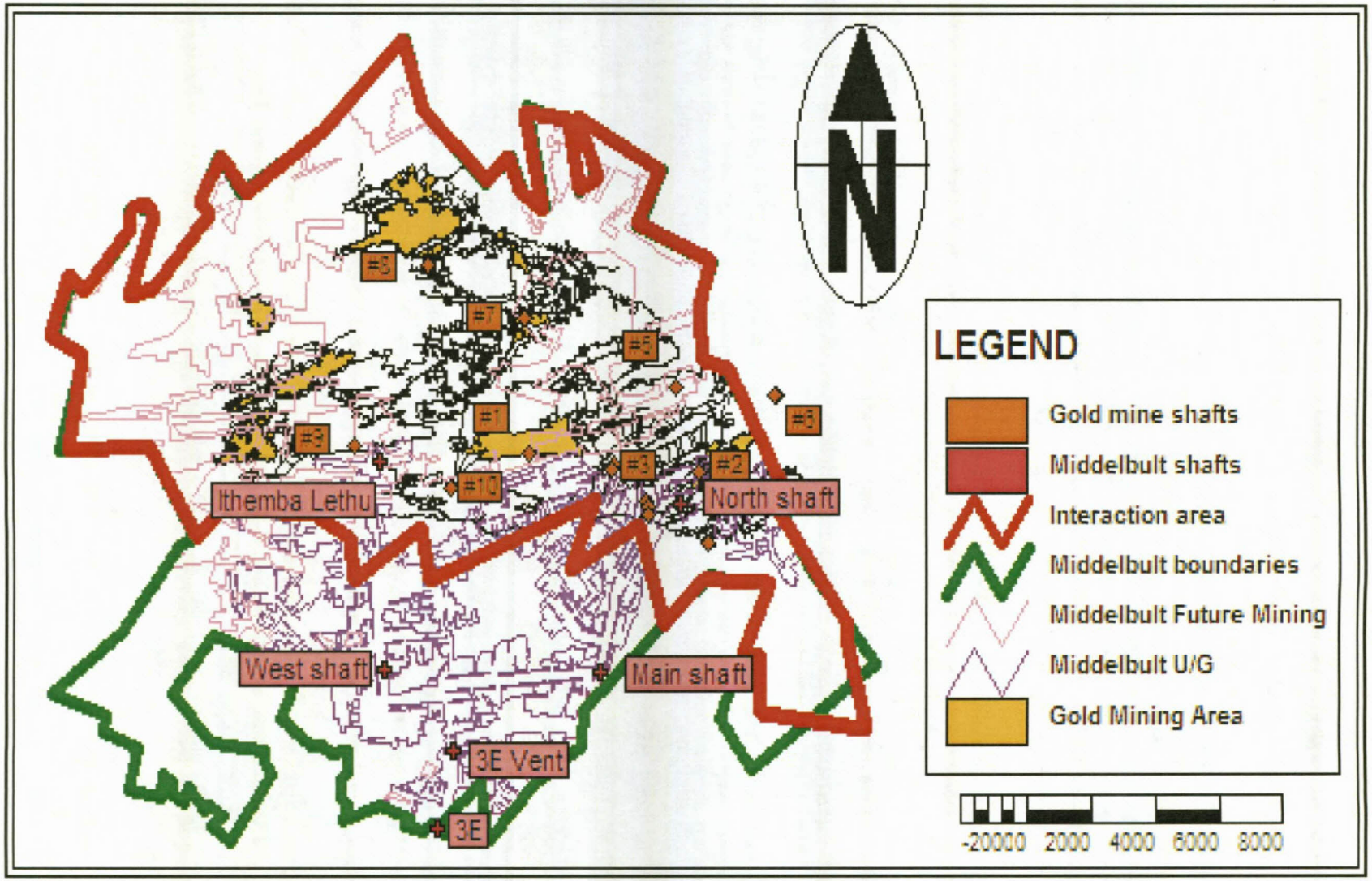

Figure 53: Sasol Mining's Middelbult (Block 8) current and future mining over Harmony Evander's gold mining activities.

6.1 Potential Interaction: Mining depths

6.1.1 Sasol coal mining

The No.4L coal seam mined by Sasol is situated at an average depth of 80 m below surface in the south and 150 m below surface in the north, or at elevations ranging between 1450 m.a.m.s.l and 1521 m.a.m.s.l in the different compartments resulting from the different dolerite sills situated throughout the study area (Figure 54). The coal seam is overlain by the Karoo Supergroup sediments compromising mainly sandstones and shales (Middelbult Mine: Block 8 Expansion EMPR, 2003). Figure 54 displays the interpolated contours of the overburden thickness covering the No. 4L coal seam in the study area. The interpolated elevations for the coal seam floor are shown in Figure 47.

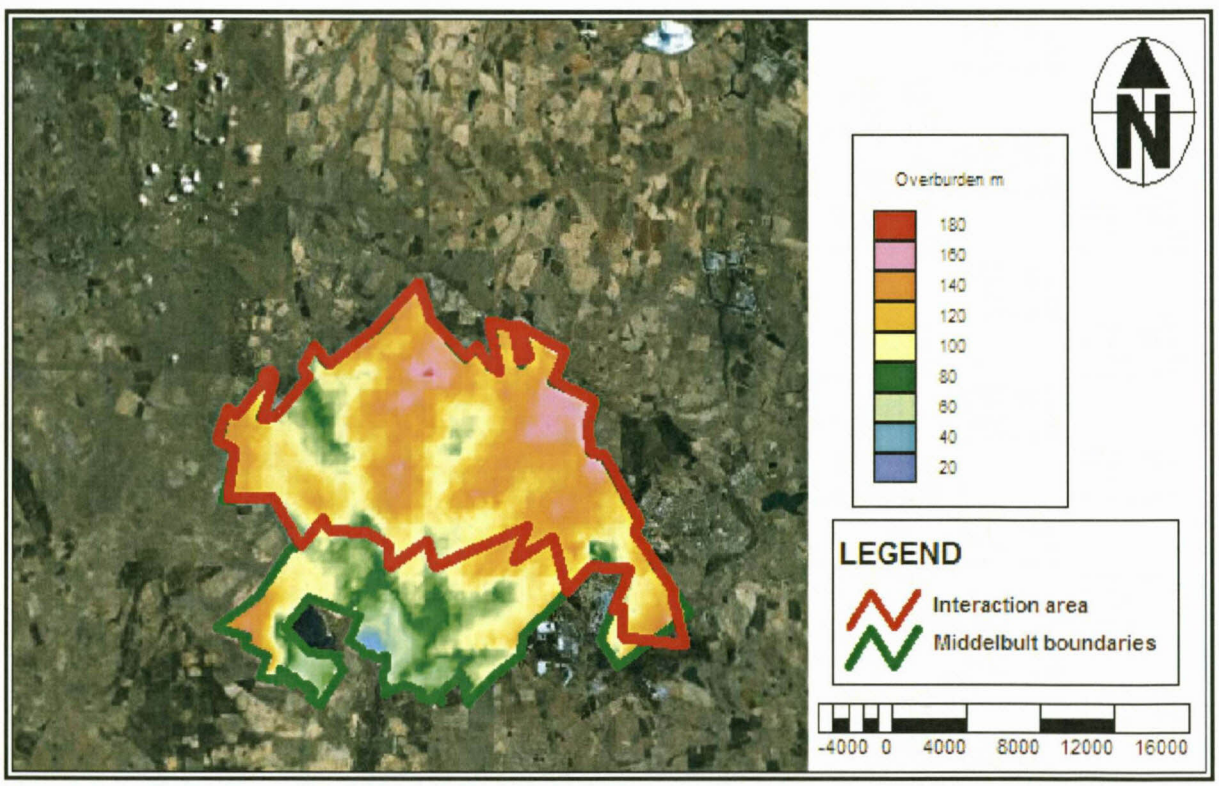

Figure 54: Overburden thickness in metres above the No.4L coal seam.

6.1.2 Harmony gold mining

The Kimberly Reef containing the gold and platinum group metals are at varying depths below surface is currently being mined. The deepest operations are 2500 m below surface, at Harmony No. 8 shaft, and the shallowest are 240 m below surface, at Harmony No. 3 shaft. This

variable depth is due to the general dip of the Kimberley reef to the north, of between 16 ° and 24° and the east-west trending faults, with downthrows to the south, which resulted in the blocks being duplicated (Tweedie *et al.*, 1986). In Figure 55, Harmony Evander's gold mining shaft system is illustrated through a cross section.

6.1.3 Difference in mining depths

In some areas, the coal mining overlaps the gold mining, as shown in Figure 53 and Figure 55. These areas have the highest risk of groundwater interaction where the coal mining and gold mining are relatively close together (less than 300 m difference in mining depths) (see Table 10). In these areas, influx of water from the coal mine into the gold mine can result from the close proximity of the mines through induced preferential flow paths.

The minimum difference in depth, of approximately 81 m between Sasol mining's No. 4L coal seam and the shallowest gold mining workings, is at Harmony Evander's No. 9 shaft (A level) and the maximum difference, of approximately 782.5 m, is at Evander's No. 8 shaft (8 level).

Table 10: Difference in mining depths.

Difference in elevation (m.a.m.s.l) of coal seam floor and shallowest gold mining operations through the study area			
Gold mine shaft	**No. 4L Coal seam floor (m.a.m.s.l)**	**Gold mining operations (m.a.m.s.l)**	**Difference in mining depths (m)**
1 Shaft	1479m	1347m (2 level)	132m
2 Shaft	1483m	912m (9 level)	571m
3 Shaft	1480m	1387m (1 level)	93m
5 Shaft	1482m	624m (13 level)	858m
7 Shaft	1490m	849m (3 level)	641m
8 Shaft	1489.5m	707 m (8 level)	782.5m
9 Shaft	1461m	1380m (A level)	81m
10 Shaft	1470m	1345m (1 level)	125m
(m.a.m.s.l) metres above mean sea level			

Currently, Sasol Middelbult Block 8 is only mining over Harmony gold mining in the southernmost parts of the study area, with the largest area covering the southeastern part (Figure 53). Future mining will cover most of the study area except for the central part of the study area around Harmony Gold Mining's No. 7 and No. 8 shafts (Figure 53).

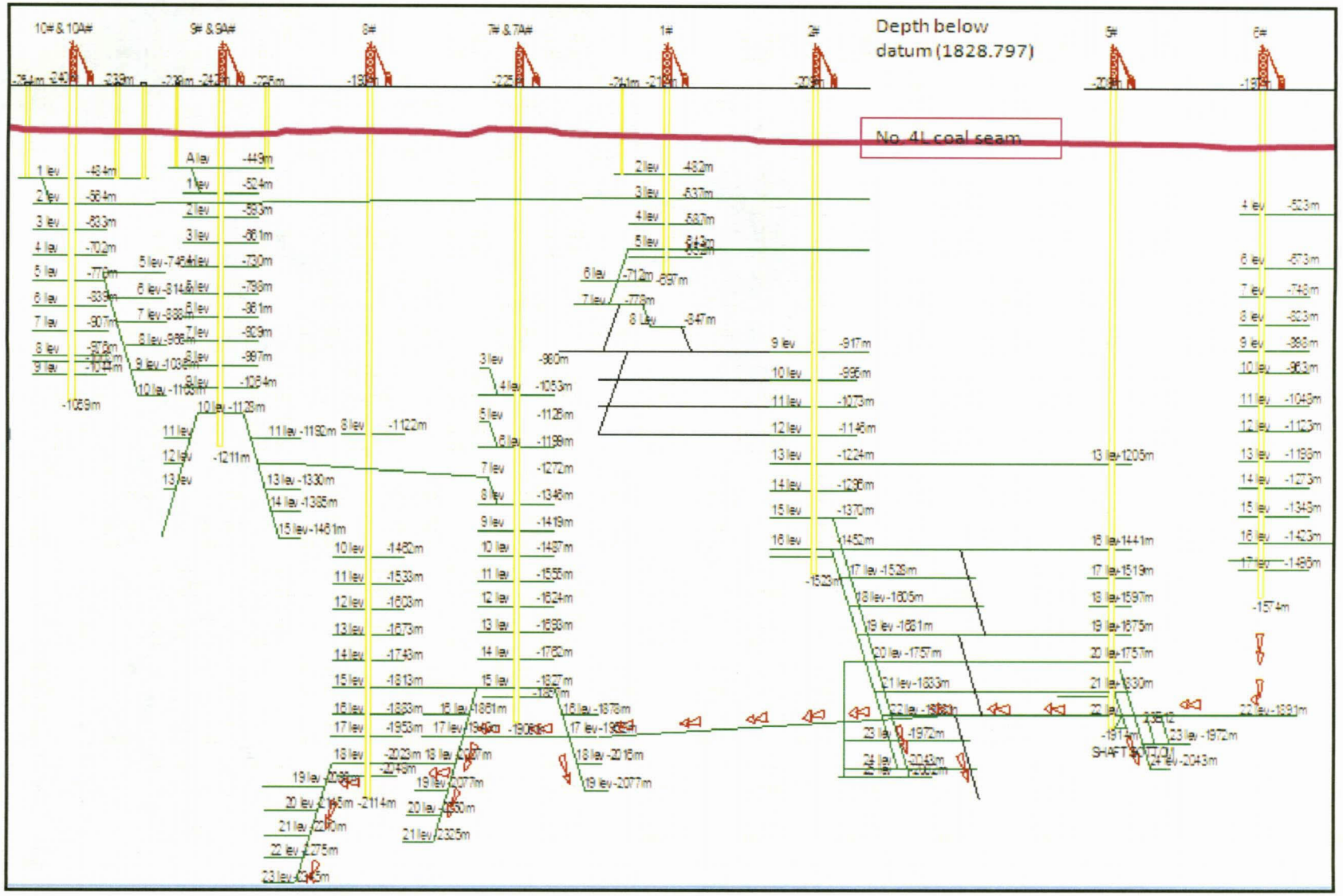

Figure 55: General Evander gold mining operations illustrating their shaft system (not to scale). (Presentation 53 Kinross, Harmony Evander).

Areas that have the highest potential for groundwater interaction according to difference in depth are:

- The area around Harmony's No. 1 Shaft (Sasol future mining);
- The area around Harmony's No. 3 Shaft (Sasol current mining);
- The area around Harmony's No. 9 Shaft (Sasol future mining);
- The area around Harmony's No. 10 Shaft (Sasol future mining);

These areas are shown in Figure 56 to Figure 59.

6.1.4 The area around Harmony's No. 1 Shaft

Sasol Coal Mining in future will mine near Harmony's No. 1 Shaft, where the No. 4L coal seam floor is situated at 1479 m.a.m.s.l or 139 m below surface (Figure 54). Harmony Gold Mining's closest mining operations at No.1 shaft to the No. 4L coal seam is situated at Level 2, which is 1347 m.a.m.s.l or 270 m below surface. The minimum difference between the No.4L coal seam and the gold mine workings at No.1 shaft is thus 132 m (Figure 56). As yet, no groundwater interaction from the coal mine into the gold mine could be established in the No. 1 shaft area, as no preferential pathways could be confirmed.

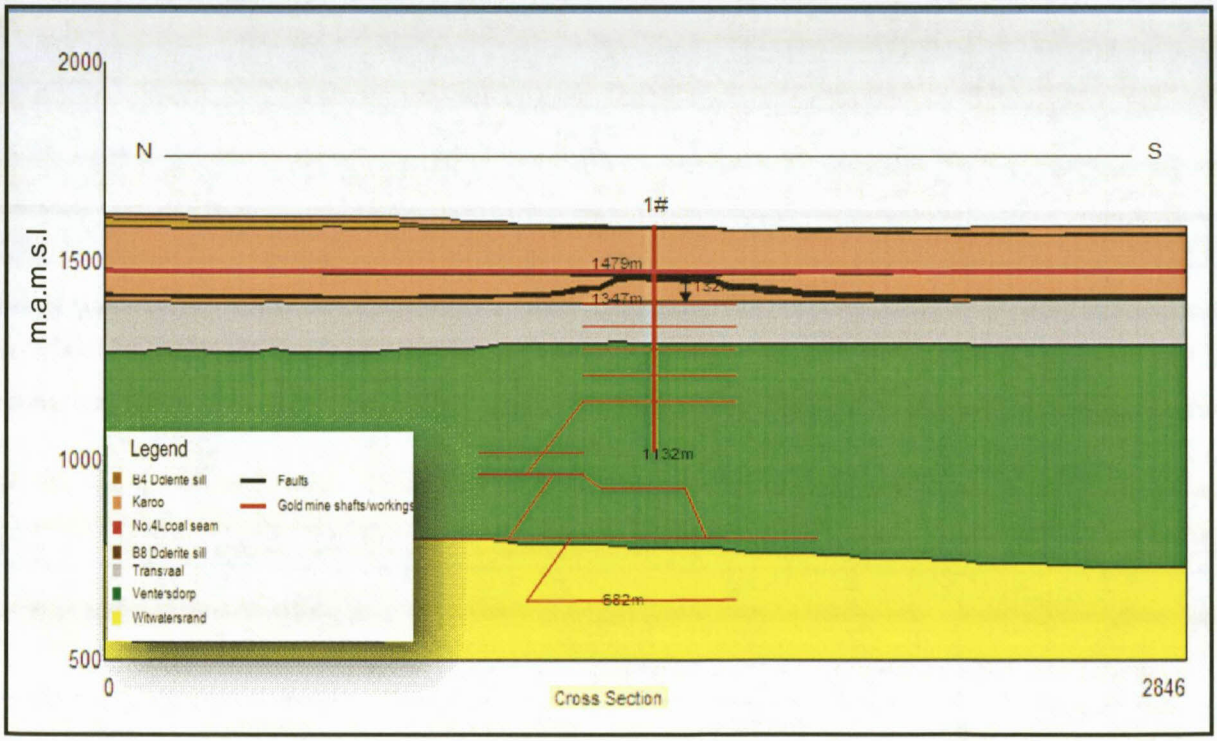

Figure 56: Cross section through Evander No.1 shaft.

6.1.5 The area around Harmony's No. 3 Shaft

Sasol is currently mining near Harmony's No. 3 shaft, where the No. 4L coal seam floor is situated at 1480 m.a.m.s.l or 136 m below surface. Harmony gold mining's closest mining operations at No.3 shaft to the No. 4L coal seam is situated at Level 1, which is 1387 m.a.m.s.l or 229 m below surface (Figure 54). The minimum difference between the No.4L coal seam and the gold mine workings is thus 93 m at No. 3 shaft (Figure 57). As yet, no groundwater interaction from the coal mine into the gold mine could be established in the No. 3 shaft area, as no preferential pathways could be confirmed.

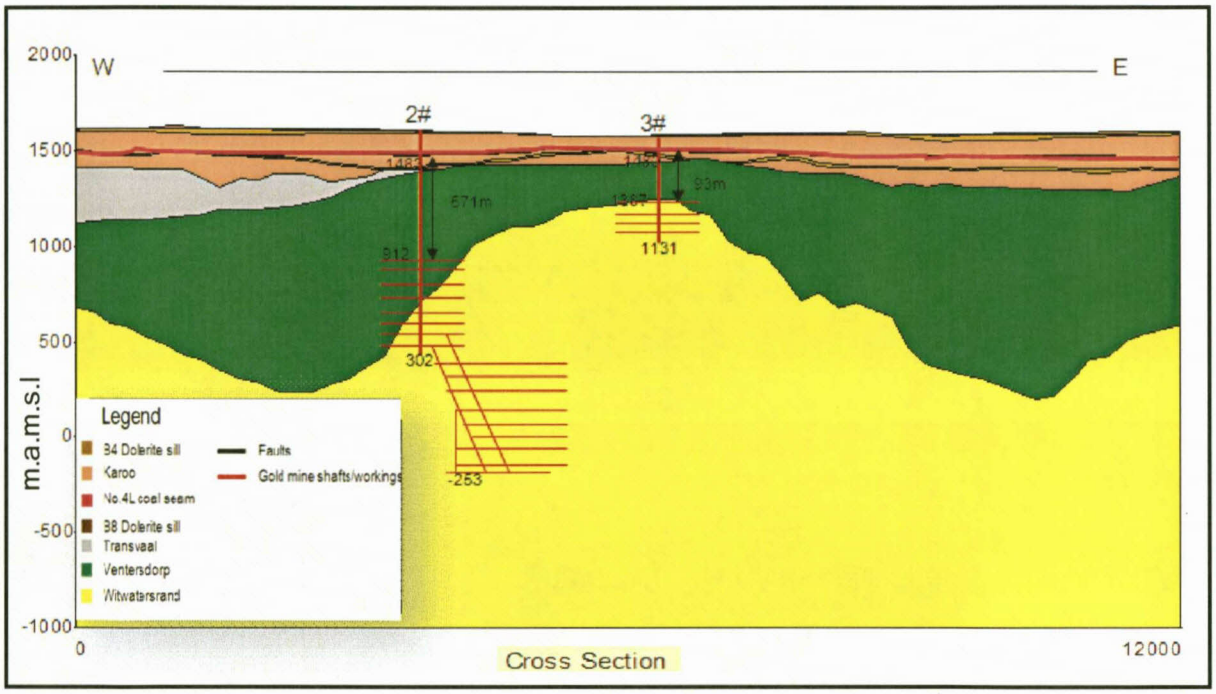

Figure 57: Cross section through Evander No. 2 and No.3 shaft.

6.1.6 The area around Harmony's No. 9 Shaft

Sasol is proposing to mine in future near Harmony's No. 9 shaft, where the No. 4L coal seam floor is situated at 1461 m.a.m.s.l or 126 m below surface (Figure 54). Harmony Gold Mining's mining operations at No.9 shaft, closest to the No. 4L coal seam, is situated at A level which is 1380 m.a.m.s.l or 207 m below surface. The minimum difference in metres between the No.4L coal seam and the gold mine workings is approximately 81 m at No. 9 shaft (Figure 58). Two preferential flow paths bearing water at No. 9 shaft (Level 1) directly underneath Level A (shown

in Figure 55) were found in this study (Table 5). These fractures could link the Karoo aquifer affected by coal mining to the gold mine workings in the Witwatersrand aquifer.

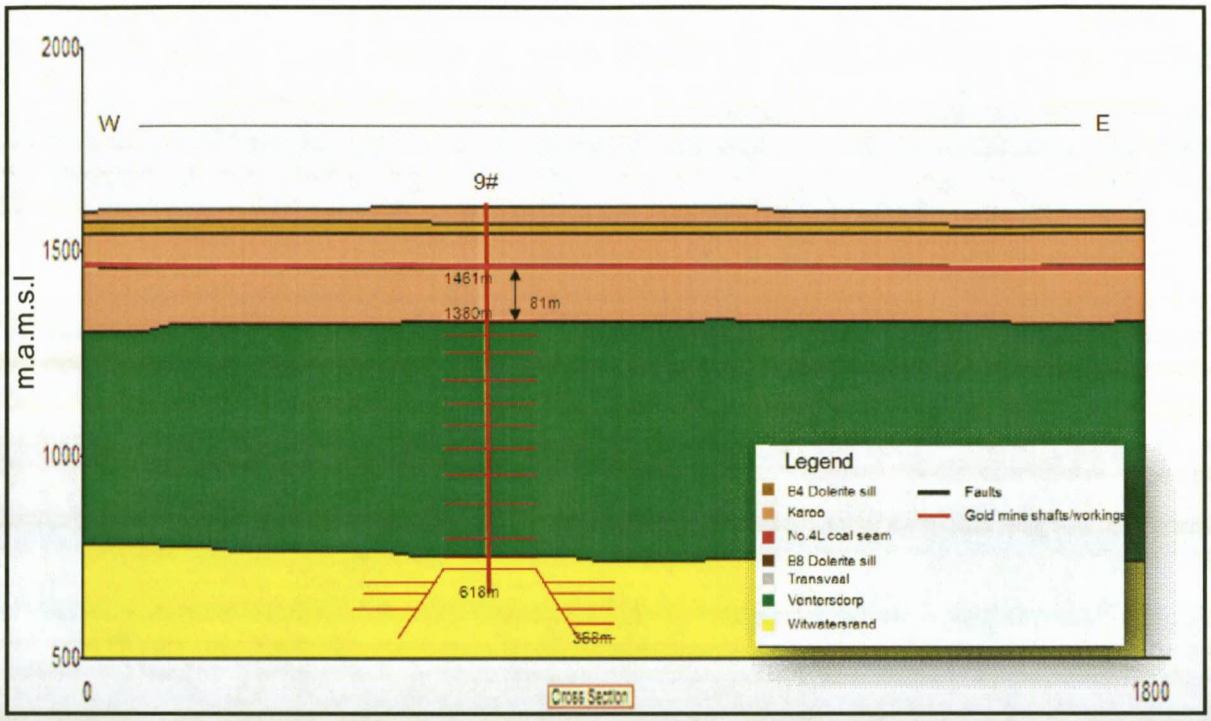

Figure 58: Cross section through Evander No.9 shaft.

6.1.7 The area around Harmony's No. 10 Shaft

Sasol is currently mining near Harmony's No. 10 shaft, where the No. 4L coal seam floor is situated at 1470 m.a.m.s.l or 119 m below surface. Harmony Gold Mining's mining operations at No.10 shaft, closest to the No. 4L coal seam, are situated at Level 1, which is 1345 m.a.m.s.l or 244 m below surface. The minimum difference between the No.4L coal seam and the gold mine workings is approximately 125 m (Figure 59). As yet, no groundwater interaction from the coal mine into the gold mine could be established in the No. 10 shaft area, as no preferential pathways could be confirmed.

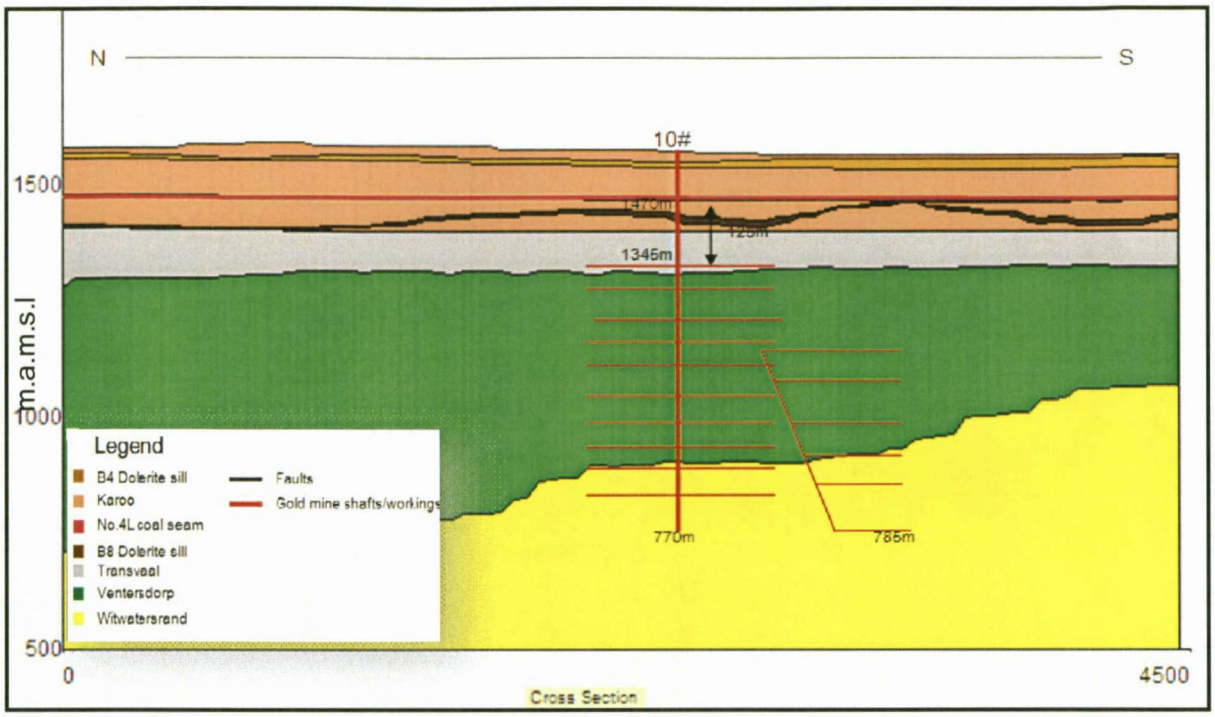

Figure 59: Evander No. 10 shaft.

6.2 Potential Interaction: Evander tailings storage facilities

The potential for groundwater interaction resulting from Harmony Evander Tailings Storage Facilities (TSF) found on surface can be attributed to the extent of subsidence resulting from the coal mining directly underlying or near the TSF. There has been coal mining underneath the Winkelhaak and Leslie slimes dams, with proposed future coal mining underneath the Kinross slimes dams, as shown in Figure 60.

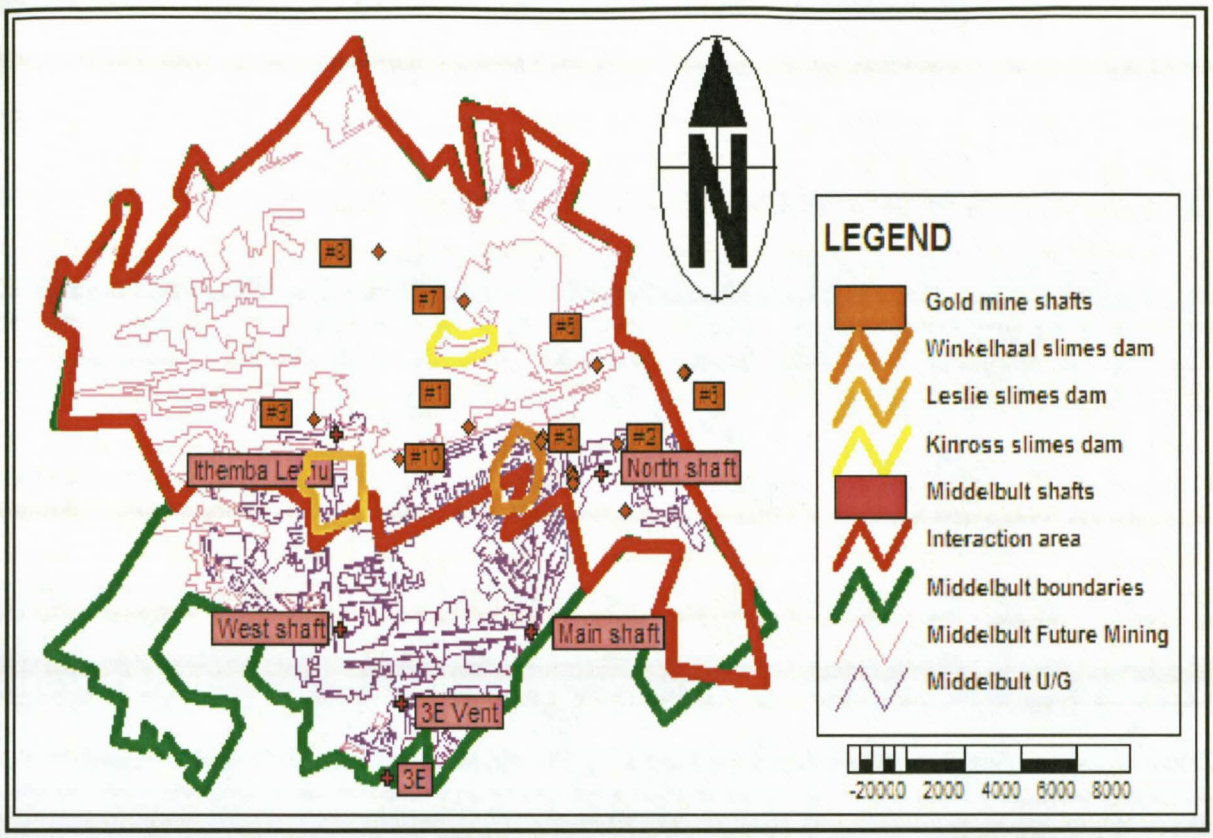

Figure 60: Harmony Evander gold mine tailings storage facilities.

6.2.1 Subsidence due to High Extraction coal mining

As the coal seam that supports the overlying rock mass is removed, the immediate roof of the seam fails and collapses, forming rubble fill (goaf). The caved rock breaks up into blocks varying in size from a few centimetres to tens of centimetres. These blocks rotate and pile up, partially filling the mined void. A stage will be reached when the mine workings are filled due to bulking of the rubble (Vermeulen & Usher, 2003).

As the coal mining face advances, higher-lying beds fall, settle and compress the caved layer. The stress in this "secondary caving zone" depends on the degree of compression of the "goafed" material. Typically, an extensive network of horizontal and vertical cracks develops, although the degree of displacement is not such that the beds lose their relative positions (Vermeulen & Usher, 2003).

Strata overlying the secondary caving zone bend and sag under their own weight and compress the goaf. As a result, the strata part along bedding planes. Continuity of the beds is maintained,

although some fractures develop from the stress of bending and sagging. The sagging will result in tension zones, compression in the rock strata and the development of cracks (Figure 61).

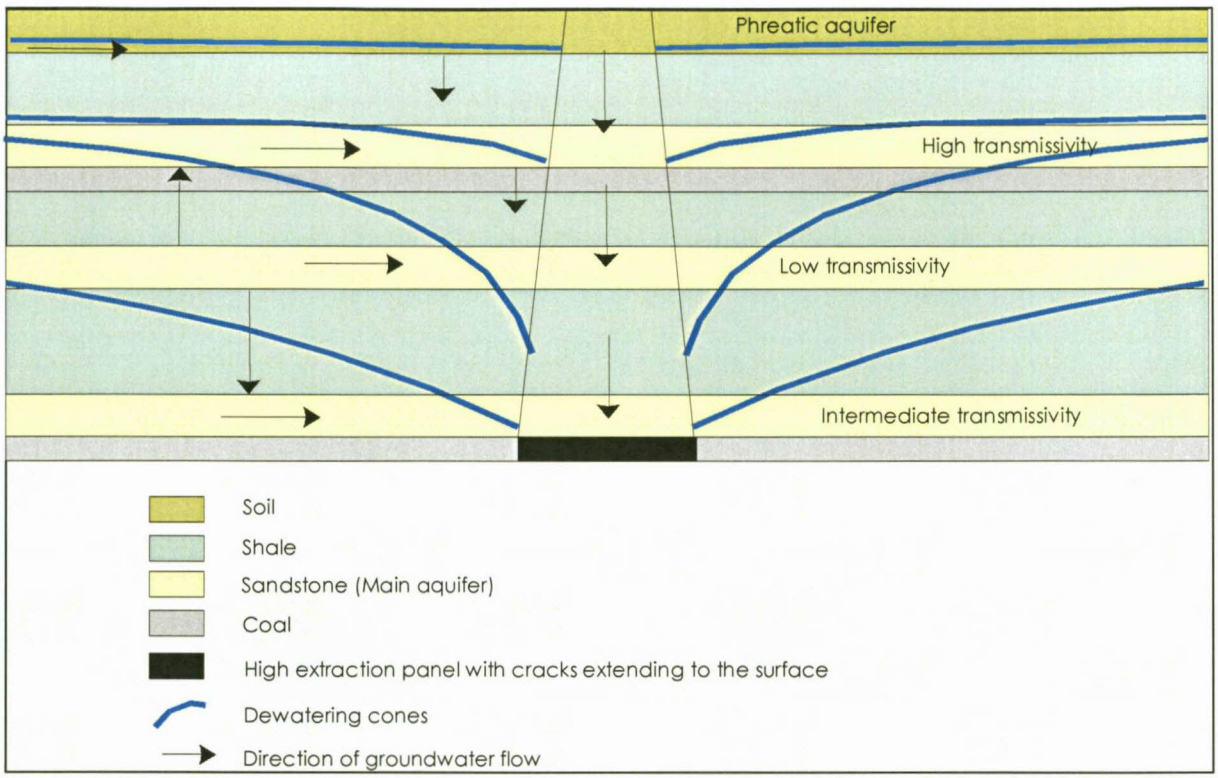

Figure 61: Schematic cross-section of a subsided high extracted panel (Grobbelaar, 2001).

Pillar extraction will present the greatest risk to groundwater influx into the underground coal mine due to potential surface subsidence as well as the expansion of preferential flow paths such as dolerite dykes, geological contact zones, dolerite sill contact zones, faults, fissures and unsealed exploration boreholes situated in the study area (refer to Figure 18). Influx of groundwater into the mine workings, as a result of high extraction mining will therefore be much more severe than for board & pillar underground mining activities.

The main contributors to the influx volumes as described by Vermeulen & Usher (2003) are:

- Annual rainfall recharge;
- Lateral inflows from the surrounding rock mass - deep (fractured) Karoo aquifer;
- Water released from storage in the overlying rock mass - shallow and deep aquifers;
- Inflows related to geological features;
- Inflows from surrounding mined out areas.

The actual increase in groundwater influx to the coal mine will be a function of:

- The actual extent of surface depressions forming ponds on the surface;
- The occurrence of areas that have a higher recharge potential because of the type of soil and vegetative cover; and
- The dimensions of apertures (cracks), and the infilling of these cracks with sediment.

A possible influx of groundwater into the coal mine could be as a result of board-and-pillar mining into the coal mine from the 3 tailings facilities situated on the surface of the study area and owned by Harmony Gold's Evander operations. These slimes dams are:

- Kinross slimes dam,
- Leslie slimes dam,
- Winkelhaak slimes dam.

The 3 tailings facilities with the possible subsidence are shown in Figure 62.

6.2.1.1 Kinross slimes dam

The Kinross slimes dam is situated in the centre of the study area with Sasol future mining underneath it as shown in Figure 60. No subsidence is expected underneath the Kinross mine as shown in Figure 62 and Figure 63. This is a result of no high extraction coal mining directly underneath of near the Kinross slimes dam (Figure 63).

6.2.1.2 Leslie slimes dam

The Leslie slimes dam is situated to the south-southwest of the study area. Some existing high-extraction coal mining panels occur as close as 20-50 m of the southwestern corner of the slimes dam. The B4 dolerite sill restricting vertical groundwater is very thin to the southwest of the slimes dam (Figure 64 and Figure 66).

Therefore subsidence is likely to the south-southwest of the Leslie slimes dam, as high-extraction coal mining will occur and it is expected that preferential pathways (fractures) linking the slimes dam with the underground coal mine working will be induced (Figure 64). Although subsidence is expected near the Leslie slimes dam groundwater interaction from the slimes dam could not be confirmed due to inaccessibility.

6.2.1.3 Winkelhaak slimes dam

The Winkelhaak slimes dam is situated south-southeast in the study area. Some existing high-extraction coal mining panels occur as close as 50-80 m to the southeastern corner of the

slimes. The B4 dolerite sill is very thin to the south-southeast of the slimes dam (Figure 65 and Figure 66).

Therefore subsidence is most likely to occur southeast of the Winkelhaak slimes dam, as high extraction coal mining will occur and it is expected that preferential pathways (fractures) linking the slimes dam with the underground coal mine working will be induced (Figure 66). Although subsidence is expected near the Winkelhaak slimes dam groundwater interaction from the slimes dam could not be confirmed due to inaccessibility.

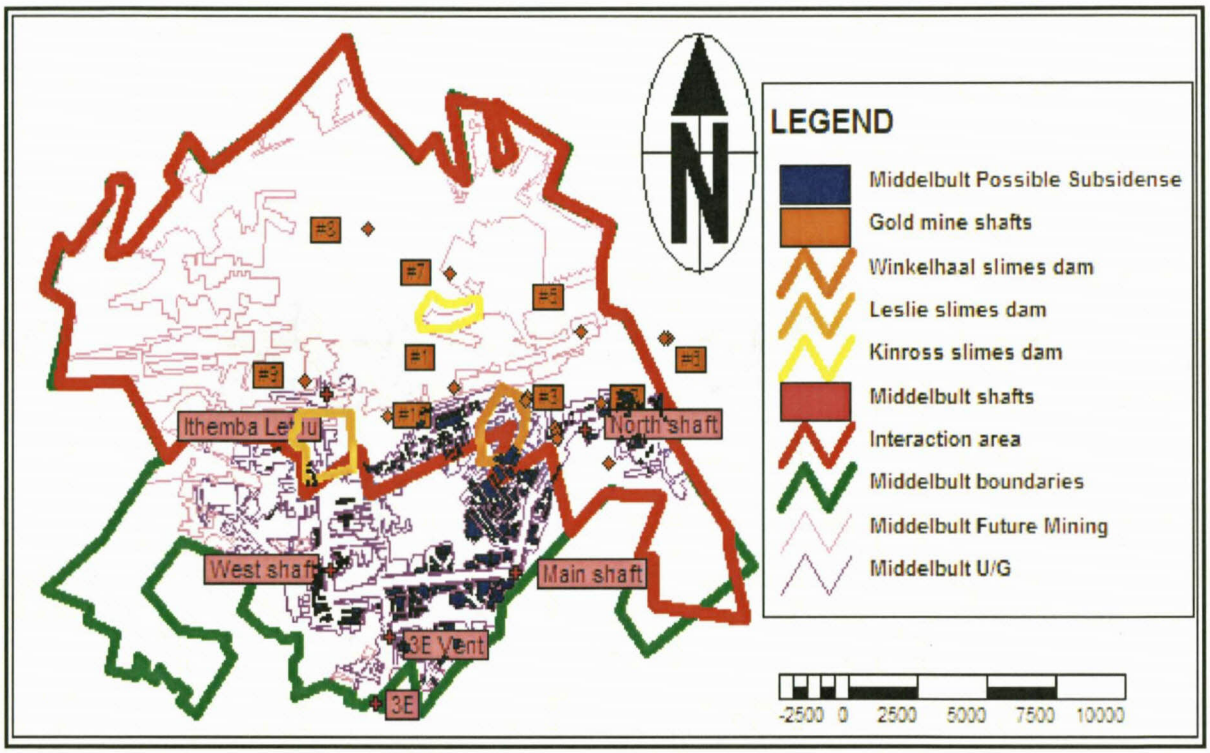

Figure 62: Possible areas of subsidence resulting from high extraction coal mining.

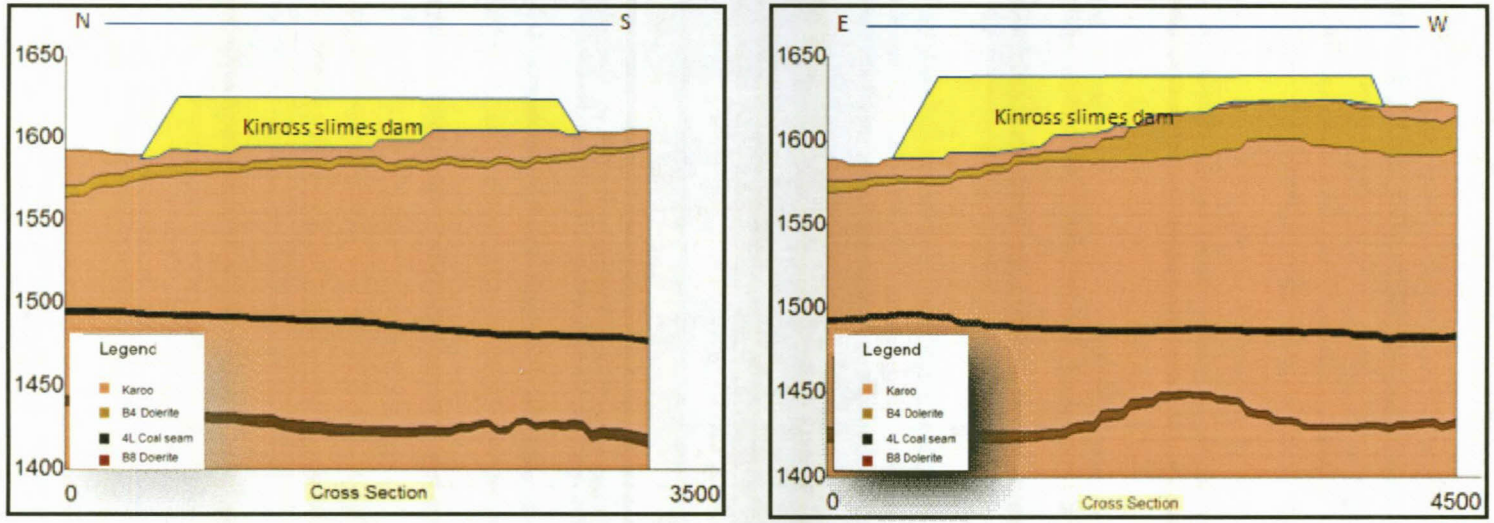

Figure 63: Kinross slimes dam conceptual cross sections.

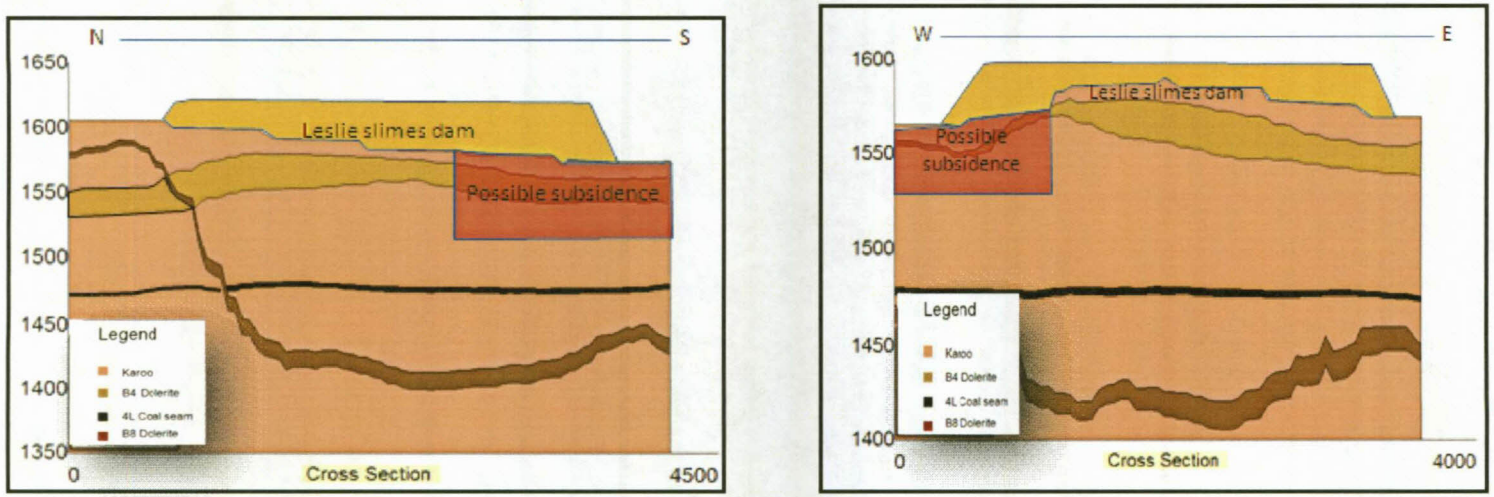

Figure 64: Leslie slimes dam conceptual cross sections.

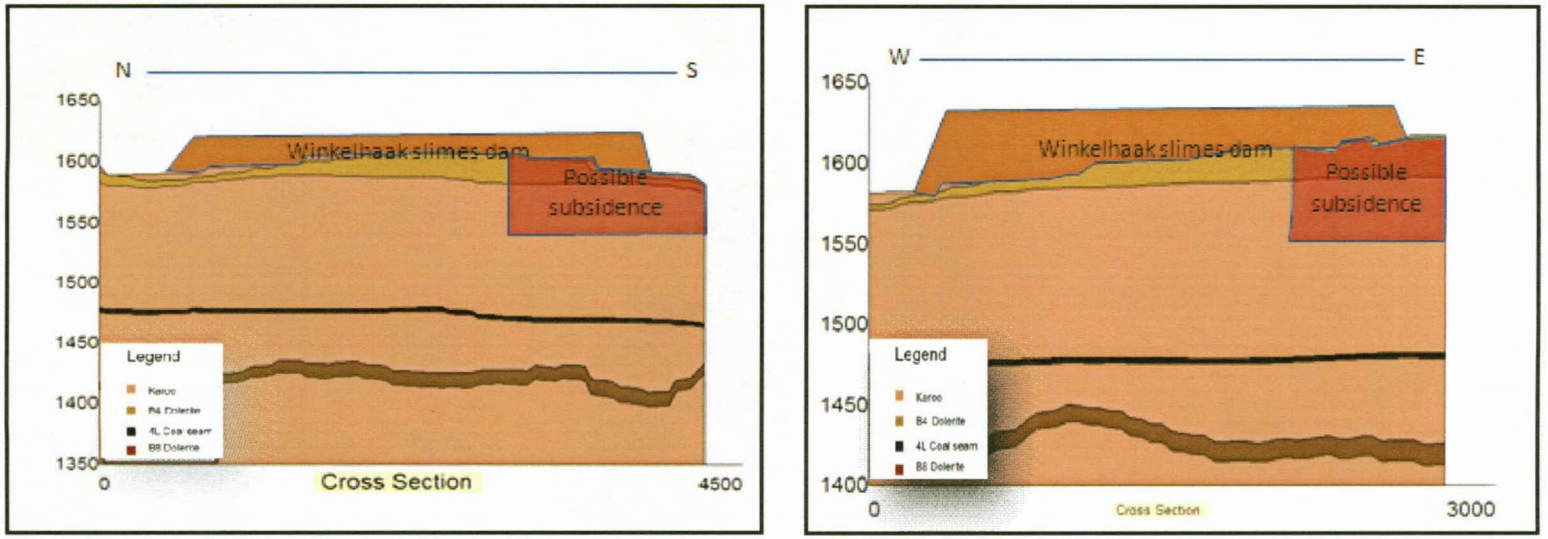

Figure 65: Winkelhaak slimes dam conceptual cross sections.

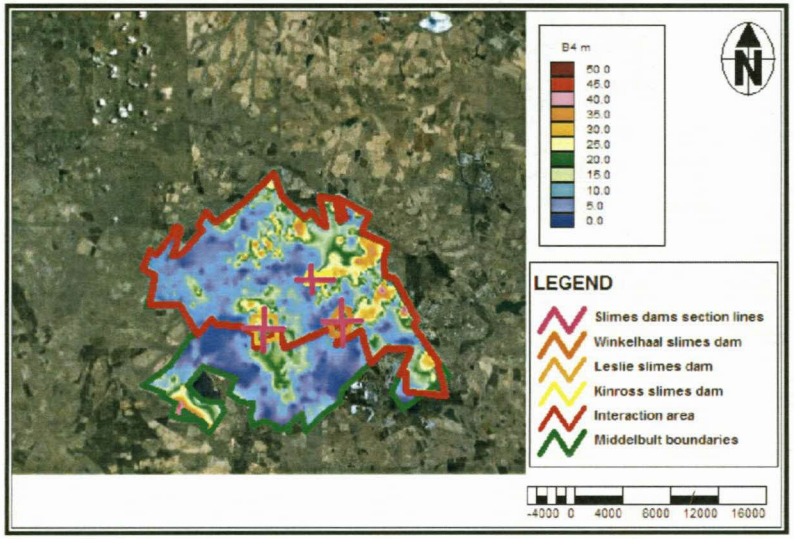

Figure 66: B4 dolerite thickness in metres with the west-east and north-south section lines.

6.3 Potential Interaction: Geology

Geology plays a major role in the possible groundwater interaction between the two mines situated in the study area. It is expected that the Transvaal Supergroup dolomites and the Ventersdorp Supergroup lavas will act as aquicludes restricting groundwater movement from the overlying coal mining into the underlying gold mining (refer to section 5.3 Impermeable layers). As a rule of thumb, it is safe to assume that a cover of 50 m (based on K-values, Kruseman & De Ridder, 1994) or more of Ventersdorp Supergroup lavas in this study area will form an impermeable layer restricting movement of groundwater from the overlying coal mine into the underlying gold mine.

The Ventersdorp Supergroup lavas appear to thin towards the south-southeast of the study area, with the exception of the southern boundary of the study area where the Ventersdorp Supergroup lava is either very thin or sub-outcrop against the Karoo Supergroup as shown in Figure 67 and Figure 68. In these areas the potential for groundwater interaction between the two mines is much higher than in the areas where the Ventersdorp lava is thicker than 50 m.

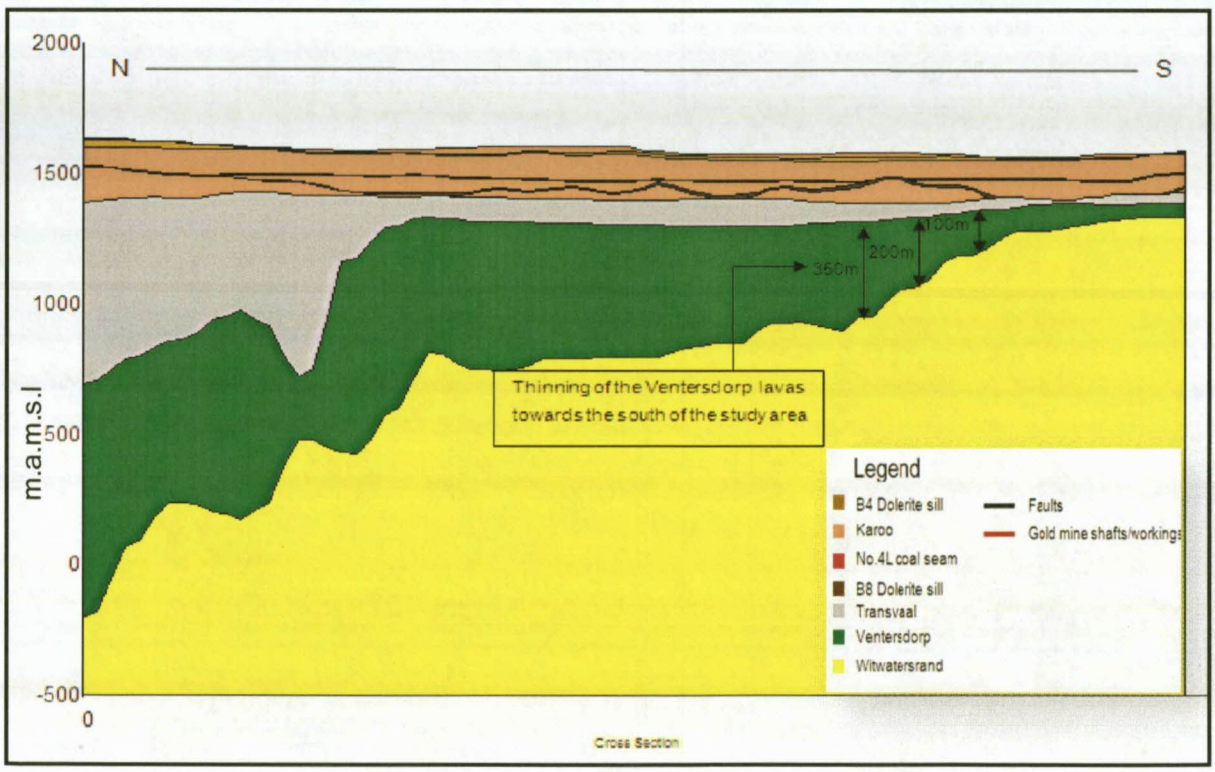

Figure 67: Thinning of the Ventersdorp Supergroup from north to south.

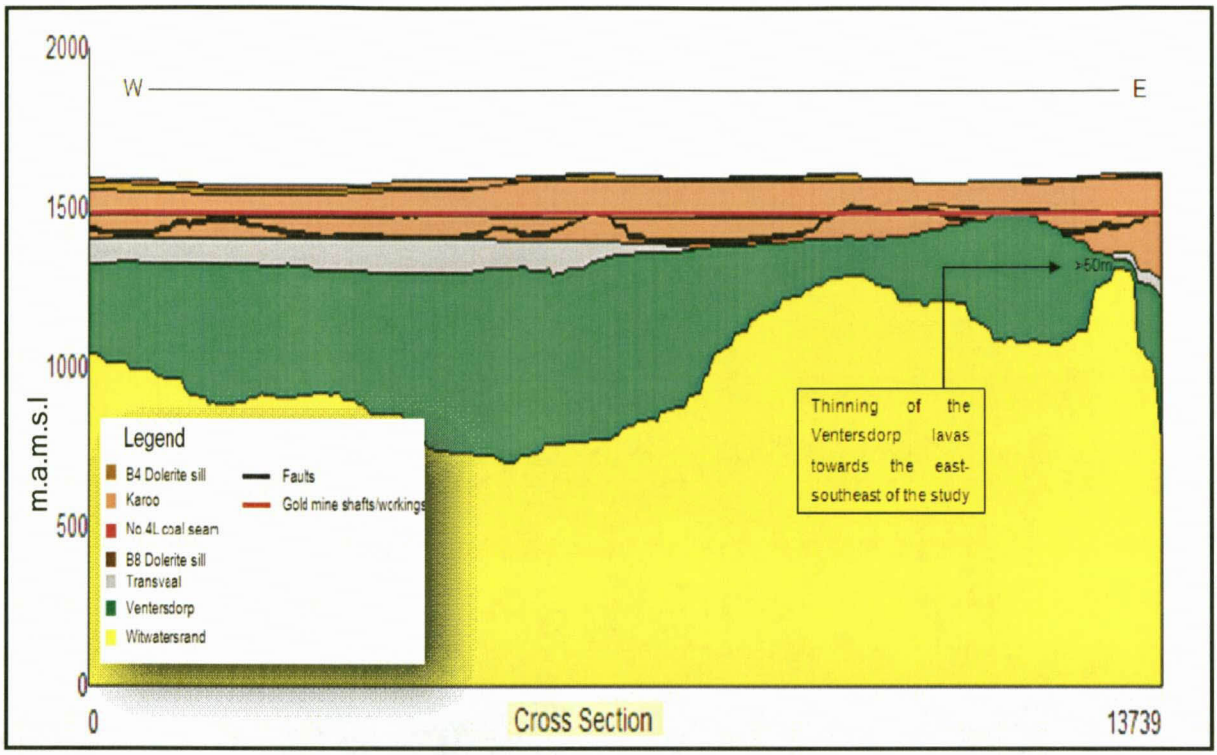

Figure 68: Thinning of the Ventersdorp Supergroup from west to east.

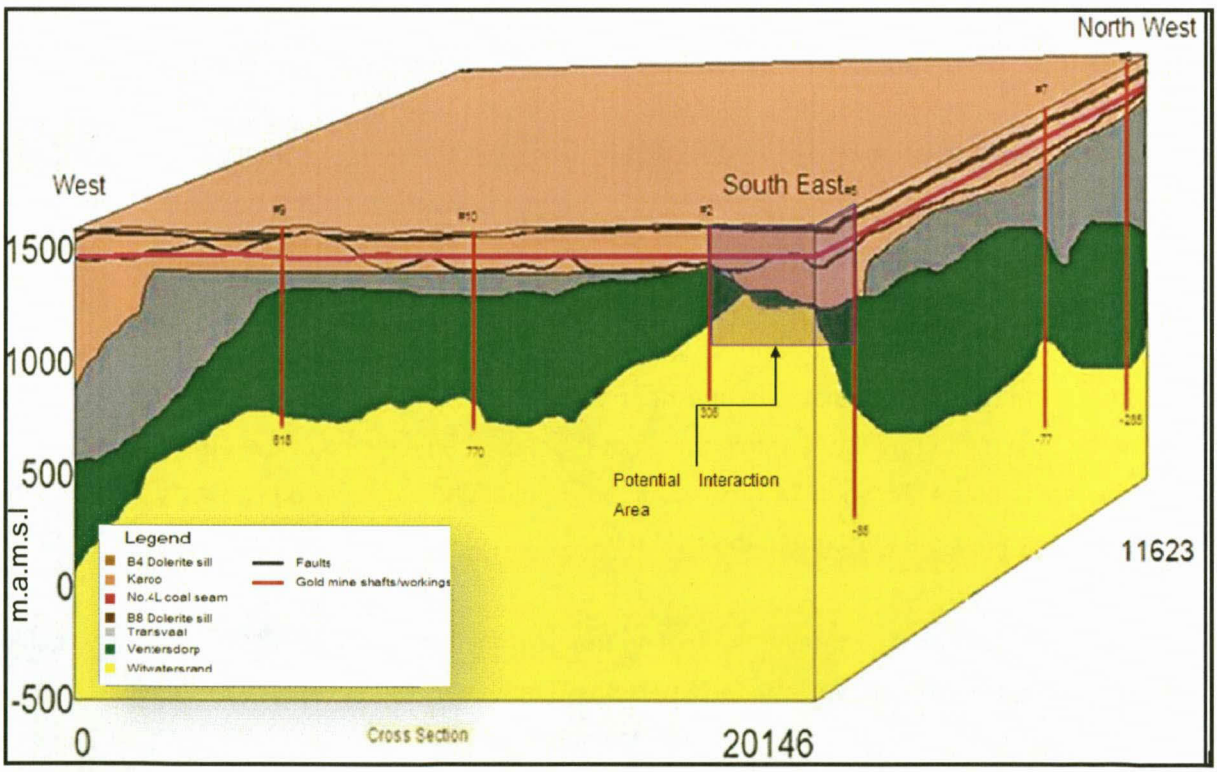

Figure 69: Potential Interaction area based on geology.

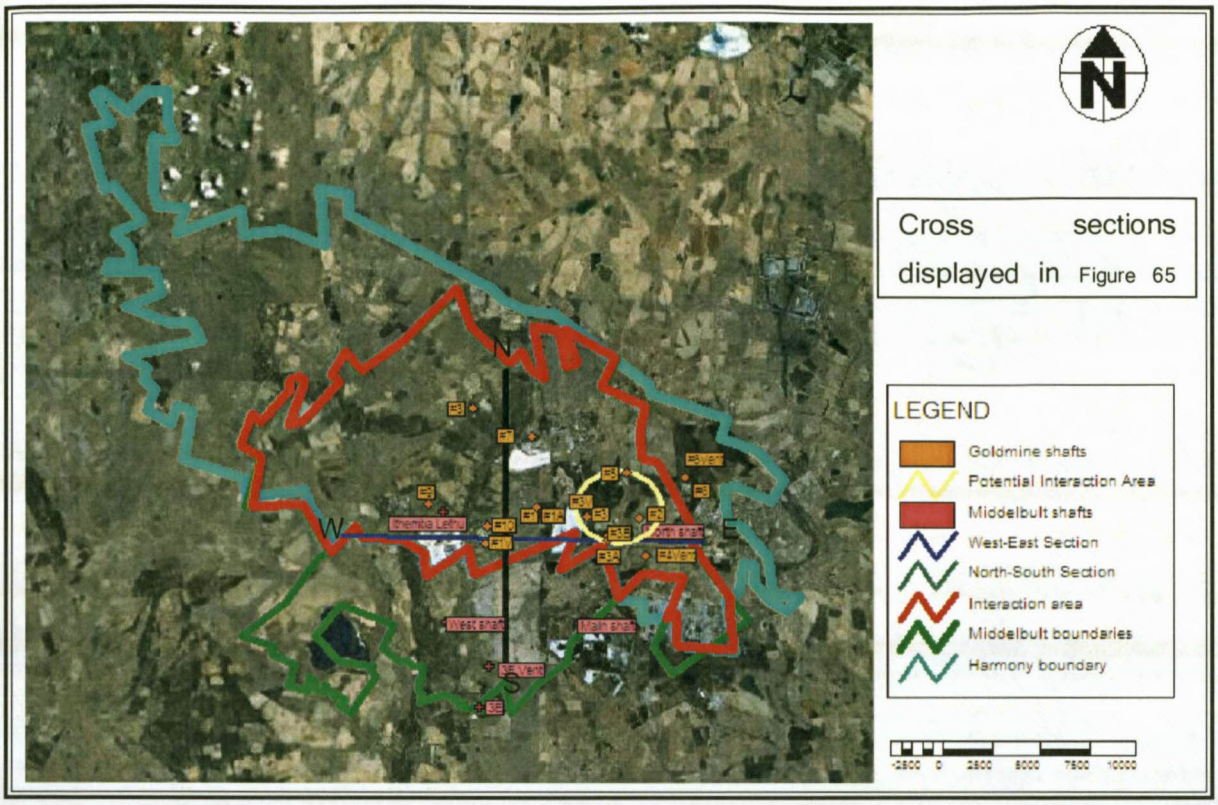

Figure 70: Surface view of the Potential Interaction Area combined with the west-east and north-south cross sections.

6.4 Potential Interaction: Preferential pathways

Samples were collected from all water-bearing structures intersecting the gold mine and these are summarised in Table 7. It should be noted that these points are the only water- bearing structures found in the study and therefore the only known pathways potentially connecting the Karoo aquifer with the Witwatersrand aquifer. Also of importance from the mining layout and the positions of the samples is that only the deep gold mine samples **H6**, **H7** and **H10** could be affected by coal mining as future mining has not reached the positions of the other underground gold mine samples as shown in Figure 74. All preferential pathways were physically and visually inspected were possible throughout the gold mine.

- **H1 and H4** - Water from faults intersecting the gold mine, the origin of this water is possibly from the base of the Karoo aquifer where the Transvaal Supergroup (aquiclude) is absent and where the faults went through the Ventersdorp Supergroup (aquiclude) and into the Witwatersrand aquifer. Groundwater will move along these faults until they intersect the gold mine workings. The position of the faults are at Evander No. 8 shaft, 11 level 1340 m below

surface (Figure 42) and at Evander No. 8 shaft, 18 level 1830 m below surface. It unlikely that the coal mining will reach the area where these faults are (Figure 53) and therefore it is unlikely that the coal mine will have an impact on the gold mining through these specific faults (Table 7).

- **H2** - Water from fractures next to dyke and exposed in the gold mine workings the origin of this sample will be where fractures next to the dyke allowed for groundwater flow (Cook, 2003). These fractures may or may not be directly connected to surface (Cook, 2003) and therefore recharge may occur in the sub-surface at different depths through the influx of overlying aquifers or directly by surface precipitation. The position of the fractures next to a dyke were encountered at Evander No. 8 shaft, 11 level approximately 1340 m below surface shown in Figure 41. It is unlikely that the coal mining will reach the area where this dyke is encountered (Figure 53) and therefore it is unlikely that the coal mine will have an impact on the gold mining through this specific dyke (Table 7).
- **H3** - Water from exploration borehole intersecting the gold mine workings. According to Middelbult Mine, Block 8 Expansion EMPR (2003) all gold mine exploration boreholes will be sealed off with a non-reactive material to prevent the drainage of groundwater from the coal mine to the gold mine. It is unlikely that the coal mining will reach the area where this borehole is situated (Figure 53). Therefore coal mining will have no impact on the gold mining through this specific exploration borehole. The position of the exploration borehole is at No. 8 shaft 15 level 1620 m below surface (Table 7).
- **H5, H6, H7 and H10** - Water dripping out of the mine roof which origin is difficult to determine. The origin of these samples is thought to be flux from fissures/fractures and joints from overlying aquifers. The position of the samples can be seen in Table 7. All of these positions can be affected by coal mining except **H5** which is at Harmony No. 8 shaft and will remain unaffected by coal mining as no coal mining will occur around No. 8 shaft area (Figure 53).
- From communications with the coal and gold mine there is explorations borehole underneath the Winkelhaak slimes dam leaking into the coal mine. The presence of this borehole could not be confirmed as the area underneath the slimes dam is inaccessible due to the flooding of the coal mine.

Chapter Seven: Hydro-chemistry and Stable Environmental Isotopes

J.D. Hem (1985) gives a detailed description of the chemical principles involved in naturally occurring water as well as the behaviour of different elements in natural waters (see Hem, H.D., 1985. "Study and interpretation of the Chemical Characteristics of Natural Waters." United States Geological Survey - Supply Paper, no. 2254). An understanding of the hydro-chemistry of groundwater systems is required for any relevant interpretation. The following is an overview of the principles and applications of natural water chemistry, gathered predominately from the work of Hem (1985).

7.1 Environmental factors affecting groundwater chemistry

Solutes are derived from a number of sources, including rocks from the earth, the oceans, animal and human activities. Water moves through the hydrogeological cycle, with solutes being added and removed from solution at various stages of the cycle (Hem, 1985). Solutes present in any form of solution represent the net effect of a series of chemical reactions. These include the dissolving of material from solid phase, the altering of previously dissolved components and the eliminating of certain components from solution by evaporation or ion-exchange reactions. The concentrations of solutes as well as the reactions occurring in a given natural groundwater system are influenced by factors such as climate, geological setting and biochemical effects from plant, animal or human interaction. The most significant factor, however, is the geological setting and its interaction with the groundwater of a given area (Hem, 1985).

7.1.1 Climate

Both temperature and precipitation influence weathering rates and hence the transfer of components from a solid or gaseous phase into a liquid. The amount of rainfall and evaporation are important parameters affecting the chemical composition of natural groundwater (Hem, 1995).

7.1.2 Geological Setting

Evaluating the composition of the rock types provides a good indication of the solutes available for uptake in the hydrogeological cycle. Elements found in groundwater in the mining sector

come from a variety of sources, but most significantly from the host rocks through which the water flows, particularly from the decomposition of minerals caused by weathering and contamination caused by mining activities.

Weathering can be both physical and chemical. The mechanical (physical) breakdown of rocks increases the surface to volume ratio, which in turn makes chemical weathering more effective (Eby, 2004). Chemical weathering is the process that adds most types of soluble minerals to natural waters.

There are four major types of chemical weathering as described by Eby (2004):

- Oxidation: the reaction with of oxygen with minerals in which reduced forms of elements are oxidised is termed oxidation. For example, the reactions of oxygen with pyrite:

  Equation 5

  $4FeS_2$ (Pyrite) + $15O_2$ + $8H_2O$ » $2Fe_2O_3$ (Hematite) + $8H_2SO_4$
- Congruent dissolution by water: simple dissolution of minerals that are soluble in water. For example, the simple dissolution of NaCl (halite) releases Na^+ and Cl^- into solution:

  Equation 6

  NaCl (halite) » Na^+ + Cl^-
- Congruent dissolution by acids: minerals are dissolved by acid attack, often organics formed in the soil. For example, the congruent dissolution of calcite by acid attack releases Ca into solution:

  Equation 7

  $CaCO_3$ (Calcite) » H_2CO_3 (aq) » Ca^{2+} + $2HCO_3^-$
- Incongruent dissolution by acids: minerals breakdown into ions in solution as well as the solid phase of different compositions. For example, the incongruent dissolution by acids of plagioclase release Na into solution while forming kaolinite:

  Equation 8

  $2NaAlSi_3O_8$ (Na-plagioclase) + $2H_2CO_3$ + $9H_2O$ » $Al_2Si_3O_5$ (kaolinite) + $2Na^+$ + $2HCO_3^-$ + $4H_4SiO_4$ (aq)

Once in solution, various other mechanisms remove the solutes, again altering the chemistry. Yechieli & Wood (2002) describe these mechanisms as:

- Precipitation of salts;
- Dissolution precipitation processes;
- Ion-exchange and adsorption;
- Redox reactions.

Precipitation is a major sink for solutes, causing a change in the residual brine. Throughout the groundwater regime, minerals can be dissolved by water as well as precipitated out of the groundwater depending on their solubility, thus adding or removing solutes from solution. Ion-exchange can have a large effect on the hydro-chemistry of groundwater (Appelo & Postma, 2005). Redox reactions associated with organic matter can have a considerable effect on groundwater chemistry. Reduction of sulphates to sulphides is one of the most common processes.

Certain physical aspects also play a role in the supply of solutes: aquifers consisting of porous rocks more readily supply solutes, through factors such as:

- the size of the crystals within the rock;
- rock texture and porosity;
- regional structure formation and length of exposure or residence time.

Furthermore, the depth below surface to which the water is transported plays a key role in water quality, since solubility increases with increasing temperature, as do dissolution rates (Eby, 2004).

Thus the geology of an area plays an important role in groundwater quality. Many sedimentary and igneous rocks in the gold and coal mines contain reactive minerals that may create acidic conditions when in contact with oxygen and water (Drever, 1997). These reactions are collectively referred to as Acid Rock Drainage reactions or more commonly as ARD.

Sulfide-bearing minerals, of which pyrite (FeS_2) is the most abundant, will react with water in an oxidising environment to form sulphuric acid (H_2SO_4). Detailed reactions are (Freeze & Cherry, 1979):

Equation 9
$FeS_2 + 7/2\ O_2 + H_2O \Rightarrow Fe^{2+} + 2SO_4^{2-} + 2H^+$

Equation 10
$Fe^{2+} + 1/4O_2 + H+ \Rightarrow Fe^{3+} + 1/2\ H_2O$

Equation 11
$Fe^{3+} + 3H_2O \Rightarrow Fe\ (OH)_3$ (yellow boy) $+ 3H^+$

Equation 12
$FeS_2 + 14Fe^{3+} + 8H_2O \Rightarrow 15Fe^{2+} + 2SO_4^{2-} + 16H^+$

Sulphuric acid is a strong acid that will mobilise most heavy metals, which will lead to widespread contamination of the aquifer system. ARD is specifically associated with coal and gold mines, as pyrites are abundant in carbonaceous material (Vermeulen & Usher, 2003).

Witwatersrand Supergroup sedimentary rocks in the gold mining area may contain water that was trapped within pores during their deposition (McKnight Geotechnical Consulting *et al.*, 2002). This water is known as pore or connate water, and is usually briny as a result of extensive ion-exchange reactions. As the pressure and temperature steadily increase (as more material is deposited), the pre-water will be released from the pores and will cause an increase in the salinity of the surrounding groundwater (Onstott *et al.*, 2006).

Geological structures such as dykes are known to create separate groundwater compartments in which the groundwater chemistry may differ from surrounding aquifers. Groundwater compartments may receive less or more recharge than the surrounding aquifer, which will lead to an increase or decrease in groundwater salinity. This can occur in gold mines as well as in coal mines (Vermeulen & Usher, 2003).

7.1.3 Biochemical effects

Reactions involved in life processes such as the decay of organic matter occur not only in freshwater bodies but also in groundwater bodies. The removal from, or addition of solutes to, the water body can occur through many varying life forms (Onstott *et al.*, 2006).

7.1.4 Other factors

7.1.4.1 Unsaturated zone

The unsaturated zone is defined as the area between the water table and the land surface. The unsaturated zone is of great importance, as it plays a role in the recharge of an aquifer as well as the quality of the groundwater (Freeze & Cherry, 1979). The unsaturated zone acts as a filter that will filter out any solids in the water before it enters the aquifer. The volume of water that will filter through the unsaturated zone is determined by its composition and thickness. If the unsaturated zone is composed of clayey or other impermeable material, only a small volume of water will filter through it and enter the aquifer. The thickness of the unsaturated zone is determined by subtracting the surface elevation from the groundwater level elevation (Freeze & Cherry, 1979).

7.1.4.2 Aquifer recharge and groundwater residence time

The residence time of groundwater refers to the time that groundwater remains within an aquifer before it is discharged into surface water bodies (Asano *et al.*, 2002). An increase in the residence time of groundwater will lead to an increase in groundwater salinity (Onstott *et al.*, 2006). When groundwater is in contact with reactive minerals, ion-exchange will cause the groundwater to become progressively more saline. Under natural geohydrological conditions, one can distinguish between groundwater within higher elevated areas and groundwater found within valley bottoms or lower elevated areas. Groundwater found within the higher elevated areas will plot within field one or two of the Expanded Durov diagram (Figure 91 and Figure 92), which represent fresh, recently recharged groundwater that has undergone a minimum degree of ion-exchange. The groundwater chemistry will therefore closely resemble the chemical composition of fresh rainwater due to the limited degree of ion exchange. As the groundwater migrates downstream, an increase in aquifer residence time will lead to an increase in the degree of ion exchange, which will ultimately lead to higher salinity in the groundwater in lower areas. A high hydraulic conductivity, good aquifer recharge, and sufficient groundwater gradients will mobilise groundwater, which will minimise the amount of time that groundwater spends within an aquifer and will lead to improved groundwater quality.

7.1.4.3 Human effects

Finally, and probably the most noteworthy, are the effects that humans have on the environment and the composition of naturally occurring groundwater. The effects of mining both coal and gold and other anthropogenic activities such as the disposal of mine waste often affect groundwater by adding solutes to naturally occurring groundwater, often resulting in significant problems in these scarce water resources. The sources and interactions of elements occurring as major cations and anions in natural waters are summarised in Table 11.

Table 11: Characteristics, sources and interactions of elements occurring as major cations and anions in natural waters (Concentrations from Appelo and Postma, 2005).

Element	General	Source	Ion interactions	Typical freshwater concentration in mg/l
Calcium	Most abundant alkali earth metal. Only one oxidation state	Pyroxenes, amfibioles, feldspars, Carbonate mineral, dolomite and calcite, gypsum fluoride.	Absorbed onto clay surfaces, often involved with cation-exchange reactions	2 to 80
Magnesium	Alkaline earth metal. Only one oxidation state. Smaller than Na and Ca, therefore more hydrated	Pyroxenes, amphiboles, micas, chlorite, olivine, serpentine, dolomite	Strongly absorbed onto clay surface, involved in exchanged reactions	1 to 50
Sodium	Abundant alkali earth metal. Only one oxidation state	Feldspars, clay minerals such as kaolinite, illite, industrial wastes	Absorbed onto clay surfaces, often involved with cation-exchange reactions	2 to 50
Potassium	Alkali metal, larger than Na. Found in 1+ oxidation state. Once in solution, tends to be reincorporated in solid, weathering state	K-feldspars, ash	Absorbed onto clay surfaces	0.5 to 80
Silicon	Second only to oxygen in abundance	Feldspars, pyroxenes, also more soluble forms of quartz, such as opal or chert	Absorbed onto mineral surfaces	0.5 to 30
Sulphur	Non-metal occurring in oxidation state, often found in high oxidation state, SO_4^{2-} or reduced form, S^{2-}	Metallic sulphides and evaporates, e.g. pyrite and gypsum, burning of fuels, smelting of ores.	Sulfide oxidation, often forms complexes	1 to 500 as SO_4^{2-}
Chloride	Most abundant of halogens. Volatile element. Chloride ion Cl- most significant oxidation state. 75 % of Cl occurs in oceans	Lower concentration in rocks compared to other rocks. Found in sedimentary rocks and evaporites.	Subdued chemical behaviour, does not take part in redox reactions, not absorbed, forms complex ions with seawater and brines at high Cl-	2 to 70
Fluoride	Lightest element of halogen group, F- is ion in solution	Fluorite, amphibole, micas, apatite, ash	May substitute -OH in minerals same size and charge, absorbed well onto gibsite	≤ 1
Nitrogen	In water as NO_2^- NO_3^- NH_4^+ Crustal rocks contain 25 % of Nitrogen	Humans, fertilisers, combustion of fossil fuels, waste disposal (CN-), sewerage.	Often indicator of pollution	0.01 to 12 as NO_3^-
Phosphorus	In water mainly as PO_4^{3-}	Apatite, phosphorites. Humans, fertilisers, sewerage, insecticides.	Co-precipitation and adsorption onto minerals	0 to 2 as PO_4^{2-}

7.2 Sampling

To determine the origin of groundwater in both mines, sampling was done at strategic positions at each mine. Samples were taken from surface boreholes as well as underground in each mine. Sampling at different depths within the mines allows water quality data to be collected for both mines. The surface view of the sampling positions is shown in Figure 71 and the underground view of sampling positions is shown in Figure 72. A summary of sampling positions is displayed in Table 12.

Table 12: Sampling summary.

Harmony & Sasol Surface Borehole Samples						
Harmony Surface	Coordinates		Elevation (m.a.m.s.l)*	Sampling depth in m below surface	Borehole depth in m below surface	Depth in m below surface
Borehole name	Y	X	Z			
KB 1 D	-2929816.932	7611.298	1591.324	28	30	3.5
KB 5 D	-2929401.146	8886.292	1615.099	28	30	1.02
WB 1 D	-2932446.352	10378.745	1589.468	28	30	1.6
WB3D	-2933838.364	10023.214	1599.229	28	30	1.3
WB 5 D	-2933225.999	11669.846	1621.612	28	30	22
Sasol Surface	Coordinates		Elevation (m.a.m.s.l)*	Depth in m below surface		Depth in m below surface
Borehole name	Y	X				
MHN 47	-2935823.037	11478.324	1578.937	110	Into mine	108.19
MHR 45	-2935046.371	10963.433	1600.137	130	Into mine	129.44
MDB Casino	-2933683.916	15952.46	1581.346	100	Into mine	97.67
m.b.g.l- metres below ground level/ m.a.m.s.l- metres above mean sea level						

Harmony & Sasol Underground Samples				
Harmony samples	Depth in m below surface	Level	Shaft or posistion	Description
H1	1340	11	8	Water from fault
H2	1340	11	8	Water next to dyke
H3	1620	15	8	Water from exploration borehole
H4	1830	18	8	Water from fault
H5	2152	24	8	Water dripping from roof stope
H6	619	1	9	Water dripping out of mine roof (minimal)
H7	619	1	9	Water dripping out of mine roof (minimal)
H10	634	8	2	Water dripping out of mine roof (minimal)
Sasol samples	Depth in (m below surface)	Level	Shaft or position	Description
S1	104	In coal mine	Near Main shaft	Borehole into mine workings
S2	113	In coal mine	Near North Shaft	Water dripping out of mine roof (minimal)
S3	105	In coal mine	Block 38	Fissure water from mine floor
S4	80	In coal mine	Near West shaft	Water dripping out of mine roof (minimal)
S5	55	In coal mine	Block 35	Water dripping out of mine roof (minimal)
(m.a.m.s.l)* metres above mean sea level				

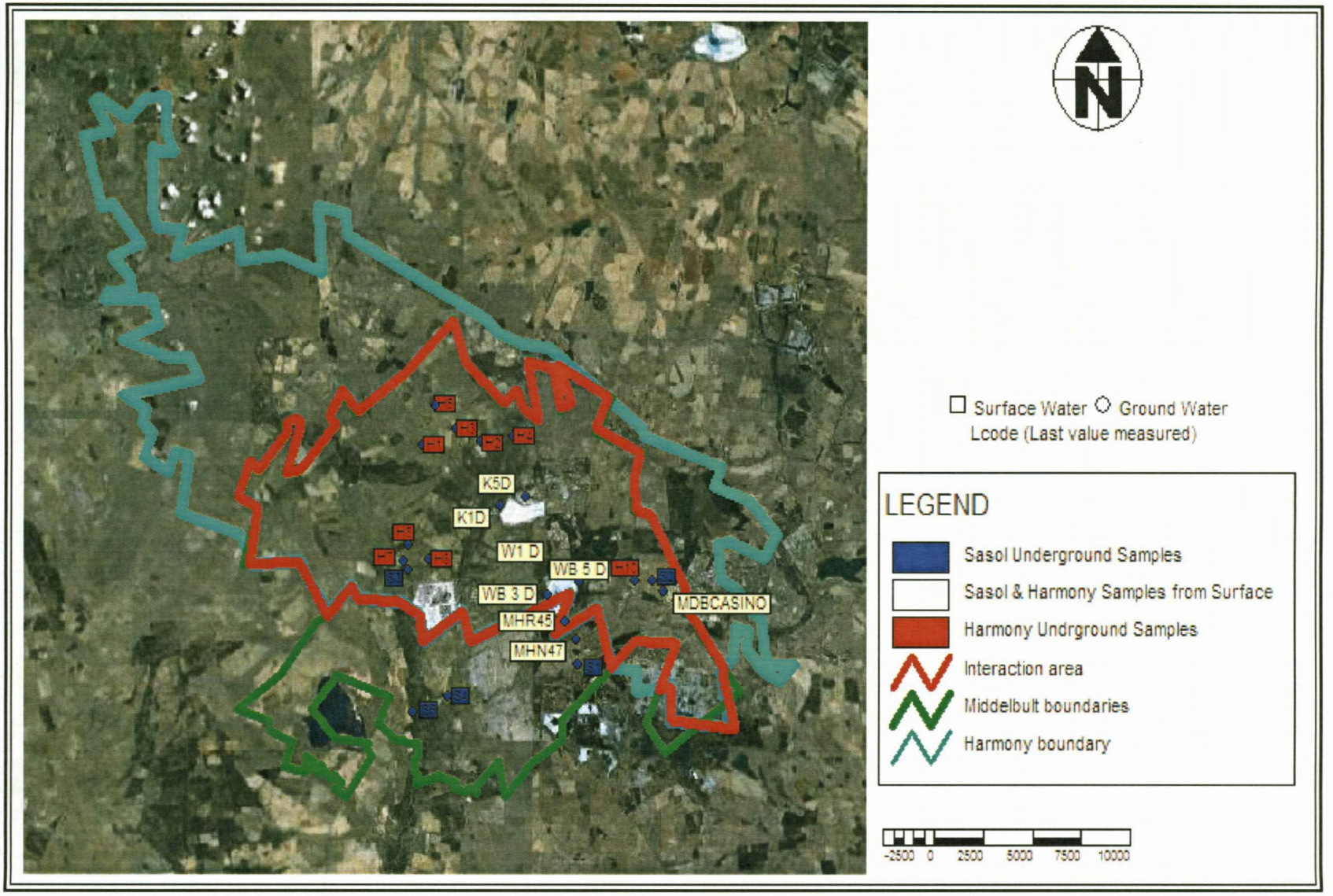

Figure 71: Surface view of the sampling positions.

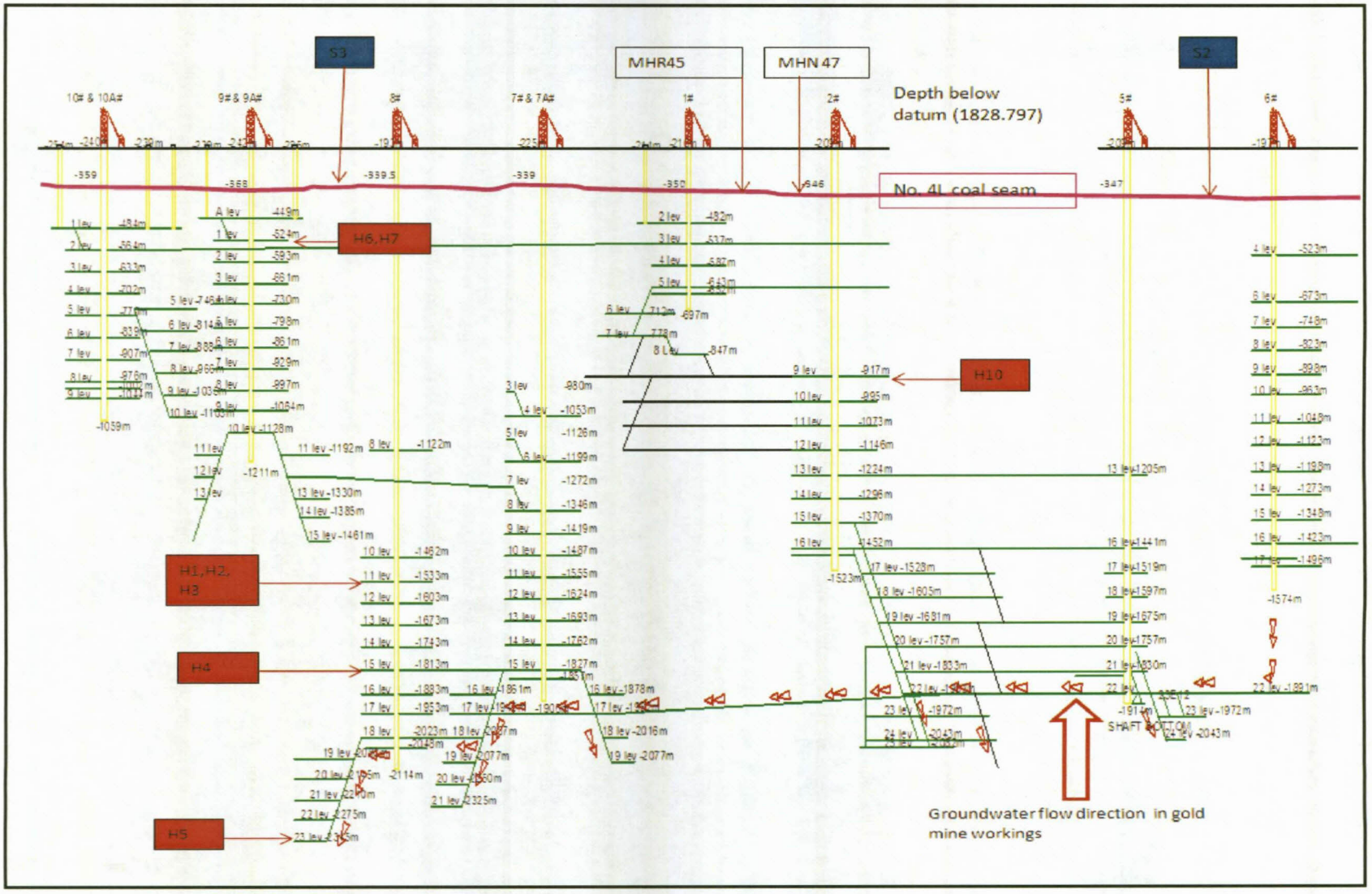

Figure 72: Underground view of the sampling positions.

7.2 Sampling Protocol

The same sampling protocol was applied during each sampling survey. Macro and trace elements as well as the stable isotopes oxygen-18 (^{18}O) and deuterium (^{2}H) were sampled for in this study.

Sampling of the hydro-chemical constituents was done by using new 250 ml plastic sampling bottles. To avoid contamination, the sampling bottle was rinsed before each sample was taken, first with sterilised water and then with water from the sampling point. Sample bottles were sealed air tight and labeled appropriately. After sampling was completed, the samples were stored in a cool (> 10°C), dry storage place until delivered to the laboratory.

Oxygen-18 (^{18}O) and Deuterium (^{2}H) samples were taken in new 250 ml, amber glass bottles to avoid contamination. The bottles were first rinsed with the sample water, then completely filled and tightly sealed. The water was not treated in any way before or after sampling. Figure 73 illustrates how the samples were taken.

Figure 73: A sample being collected in the gold mine next to a fracture.

7.3 Data interpretation techniques

In order to characterise the origin of the groundwater within the various aquifers, the following interpretation was carried out on the hydro-chemical data:

- Standard tri-linear diagrams, i.e. Piper and Expanded Durov diagrams were employed to investigate the use of these diagrams to distinguish between groundwater originating from surface or shallow Karoo aquifers or from deeper Witwatersrand aquifers.
- Various X-Y column plots of ionic ratios were used to fingerprint groundwater types with different flow paths.

There are numerous methods of displaying and defining the type of groundwater that occurs within an area.

7.3.1 Chemical parameters

Although all major elements were analysed for only the elements that are expected to show concentration increases or decreases within the coal and gold mining environment will be discussed. All analysed elements will however be studied and discussed if anomalies do occur. The chemical parameters that will be discussed in the document are the following:

- pH - pH is an important parameter, as it determines the solubility of metals in groundwater. Most metals are immobile in groundwater in which the pH varies between 5 and 9 units. pH decreases are also a good indication of the presence of acid rock drainage (ARD) reactions, which occur when sulphide-bearing minerals such as pyrite are exposed to an oxidising environment in the presence of groundwater and microbial organisms (Drever, 1997).
- Electrical Conductivity (EC) - the EC of groundwater is a good overall indication of the quality of groundwater. EC increases are generally linked to pH decreases (Drever, 1997)
- Sodium (Na) - sodium is found in high concentrations in groundwater in the Karoo Supergroup, due to its marine deposition environment. It is also found in groundwater systems that have undergone a high degree of sodium ion-exchange (Eby, 2004).
- Sulphate (SO_4^{2-}) - sulphate contamination is associated with the oxidation of sulphate-bearing minerals such as pyrite (acid rock drainage reactions - ARD). As mentioned previously, sulphate contamination will under most conditions lead to a decrease in the pH of groundwater due to the formation of sulphuric acid (Vermeulen & Usher, 2003).
- Chloride (Cl) - elevated chloride concentrations are generally due to the inherent high chloride concentrations that exist in some sedimentary rocks. High chloride concentrations are also associated with old, stagnant groundwater that has undergone a reasonable degree of ion-exchange (Eby, 2004).

- Bicarbonate (HCO_3^-) - exists in aqueous solutions containing calcium (Ca^{2+}), bicarbonate (HCO_3^-) and carbonate (CO_3^{2-}) ions, together with dissolved carbon dioxide (CO_2) (Freeze & Cherry, 1979). The relative concentrations of these carbon-containing species depend on the pH. Bicarbonate predominates within the range 6.36 to 10.25 in fresh water (Freeze & Cherry, 1979). Most groundwater in a unconfined aquifer is in contact with the atmosphere and absorbs carbon dioxide, and as these waters come into contact with rocks and sediments, they acquire metal ions, most commonly, calcium and magnesium. Therefore, most water near the surface (shallow, unconfined to semi-confined aquifers) can be regarded as dilute solutions of these bicarbonates (Freeze & Cherry, 1979).

The positions of the sampling points for which groundwater chemistry data is available are shown in Figure 71. Groundwater quality information was obtained for a total of 21 sampling points. Only once-off monitoring was done and therefore only once-off data is available, therefore no increasing or decreasing concentration trends can be identified, nor can explanations for anomalies be given with a high degree of confidence.

7.4 Hydro-chemical results interpretation

The following interpretations were made from the chemical results. It is important to note from the mining layout and the positions of the samples that only the deep gold mine samples **H6, H7** and **H10** might be affected by coal mining, as future mining has not reached the position of the other underground gold mine samples, as shown in Figure 74.

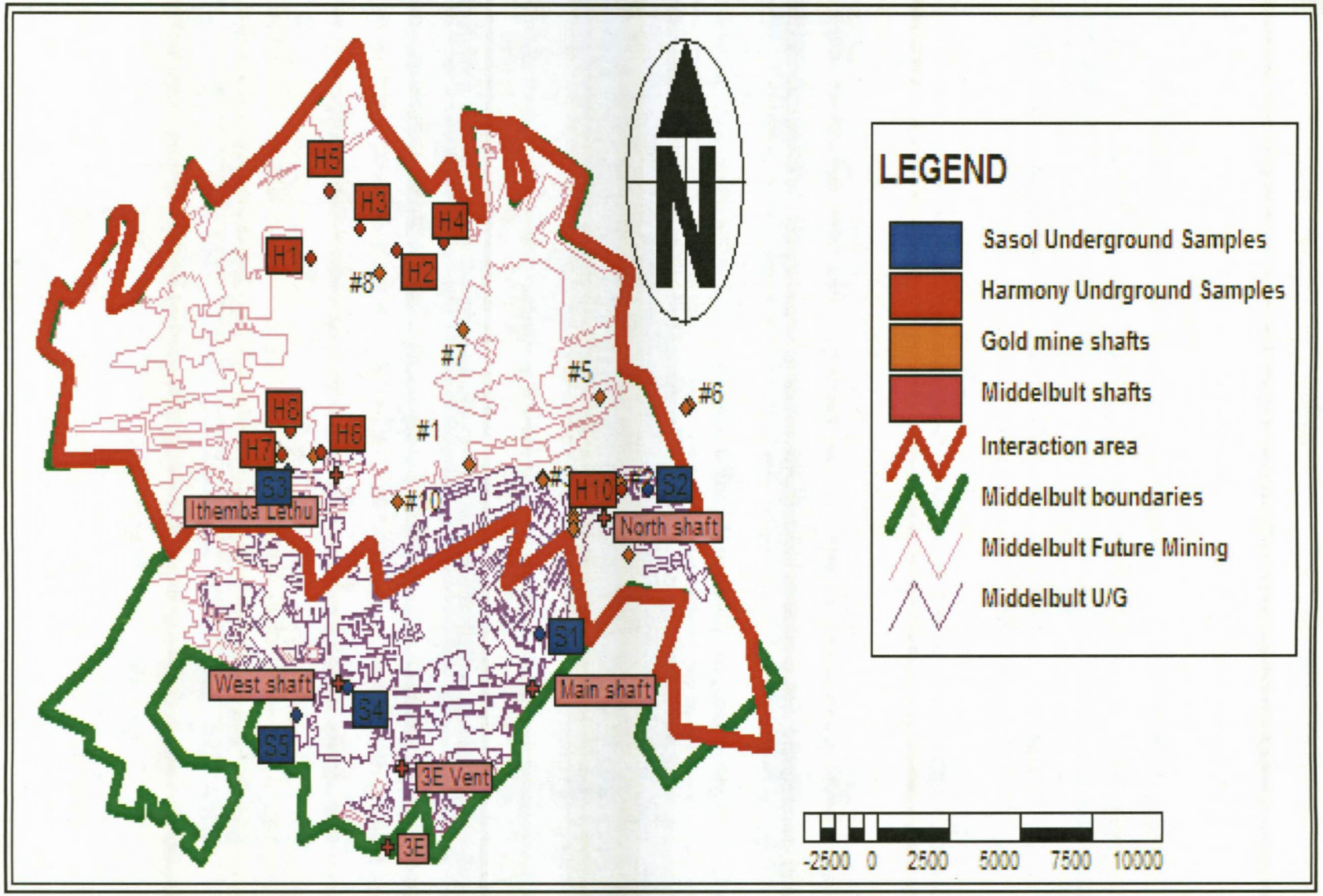

Figure 74: Underground sampling positions with the current and future coal mining layout.

7.4.1 Electrical Conductivity (EC)

EC values are a good overall indication of groundwater quality and distribution. The EC values of the sampling points range between 56.2 ms/m **(S5)** to 529 **(S1)** with an average value of 265 ms/m Figure 77 plots the EC values for the samples. The samples are plotted shallow to deep, from left to right, in Figure 76.

EC is an indication of groundwater salinity. Groundwater salinity does not appear to increase from the shallower Karoo aquifer samples (**KB1D to MHR45**) towards the deeper Witwatersrand aquifer samples (**H1 to H10**) shown in Figure 76, where **KB1D** (189) shallowest and **H5** (169) deepest are in the same order of magnitude, and this is unexpected. It can be attributed to the following factors:

- Dolerite dykes and faulting (discussed in Structural Geology Section 4.7) are known to create separate groundwater compartments in the study area (Figure 75). The groundwater chemistry differs for the different compartments. Different groundwater compartments may receive less or more recharge than the surrounding compartments, which will lead to an increase or decrease in the groundwater salinity (Hodgson & Krantz, 1995). This can be seen in samples **MDBCasino** (336), **MHN47** (156) and **MHR45** (449) all of which were taken from the already water-filled underground coal mine workings. The maximum difference is 293 between **MHR45** (449) and **MHN47** (156), indicating the difference in chemical reactions taking place in the different compartments as well as the different recharge potentials of the different compartments (Hodgson & Krantz, 1995).

- Different aquifers and depths of the samples (discussed in Hydrogeology 5.2) within the study area will lead to different recharge potentials and different chemical reactions taking place within each aquifer. This can be seen in sample **S5** (56.2) taken from the shallow Karoo aquifer compared to sample **H1** (488) taken from the deeper Witwatersrand aquifer. The difference in EC value is 431.8 ms/m between **H1** (Witwatersrand) and **MHN47** (Karoo).

- Contamination from Tailing Storage Facilities or other contamination sources may also affect the EC of the samples especially the shallow Karoo aquifer samples taken downstream and/or on preferred pathways near the gold mine tailings storage facilities. This can be seen in samples **WB1D** (89.1) and **WB3D** (500), sample **WB3D** is situated downstream and in close proximity of the Winkelhaak Slimes dam and shows elevated EC values compared to WB1D situated upstream and unaffected by the Winkelhaak slimes dam (Figure 62).

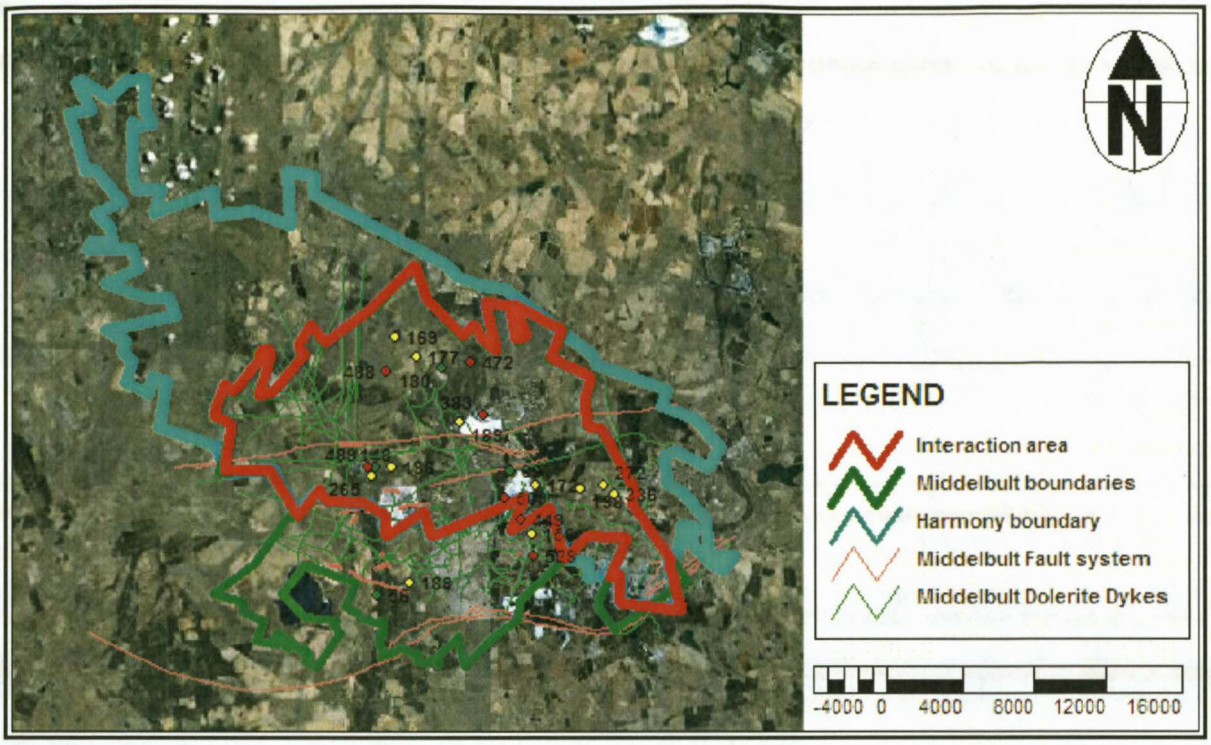

Figure 75: Dykes and faults across the study area.

- The EC values of the gold mine samples **H1** (488) and **H4** (472) are much higher than the other gold mine samples. Both these samples were taken from faults intersecting the gold mine workings, suggesting that their origin is the base of the Karoo or Transvaal Supergroup, as the faulting pre-dates the deposition of the Transvaal and hence the Karoo Supergroup (Tweedie *et al.*, 1986). They were taken at 1380 m below surface (**H1**) at 1830 m below surface (**H4**). The Karoo Supergroup is approximately 210 m thick (Figure 21). This shows that these samples had to travel approximately 1170 m (**H1**) and 1620 m (**H4**). As these samples move along the fault they react with different minerals through the process of dissolution. The more dissolution takes place, the higher the EC will be.

- **H3** (177) was taken from an exploration borehole intersecting the gold mine workings. The EC value is much lower compared to that of the fault samples **H1** (488) and **H4** (472). This suggests that it has been mixed with precipitation as the borehole is directly linked to the surface and the Karoo aquifer and that the water travelled much faster through the sub-surface, subduing dissolution with rock minerals and therefore having a lower EC value.

If the shallower Karoo Aquifer were well connected with the deeper Witwatersrand aquifer, there would have been a significant increase of EC from the shallower Karoo aquifer samples to the deeper Witwatersrand aquifer, which is not the case (Figure 76). In most of the samples, except for samples H1 and H4, the EC value decreases (Figure 76).

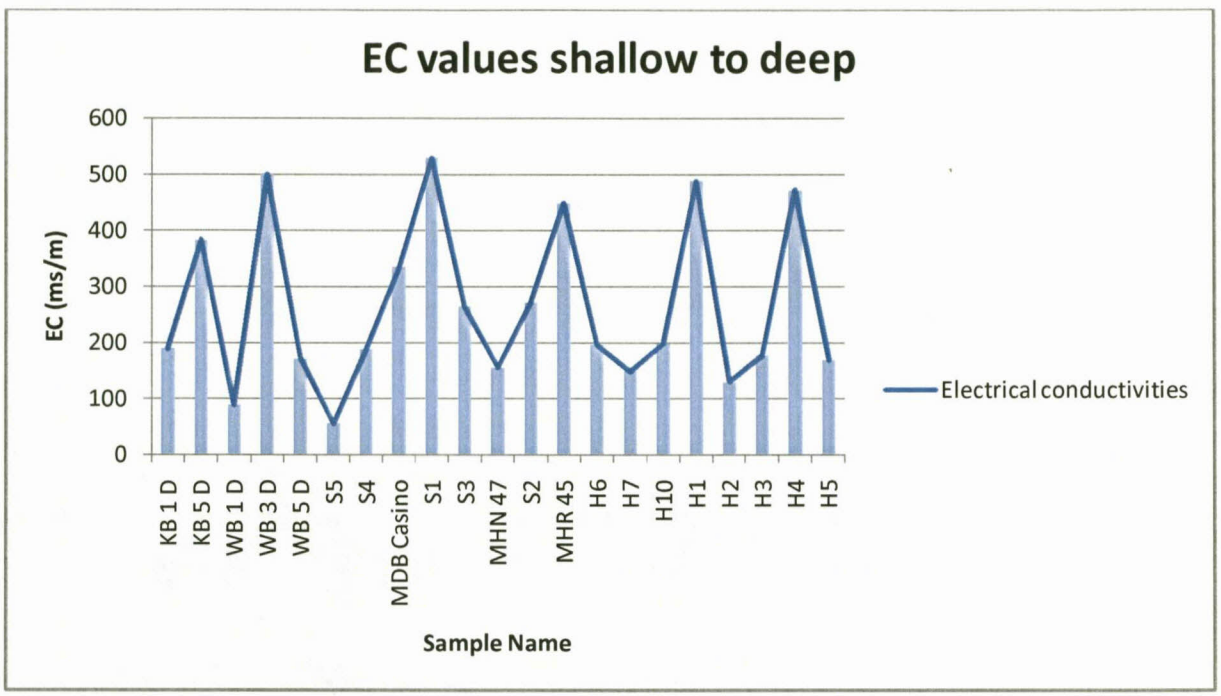

Figure 76: EC values of samples collected in this study from shallow (left) to deep (right).

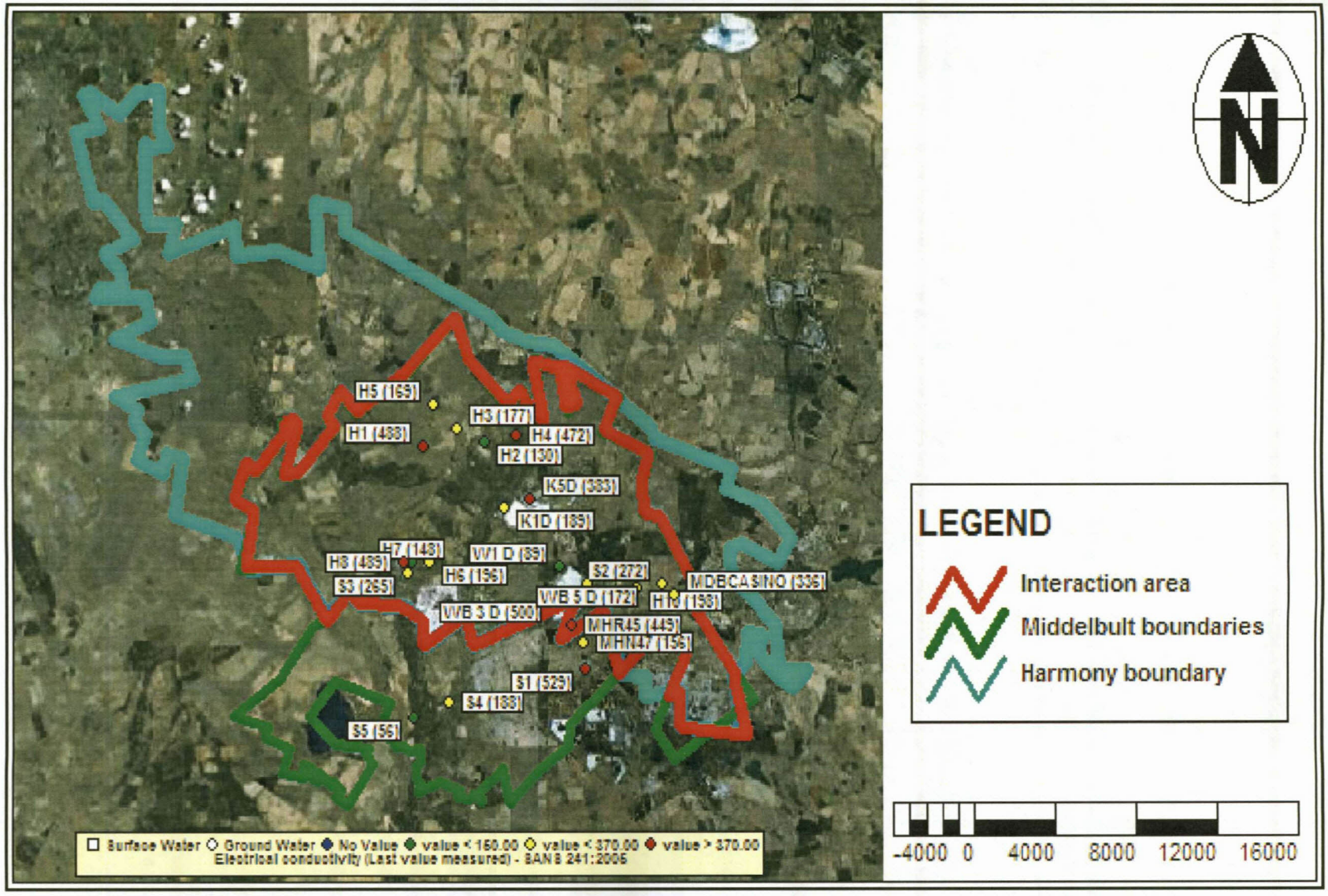

Figure 77: Electrical conductivity values for samples collected in this study.

7.4.2 pH

Groundwater pH appears to be basic throughout the samples in the study and ranges between 6.33 (**MHR 45**) to 8.8 (**H2**) with an average pH of 7.73, as shown in Figure 79. The neutralisation of the pH is due to the naturally occurring marine carbonate minerals in the Karoo Supergroup which are present in of the study area (Vermeulen & Usher, 2003). The lack of oxygen in the deeper samples will also contribute to the basic pH (Freeze & Cherry, 1979). Basic groundwater conditions are a good sign of the absence of Acid Rock Drainage reactions (Freeze & Cherry, 1979). Most metals are immobile with the basic pH values found in the study area. Groundwater pH does not appear to increase or decrease from the shallower Karoo aquifer (samples **KB1D** (7.4) towards the deeper Witwatersrand aquifer samples **H5** (8), as shown in Figure 78.

- The alkaline pH-level of the Karoo aquifer samples (**KB1D, K5D, W1D, WB3D, WB5D, S5, S4, MDBCasino, S1, S3, MHN47, S2** and **MHR45**) suggests that the Karoo aquifer has sufficient base potential to neutralise the generated acid at this point in time (Hodgson & Krantz, 1995).

- The basic pH found in the deeper Witwatersrand aquifer samples (**H1-H10**) indicates that the groundwater is deprived of oxygen and therefore basic, as oxygen is a major component for lowering the pH in Acid Rock Drainage reactions, as shown in Equation 1 to Equation 4 (Freeze & Cherry, 1979).

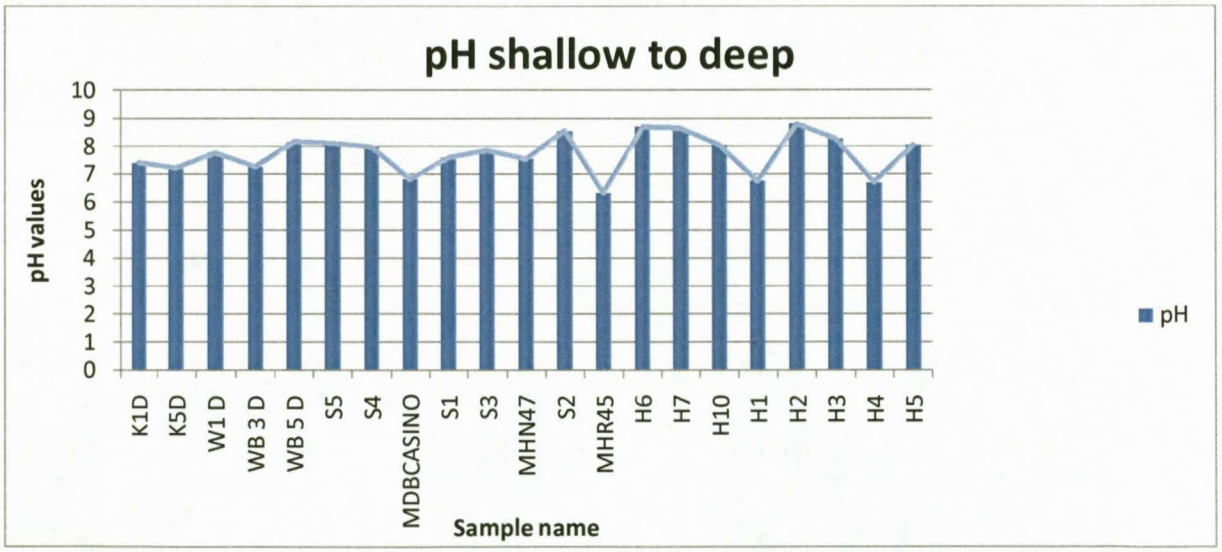

Figure 78: pH values of samples collected in this study from shallow (left) to deep (right).

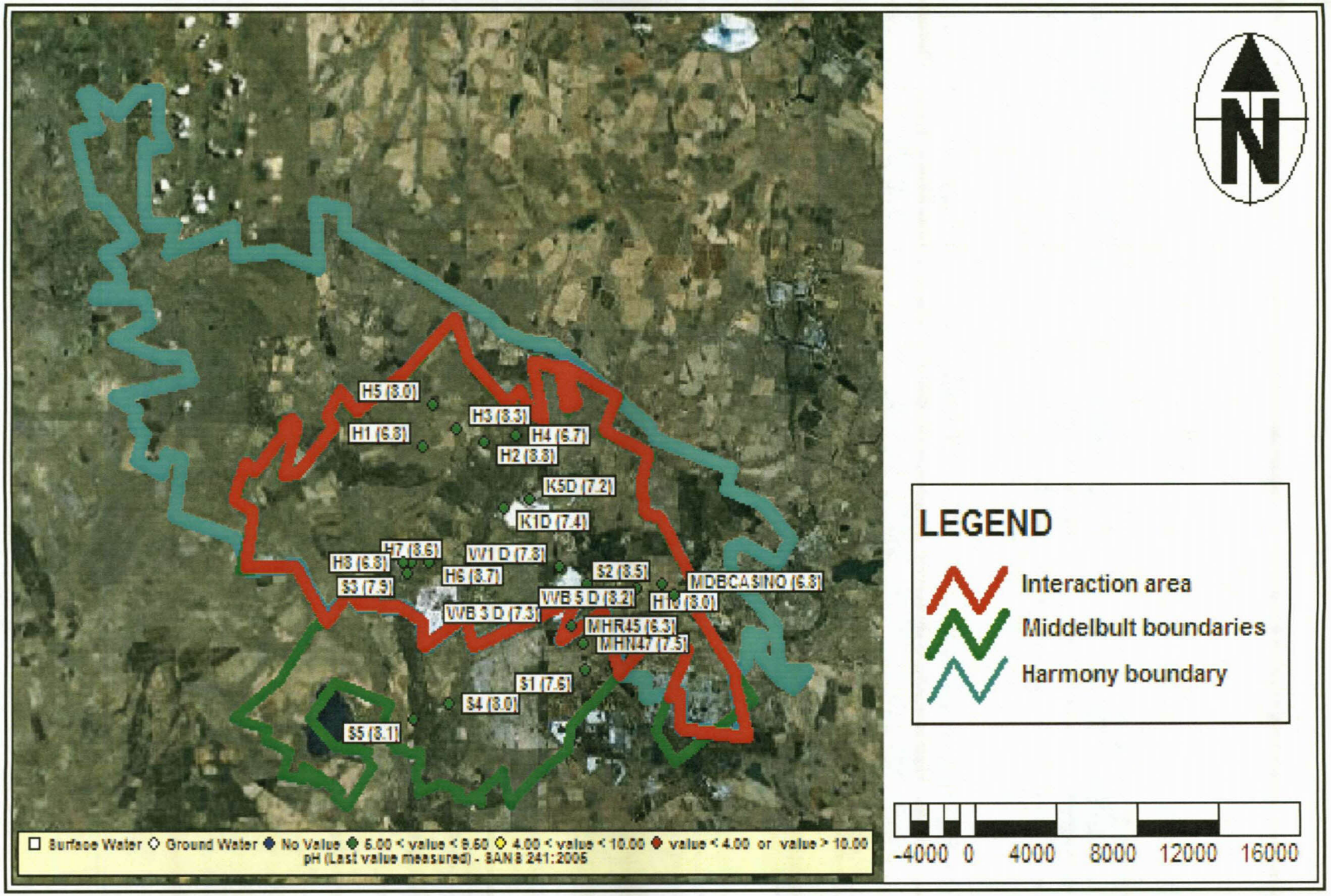

Figure 79: pH values for samples collected in this study.

7.4.3 Sodium (Na)

Sodium is a highly soluble chemical element that reacts freely with groundwater in the sub-surface. It is also found naturally in groundwater systems (Eby, 2004). It is expected that the deeper the groundwater moves through the sub-surface, the more enriched in Na it will become as it comes into contact with more minerals and more dissolution and cation-exchange will take place (see Equation 6 and Equation 8). The groundwater found in the Witwatersrand aquifer is also enriched in Na due to the long residence time of the groundwater, resulting in a longer time for dissolution to take place (Onstott *et al.*, 2006). The cation-exchange capacity is the capacity of a medium to preferentially release specific cations while binding other cations in their place. In groundwater, this process is particularly prevalent in areas of dynamic groundwater flow, such as the water-filled coal mining area, where calcium is adsorbed and sodium is released. Dissolution of sodium, potassium and chloride-bearing minerals represents the first interaction between the rock, hydrosphere and lithosphere following mining activity (Freeze & Cherry, 1979).

Figure 81 indicates that the deeper the groundwater moves in the study area, the more enriched in Na-concentration it becomes. The minimum Na-concentration is 91.34 mg/l (**S5**) and maximum is 816.13 mg/l (**H1**), with an average of 394.47 mg/l, as shown in Figure 82. This is an indication that the groundwater encountered within the deep Witwatersrand aquifer is either derived from groundwater moving slowly through the sub-surface and reacting with Na-rich minerals through dissolution and cation exchange until it reaches the end of the groundwater cycle (Figure 80), or it is paleo-meteoric water that was trapped during the deposition of the Witwatersrand sediments, which will have a high Na-concentration due to the deposition environment and relatively long residence times (Onstott *et al.*, 2006).

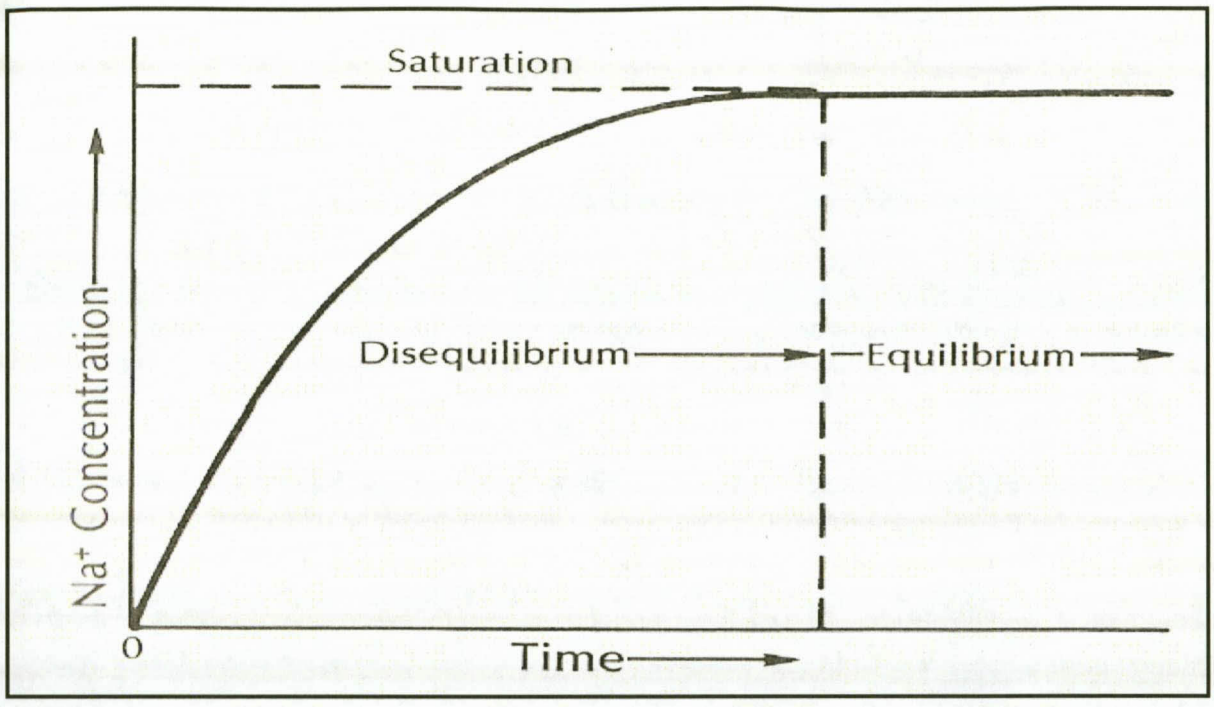

Figure 80: Sodium saturation over time.

- **H1** (816) and **H4** (717) (water from fault, Table 12) are higher in Na concentration compared to the other gold mine samples (see also EC). As these samples move along the fault, they react with different minerals through the process of dissolution and cation exchange. The more dissolution takes place, the more cation exchange takes place and the higher the Na-concentration will be.

- **H3** (347) (water from a exploration borehole, Table 12) has a lower Na concentration than samples **H1** (816) and **H4** (717) from the faults, which indicates that it has travelled at a much faster rate from the Karoo aquifer to the Witwatersrand, giving it less time for dissolution and therefore cation exchange.

- **MDBCasino** (595), **S1** (729), **S2** (691) and **MHR45** (740) are all elevated in Na concentration. They were samples taken within the coal mine filled with water. Surface water that drains towards and into the collapsed columns above high extraction areas undergoes base exchange. Calcium and magnesium are adsorbed onto clays within the sediments, in exchange for sodium (Eby, 2004). Interstitial release of sodium from the shale occurs as the water falls down the fractured columns (Hodgson & Krantz, 1995). The degree to which

cation exchange has affected the chemistry of the water is a function of the distance that the water has travelled and the composition of the rock through which it has moved. The resultant water that ends up on the coal seam horizon ranges from water almost totally devoid of calcium and magnesium, to water that may be slightly enriched in sodium (Hodgson & Krantz, 1995). The conclusion drawn from the samples is that the initial character of water in coal extraction areas is one of high sodium water.

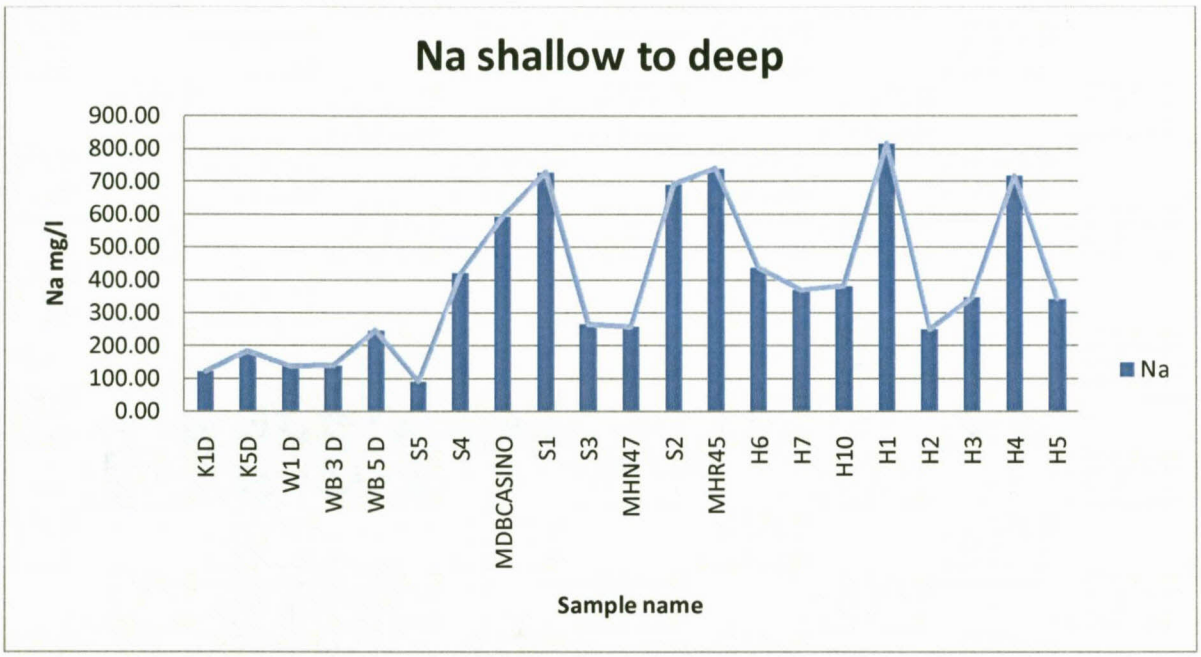

Figure 81: Sodium concentrations for the samples collected in this study from shallow (left) to deep (right).

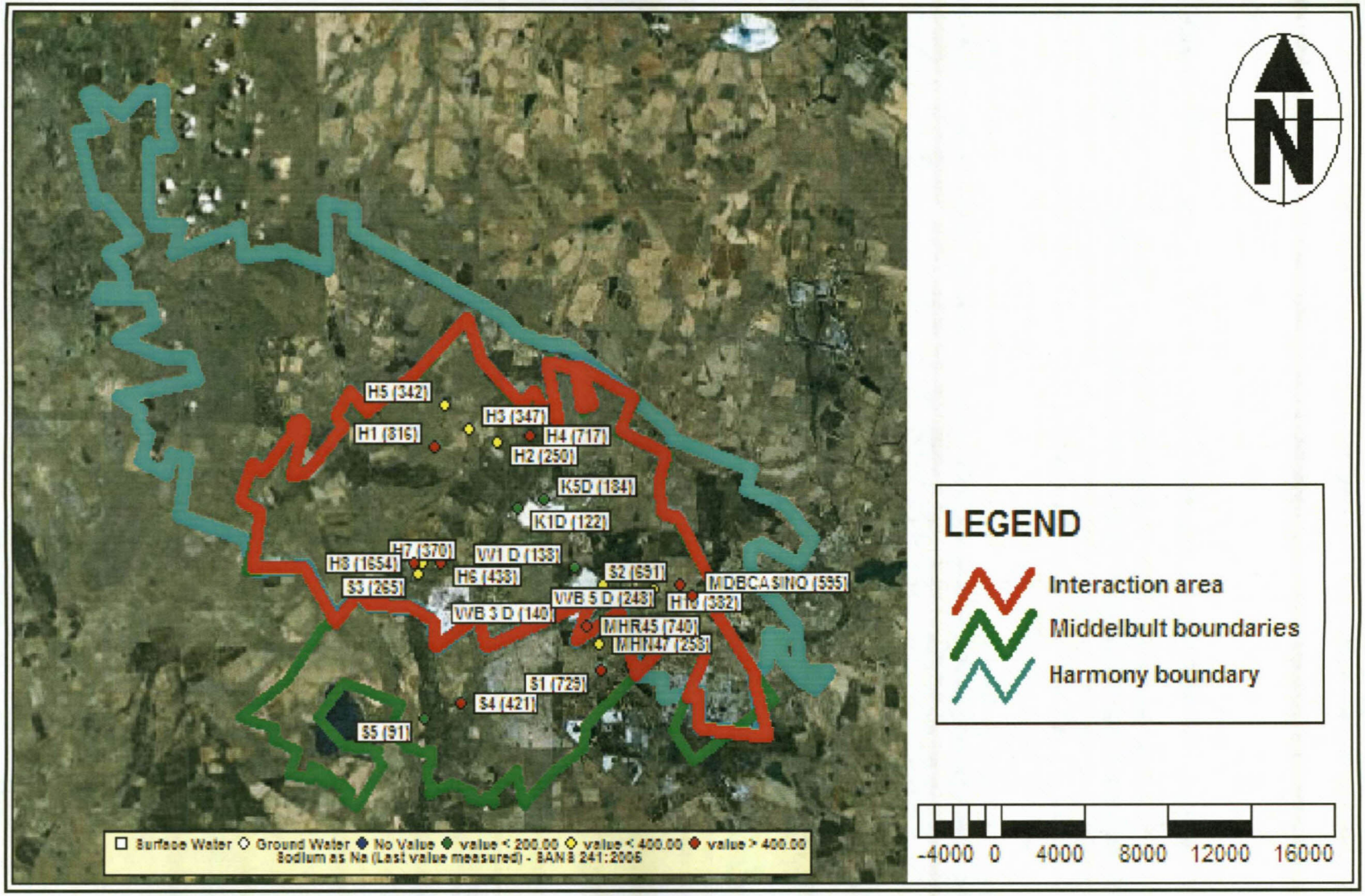

Figure 82: Sodium concentrations of the samples collected in this study.

7.4.4 Sulphate (SO_4^{2-})

The SO_4^{2-} concentration ranges from 4 mg/l (**H2**) to 2759 mg/l (**S1**), with an average value of 397.77 mg/l, as shown in Figure 84. Figure 83 shows that most of the shallower samples taken from the Karoo aquifer (**KB 5 D, WB3D, MDBCASINO, S1, S3, MHN47, MHR45**) have a higher SO_4^{2-} concentration than the deeper samples (**H1-H10**) taken from the Witwatersrand aquifer.

- Samples taken from the Witwatersrand aquifer (**H1-H10**) were either water dripping from the mine roof, fault or an exploration borehole. They have a much lower SO_4^{2-} concentration than the shallower Karoo aquifer samples. This can be attributed to a reducing environment (lack of oxygen) that inhibits oxidising reactions with sulphate rich minerals in groundwater, as explained in Equation 1 to Equation 4.

- The varying SO_4^{2-} concentration could also be attributed to the varying geology and compartmentalisation, which in some places may or may not contain sulphate-rich minerals with more or less water and oxygen.

- Samples **WB3D, MDBCASINO**, **S1** and **MHR45,** all taken from the Karoo aquifer, have relatively high concentrations of SO_4^{2-} compared to the other samples taken in the Karoo aquifer. **WB3D**'s elevated concentration can be attributed to its close downstream proximity to the Winkelhaak slimes dam, whereas elevated concentrations in samples **MDBCASINO, S1** and **MHR 45** can be attributed to the oxidation of sulphate minerals within the coal mine (Vermeulen & Usher, 2003).

- The elevated sulphate concentrations in samples **MDBCasino** (1024) and **S1** (2749) indicate that the coal seam has a high acid-generating potential (Hodgson & Krantz, 1995). However, the alkaline pH-level of the samples suggests that the coal seam also has sufficient base potential to neutralise the generated acid at this point in time. The sulphate concentrations in the underground gold mine samples (**H1-H10**) are much lower than those of the shallow Karoo aquifer samples (Figure 83). This is due to lack of oxygen and sulphate-bearing minerals such as pyrite in the deeper gold mine inhibiting the reactions shown in Equation 1 to Equation 4. Static acid base accounting tests were conducted on samples of dust on rocks obtained from mined strata in order to provide a qualitative predication of the net acidity, a function of the relative content of acid-generating minerals (sulphides) and acid-consuming or neutralising minerals (carbonates) (Winkelhaak Mine EMPR, 1988). When the

acid-generating capability exceeds the acid-consuming capacity, the pH of the water decreases, with the consequent mobilisation of sulphates and heavy metals, resulting in acid rock drainage (Winkelhaak Mine EMPR, 1988).

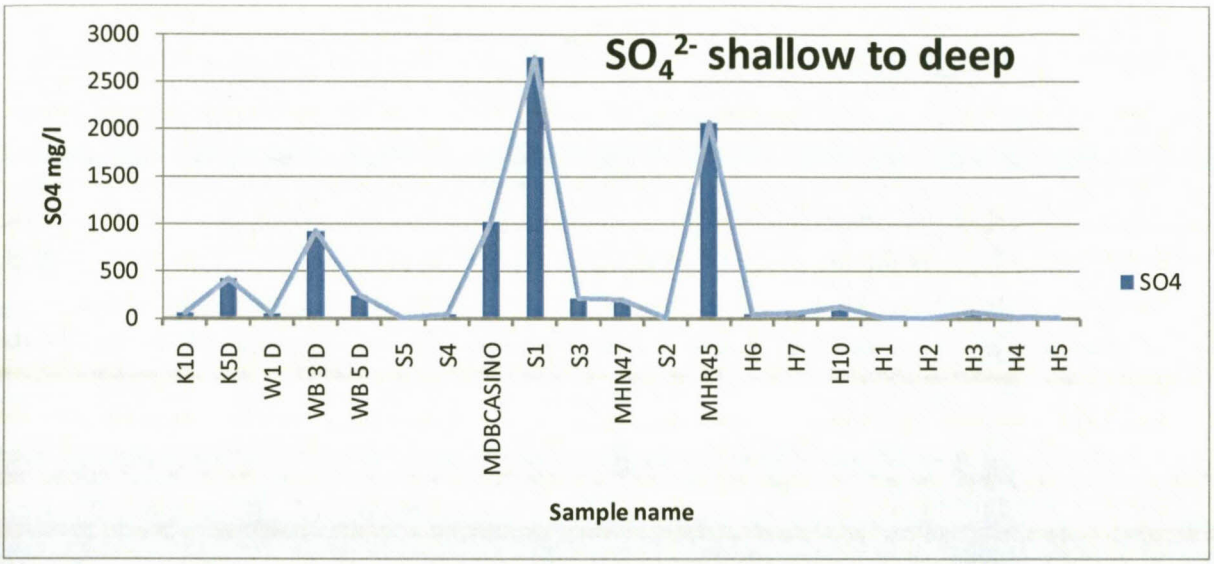

Figure 83: Sulphate concentrations in the study area from shallow (left) to deep (right).

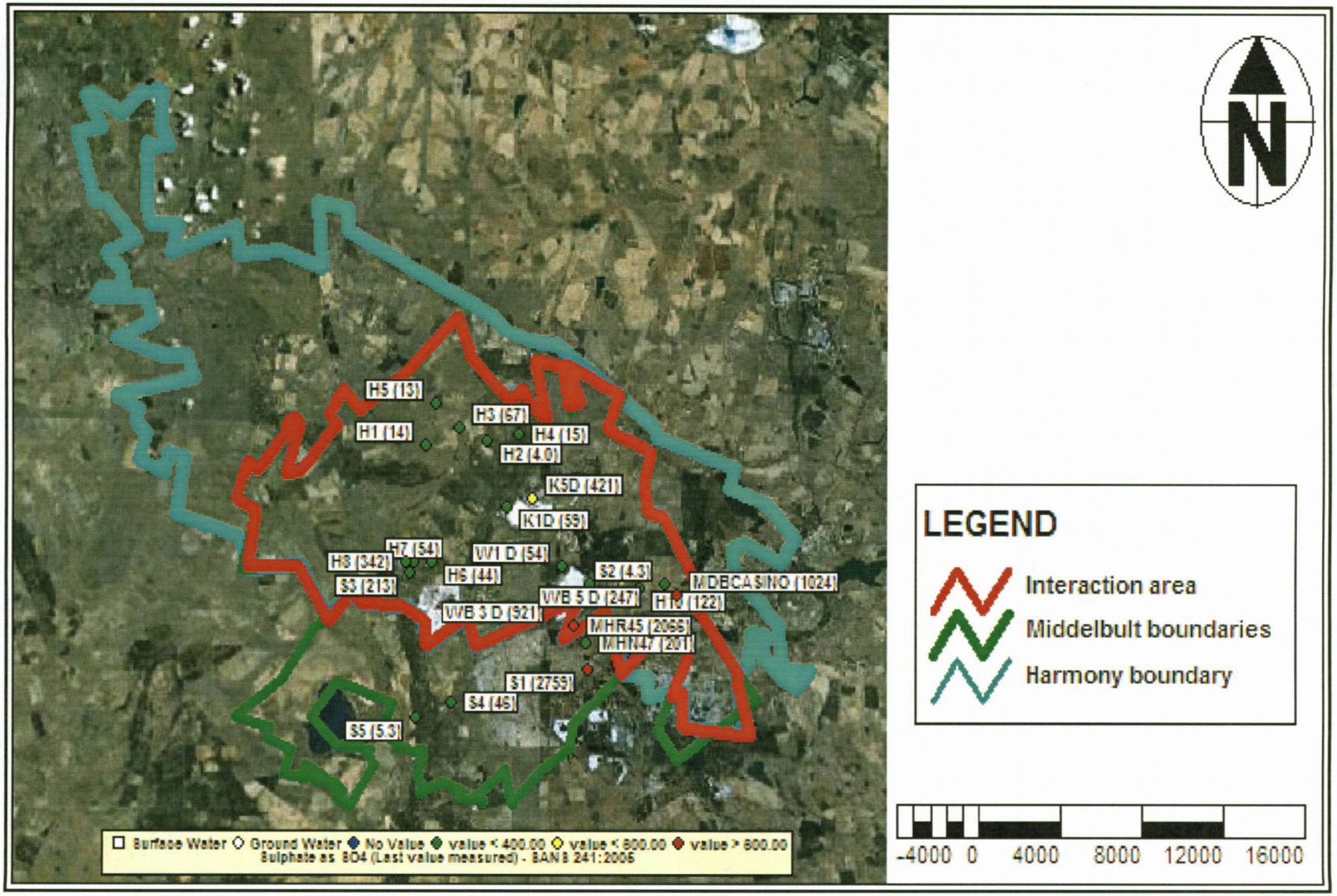

Figure 84: Sulphate concentrations for samples collected in this study.

7.4.5 Chloride (Cl)

The chloride concentrations range from 24.8 mg/l (**S5**) to 1612 (**H4**) mg/l, with an average value of 476.9 mg/l. From the linear trend line there is an increase of Cl from shallow to deep. Cl has a subdued chemical behaviour, meaning it does not take part in redox reactions and is not absorbed by minerals (Appelo & Postma, 2005).

- Samples **KB1D, KB5D** and **WB3D** are elevated in Cl and this can be attributed to the dissolution of the Cl-rich shales found in the Ecca formation of the Karoo Supergroup, which contain a relatively high amount of Cl, combined with the fact that the major anion of rainwater in the study area is Cl (USGS, 2004).

- The elevated Cl concentrations of **H1** and **H4** can be associated with groundwater that has undergone a reasonable degree of ion-exchange and has reached the end of the groundwater cycle (Phillips, 2009). As these samples are from a fault, it was expected that they would have a high Cl concentration due to high dissolution and ion exchange taking place as the water travels along the fault.

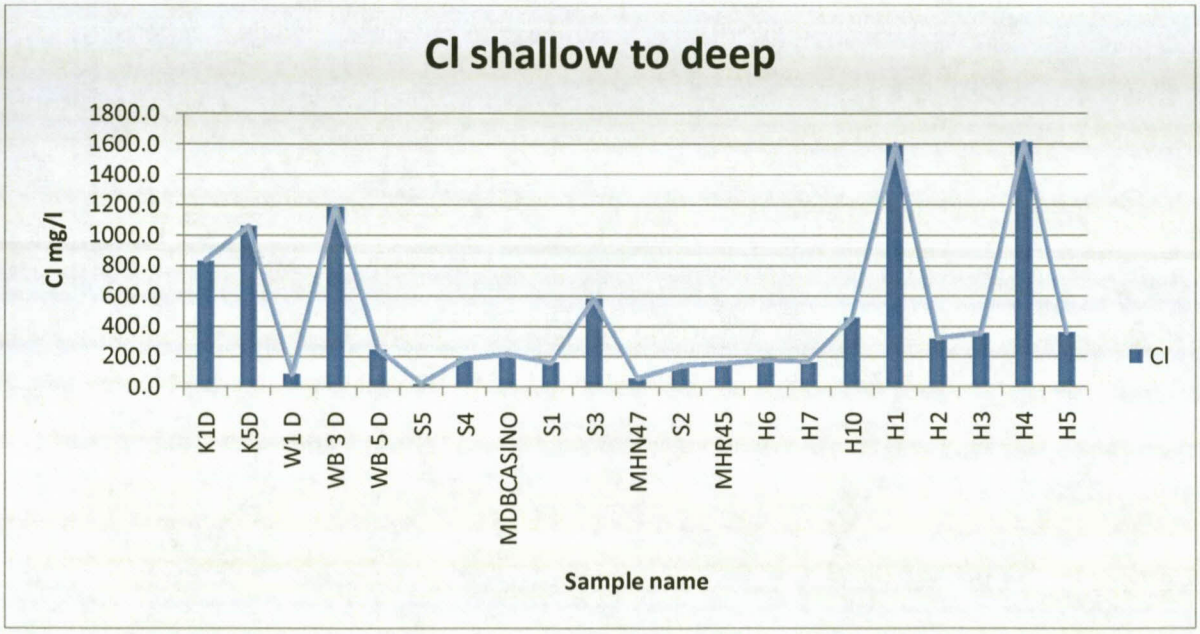

Figure 85: Chloride concentrations in the study area from shallow (left) to deep (right)

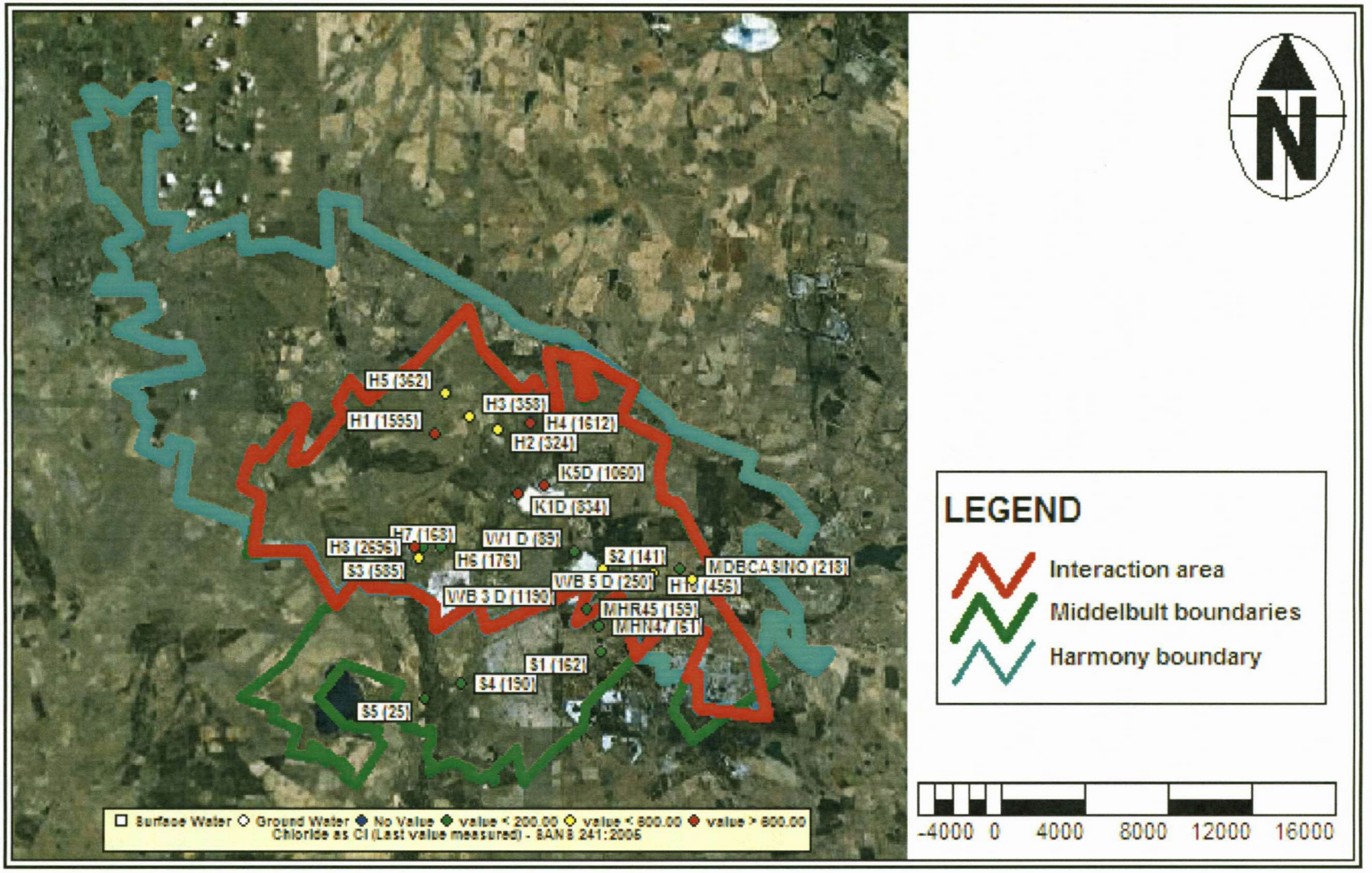

Figure 86: Chloride concentrations for samples collected in this study.

7.4.6 Bicarbonate (HCO_3^-)

HCO_3^- only exists in aqueous solutions containing calcium (Ca^{2+}), bicarbonate (HCO_3^-), and carbonate (CO_3^{2-}) ions, together with dissolved carbon dioxide (CO_2) (Freeze & Cherry, 1979). The relative concentrations of these carbon-containing species depend on the pH. Bicarbonate predominates within the pH range from 6.36 to 10.25 in fresh water (Freeze & Cherry, 1979).

Most groundwater in an unconfined aquifer is in contact with the atmosphere and absorbs carbon dioxide. As these waters come into contact with rocks and sediments, they acquire metal ions, most commonly calcium and magnesium. Therefore, most water near the surface (shallow unconfined to semi-confined aquifers) can be regarded as dilute solutions of these bicarbonates (Freeze & Cherry, 1979).

CO_2 occurs from atmosphere and is enriched in the soil, as precipitation moves through the unsaturated zone and CO_2 dissolves to form carbonic acid (Equation 13). Detailed reactions from Freeze and Cherry (1979):

Equation 13

$$H_2O + CO_2 \Leftrightarrow H_2CO_3^-$$

Carbonic acid is a weak acid that dissociates to form bicarbonate (Equation 14).

Equation 14

$$H_2CO_3 \Leftrightarrow H^+ + HCO_3^-$$

In

Figure 87, the decreasing trend of the bicarbonate concentrations can be seen in the samples taken from the Karoo aquifer, indicating their relative recharge histories, as more bicarbonate is in solution in the shallow Karoo aquifer, which is recharged by precipitation, compared to the deeper Witwatersrand aquifer, which is recharged by influx from the Karoo aquifer. H1 has 0 mg/l bicarbonate in solution compared to S2, which has 1585 mg/l bicarbonate in solution.

- **KB1D, KB5D, W1D, WB3D, WB5D, S5, S4, MDBCasino, S1, S3, MHN47, S2, MHR45, H6 and H7** - All have relatively high concentrations of bicarbonate, suggesting that they are recharged by precipitation or water in the shallow unconfined Karoo aquifer that freely reacts with the atmosphere. Although **H6** and **H7** were not taken directly from the Karoo aquifer, their bicarbonate concentration indicates that they are of Karoo aquifer origin.

- **H2, H3, H5 H10** - have higher bicarbonate concentrations compared to the other gold mine samples if **H6** and **H7** are excluded. **H3** is from an exploration borehole intersecting the gold mine and therefore its bicarbonate concentration is expected to be a mixture of precipitation and flux from confined aquifers. **H2, H5, H10** represent an influx of confined aquifer water as they were taken from fractures intersecting the gold mine. Their lower bicarbonate concentrations compared to **H3** are attributed to the reverse of Equation 14 in a closed system (confined aquifer) where there is no CO_2 present, resulting in the slow loss of HCO_3^- (Freeze & Cherry, 197). This explains the lower bicarbonate concentrations in **H2** and **H5.** It indicates that they are recharged by the shallower Karoo aquifer but that they have had a long residence time in the sub-surface.

- **H1 and H4** - Both these samples were taken from faults, and their bicarbonate concentrations suggest that they are recharged by influx from a confined aquifer below the No. 4L coal seam, presumably the deep fractured Karoo aquifer or from the Transvaal dolomites.

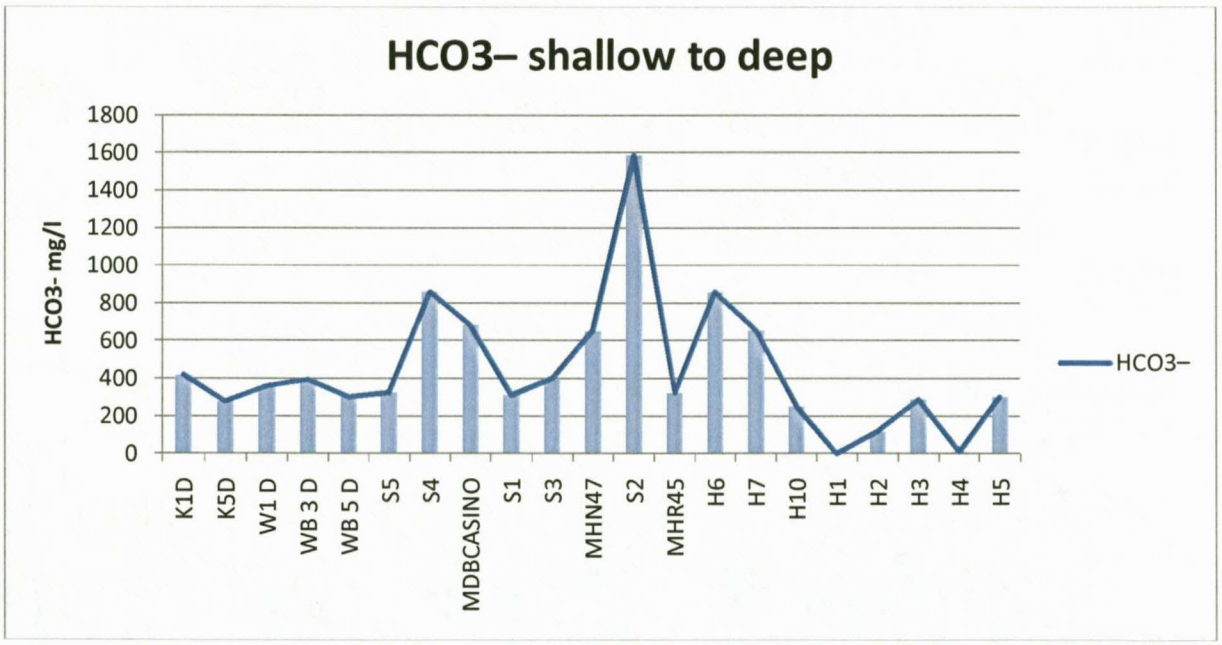

Figure 87: Bicarbonate concentrations from shallow to deep.

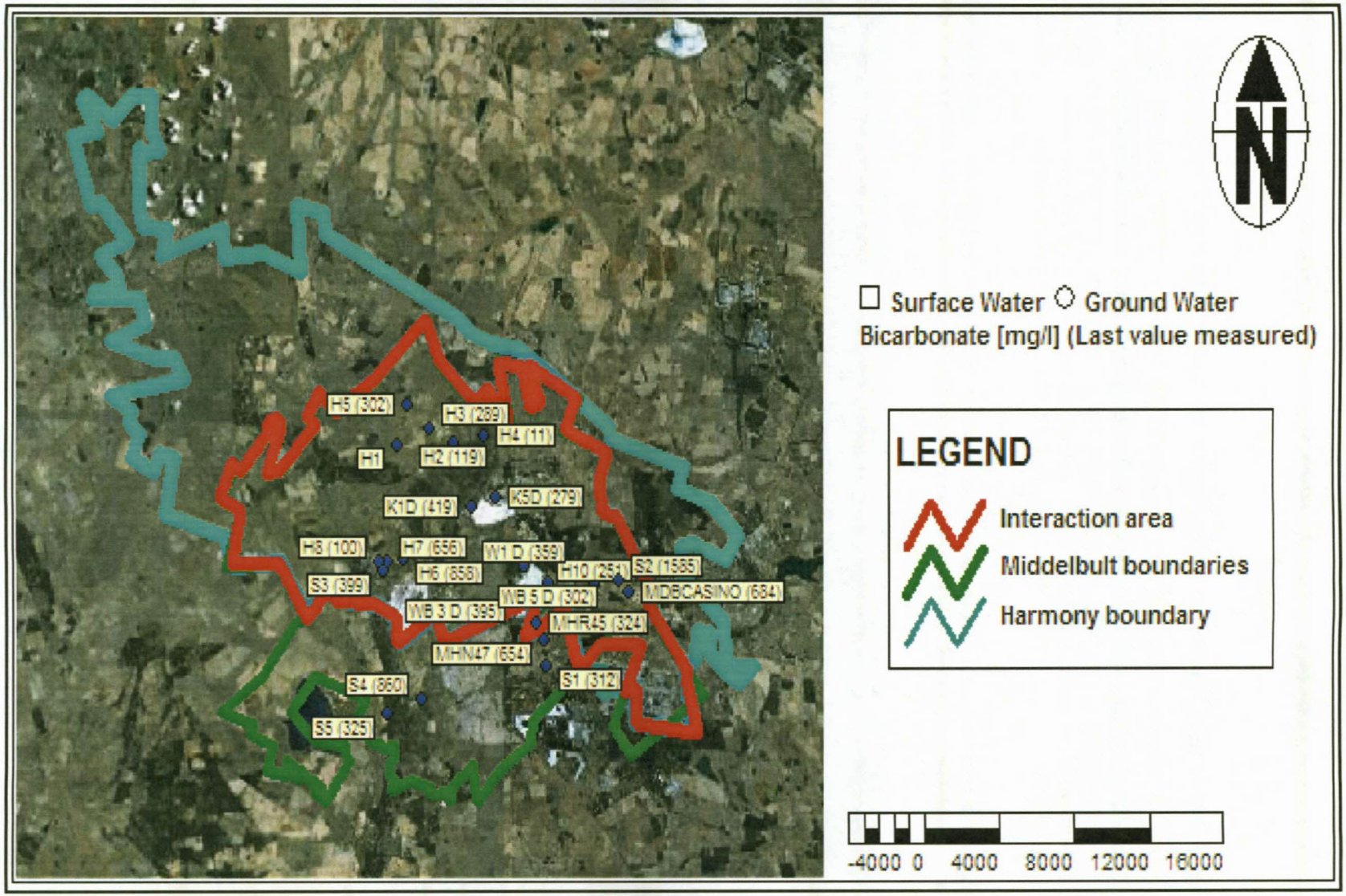

Figure 88: Bicarbonate concentrations for samples collected in this study.

7.4.7 Piper diagrams

The Piper diagram is a useful tool in providing a quick comparison of numerous individual chemical analyses. The Piper diagram allows for both anion and cation compositions to be represented on a single graph. In the Piper diagram, the ion concentrations are plotted as percentages, with each point representing a chemical analysis (Piper, 1944).

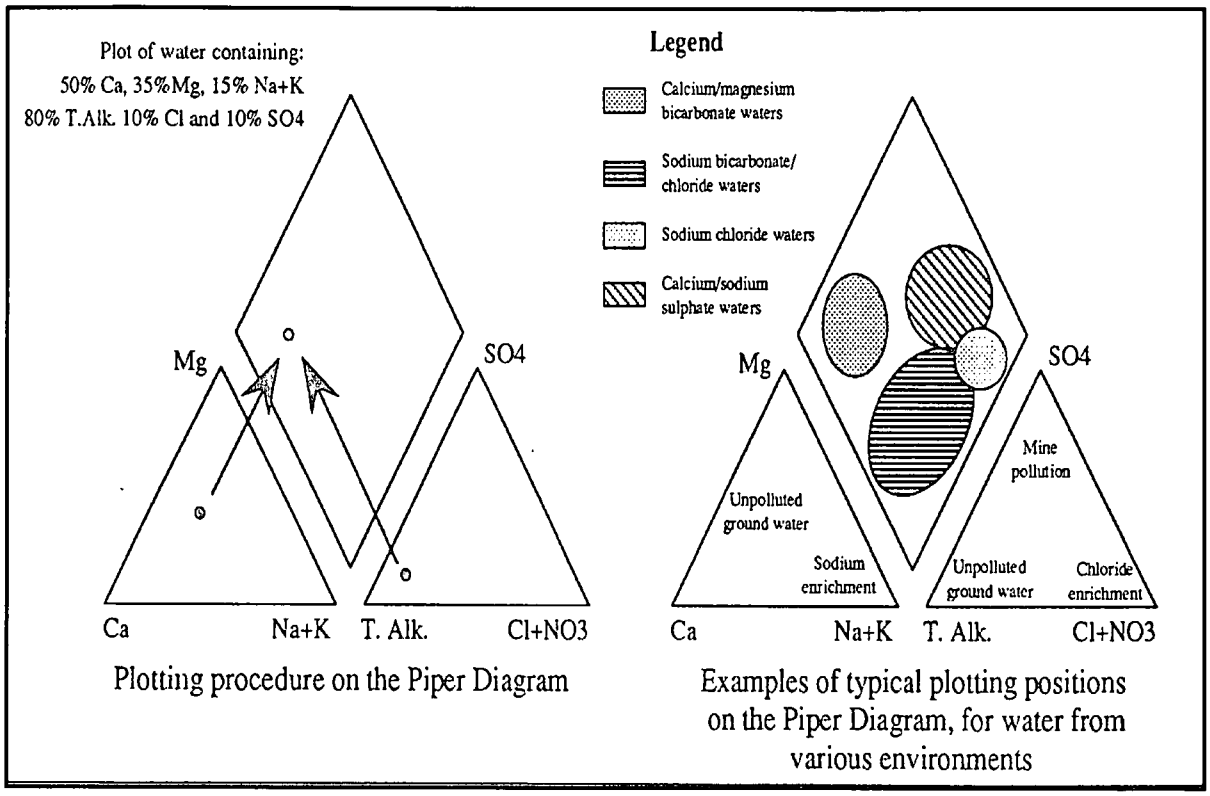

Figure 89: Piper diagram, adapted from Piper (1944).

7.4.8 Piper diagram for the study area

From Figure 90, samples **S1, H4, H1, S3, MHR 45, WB5D** and **MDB CASINO** are grouped together in the Piper diagram, indicating sodium-sulphate dominated groundwater. Samples **H10, H2, H3 and H5** are grouped together, indicating sodium-chloride dominated groundwater and samples **S5, MHN47** and **W1D** are grouped together, indicating sodium-bicarbonate/chloride dominated groundwater.

- Sodium-sulphate dominated samples (**S1, H4, H1, S3, MHR45, WB5D** and **MDBCASINO**). All these are shallow Karoo aquifer samples except for **H1** and **H4**, which are samples collected from faults intersecting the gold mine workings. This indicates that the **H1** and **H4**

origin is from the base of the Karoo aquifer, as all faults are cut off at the base of the Karoo Supergroup.

- Sodium-chloride dominated samples (**H2, H3, H5** and **H10**). These are samples collected from the gold mine in the Witwatersrand aquifer. Due to the high sodium and chloride content they can be regarded as water that has reached the end of the water cycle or water with relative long residence times that is unaffected by coal mining.

- Sodium-bicarbonate/chloride dominated samples (**S5**, **MHN47** and **W1D**). These are samples taken in the Karoo aquifer. These samples are typical of water that has been mixed with recent precipitation. This is seen in the bicarbonate content. CO_2 in the atmosphere combines with water to form carbonic acid, which gives rise to the bicarbonate in the groundwater, as shown in the reaction in Equation 15.

Equation 15
$H_2O + CO_2 \leftrightarrow H_2CO_3$ (Eby, 2004)

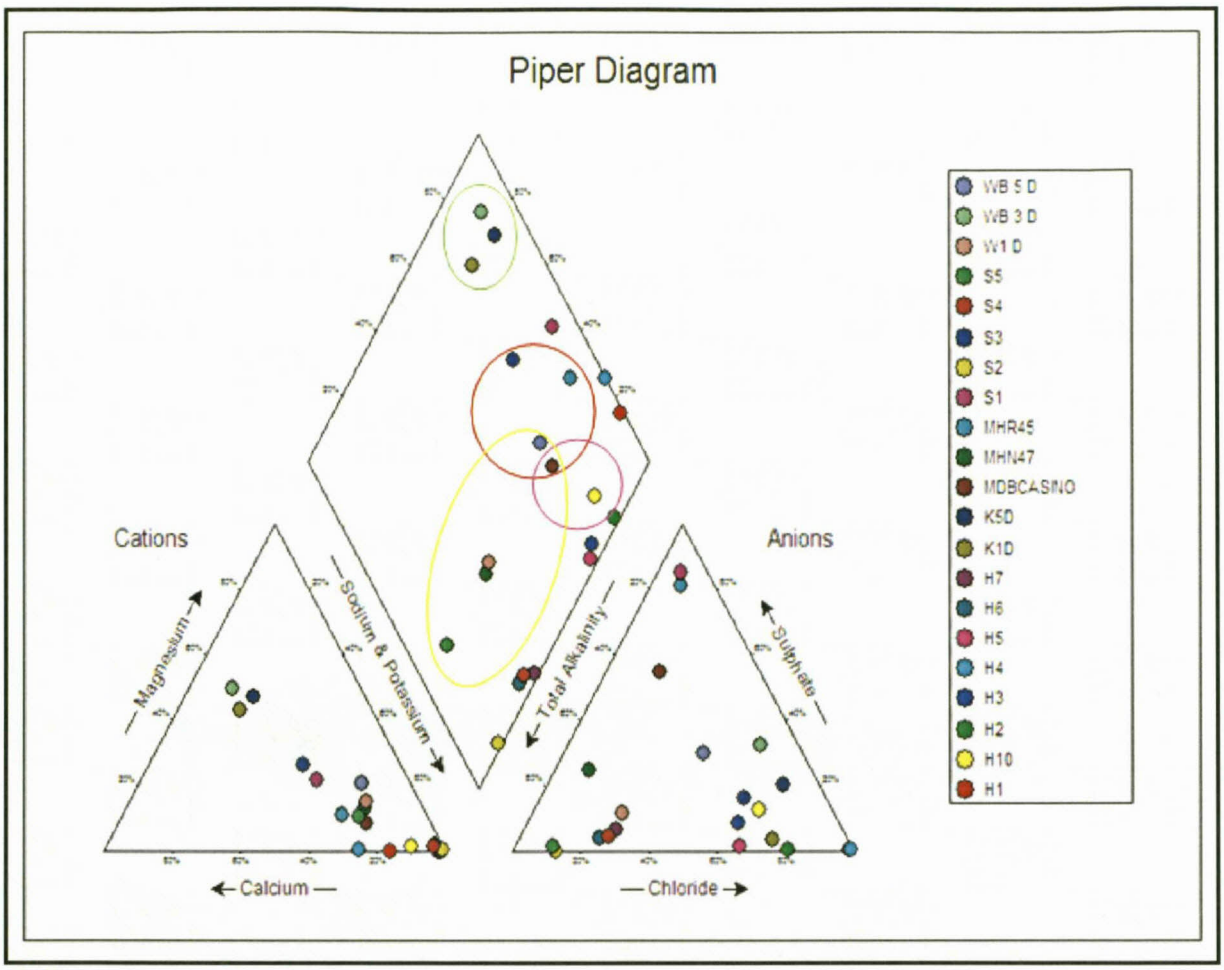

Figure 90: Piper diagram for the samples collected in this study.

7.4.9 Expanded Durov Diagram

Each field of the Expanded Durov Diagram represents groundwater dominated by different anions and cations, which in turn represents groundwater that is at different stages of the hydrogeological cycle. The different fields of the EDD are indicated in Figure 91 and Figure 92, after which a short description of each field follows. The expanded Durov diagram offers a distinct advantage over the Piper diagram in that nine groundwater fields display the different hydro-chemical types and processes on the diagram.

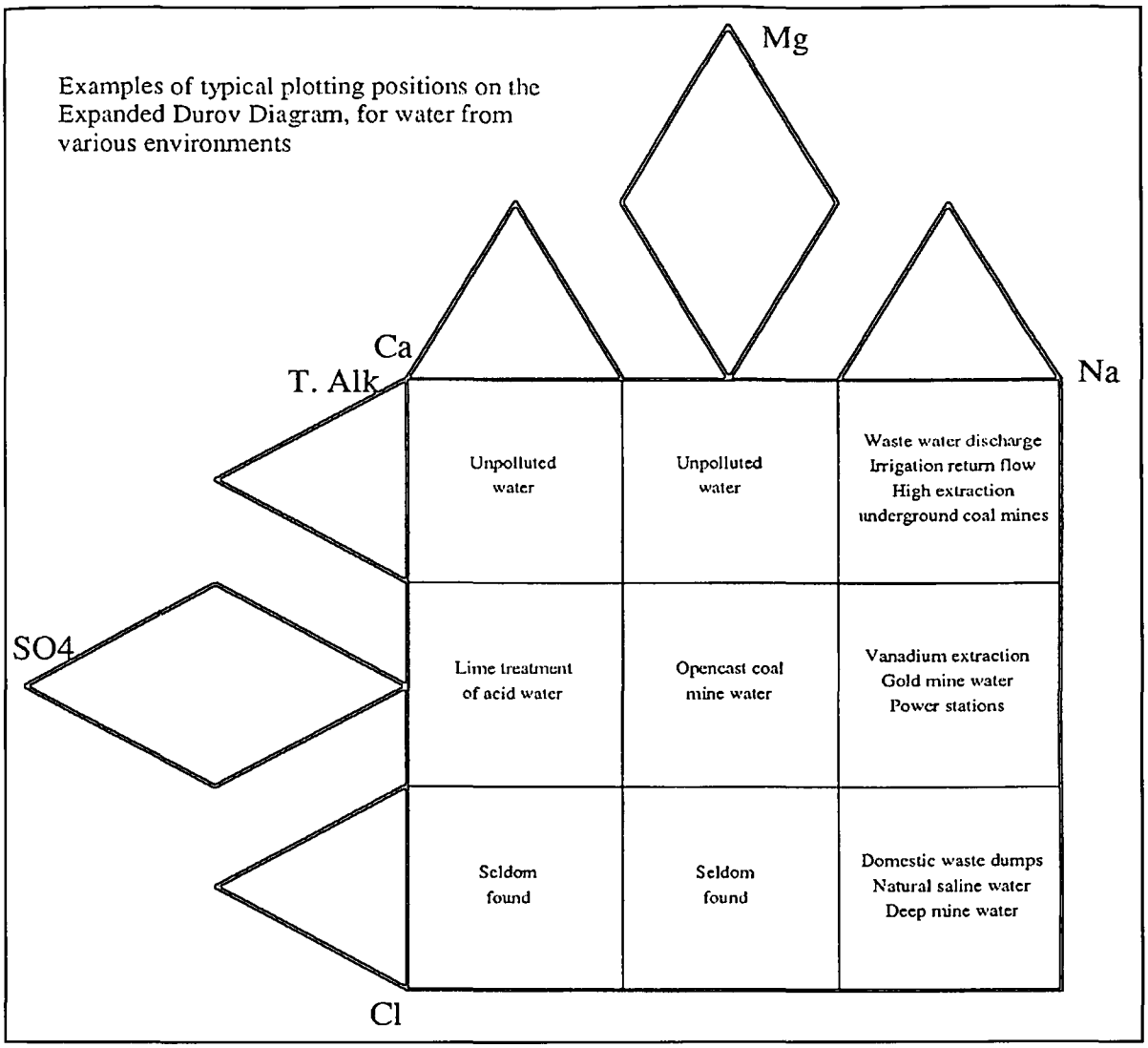

Figure 91: Interpretations from the Expanded Durov Diagram (1).

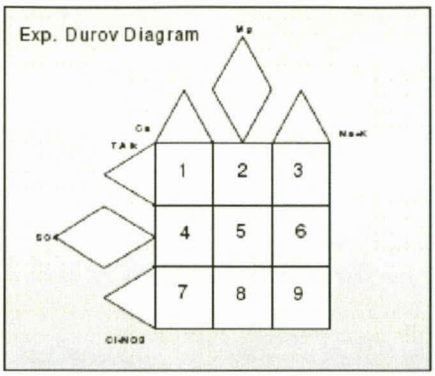

- Field 1: Fresh, very clean recently recharged groundwater with HCO_3 and CO_3 dominated ions.
- Field 2: Field 2 represents fresh, clean, relatively young groundwater that has started to undergo Mg ion-exchange, often found in dolomitic terrain.
- Field 3: This field indicates fresh, clean, relatively young groundwater that has undergone Na ion-exchange (sometimes in Na-rich granites or other felsic rocks), or because of contamination effects from a source rich in Na.
- Field 4: Fresh, recently recharged groundwater with HCO_3 and CO_3 dominated ions that has been in contact with a source of SO_4 contamination, or that has moved through SO_4 enriched bedrock.
- Field 5: Groundwater that is usually a mix of different types – either clean water from Fields 1 and 2 that has undergone SO_4 and NaCl mixing/contamination, or old stagnant NaCl dominated water that has mixed with clean water.
- Field 6: Groundwater from Field 5 that has been in contact with a source rich in Na, or old stagnant NaCl dominated water that resides in Na-rich host rock / material.
- Field 7: Water rarely plots in this field that indicates NO_3 or Cl enrichment, or dissolution.
- Field 8: Groundwater that is usually a mix of different types - either clean water from Fields 1 and 2 that has undergone SO_4, but especially Cl mixing / contamination, or old stagnant NaCl dominated water that has mixed with water richer in Mg.
- Field 9: Very old, stagnant water that has reached the end of the geohydrological cycle (deserts, salty pans, etc.) or water that has moved a long time and/or distance through the aquifer and has undergone significant ion-exchange.

Figure 92: Interpretations from the Expanded Durov Diagram (2).

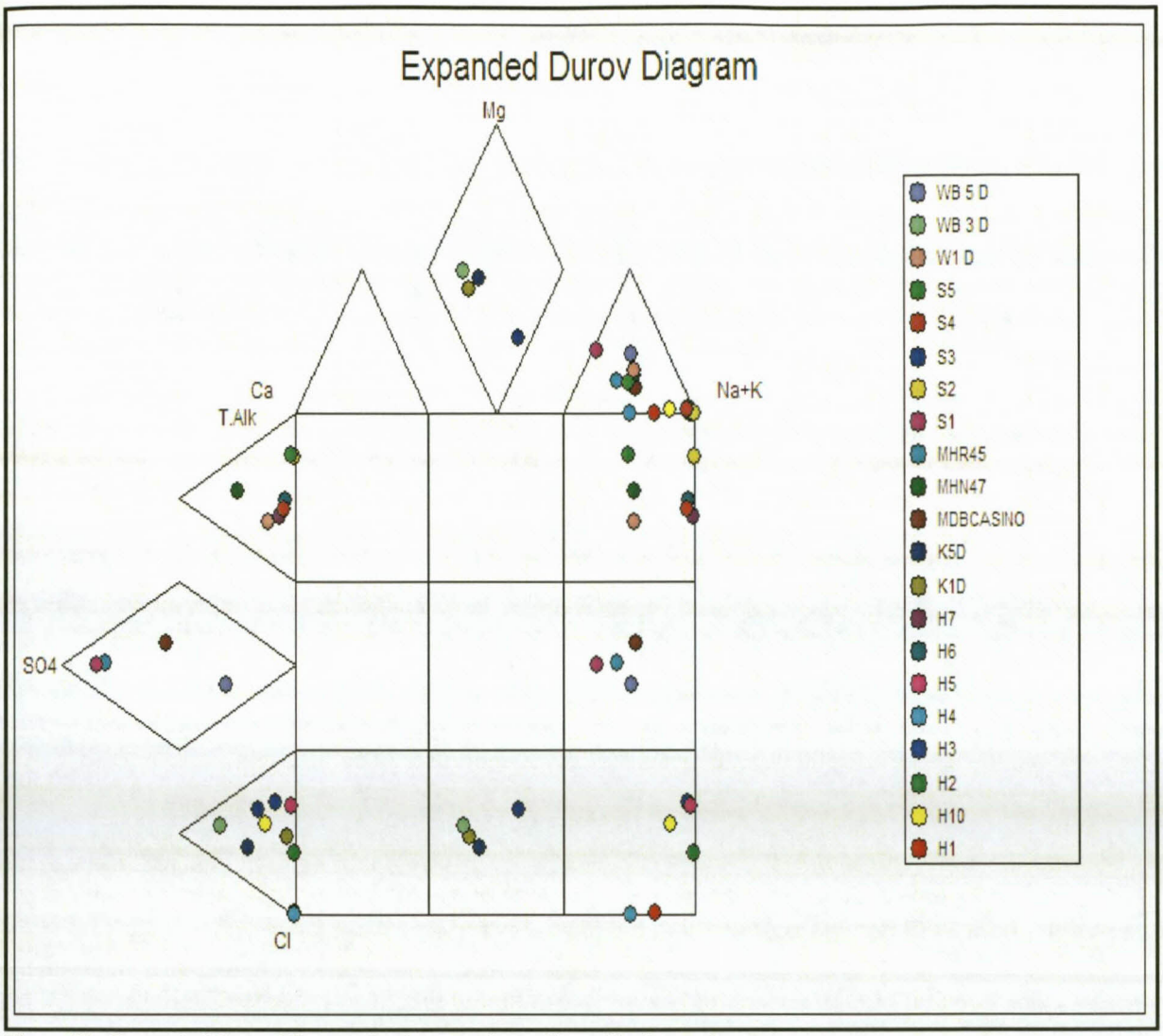

Figure 93: Expanded Durov Diagram for the samples collected in the study area.

From the EDD displayed in Figure 93, certain groupings according to each Field mentioned can be made:

- **Field 3 - (W1D, MHN47, S4, S5, S2, H7 and H6).** High extraction coal mining or fresh clean relatively young water that has undergone a degree of Na- ion exchange, although the reduction of SO_4^{2-} at depth can produce H_2S and CO_2 in the case of Na^+ dominant water. Water emanating from this field in the study area has most probably undergone ion-exchange reactions in reducing conditions on its flow path through the Ecca shales. All the samples except **H6** and **H7** are samples taken from the Karoo aquifer. **H6** and **H7** represent

fracture water dripping out of the roof of the mine, indicating that it is of Karoo aquifer origin and flows along the fracture until it intersects the gold mine workings.

- **Field 6** - (**WB5D**, **MHR45**, **MDBCASINO** and **S1**). These samples are indicative of water that has been in contact with a source rich in Na, or old stagnant NaCl dominated groundwater that has been influenced by Na-Cl host rock/material. As these samples were collected in the Karoo aquifer. They will have high Na- concentrations through the processes of dissolution and cation exchange, where calcium and magnesium are adsorbed onto clays within the sediments, in exchange for sodium (Eby, 2004).

- **Field 8** - (**WB3D**, **K1D**, **K5D** and **S3**). Groundwater that is usually a mix of different types, either clean water from **Fields 1** and **2** that has undergone SO_4, but especially Cl mixing, or old stagnant NaCl-dominated groundwater that has mixed with sources richer in Mg. These are all samples collected in the Karoo aquifer.

- **Field 9** - (**H3, H4, H1, H2, H10, H5**). Very old stagnant water that has reached the end of the geohydrological cycle or water that has moved a long time and/or distance though the sub-surface and has undergone significant ion-exchange. End-point water is normally saline water (old brackish water), which is true for the samples plotted in **Field 9**.

Stiff diagrams

A Stiff diagram plots major cations and anions on opposite sides of a y-axis, with the x-axis representing the concentration of the ions in meq/l. By plotting the ions in this manner, each sample will have its own unique geometry (Appelo & Postma, 2005).

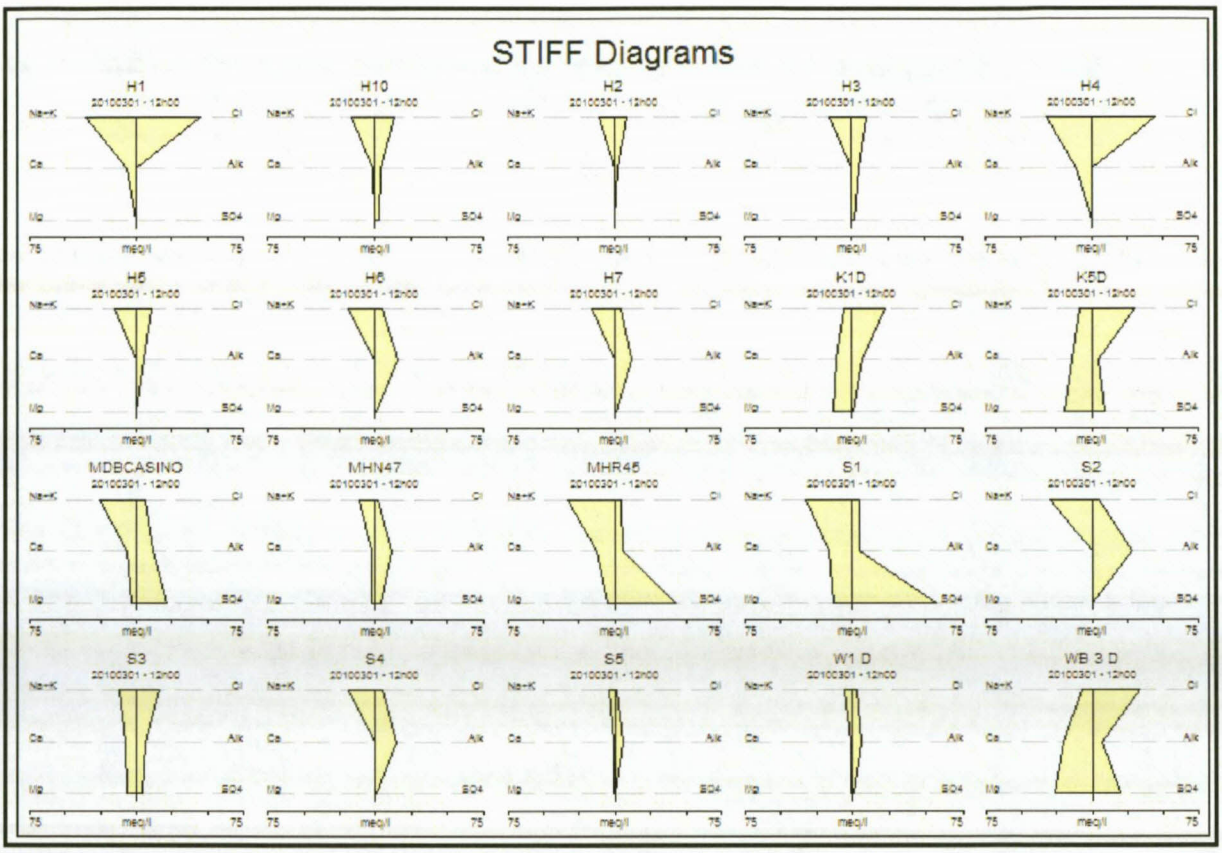

Figure 94: Stiff diagram for the underground samples collected in this study.

From the Stiff diagrams, we see that some samples are dominated by major anions or cations. The samples that show a clear dominance are listed below:

- (**H1, H4, H10, H2, H3** and **H5**) - Na+K and Cl dominated groundwater. Samples collected in the gold mine. **H2**, **H3**, **H5** and **H10** geometry is different than that of **H1**, **H4** and **H10**, suggesting that they are the same water but affected by different hydro-chemical reactions.

- (**H6, H7, S4** and **S2**) - Na+K dominated groundwater with a high alkalinity. H6 and H7 were collected in the gold mine whereas **S4** and **S2** were collected in the water-filled coal mine.

- (**MDBCASINO, MHR45** and **S1**) - Na+K and SO_4 dominated groundwater. Samples collected in the water-filled coal mine. They will have high Na- concentrations though the processes of dissolution and cation exchange. Calcium and magnesium are adsorbed onto clays within the sediments, in exchange for sodium (Eby, 2004).

- (**WB3D, K1D, K5D**) - Cl and Mg dominated groundwater. Samples collected in the shallow Karoo aquifer. The processes of dissolution and cation exchange are limited and the calcium and magnesium has not been adsorbed onto clays within the sediments in exchange for sodium (Eby, 2004).

7.5 Discussion of Chemical Results

From the chemical parameter plots, Piper diagram, Expanded Durov diagram and Stiff diagrams, the origin of some of the groundwater samples can be "fingerprinted" according to their composition. Their origin of the samples can be "fingerprinted" from the shallow Karoo aquifer affected/unaffected by coal mining or from the deeper Witwatersrand aquifer. The following section discusses the origin of the samples with reference to their hydro-chemical composition and the different aquifers found in the study area.

7.5.1 Samples taken from boreholes on surface

Table 13: Summary of samples taken from boreholes on surface of the study area.

Harmony Surface	Coordinates		Elevation (m.a.m.s.l)*	Sampling depth m below surface	Sampling depth m below surface	water level depth m below surface
Borehole name	Y	X	Z			
KB 1 D	-2929816.932	7611.298	1591.324	28	30	3.5
KB 5 D	-2929401.146	8886.292	1615.099	28	30	1.02
WB 1 D	-2932446.352	10378.745	1589.468	28	30	1.6
WB3D	-2933838.364	10023.214	1599.229	28	30	1.3
WB 5 D	-2933225.999	11669.846	1621.612	28	30	22
Sasol Surface	**Coordinates**		**Elevation (m.a.m.s.l)***	**Sampling depth m below surface**	**Borehole depth m below surface**	**water level depth m below surface**
Borehole name	Y	X	Z			
MHN 47	-2935823.037	11478.324	1578.937	110	Into mine	108.19
MHR 45	-2935046.371	10963.433	1600.137	130	Into mine	129.44
MDB Casino	-2933683.916	15952.46	1581.346	100	Into mine	97.67
m.a.m.s.l- metres above mean sea level						

According to the chemical parameters, Piper diagram, Durov diagram and Stiff diagrams, the surface borehole samples are indicative of Karoo aquifer water that has been affected by both underground coal and surface gold mining activities in the study area.

- We can distinguish between samples taken directly from the coal mine filled with water (**MHN47, MHR45, MDBCasino**) through the chemical parameter of sodium (Na). Dissolution and cation exchange has taken place in these samples, replacing the Mg and Ca. The Stiff diagrams also show this characteristic Na+K dominated water, which is indicative of the coal mine filled with water (Hodgson & Krantz, 1995).

- **KB1D, KB5D, WB1D, WB3D, WB5D** are samples taken from the shallow Karoo aquifer. According to their Stiff diagram, they are characteristic of Mg and Cl dominated water. These samples have been exposed to Cl mixing and are dominated by groundwater that has mixed with sources richer in Mg, found in the shallow Karoo aquifer. The Cl concentrations can be attributed to the dissolution of the Cl rich shales found in the Ecca formation of the Karoo Supergroup, which contain a relatively high amount of Cl, combined with the fact that the major anion of rainwater in the study area is Cl^- (USGS, 2004).

- SO_4 concentration is the main contributor to ARD and it is thought that Harmony's slimes dam may contribute to ARD in Sasol's coal mine. From the samples analysed in this study for SO_4 concentrations, it is clear that if there is a contribution of SO_4 concentrations from Harmony gold mining's slimes dams it is minimal, as Sasol coal mining's samples (**MDBCASINO** and **MHR45**) are more than double the highest SO_4 concentrations found in Harmony's highest sample (**WB3D**), as shown in Figure 83 and Figure 84.

- **KB1D, KB5D, W1D, WB3D, WB5D, S5, S4, MDBCasino, S1, S3, MHN47, S2, MHR45, H6** and **H7** - All have relatively high concentrations of bicarbonate, suggesting they are recharged by precipitation or water in the shallow unconfined Karoo aquifer that freely reacts with the atmosphere.

- Referring to the EDD and Piper diagram in Figure 93 and Figure 90, a correlation exists between the surface borehole samples (**KB1D, KB5D, WB1D, WB3D, WB5D**) and the underground samples (**S1, S2, S3, S4, S5, H6** and **H7**) taken from both mines, as they plot in areas of the same hydro-chemical characteristic. This is a confirmation that there is dynamic interaction between the aquifers situated in the Karoo Supergroup as there is a

direct link with recharge from precipitation into the shallow perched aquifer and the shallow weathered aquifer. This water then flows through preferential pathways from these aquifers into the deeper artificial coal mine aquifer and into the fractured aquifer. Therefore, the deeper Karoo aquifer is not directly recharged by precipitation but by flux from shallower Karoo aquifers. Furthermore, Karoo aquifer flux flows into Sasol's underground coal mine and in some places through fractures into Harmony's gold mine workings, as seen in samples **H6** and **H7** (fracture water dripping from roof - Table 14) taken from Level 1 at Harmony's No. 9 shaft, which is in close proximity to the overlying Sasol coal mine workings (Figure 95).

7.5.2 Samples taken directly from underground

Only **H6**, **H7** and **H10** could possibly be affected by coal mining, as shown in Figure 74. They are the only samples taken where current coal mining is near the gold mine workings.

Table 14: Summary of samples taken directly from underground in this study.

	Depth in m below surface	Level	Shaft or posistion	Description
H1	1340	11	8	Water from fault
H2	1340	11	8	Water next to dyke
H3	1620	15	8	Water from exploration borehole
H4	1830	18	8	Water from fault
H5	2152	24	8	Water dripping out of roof of stope
H6	282	1	9	Water dripping out of mine roof (minimal)
H7	282	1	9	Water dripping out of mine roof (minimal)
H10	635	8	3	Water dripping out of mine roof (minimal)
Sasol samples	**Depth in m below surface**	**Level**	**Shaft or position**	**Description**
S1	104	In coal mine	Near Main shaft	Borehole into mine workings
S2	113	In coal mine	Near North Shaft	Water dripping out of mine roof (minimal)
S3	105	In coal mine	Block 38	Fissure from floor
S4	80	In coal mine	Near West shaft	Water dripping out of mine roof (minimal)
S5	55	In coal mine	Block 35	Water dripping out of mine roof (minimal)

According to the chemical parameters, Piper diagram, Durov diagram and Stiff diagrams, the underground groundwater samples can be grouped together. The grouping is as follows:

- **(H1, H2, H4, H5 and H10)** - The Na- concentrations in these samples (Figure 81) generally increases with depth, while their SO_4^{2-} concentration is much more depleted than the samples taken in the Karoo aquifer (Figure 83) These samples have the same hydro-

chemical characteristic of groundwater expected to be found in deep confined aquifers or gold mines. The samples are a mixture of old stagnant water (possibly connate water or paleo-meteoric water) and water that has travelled a long distance in the sub-surface with a relatively long residence time and has reached the end of the groundwater cycle. **H2**, **H3**, **H5** and **H10** have higher concentrations of bicarbonate compared to the other gold mine samples, if **H6** and **H7** are excluded (

- Figure 87).

- **H3** is water from an exploration borehole intersecting the gold mine and therefore its bicarbonate concentration is expected to be higher, as it has been recharged by a mixture of precipitation and influx from confined aquifer water. **H2, H5** and **H10** (samples from fractures) have lower bicarbonate concentrations compared to **H3**, which is attributed to the reverse of Equation 14 in a closed system (confined aquifer) where there is no CO_2 present, resulting in the slow loss of HCO_3^- (Freeze & Cherry, 1979). Therefore there are lower bicarbonate concentrations in **H5, H2** and **H10.** This indicates that they are recharged by the shallower Karoo aquifer but that they have had a long residence time in the sub-surface.

- **H4** and **H1** - Both these samples were taken from faults, and their bicarbonate concentrations suggest that they are recharged by influx from a confined aquifer below the No. 4L coal seam, presumably the base of the fractured Karoo aquifer or from the Transvaal dolomites.

- **H1** and **H4** are unaffected by coal mining (Table 14 and Figure 74). In the Stiff diagram (Figure 94) they have a much more pronounced Na+K and Cl geometry compared to the other samples taken in the gold mine. This indicates that **H1** and **H4** (water from fault) originated from the base of the Karoo Supergroup and that groundwater in some faults moves from the base of the Karoo aquifer, unaffected by coal mining, towards the deeper Witwatersrand aquifer. They are unaffected by coal mining as coal mining has not reached the area where these samples were taken (Figure 74).

- **H3** - This sample was taken from an exploration borehole intersecting the gold mine workings. It resembles water of Karoo aquifer origin that has travelled in the borehole through the Ventersdorp Supergroup and reached the gold mine workings. The travelling time of the sample is less than samples **H1** and **H4** taken from the faults, as its Na

concentration is much lower than samples **H1** and **H4**, indicating that it has not undergone the degree of ion-exchange these samples have, due to less time of exposure to minerals and therefore less travelling time. As coal mining has not reached No. 8 shaft, it has remained unaffected by coal mining, which is indicated by the EDD (Figure 93). If the coal mining intersects the exploration borehole it will be sealed (Block 8 Expansion EMPR, 2005).

- **S1, S2, S3, S4, S5, H6** and **H7** have been grouped together in **Field 3** of the EDD (Figure 93). They also have the same geometry in the Stiff diagram (Figure 94). These samples are groundwater expected to be found in high extraction coal mining. They have most probably undergone ion-exchange reactions in reducing conditions on their flow path through the Ecca shales. All the samples except **H6** and **H7** are samples taken from the water-filled coal mine in the Karoo aquifer. **H6** and **H7** are fracture water dripping out of the roof of the mine (Table 14). Through the EDD (Figure 93) and from their bicarbonate concentrations (

- Figure 87) it can be seen that they are of Karoo aquifer origin, affected by coal mining (water dripping from roof, Table 14). They were taken from Level 1 at Harmony's No. 9 shaft, which is in close proximity to the overlying Sasol coal mine workings (Figure 95).

- **H10** is also fracture water dripping out of the mine roof (Table 14). As it is near the current coal mining of Middelbult Mine Block 8, it may be affected by coal mining (Figure 74). According to the hydro-chemical data, however, there is no indication of **H10** being influenced by coal mining.

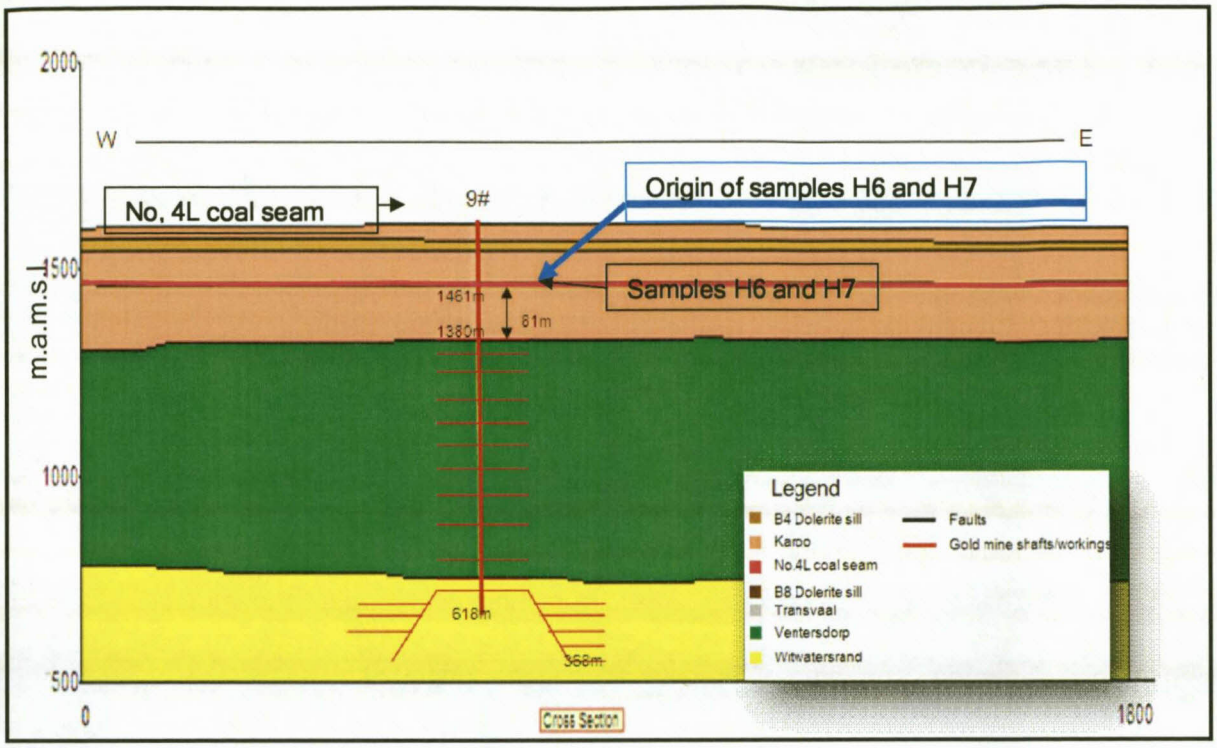

Figure 95: Origin of samples H6 and H7 according to Hydro-chemistry.

7.6 Environmental Stable Isotopes

The use of stable isotope ratios of deuterium (δD) and oxygen (δ^{18}) in hydrogeology can be a reliable indicator of the origins and movement of surface water as well as groundwater. Stable isotopes have been successfully used to determine the relative ages of the contribution of "new water" to groundwater flow in previous studies, such as Saayman *et al.* (2003) and Weaver *et al.* (1999).

As water molecules are made up of hydrogen and oxygen atoms, the hydrogen (deuterium) and oxygen (oxygen-18) stable isotopes can be seen to be of key importance in most groundwater studies. These isotopes are commonly used to determine the average elevation of recharge for a particular mass of groundwater. The ratios of deuterium (δD) and oxygen (δ^{18}) in the water molecule undergo small changes through fractionation processes such as evaporation and condensation (Fritz *et al.*, 1980).

The values for the individual ratios are expressed as δ values, which are defined as:

Equation 16

$$\delta = [(R_{sample}/R_{ref})-1] \times 1000\ ‰$$

where R_{sample} and R_{ref} are the isotope ratios ($^{2}H/^{1}H$ and $^{18}O/^{16}O$) for the sample and a reference standard respectively. The universal reference standard is the standard mean ocean water (SMOW). On a graph of deuterium (δD) against oxygen (δ^{18}), with respect to SMOW, all current precipitation (meteoric water) worldwide plots along a linear regression trend called the world meteoric water line (WMWL) or the universal meteoric water line (UMWL). Their position on the line will be determined by geographic, climatologic and physiographic factors. Their isotopic ratios in groundwater are conservative in the sense that they are not readily altered by processes in closed systems and in the saturated zone. Even where subsequent changes in hydrochemistry might occur, the isotopic composition remains diagnostic of the origin of groundwater. For example, during condensation of the water molecule the lighter isotope has a higher vapor pressure and hence is enriched in the gas phase, while the heavier isotope forms precipitation more readily (Figure 96).

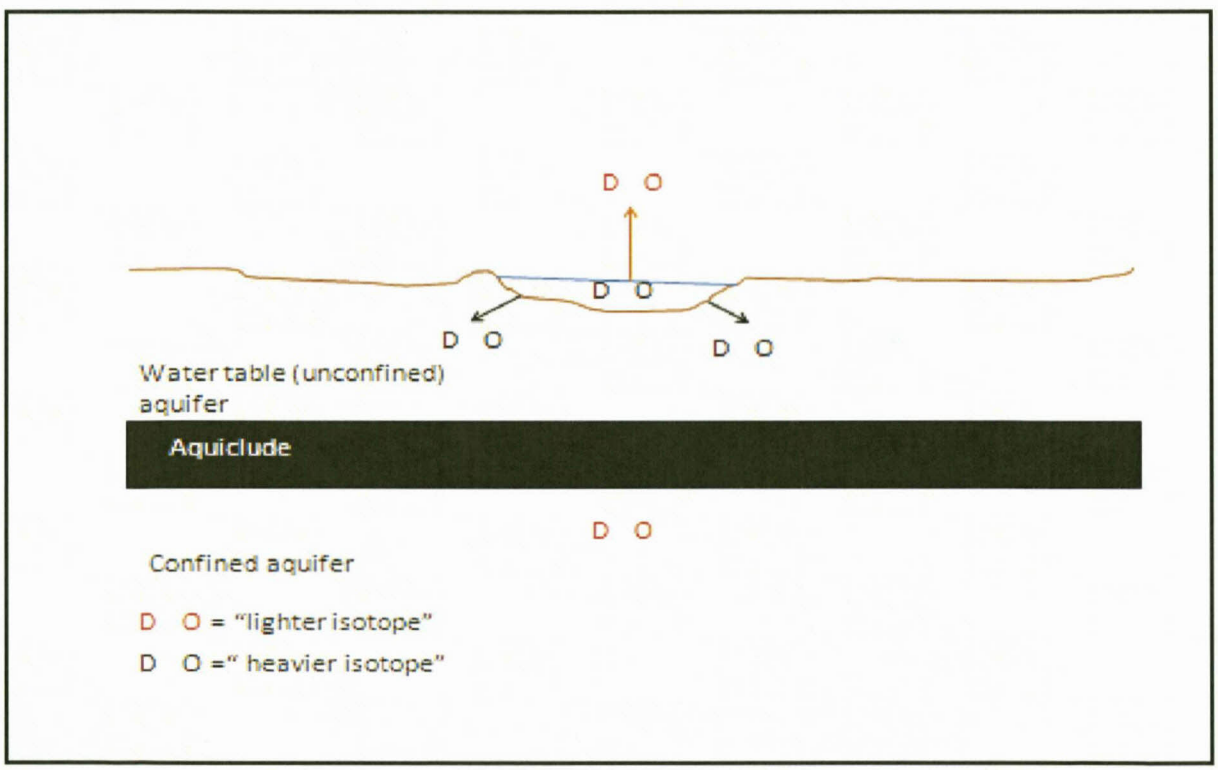

Figure 96: Schematic of isotope enrichment/depletion in the vapor and condensation phase.

Equilibrium phase changes affect deuterium and ^{18}O in a constant ratio and their values are linearly related in rain water according to a general worldwide equation:

Equation 17
$\delta D = 8 \times \delta^{18}O+10$ (Fritz *et al.*, 1980).

Oxygen and hydrogen are in some ways the perfect tracers of water because their concentrations are not subjected to changes by interactions with the aquifer material (Unesco, 1973). Once underground and removed from zones where fractionation through evaporation and condensation can occur, the isotope ratios are conservative and can only be affected by mixing. When precipitation infiltrates to recharge groundwater, mixing in the unsaturated zone smoothes the isotopic variations, meaning water in the saturated zone has a composition corresponding to the mean isotopic composition of infiltration in the area. This may differ slightly from the mean isotopic composition of precipitation, due to the fact that not all precipitation during the year infiltrates in the same proportion (Unesco, 1973).

Analyses of deuterium (δD) and oxygen (δ^{18}) can be used to identify the probable source of undergroundwater. If the isotopic composition of undergroundwater plots close to the meteoric water line in a position similar to that of present-day precipitation in the same region, the water is almost certainly meteoric (Figure 97). Although the isotopic composition of precipitation at a particular location is approximately constant, it varies from season to season and from one rainstorm to another. The variations can be used to identify the season at which most of the recharge takes place (Drever, 1997).

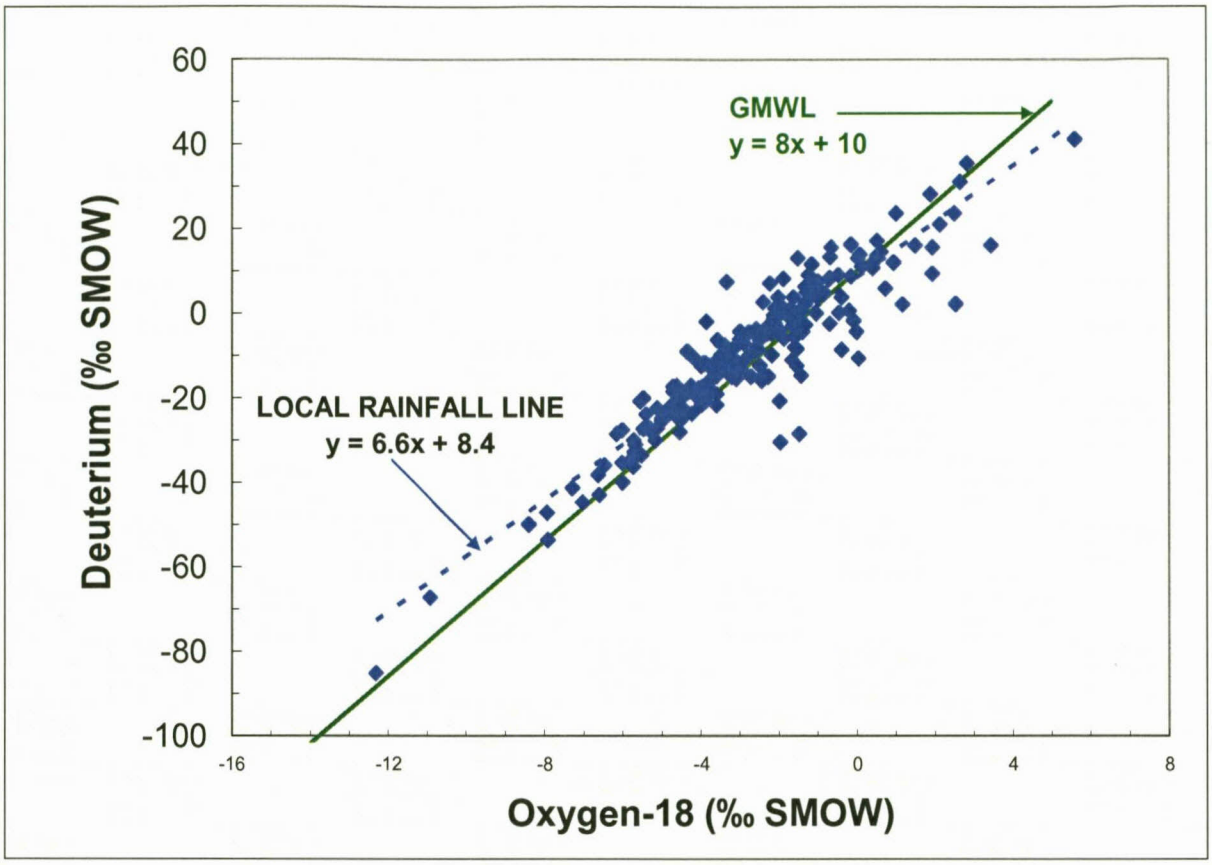

Figure 97: The relationship between δ18O and δD for Pretoria rainfall (Talma, 2003).

Surface water bodies such as dams, lakes and pans are enriched in the heavy isotope content during evaporation (Figure 96). Light isotopes are preferentially transferred to the vapour phase. The resulting surficial layer enriched in the heavy isotope is then readily mixed into the bulk of the water body through convective processes (Figure 99). This evolutionary enrichment produces δD and $\delta^{18}O$ values that lie to the right of the meteoric water line, and plot on an evaporation line of lesser slopes (usually 4 to 5) and lower d than the GMWL. Groundwater derived through infiltration from such water bodies will carry this distinctive evaporative isotopic signal (Gat, 1996).

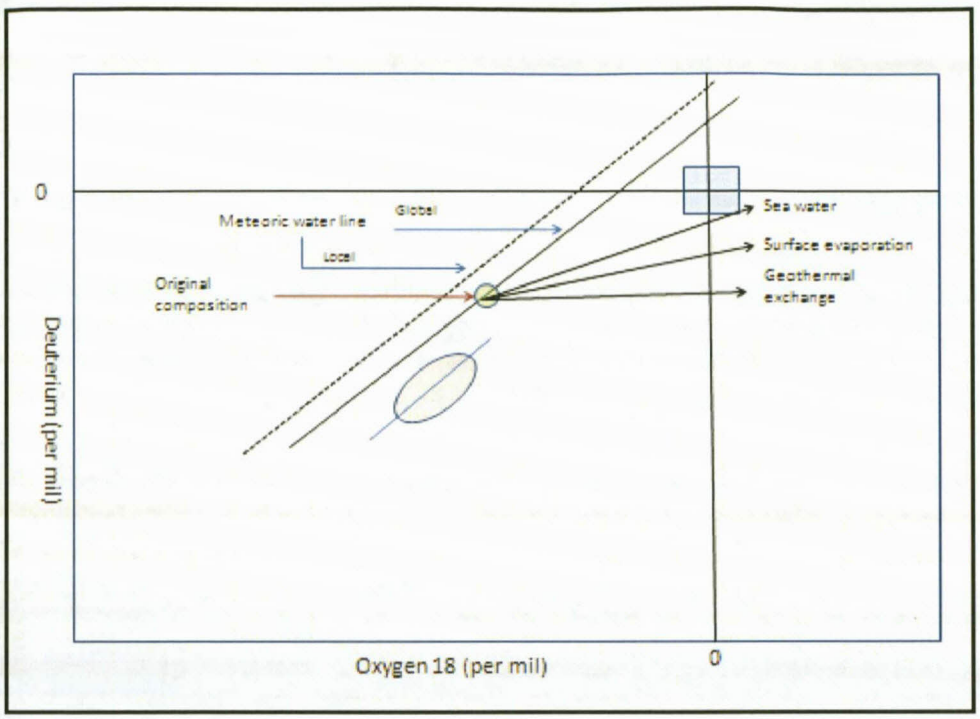

Figure 98: Meteoric water lines (adapted from Gat, 1996).

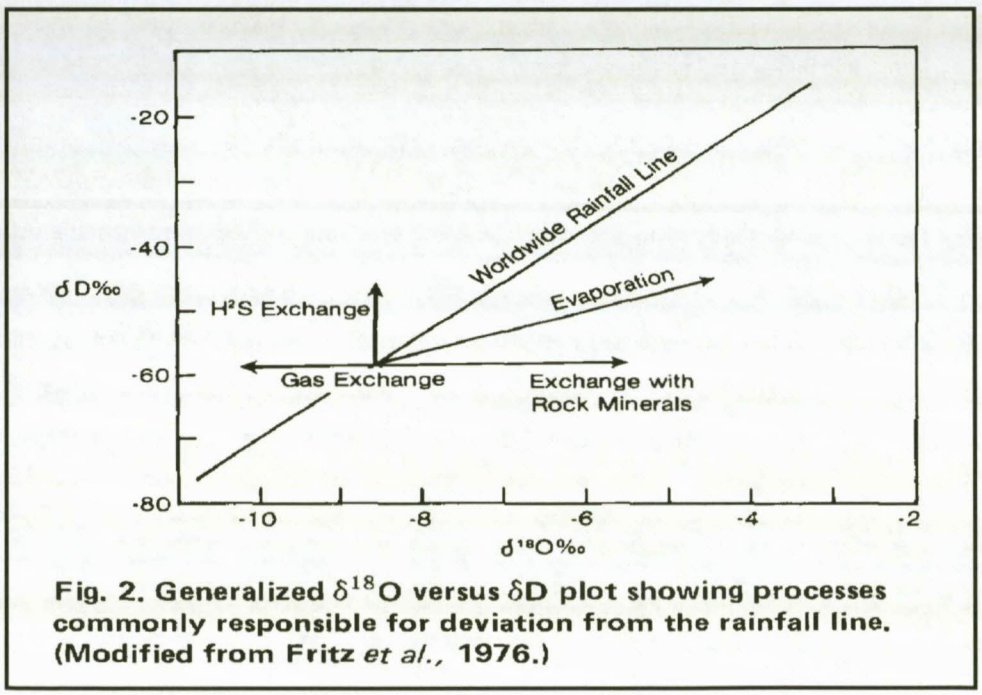

Fig. 2. Generalized $\delta^{18}O$ versus δD plot showing processes commonly responsible for deviation from the rainfall line. (Modified from Fritz *et al.*, 1976.)

Figure 99: Generalised δD versus $\delta^{18}O$ plot showing the world rainfall (meteoric) line and processes commonly associated of deviation from the rainfall line (Fritz *et al.*, 1980).

Regional groundwater flow in the study area follows a complex system of interconnected, structurally controlled flow paths, incorporating multiple lithologies with both fracture and matrix dominated flow (Rison Groundwater Consulting, 2007). The use of oxygen and hydrogen isotopic composition could prove to be a useful tool to "fingerprint" the origin of groundwater found in the study area and more specifically the origin of the deeper groundwater found in the gold mining areas of Harmony Evander's gold mining operations. The isotopes δD and $\delta^{18}O$ could assist in determining the type of water as well as whether any groundwater flux exists between the mines. The thought process behind this is that if there is any water interaction between Sasol Mining's Middelbult (Block 8) and Harmony Evander operations, the groundwater in both mines will have the same relative isotopic composition, or if the contrary is true and there is no groundwater interaction between the mines, that the relative isotopic composition may differ.

7.6.1 Application of environmental isotope and hydro-chemistry in this study

Environmental isotopes and hydrochemistry data analysis methodologies were applied in this study to establish the different groundwater types and hydraulic interconnection between the shallower Karoo aquifer and the deeper Witwatersrand aquifer.

Specific applications of the environmental stable isotopes $\delta^{18}O$ and δD in this study are:

- To assist structural geological and hydrogeological data with the conceptualisation of the aquifer systems in the study;
- To determine the existence of mine interflow systems between the coal and the gold mine by comparing the $\delta^{18}O$ and δD signatures with a hydro-chemical analysis of groundwater emanating from the underground mining activities of each mine.

In order to test the applicability to interpretation of hydro-chemical and environmental isotope data analyses methodologies for the two aquifers, the data was interpreted with the following:

Standard groundwater chemistry diagrams: Piper and Expanded Durov and Stiff diagrams are used to define the general study area's groundwater chemistry characteristics relative to other groundwater types.

Diagnostic chemistry diagrams: In the format of X-Y scatter plots or composition diagrams of selected pairs of measured parameters. In general, positive correlations are indicated as straight lines, representing mixing of end-members in different proportions. Clusters of data indicate similar groundwater types or groundwater fed by the same aquifer.

δ18O versus δD diagram: This "fingerprints" the different groundwater in the different aquifers, by comparing their relative isotopic ratios.

7.6.2 Stable environmental isotope data

Figure 100 represents the δ18O and δD relationships for groundwater of the study area. Given the fact that residence times for groundwater in the study area are likely to be spatially variable, infiltrating rainwater with a Karoo aquifer isotopic "signature" can coexist with groundwater with a Witwatersrand isotopic "signature". The lack of connectivity within the aquifer(s) is also suggested by the spatial distribution of the samples within the aquifer system. A rainfall signature prevails in Karoo aquifer samples taken in the study area (Figure 100). These samples are affected by a relatively large annual precipitation and apparent short residence times, since their isotopic signature is very close to that of rainfall. Therefore, most of the shallow groundwater samples most probably reflect the character of the largest rainfall events during the previous year. By contrast, the Witwatersrand aquifer samples generally have a different "signature" to that of rainfall (Figure 100). Apparently, rainfall events have not recharged the deep aquifer over a short period of time to make a significant contribution to the isotopic "fingerprint" of the deeper groundwater found in the Witwatersrand aquifer (Figure 100). In deep aquifers such as the Witwatersrand aquifer, complex flow patterns originating from the geological structures often lead to difficult predictions of water origin(s), determination of the main flow paths, and potential mixing of waters (Drever, 1997). All these uncertainties prevent an efficient interpretation from isotopic composition data alone. A much more efficient way is to combine isotopic ratios with the major ionic ratios and depth to "fingerprint" the origin of the groundwater in the different aquifers.

From the data plotted in Figure 100 the following samples can be "fingerprinted":

- Rainfall selectivity: The singular rainwater sample can be disregarded as it was a once of sampling event and may vary due to seasonal rainfall events (Drever, 1997).
- The deeper Witwatersrand aquifer samples (**H1**, **H2, H3, H4** and **H5**) are more depleted in $\delta^{18}O$ and δD than the shallower Karoo aquifer (**WB1D, WB3D, MHR47, MHN 45, S1, S3, S4,** and **S5**). This is explained by different intake histories. The Witwatersrand aquifer is not constantly recharged from precipitation, compared to the shallower Karoo aquifer, which is recharged by precipitation (Drever, 1997). This means that the Karoo aquifer is generally enriched in both $\delta^{18}O$ and δD (less negative) compared to the Witwatersrand aquifer.

- **H1** and **H4** are more depleted in $\delta^{18}O$ and δD than the other gold mine samples (Figure 100). **H1** and **H4** are samples taken from faults intersecting the gold mine workings (Table 14), indicating water that has had a fair amount of exchange with rock minerals when it travelled along the fault from the base of the Karoo and into the gold mine, thus depleting the $\delta^{18}O$ and δD (Figure 99).
- **H7** is water dripping out of the roof of the gold mine. Its isotopic "signature" is unrelated to the other gold mine samples. It plots with samples **WB1D, WB3D, MHR47, MHN45, S1, S3, S4** and **S5**, which are samples taken from the coal mine and the Karoo aquifer. This indicates that **H7**'s origin is that of the Karoo aquifer affected by coal mining.
- The other samples were difficult to distinguish between as they plot in the same area on the $\delta 18O$ and δD relationship isotope plot (Figure 100) with no unique isotopic "signature". They all plot close to the local rainfall line (Figure 100), suggesting that they have been affected in some way by precipitation directly or indirectly (mixing) over a period of time.

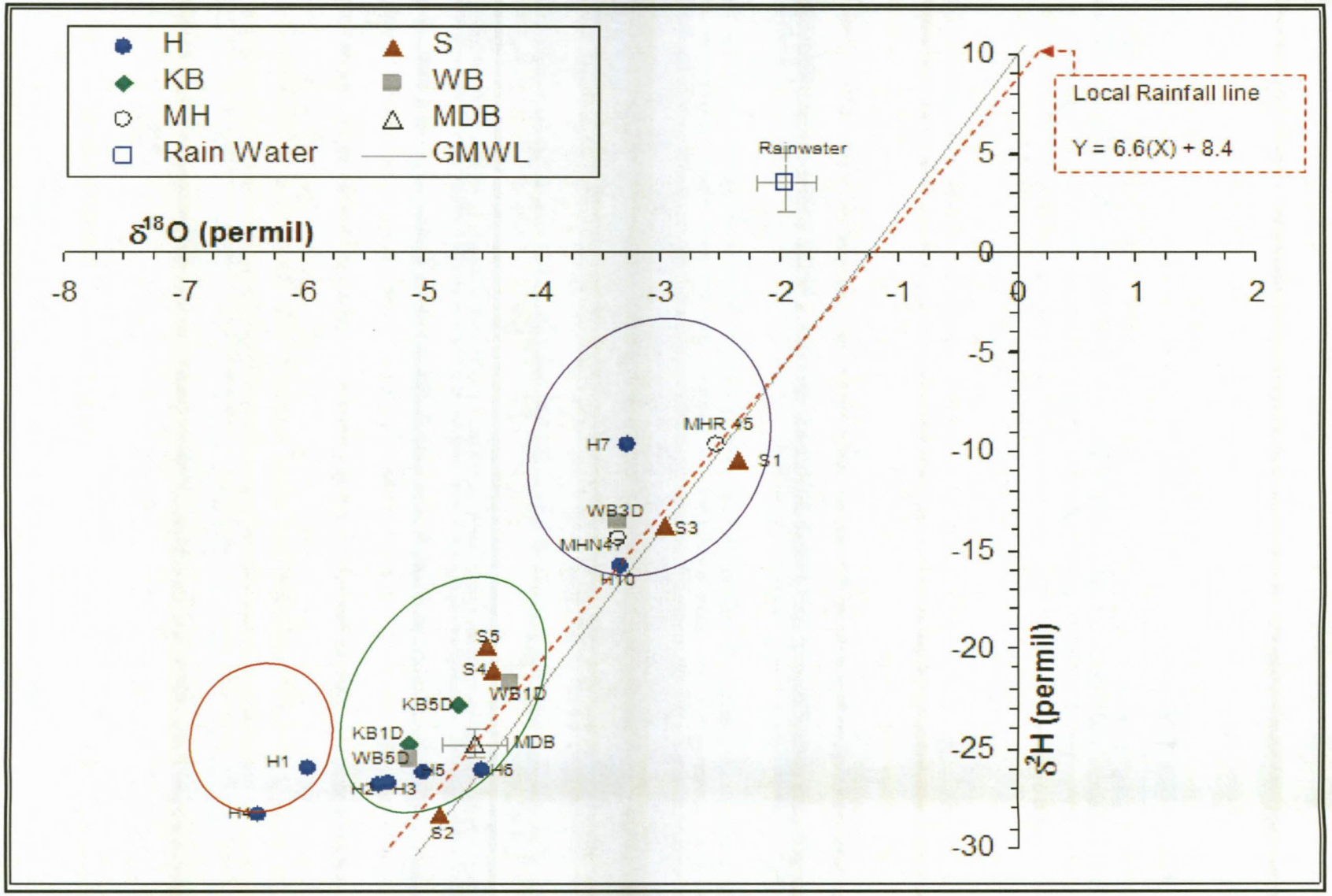

Figure 100: δ18O and δD relationship isotope plot for the samples collected in the study.

7.6.3 Major ion chemistry and stable environmental isotopes

Various X-Y scatter plots of ionic ratios and/or environmental isotopes are used to "fingerprint" the different origins of groundwater in the aquifers. One of these plots is the $\delta^{18}O$ versus EC plot.

From the $\delta^{18}O$ versus EC plot (Figure 101) it is possible to distinguish between samples originating from the different aquifers. Although no direct relationship between $\delta^{18}O$ and EC exists, combination of the information obtained independently from $\delta^{18}O$ and EC is significant. The $\delta^{18}O$-signature provides information on the recharge whereas EC provides information on dissolution processes in the aquifer, flow process and path. The Witwatersrand aquifer groundwater clusters around $\delta^{18}O$ and EC values between -4.5 to -6.4 ‰ and 200 to 500 mg/l, respectively, whereas the Karoo aquifer's sample clusters around ^{18}O and EC values between -2.3 to -5.15 ‰ and 89 to 500 mg/l, respectively (Figure 101).

From Figure 101, it is possible to distinguish the following three different groups of groundwater:

- **S1, WB 3D, MHR 45** - Groundwater originating from the Karoo aquifer and which is recharged by rainfall on a fairly constant basis with relative short residence time (Fritz *et al.*, 1980).

- **H1, H4** - Groundwater originating from the faults with a relative long travel time and exchange with rock minerals, as seen in Figure 99 (Fritz *et al.*, 1980).

- **H2, H3, H5, H6, H7, H10, S2, S3, S4, S5, KB1D, KB5D, WB1D, WB5D** and **MHN47** - Groundwater that has undergone a fair amount of mixing and mineralisation. It is not possible to determine which aquifer these samples originate from using isotopic compositions alone. They all plot close to the local rainfall line (Figure 100), suggesting that they have been affected in some way by precipitation directly or indirectly (mixing) over a period of time.

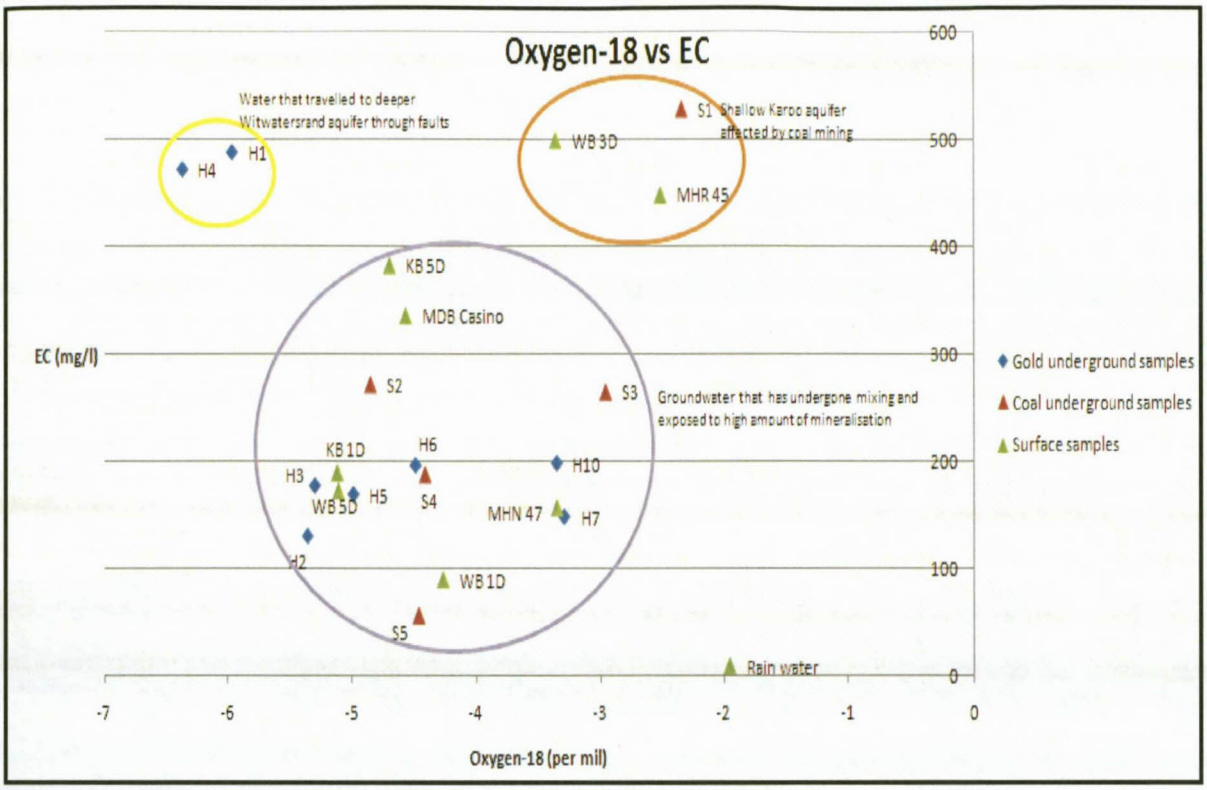

Figure 101: $\delta^{18}O$ vs. electrical conductivity plot.

7.6.4 Depth and stable environmental isotopes

In Figure 102, the samples were plotted from shallowest (**KB1D**) 28 m to deepest (**H5**) 2152 m below surface. Figure 103 show the depleted $\delta^{18}O$ signature of the deeper gold mine samples, suggesting that water was recharged at a much earlier time with a much longer flow path.

- Figure 102 and Figure 103 show the depleted $\delta^{18}O$ signature of the gold mine samples **(H1, H2, H3, H4, H5** and **H10)** with depth. This indicates their long residence and flow paths to reach the gold mine.

- Figure 102 and Figure 103 show that the $\delta^{18}O$ signature for **H6** and **H7** is in the same order of magnitude as that of the coal mine samples. They are of Karoo aquifer origin and they are the closest samples taken to the floor of the No. 4L coal seam. **H1** and **H4** are also believed to be of Karoo aquifer origin but are much more depleted compared to **H6** and **H7.** This is attributed to **H1** and **H4** originate from a fault that connects the base of the Karoo aquifer

with the Witwatersrand aquifer and therefore a confined aquifer with a long travel time, giving rise to their depleted $\delta^{18}O$ signature (Figure 98).

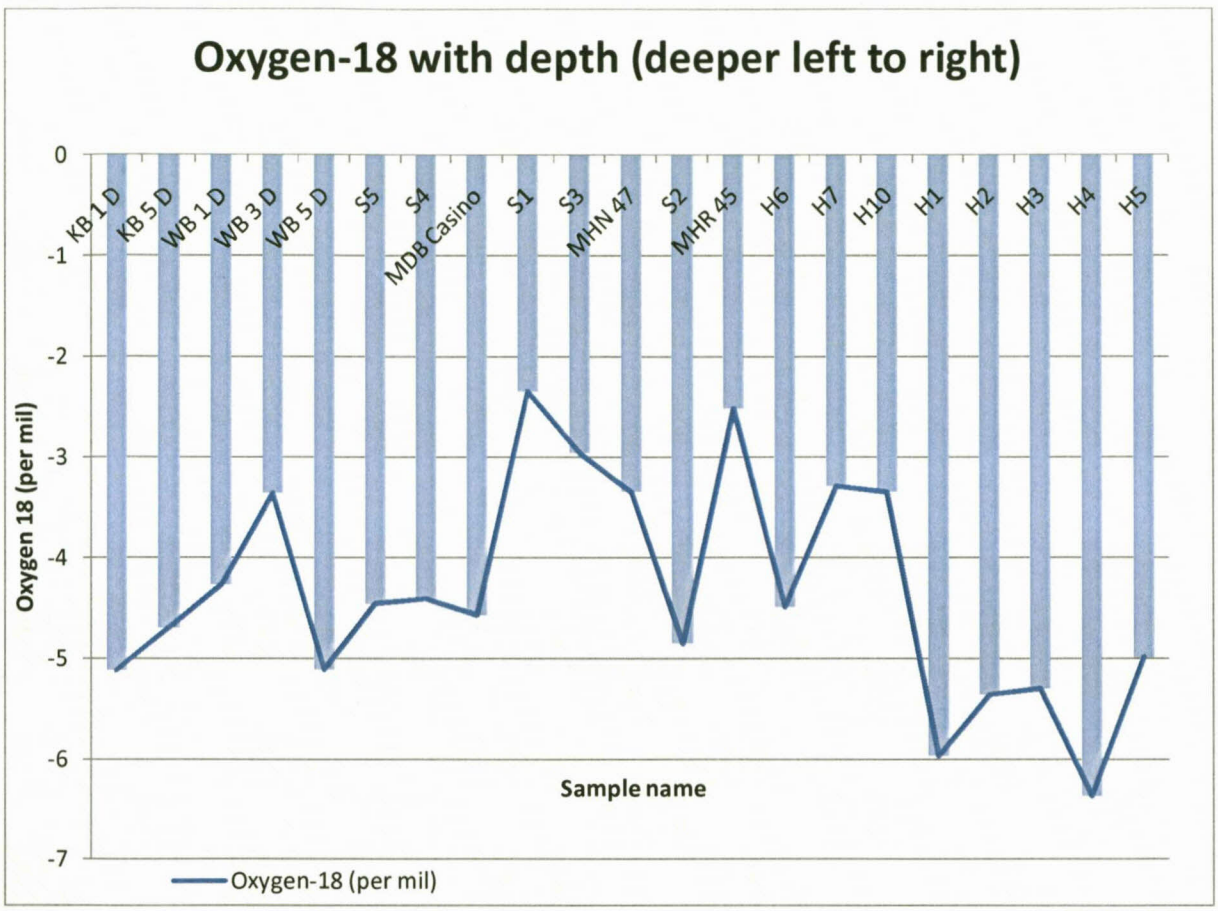

Figure 102: $\delta^{18}O$ vs. depth for samples in the study area.

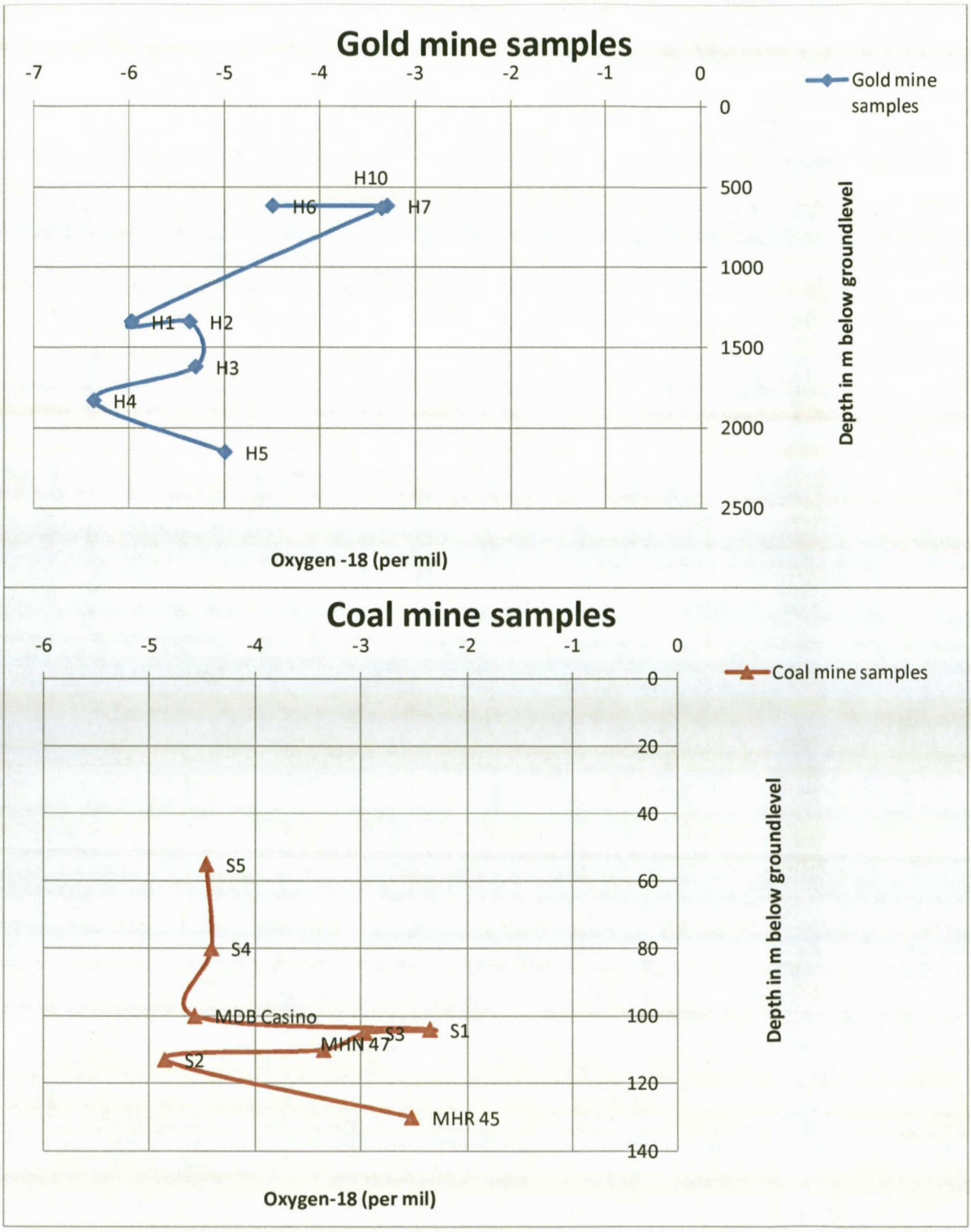

Figure 103: $\delta^{18}O$ vs. depth for underground samples originating in the different mines.

7.7 Discussion of isotope results

A rainfall signature prevails in the shallower groundwater samples (**KB1D, KB5D, WB1D, WB3D, WB5D, MDBCasino, S1, S2, S3, S4, S5**) taken from the Karoo aquifer in the study area (Figure 100). These samples are affected by a relatively large annual precipitation and apparently short residence time, since their isotopic signature is very close to that of rainfall (Figure 100). Therefore, most of the Karoo aquifer samples most probably reflect the character of the largest rainfall events during the previous year. By contrast, the deep groundwater samples generally have a different "signature" to that of rainfall (Figure 100). It is apparent that rainfall events have not recharged the deep aquifer over a short period of time to make a significant contribution to the isotopic "fingerprint" of the samples found in the Witwatersrand aquifer.

This means that the Karoo aquifer is generally enriched in both $\delta^{18}O$ and δD as shown in Figure 100 (less negative).The deeper Witwatersrand aquifer (as seen in samples **H1-H5** and **H10** in Figure 103) is more depleted in $\delta^{18}O$ and δD than the shallower Karoo aquifer seen in samples **WB1D, WB3D, MHR47, MHN 45, S1, S3, S4, S5** and **H7** in Figure 103. This is explained by different intake histories and long travelling times. The Witwatersrand aquifer is not directly recharged by precipitation compared to the shallower Karoo aquifer, which is directly recharged by precipitation.

H1 and **H4** are the most depleted samples in $\delta^{18}O$ and δD (Figure 100) as they were taken from faults it suggest that reactions with rock minerals have taken place in the water as it travelled along the fault depleting its $\delta^{18}O$ and δD composition (Figure 99).

7.8 Isotopes and Hydro-chemistry conclusions

From the 21 water samples that were collected from different localities (Figure 71 and Figure 72) widely dispersed over the study area covering a depth range of between 28 and 2152 m below surface. Three different types of sub-surface water were encountered in the study area and can be differentiated between.

7.8.1 Karoo aquifer origin samples recharged by precipitation (KB1D, KB5D, WB1D, WB3D, WB5D, MHN47, MHR 45, MDBCasino and S1-S5).

The shallow Karoo aquifer samples and those affected by coal mine activities (**KB1D, KB5D, WB1D, WB3D, WB5D, MHN47, MHR 45, MDBCasino** and **S1-S5**) are generally lower in Na concentrations (Figure 81) and higher in SO_4 concentrations (Figure 83) than the deeper

Witwatersrand aquifer samples. All have relatively high concentrations of bicarbonate, suggesting they are recharged by precipitation or water in the shallow unconfined Karoo aquifer that reacts freely with the atmosphere. They all plot close to the local rainfall line (Figure 100), which also suggests that they have been affected in some way by precipitation, directly or indirectly (mixing). They are relatively enriched in $\delta^{18}O$ and δD, suggesting that they have had a relatively short residence time in the sub-surface (Figure 103).

7.8.2 Witwatersrand samples recharged by influx from shallower Karoo aquifers (H1, H4, H6, H7).

Samples **H1, H4, H6** and **H7** are also regarded as Karoo aquifer origin samples, based on the elevated Cl concentrations of **H1** and **H4,** shown in Figure 85 (ion-exchange). The Na-SO_4 grouping of the shallower samples (**S1, S3, MHR45, WB5D** and **MDBCasino**) in the Piper diagram (

Figure 90) have an isotopic signature shown in their depleted $\delta^{18}O$ and δD (Figure 100) and their unique Stiff diagram geometry (Figure 94), combined with the fact that they were taken from faults intersecting the gold mine workings linking the base of the Karoo aquifer with the Witwatersrand aquifer (Table 14).

H1 and **H4** are the samples most depleted in $\delta^{18}O$ and δD (Figure 100), as they were taken from faults. This suggests that reactions with rock minerals have taken place in the water as it travelled along the fault, depleting its $\delta^{18}O$ and δD composition (Figure 99).

H6 and **H7** are of Karoo aquifer origin, based on their Stiff diagram (Figure 94) general geometry being the same as the coal mine samples (**S1-S5**) and their EDD plotting position in **Field 3** with the coal mine samples (**S1-S5**), which are expected to be found in high extraction coal mining. These samples have most probably undergone ion-exchange reactions in reducing conditions on the water's flow path through the Ecca shales. **H6** and **H7** are the samples taken closest to the No. 4L coal seam (Figure 95). **H6, H7** and **H10** are also the only samples that could have been affected by coal mining as coal mining has not reached the area of the other underground gold mining samples (Figure 74).

7.8.3 Witwatersrand aquifer water recharged by influx from shallower Karoo aquifer with a long residence time and possibly mixed with connate water or paleo-meteoric water (H2, H3, H5, H10)

Sample **H2** (next to dyke), **H3** (exploration borehole), **H5** (out of stope) and **H10** (out of mine roof) all show depleted $\delta^{18}O$ and δD (Figure 100). They have relatively high Na- concentrations (Figure 81) and low SO_4 concentrations (Figure 83) compared to Karoo aquifer samples, but have lower Na- concentrations compared to the **H1** and **H4** samples (from faults), believed to be water from the base of the Karoo aquifer. **H2, H3, H5** and **H10** all plot within **Field 9** of the EDD which is very old, stagnant or paleo-meteoric water that has reached the end of the geohydrological cycle or water that has moved a long time and/or distance though the sub-surface and has undergone significant ion-exchange. **H3**'s bicarbonate concentrations are a mixture of precipitation and flux of confined aquifer water. **H2, H5,** and **H10** represent a flux of confined aquifer water, as they were taken from fractures intersecting the gold mine workings. Their lower bicarbonate concentrations compared to **H3** is attributed to the reverse of Equation 14 in a closed system (confined aquifer) where there is no CO_2 present, resulting in the slow loss of HCO_3^- (Freeze & Cherry, 1979). This indicates that they are recharged by the shallower Karoo aquifer but that they have had a long residence time in the sub-surface.

7.8.4 Groundwater interaction between the Karoo aquifer and the Witwatersrand aquifer based on hydro-chemical interpretations

There is interaction between the aquifers, as seen in samples **H1 H3 H4 H6** and **H7,** through preferred pathways such as faults and fractures. Important is the fact that **H1, H3** and **H4** interaction occurs without the influence of the coal mine, as coal mining has not reached the areas where these samples were taken.

H6, H7 and **H10** were taken near current coal mining activities. Only **H6** and **H7** show a "fingerprint" that is characteristic of a Karoo aquifer affected by coal mining. Therefore, the only current interaction between the coal mine and the gold mine is at No. 9 shaft, Level 1 (Figure 95). Therefore not all preferential pathways bearing water from the Karoo aquifer have been affected by coal mining.

It can be stated categorically that very little water was encountered in gold mines- indicating that very little seeps through from the Karoo aquifer into the Witwatersrand aquifer.

7.8.5 Limitations of sampling

The following are the limitations of sampling:

- Only once of sampling was done and therefore no trends over time could be established.
- Not all areas within the gold and coal mine were accessible. This was due to flooding of some compartments within the coal mine and shafts that have been decommissioned and unsafe within the gold mines.

Chapter Eight: Decant

After mining of the coal and gold in the study area, the mining voids resulting from the mining will be left to flood with water. Therefore, this study considers the possibility of groundwater decanting onto the surface and from the deeper situated gold mine into the shallower coal mine.

If decant in the study area will occur it will be a function of:

- Type of mining,
- Topography,
- Depth of mining,
- Interconnectivity of the different mines, and
- Piezometric levels of the different mines and different aquifers.

8.1 Mining and recharge in Sasol's Middelbult (Block 8)

The underground workings of Sasol's Middelbult Block 8 consist and in future will consist of various layouts and configurations (refer to Section 3.1 Sasol coal mining complex, Figure 11). These configurations can be broadly classified under board-and-pillar and high extraction methods. The common characteristic of these mining methods especially high extraction is that the removal of the coal seam results in the caving of the overlying strata into the mined void. This disruption of the overlying rock mass has a significant effect on the hydrogeology, especially where high extraction has been done, resulting in subsidence (refer to Section 6.2.1 Subsidence due to high extraction coal mining, Figure 62)

The overburden covering the No. 4L coal seam consists of Karoo Supergroup formations, which are sandstone, shale, interbedded siltstone, mudstone and coal of variable thickness (Vermeulen & Dennis, 2009). The total thickness of the overburden covering the No. 4L coal seam ranges from 60 m to 180 m, at an average of 90 m (refer to Karoo Supergroup, Figure 22). Dolerite intrusions in the form of dykes and sills are present over the entire study area (refer to Section 4.8.1 Karoo age intrusives). Subsidence is most likely to occur where the coal seam is closest to the surface and where the B4 dolerite sill covering the study area is very thin to non-existent.

Recharge of between 5 to 7 % can be expected at the subsidence areas. Low recharge of between 1 to 3 % can be expected where no subsidence occurs, with a tendency towards 1 % where the B4 dolerite sill is thick (Vermeulen and Usher, 2006).

8.2 Groundwater systems within the coal mine

Three distinct and superimposed groundwater systems are present in the coal mining area of the study area, as described in (Section 5.2 Aquifer types). They are the upper weathered Karoo aquifer system, the lower fractured Karoo aquifer system and the artificial coal mining aquifer system.

8.3 Conceptual decant model for Sasol Middelbult Block 8

After the mining voids have filled up with water, the piezometric level of the artificial coal mine aquifer will rise with the storage coefficient value of the artificial coal mine aquifer (not the specific yield) as conditions in the artificial mine aquifer have changed from an unconfined aquifer to a confined aquifer (Vermeulen & Dennis, 2009). The influx of water from the overlying aquifers into the mine aquifer will decrease as the two water levels approach each other, as shown in Figure 104 below (Vermeulen & Dennis, 2009). The lowest point on the surface through this particular section is at 1566 m.a.m.s.l, while the lowest point on the surface in the Middelbult Block 8 area is at 1560 m.a.m.s.l. The highest point of the No. 4L coal seam roof through this particular section is 1505 m.a.m.s.l, while the highest point in the Middelbult Block 8 area is at 1521 m.a.m.s.l. The minimum difference in height between the surface and the No. 4L coal seam roof in the Middelbult Block 8 area is thus more than 39 m.

For groundwater affected by the coal mining activities and left to fill the mining voids to decant it will have to overcome more than four bars of pressure (10 m = 1 bar), which is unlikely. In the unlikely event that the piezometric level from the mine and the water level in the fractured zone combine, the excess water will seep out as water that is unaffected by underground coal mining activities (Vermeulen & Dennis, 2009). The average thickness of the overburden above the No. 4L coal seam of the Middelbult Mine Block 8 area is approximately 90 m (refer Karoo Supergroup, Figure 22), while the average thickness of the overburden covering the Sasol Secunda mining complex is more than 100 m (Vermeulen & Dennis, 2009).

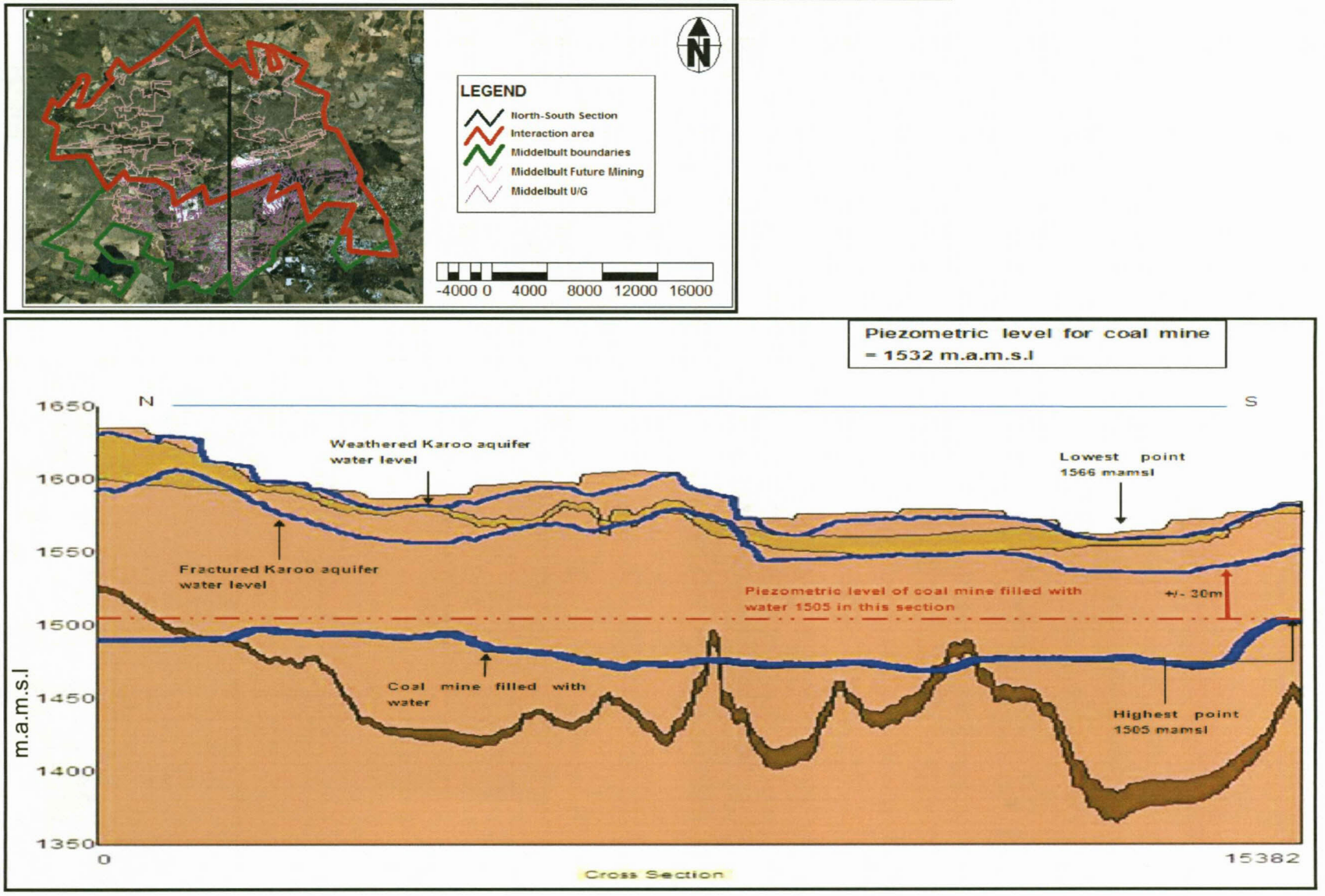

Figure 104: North-south cross-section of the conceptualisation of the different water levels.

8.4 Mining and recharge in Harmony Evander gold mining operations

Evander is a deep-level gold mine, with no opencast or shallow workings. The underground workings of Harmony Evander gold mining consist of various layouts and configurations (refer to Section 3.4 Harmony Evander gold mining operations, Figure 14). These configurations are a function of mine planning and method, and can broadly be classified under conventional mechanised face and strike gully stoping methods. The overburden covering the viable Kimberley Reef consist of Karoo super group formations which are sandstone, shale, interbedded siltstone, mudstone and coal the Transvaal Supergroup consisting of dolomites, shales and conglomerates and the Ventersdorp Supergroup consisting of basalts.(refer to Chapter 4: Geology of the Study Area). The total thickness of the overburden covering the Witwatersrand Supergroup in the study area ranges from 208 m to 2500 m at an average of 1392 m (Figure 105). Faulting is common throughout the study area (refer to Figure 32). Naturally occurring recharge to the gold mine is considered less than 1 % due to the immense thickness of the overburden covering the study area. Influx into the gold mine may occur from the overlying Karoo aquifer through preferred pathways such as:

- Fractures,
- Faults,
- Shafts,
- Exploration boreholes.

Influx may also occur from the water trapped in the Witwatersrand sediments or from connate water (Onstott *et al.*, 2006). This recharge is limited and could be depleted due to pumping activities. Influx into gold mine voids will allow the mine to fill up with water, when the possibility of decant to surface or the overlying coal mine may arise.

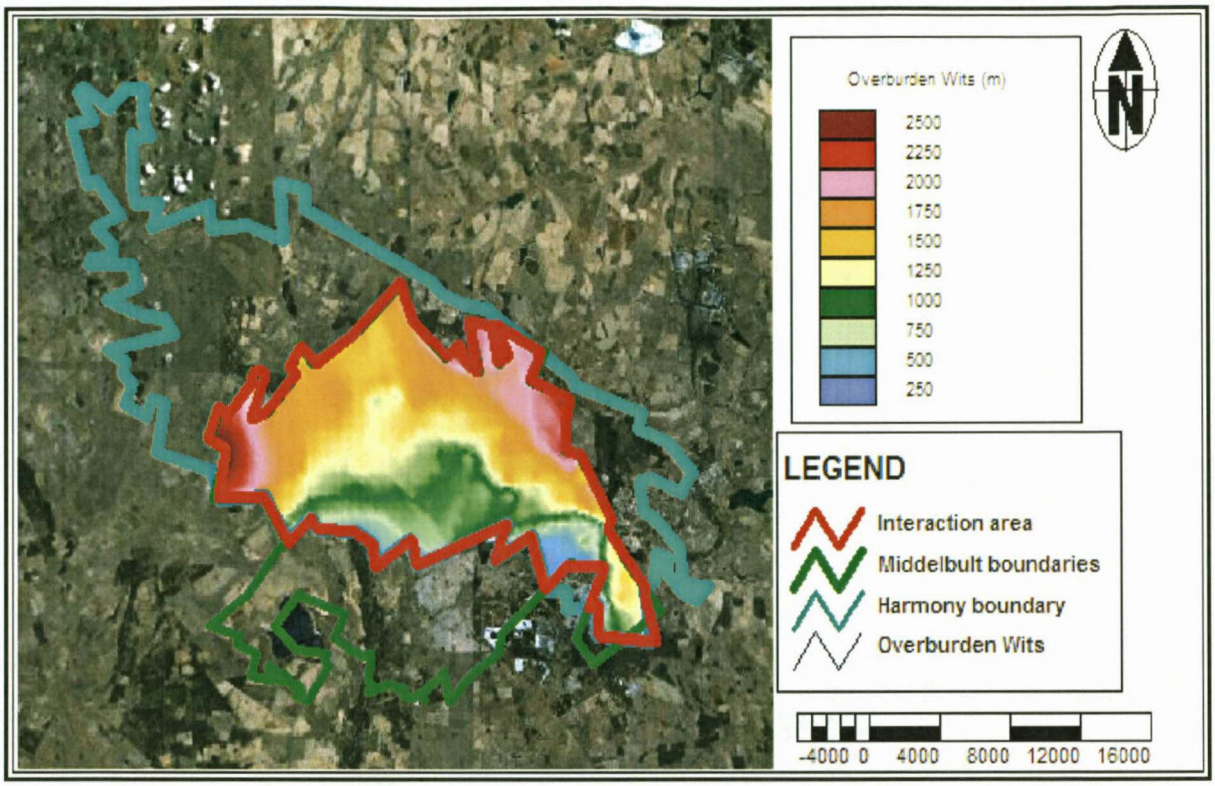

Figure 105: The interpolated thickness of the overburden covering the Witwatersrand Supergroup.

8.5 Groundwater systems within the gold mine

Two distinct and superimposed groundwater systems are present in the gold mining area of the study area. They are the fractured Witwatersrand aquifer and the artificial gold mining aquifer, which are both confined due to the overlying Ventersdorp Supergroup. (refer to Section 5.3 Aquicludes/Impermeable layers).

8.6 Study area conceptual decant model for the gold mine

If undisturbed, the water level in the Witwatersrand aquifer (confined aquifer) will not rise above the Ventersdorp Supergroup (lavas) as the Ventersdorp Supergroup acts as an aquiclude restricting groundwater movement. However, shafts from gold mining operations have intruded through the Ventersdorp Supergroup, puncturing the Witwatersrand aquifer and effectively creating a piezometric level within the aquifer. The average thickness of the Ventersdorp Supergroup is 577 m with a range of 0 m to 1324 m throughout the study area (Figure 106).

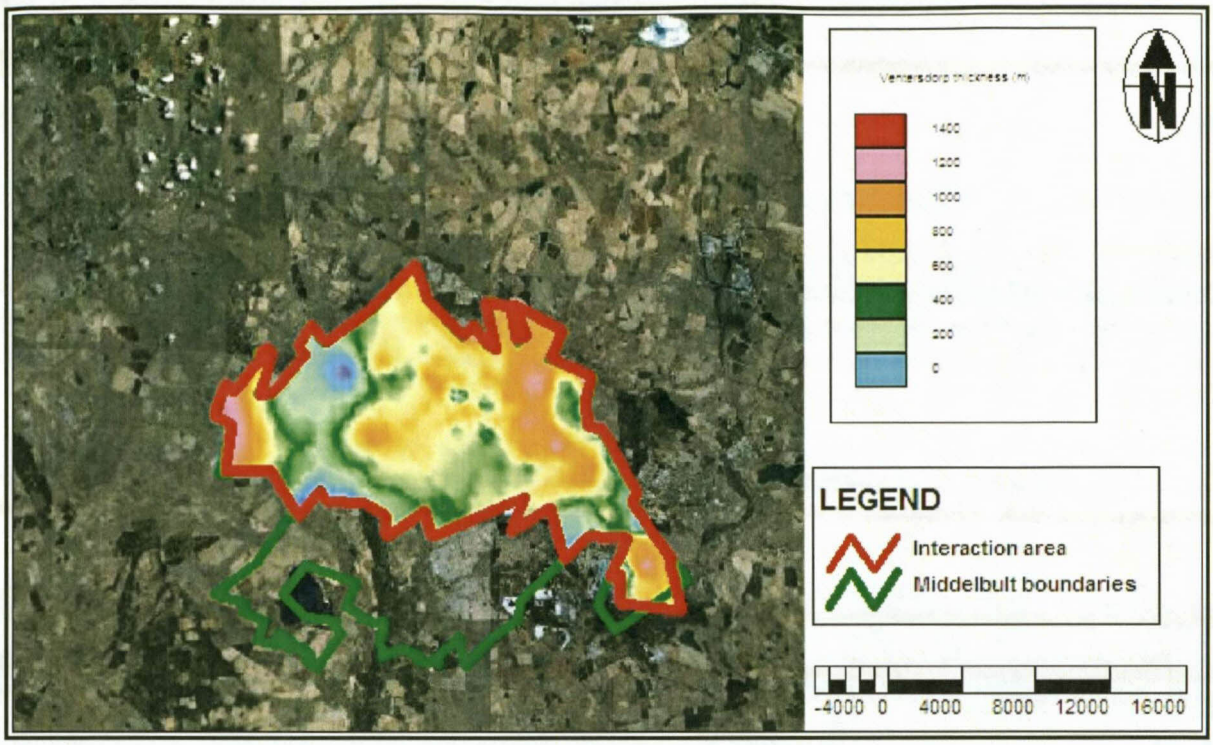

Figure 106: Interpolated thickness of the Ventersdorp Supergroup.

Earlier reports by Pritchard-Davies (1962), Mulholland (1982), Rison Groundwater Consulting (2002), Rison Groundwater Consulting (2003) and Rison Groundwater Consulting (2003) indicate that the original Witwatersrand aquifer water level was at approximately 1533 m.a.m.s.l pre-mining where exploration boreholes intersected the Witwatersrand aquifer. The average interpolated thickness of the overburden above the Witwatersrand aquifer has a maximum of 2550 m and a minimum of 254 m at an average of 1400 m. This indicates that the original water level measured by Pritchard-Davies (1962) is not an actual water level but a piezometric level as there are aquicludes confining the Witwatersrand aquifer resulting in the piezometric level of 1533 m.a.m.s.l. that is within the Karoo Supergroup.

The piezometric level is the hypothetical surface of the hydraulic head in a confined or semi-confined aquifer. The piezometric level will be the closest to surface where the confined aquifer is open to atmospheric pressure or where hydraulic pressure is equal to atmospheric pressure, which is zero. A conceptual model of piezometric levels is shown in Figure 107. Important to note is that shafts and exploration boreholes situated on the surface of the study area go through the Ventersdorp Supergroup and intersect the Witwatersrand aquifer, creating piezometric levels within the shafts and exploration boreholes, shown in Figure 110 where the

water levels of No. 6 shaft and No. 10 shaft have risen above the confined water level within the Witwatersrand aquifer. During the period 1956 to 1969, a dewatering cone developed around the mine workings and the groundwater level was lowered to a deepest point of 841 m below surface or 728 m.a.m.s.l. (Rison Groundwater Consulting, 2007). Pumping in one mine affected the water levels in adjacent mines. Groundwater drawdown therefore occurred at variable rates at the different mines. The water level in Winkelhaak dropped 305 m between August 1956 and July 1962. The water level in Bracken dropped 190 m between February 1961 and July 1962 and the water level in Leslie dropped 170 m between February 1961 and July 1962 (Pritchard-Davies, 1962). Currently, the water levels of No. 10 and No. 6 shaft, where the pumping stations have been decommissioned for over 10 years (Table 9), is at 736 m below surface or 853 m.a.m.s.l at No. 10 shaft and at 701 m.a.m.s.l. or 925 m below surface at No. 6 shaft. This suggests that their piezometric levels have stabilised at these levels as a result of pressure release in the confined Witwatersrand aquifer combined with the effects that pumping has had on these two shafts, lowering the water level around the gold mining. Thus the inflow of water is equal to the outflow in the gold mine if No. 10 and No. 6 shaft are considered.

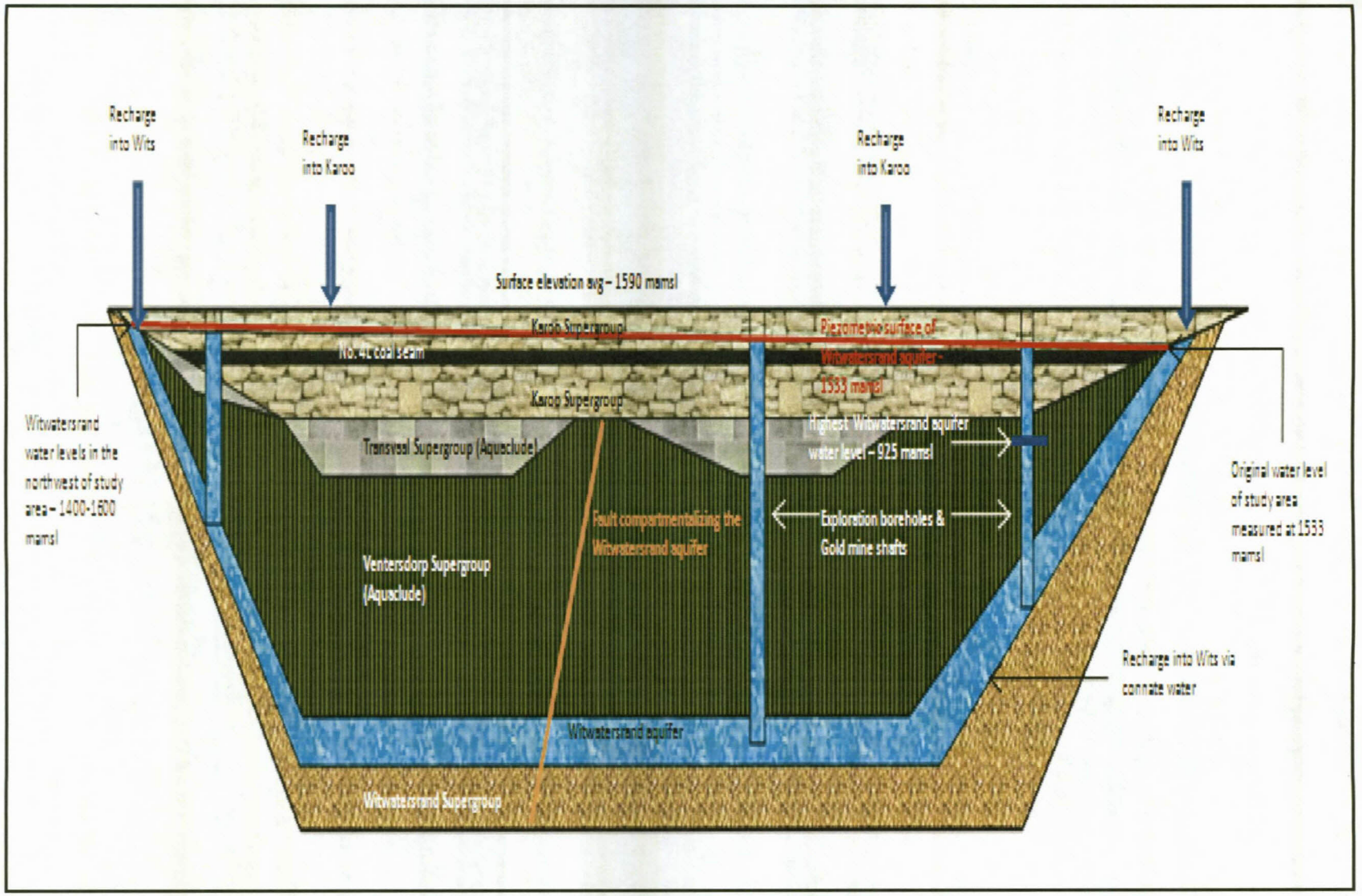

Figure 107: Conceptual models for piezometric levels.

8.6.1 Current conceptual model for decant in Harmony Evander gold mining operations under pumping conditions

The original water level was recorded at approximately 1533 m.a.m.s.l (Pritchard-Davies, 1962) and the current water levels in No.6 shaft and No.10 shaft (Table 9) are at 925 m.a.m.s.l or 1226 m below surface (No.6 shaft) and 853 m.a.m.s.l or 818 m below surface (No.10 shaft). This indicates that rate of pumping (outflow) was higher than the rate of recharge (inflow), thus lowering the piezometric levels in the Witwatersrand aquifer by approximately 608 m in No. 6 shaft and approximately 680 m in No. 10 shaft from the original piezometric level of 1533 m.a.m.s.l.

It is not expected that the current Witwatersrand aquifer water level (pumping level) will reach the coal mine, as the current piezometric level (pumping level) of the Witwatersrand aquifer in the study area is below 925 m.a.m.s.l. The lowest point in the Middelbult Block 8 area of the coal seam floor is at 1450 m.a.m.s.l. The highest point of the current Witwatersrand aquifers piezometric level (pumping level) is 925 m.a.m.s.l (No. 6 shaft). Under current pumping conditions, the minimum difference of the Witwatersrand aquifer's piezometric level (pumping level) and the coal seam floor is 525 m.

8.6.2 Conceptual model for decant in Harmony Evander gold mining operations (Post-closure)

The Witwatersrand aquifer water levels in the Poplar and Rolspruit Project areas situated to the north-northwest of the study area have been recorded at between 1400 to 1600 m.a.m.s.l (Rison Groundwater Consulting, 2007). The project areas of Poplar and Rolspruit are shown in Figure 109. These water levels have been unaffected by mining and pumping and are in the same order of magnitude as the water level of 1533 m.a.m.s.l recorded by Pritchard-Davies (1962). This suggests that:

- The dewatering at the Harmony Evander gold mine shafts has had no influence on the groundwater levels in the Poplar and Rolspruit area, suggesting some compartmentalisation within the Witwatersrand aquifer. With reference to Figure 108, it can be seen that there are major NE-SW trending faults and dykes between the two areas and based on the geological done by McKnight Geotechnical consulting (2002) evidence it is concluded that these faults form impermeable barriers and allow selected parts of the basin to be dewatered independently.

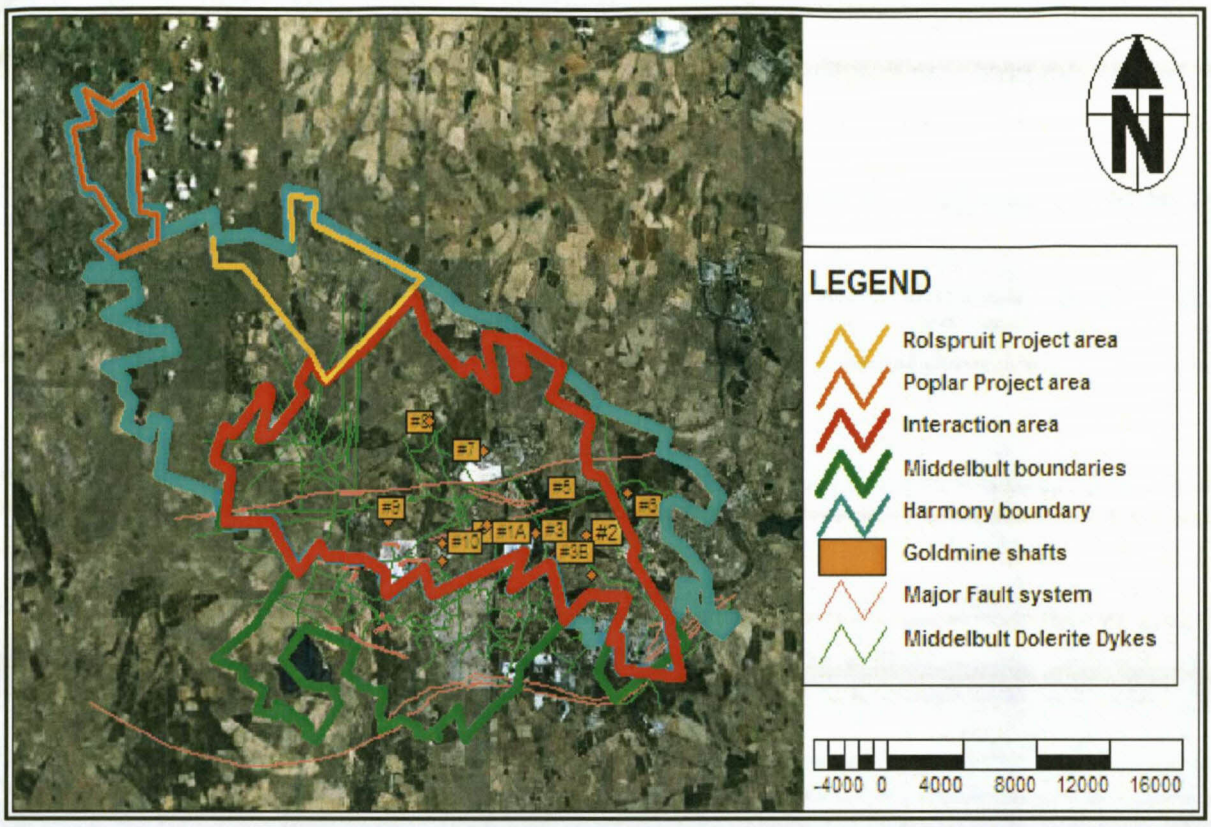

Figure 108: Compartmentalisation within the Witwatersrand aquifer resulting from faults and dykes.

- The current water levels measured in the shafts are not water levels but pumping levels and they can only rise to the piezometric surface of maximum 1533 m.a.m.s.l. found in the Karoo Supergroup where Sasol Middelbult Block 8 coal mining activities operate which is unlikely as there has been significant pressure decrease due to mining within the confined Witwatersrand aquifer. The highest point of the No. 4L coal seam roof in the Middelbult Block 8 area is at 1521 m.a.m.s.l. (Table 1).

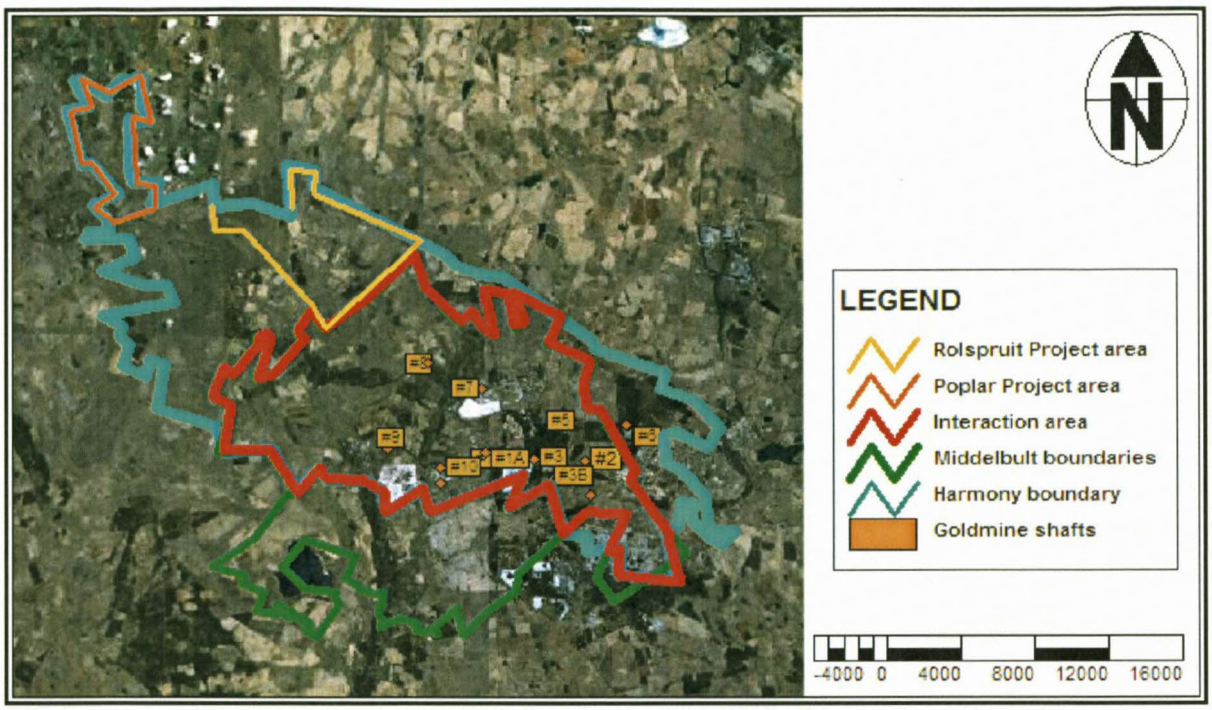

Figure 109: Poplar and Rolspruit Project areas.

After the mining voids have filled up with water, the piezometric level of the artificial gold mine aquifer will rise with the storage coefficient value of the artificial gold mine aquifer (not the specific yield) as conditions in the artificial mine aquifer change from an unconfined aquifer to a confined aquifer. The influx of water from the overlying aquifers into the mine aquifer will decrease as the Witwatersrand piezometric level approaches the Karoo aquifers water level in the gold mine shafts shown in Figure 110. The lowest point of the coal seam floor is at 1450 m.a.m.s.l. Once the water level in the shafts reaches this elevation, the Witwatersrand aquifer's piezometric level and the Karoo aquifer's water level will become one. As the piezometric level from the gold mine and the water level in the Karoo aquifer combine, the excess water will seep out as water that is unaffected by underground gold mining activities (Vermeulen & Dennis, 2009). For groundwater affected by the gold mining activities and left to fill the mining voids to decant, it will have to overcome the same four bar of pressure as the coal mine artificial aquifer, which is unlikely.

This concept is shown in Figure 110. Important to note is that the piezometric level will only rise in the shafts and not through the Ventersdorp Supergroup, which is an aquiclude (confining) layer that will restrict vertical groundwater flow. Although the original piezometric level was at 1533 m.a.m.s.l., the Witwatersrand aquifer piezometric level can never rise to 1533 m.a.m.s.l.

There are numerous voids and shafts from gold mining activities greatly reducing the pressure within the confined Witwatersrand aquifer and thereby significantly lowering the Witwatersrand aquifer's piezometric level.

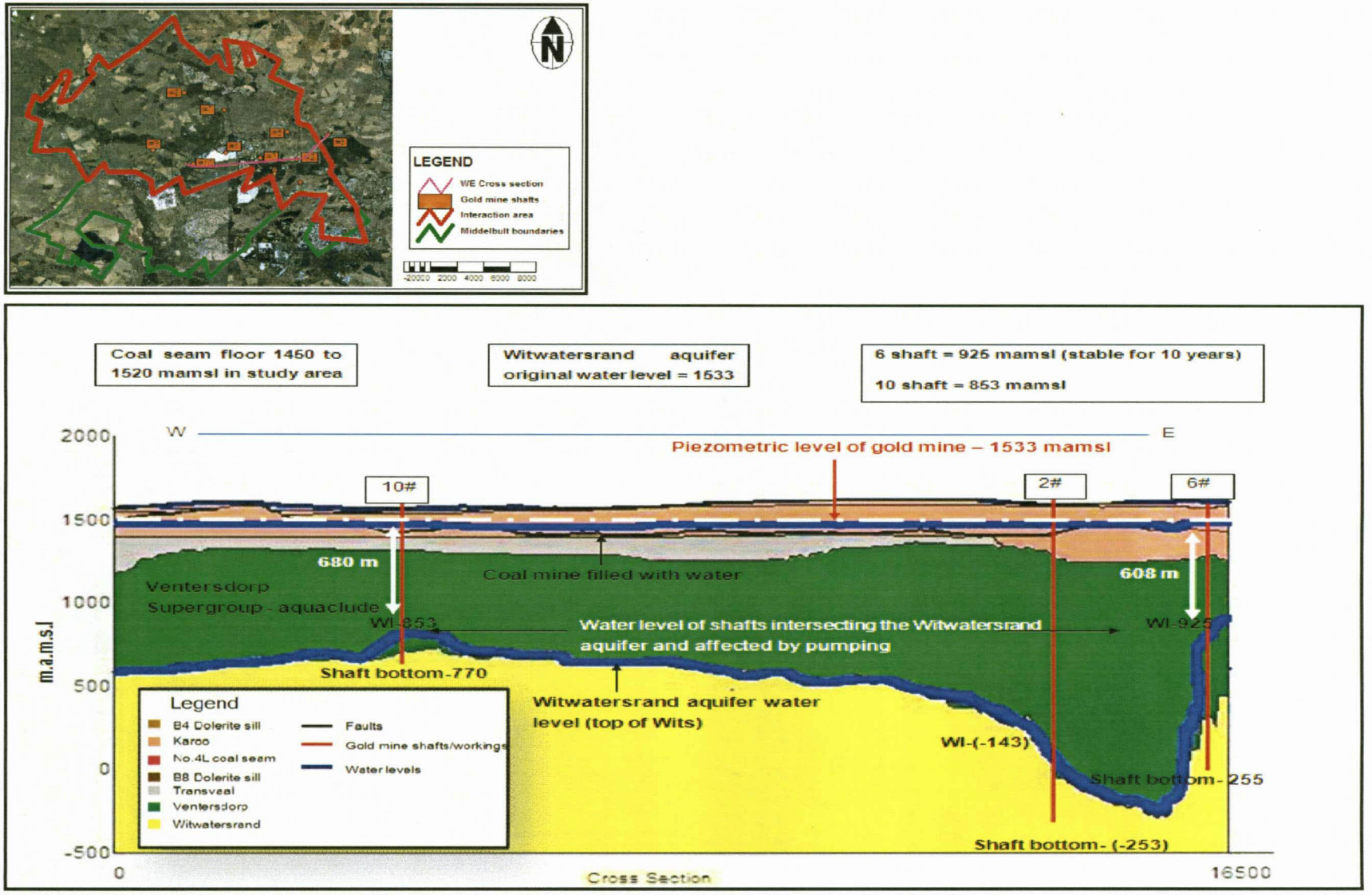

Figure 110: Conceptual model with the interpolated Witwatersrand aquifer water levels.

8.7 Time of gold mine piezometric level to reach coal seam floor

The time for the piezometric level of the gold mine to reach the coal seam floor can be calculated by using the total volume of voids per level and the total volume of inflow of the gold mine (Table 15). The voids were calculated using the tons milled by the gold mine and dividing it by it the specific gravity of most rocks (G ≈ 2.65) given by Freeze & Cherry (1979).

Table 15: Harmony gold mine data used to calculate volume of voids/flooding.

Mine Complex Name	Harmony gold mine total voids (m^3)	Volume of inflow into mine per annum (m^3)	Number of shafts
Winkelhaak	28223773.58	1170500	6
Kinross	24454339.62	2284290	2
Leslie	15635471.7	0	1
Bracken	9980000	0	1
Total	78293584.91	3454790	10

8.7.1 Assumptions

Due to lack of data, numerous assumptions had to be made to determine the flooding of the gold mine. These assumptions are as follows:

- The gold mine only has tonnages for mining complexes and not for individual shafts or levels. Therefore, percentages of volumes were calculated for each complex according to the number of shafts and levels. These uniform values were then assigned to each level of the individual shaft. The values are shown in Table 16. Furthermore the volume of the individual shaft from the bottom of the coal seam roof to the shallowest gold mine workings in each gold mine shaft was calculated by using 12 m x 12 m x difference in depth.
- The total volume of groundwater inflows was calculated using data from Harmony Gold Mining. The estimated groundwater inflow was calculated at 3 454 790 m^3 per annum or 9461 m^3 per day (Table 15). This is in the same order of magnitude as calculated by Rison Groundwater Consulting (2002) and Rison Groundwater Consulting (2003) at 8300 m^3 per day. This roughly equates to 0.5 % of annual recharge, which is the expected range of recharge. The recharge was calculated by using the entire Evander Basin as the surface area for recharge. As not all recharge will accumulate in the underground gold mine workings, this is a very rough estimate.

- All the gold mine shafts are interconnected and will therefore be affected by the same volume of influx. The assumption was made that the gold mine will fill according to elevation and not according to level, meaning that the gold mine will fill uniformly and not according to shaft, where the shaft will fill until the water rises to where the shaft is connected to another shaft, from where it will flow to the adjacent shaft. This is very difficult to simulate and requires a very intricate simulation model. Important to note is that this will affect the different filling rates of the shafts and levels but not the final piezometric level of the gold mine.

Table 16: Values of individual shafts and levels.

Shaft name	Volumes in m^3	Volumes in m^3 to each level	Volumes in m^3 from shallowest gold mine gold to coal seam floor
Shaft No. 1	3669090.566	521440.3666	19008
Shaft No. 2	8184894.34	506416.8962	82224
Shaft No. 3	4515803.774	500267.9748	13392
Shaft No. 5	5080279.245	495672.7245	123552
Shaft No. 6	6773705.66	519016.1277	26496
Shaft No. 7	13694430.19	13602126.19	92304
Shaft No. 8	10759909.43	10738885.43	21024
Shaft No. 9	15635471.7	976487.9811	11664
Shaft No. 10	9980000	1106984.889	1679616
Total	**78293584.91**		

8.7.2 Estimate of the piezometric level to reach coal seam floor with a constant inflow rate

The time for the water level to reach the coal seam is estimated at 22 years and 6 months if current pumping conditions are ceased and a constant rate of 3454790 m^3 is used (Figure 111 and Figure 112). This scenario is unlikely as a rate of inflow will decrease with an increase in elevation or decrease in gradient according to Darcy's law:

Equation 18

$Q = K (dh/dl) A$

$Q = K_{(constant)} \, i \, A_{(constant)}$

Therefore

$Q \propto i$

where:

Q = Rate of inflow

K = Hydraulic conductivity

A = Area

i = Gradient

If K and A remain constant, Q will be directly proportional to *i*. Therefore a decrease in elevation will result in a decrease in inflow rate. Thus the time taken for the gold mine to flood will increase significantly.

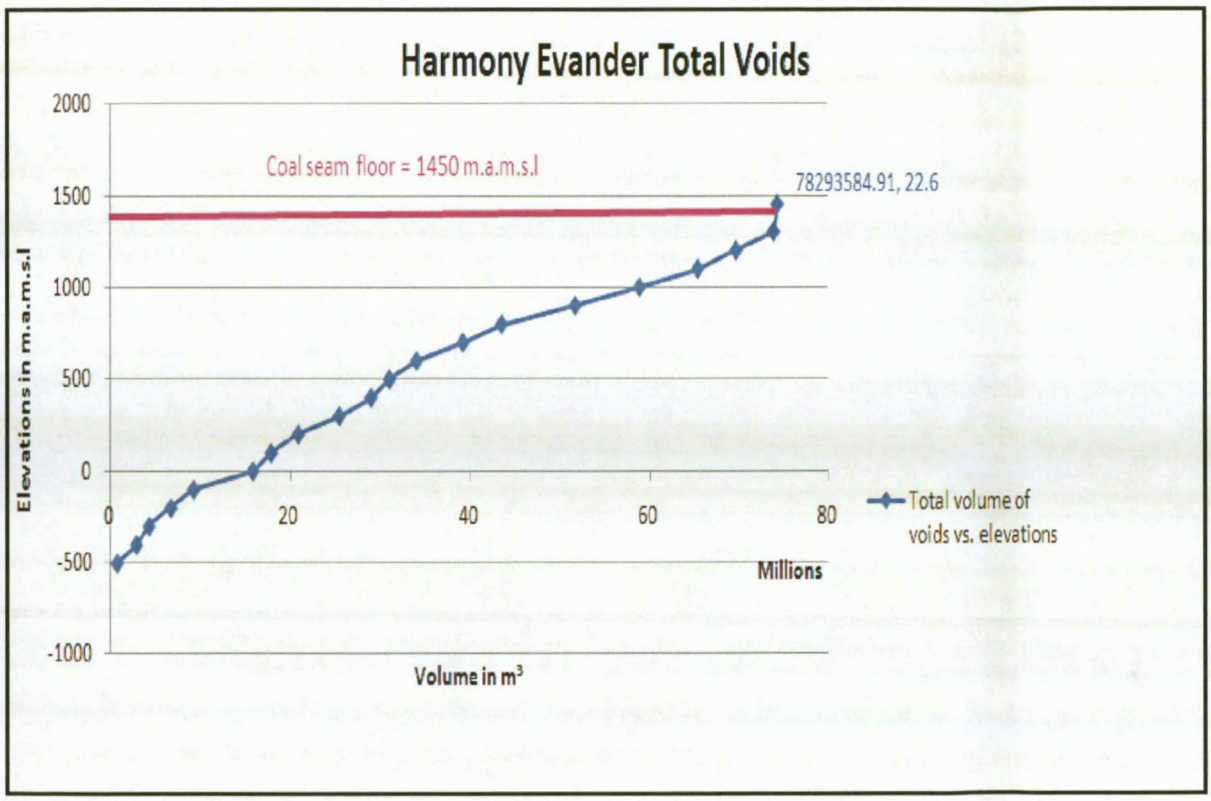

Figure 111: Volume of voids versus elevations.

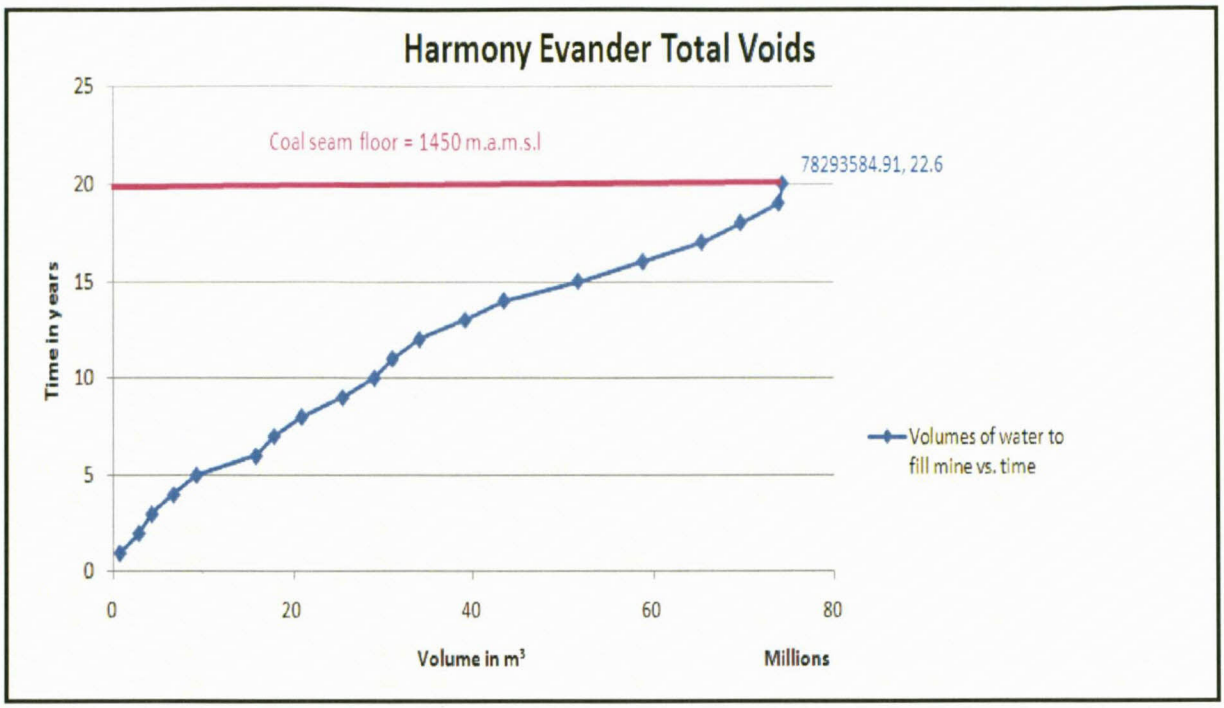

Figure 112: Influx over time.

8.7.3 Estimate of piezometric level to reach coal seam floor applying Darcy's law

If the current inflow rate for the total Harmony gold mine is taken as 3 454 790 m^3 per annum (Table 15) the time for Harmony Evander gold mine workings to flood to the coal seam floor of 1450 m.a.m.s.l will be **406 years**. The piezometric level of the artificial gold mine aquifer will rise with the storage coefficient value of the artificial gold mine aquifer (not the specific yield). The inflow of water from the overlying aquifers into the mine aquifer will decrease as the piezometric level in the shafts rises, decreasing the gradient and thereby decreasing the inflow rate (Equation 18). The inflow of water in the shafts will be high in the beginning but will decrease over time, as shown in Figure 113 and Figure 114.

The time for the water level to reach the coal seam is estimated at 406 years if current pumping conditions are ceased at an inflow rate of 3 454 790 m^3.

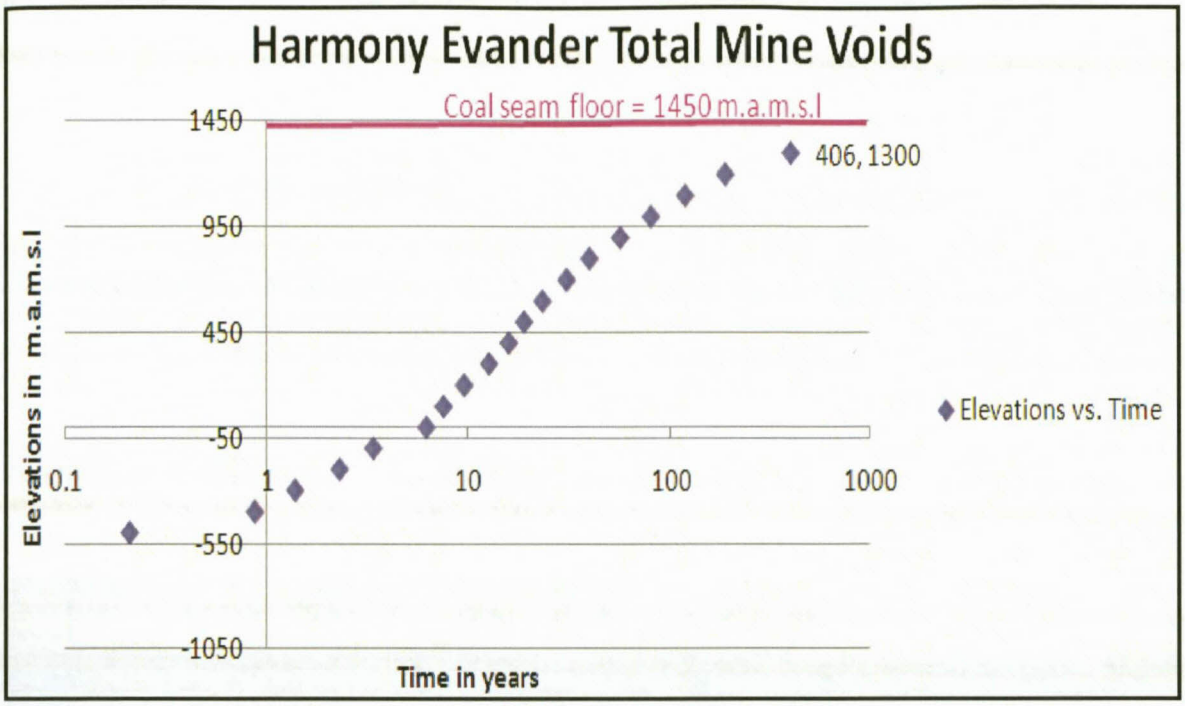

Figure 113: Influx with elevations over time.

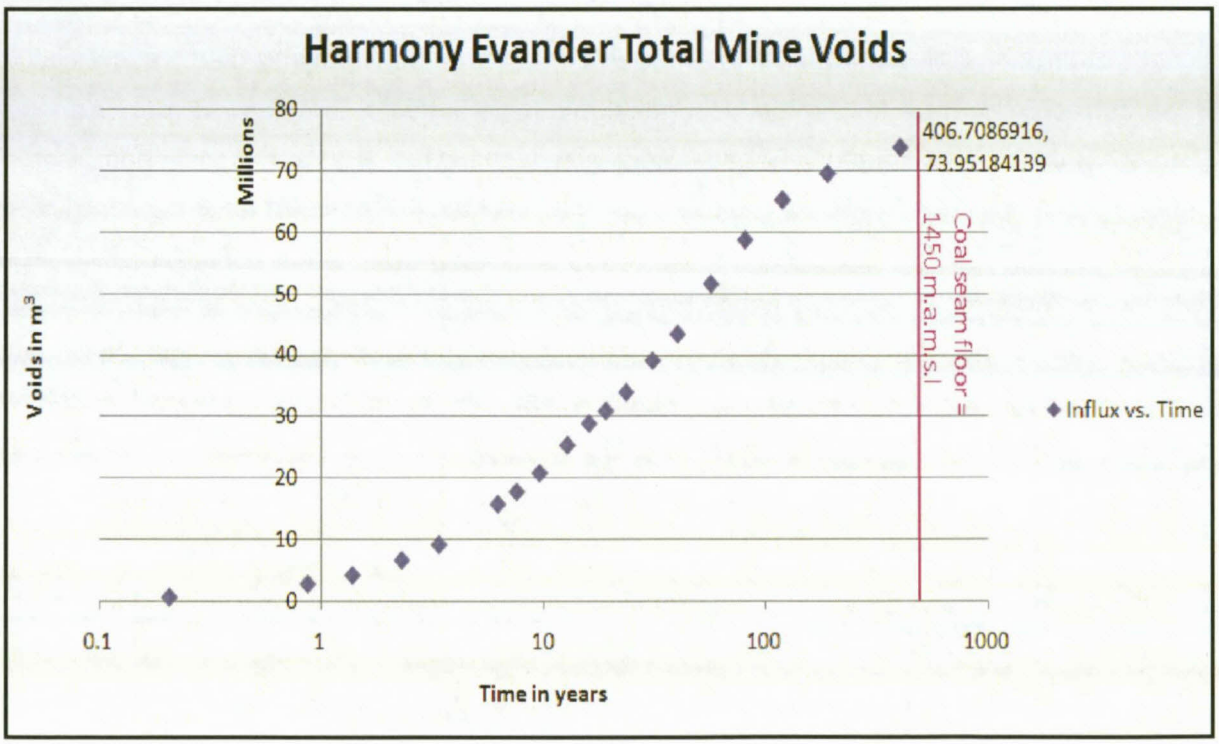

Figure 114: Influx over time indicating years for the gold mine to fill with water.

8.7.4 Conceptual scenario when pumping ceases

With reference to Table 9, the following scenario is envisaged for Harmony gold mine once pumping has ceased:

- Water in No. 1 shaft will fill to level 12, from where it will flow to No. 2 shaft.
- Water in No. 3 shaft will fill to level 5, from where it will flow to No. 2 shaft.
- Water in No. 5 shaft will fill to level 22, from where it will flow to No. 2 shaft.
- The water from No. 2 shaft will flow from level 22 towards No. 7 shaft level 17.
- Water in No. 10 shaft will fill to level 2, from where it will flow to No. 8 shaft.
- Water in No. 9 shaft will fill to level 12, from where it will flow to No. 8 shaft.
- Water in No. 8 shaft will fill to level 12, from where it will flow to No. 7 shaft.

Therefore, No.7 shaft will flood to the point where it is interconnected to the other shafts before further flooding. Only when the other shafts are flooded to the same level, will further flooding in No. 7 commence. When all the shafts are flooded to the same level (elevation), the piezometric level in one shaft will fill simultaneously with the piezometric level of the other shafts.

Chapter Nine: Conclusions and Recommendations

9.1 Conclusions

The objective and aim of the study was to determine potential groundwater interaction between Sasol Mining's Middelbult (Block 8) and Harmony Evander Operations including the combined impacts on the environment. Tools used to establish whether such interaction exists comprised geological data, water sample chemical analysis, water sample stable isotope environmental analysis, and geohydrological information. It is important to list all the various characteristic indicators identified across various geological lithologies and the different aquifers. Of interest is to briefly compare the water samples with each other, with thought given to sample location, depth, mining activity and aquifer. The following overall conclusions are drawn from this investigation:

The study area is located in the quaternary sub-catchments C24D, C23G and C23H of the Waterval River Catchment drainage region as shown in Figure 2. Grootspruit, Winkelhaakspruit, and Trichardtspruit drain over the area and join the Waterval River upstream of the confluence. The surface elevation varies from 1560 to 1695 m.a.m.s.l. The topography dips towards the rivers (Figure 5).

Sasol's mines are located in the Vryheid Formation of the Ecca Group, Karoo Supergroup. These rocks consist primarily of sandstones, shales and coal beds and are extensively intruded by dolerites of Jurassic age. The coal seams in the Highveld Coalfield are mainly flat to gently undulating, with a very gentle regional dip to the south. Coal seam topography and distribution, however, are commonly controlled by pre-Karoo topography on the northern and western margins of the coalfield. Steeper dips are encountered where seams are situated against pre-Karoo hills. The dolerites occur both as sills and linear dyke structures that may extend over tens of kilometres. A large sill-like dolerite structure the B4 sill covers most of the study area.

Harmony's gold mining operations are situated in the Witwatersrand Supergroup, predominantly consisting of quartzite with subordinate lava, shale and conglomerate. The Kimberley Shale separates the two units and is marked by a basal unconformity. Immediately above this

unconformity is a conglomerate layer known as the Kimberley Reef, which is mined by Harmony.

In the major part of the study area, the Witwatersrand Supergroup unconformably overlies the Archaean Basement. These Witwatersrand sediments are in turn overlain by rocks of the Ventersdorp Supergroup, Transvaal and Karoo Supergroups. The study area has undergone extensive structural dislocation and faulting is the most common form of deformation with both primary and secondary fault-features being observed in the study area below the Karoo Supergroup. ***For most of the study area, the Ventersdorp Supergroup forms a thick wedge between the Karoo/Transvaal Supergroup and the Witwatersrand Supergroup.*** The average thickness of the Ventersdorp Supergroup is 577 m and ranges from 0 in the southeast to 1324 m in the central part of the study area.

Early compression tectonics and later extensional tectonics affected both the Witwatersrand and Ventersdorp Supergroups in the Evander Basin, but pre-dated the deposition of the Transvaal Supergroup and hence the Karoo Supergroup (i.e. >2500 Ma). ***This resulted in all major faulting being "cut-off" at the base of the Karoo Supergroup and Transvaal Supergroups.***

There are seven different aquifer types within the study area:

- shallow perched Karoo aquifers (unconfined);
- shallow weathered zone Karoo aquifers (semi-confined);
- deep Karoo fractured aquifers (zone below the weathered zone & confined);
- coal mine artificial aquifer (confined);
- Transvaal dolomitic aquifer (confined);
- gold mine artificial aquifer (confined);
- deep Witwatersrand aquifer (confined).

There is dynamic interaction between the aquifers situated in the upper Karoo Supergroup as there is a direct link with recharge from precipitation into the shallow perched aquifer and the shallow weathered aquifer. This water flows through preferential pathways from these aquifers into the deeper artificial coal mine aquifer and fractured Karoo aquifer. Therefore, the deeper Karoo aquifer is not directly recharged by precipitation but by influx from shallower Karoo aquifers. The water is prevented from moving further downward at the base of the Karoo Supergroup by the Dwyka Tillite, and further down by the Transvaal dolomites and the Ventersdorp Supergroup lavas that separate the Karoo aquifer affected by coal mining from the Witwatersrand aquifer affected by gold mining.

Recharge in the coal mine of between 5 and 7 % can be expected at the subsided areas. Low recharge of between 1 and 3 % can be expected where no subsidence occurs, with a tendency towards 1 % where the B4 sill is thick.

Recharge in the gold mine of a maximum of 1 % can be expected in the gold mine due to the thickness of the overburden ranging from 208 m to 2500 m at an average of 1392 m and the lack of water-bearing structures encountered in this study. Calculated recharge from data of the gold mine was in the range of 0.5 %.

For the purposes of this study, the Karoo aquifers were regarded as one significant aquifer situated above the Ventersdorp Supergroup and the deeper Witwatersrand aquifer situated below the Ventersdorp Supergroup was regarded as the other significant aquifer (refer to Figure 36).

Thus there are two major aquifers dominating the geohydrology of the study area namely:

- The Karoo aquifer (unconfined to confined),
- The deeper Witwatersrand aquifer (confined).

The shallower Karoo aquifer is regarded as an unconfined to confined aquifer and its recharge can be linked directly to recharge by precipitation (1-3 % of annual precipitation and 5 % to 7 % where high extraction mining has occurred). The deeper Witwatersrand aquifer is regarded as a confined aquifer that has no direct link of recharge to precipitation and has a very low flux from shallower Karoo aquifers though preferential pathways or where the Witwatersrand Supergroup sub-outcrops against the base of the Karoo Supergroup (>1 % of annual precipitation).

The No.4L coal seam mined by Sasol is situated at an average depth of 80 m below surface in the south and 150 m below surface in the north, or at elevations ranging between 1450 m.a.m.s.l and 1521 m.a.m.s.l throughout the different compartments resulting from the different dolerite sills situated throughout the study area (Figure 54). The Kimberly Reef containing gold and platinum group metals at varying depths below surface is currently being mined, the deepest being ± 2500 m below surface at Harmony No. 8 shaft and the shallowest being 240 m below surface at Harmony No. 3 shaft.

Currently, Sasol Middelbult Block 8 is only mining over Harmony gold mining in the southernmost parts of the study area, with the largest area covering the southeastern part (Figure 53). Future mining will cover most of the study area except for the central part of the study area around Harmony gold mining No. 7 shaft and No. 8 shaft (Figure 53).

Sasol coal mining will mine in future near Harmony's No. 1 Shaft, where the No. 4L coal seam floor is situated at 1479 m.a.m.s.l or 139 m below surface (Figure 54). Harmony gold mining's mining operations at No.1 shaft, closest to the No. 4L coal seam, are situated at Level 2, which is 1347 m.a.m.s.l or 270 m below surface. The minimum difference between the No.4L coal seam and the gold mine workings at No.1 shaft is thus 132 m (Figure 56). As yet, no groundwater interaction from the coal mine into the gold mine could be established in the No. 1 shaft area, as no preferential pathways could be confirmed.

Sasol is currently mining near Harmony's No. 3 Shaft where the No. 4L coal seam floor is situated at 1480 m.a.m.s.l or 136 m below surface. Harmony gold mining's mining operations at No.3 shaft, closest to where the No. 4L coal seam is situated at Level 1, which is 1387 m.a.m.s.l or 229 m below surface (Figure 54). The minimum difference between the No.4L coal seam and the gold mine workings is thus 93 m at No. 3 shaft (Figure 57). As yet, no groundwater interaction from the coal mine into the gold mine could be established in the No. 3 shaft area, as no preferential pathways could be confirmed.

Sasol is proposing to mine in future near Harmony's No. 9 Shaft, where the No. 4L coal seam floor is situated at 1461 m.a.m.s.l or 126 m below surface (Figure 54). Harmony gold mining's mining operations at No.9 shaft, closest to the No. 4L coal seam, are situated at A Level, which is 1380 m.a.m.s.l or 207 m below surface. The minimum difference in metres between the No.4L coal seam and the gold mine workings is approximately 81 m at No. 9 shaft (Figure 58). Two preferential flow paths bearing water at No. 9 shaft (Level 1) directly underneath Level A (as shown in Figure 55) were found in this study (Table 5). These fractures could link the Karoo aquifer affected by coal mining to the gold mine workings in the Witwatersrand aquifer.

Sasol is currently mining near Harmony's No. 10 Shaft, where the No. 4L coal seam floor is situated at 1470 m.a.m.s.l or at approximately 119 m below surface. Harmony gold mining's closest mining operations at No.10 shaft to the No. 4L coal seam is situated at (1 level) which is 1345 m.a.m.s.l or 244 m below surface. The minimum difference in metres between the No.4L coal seam and the gold mine workings is approximately 125 m (Figure 59). As yet, no groundwater interaction from the coal mine into the gold mine could be established in the No. 10 shaft area, as no preferential pathways could be confirmed.

The potential for groundwater interaction resulting from Harmony Evander Tailings Storage Facilities (TSF) found on surface can be attributed to the extent of subsidence resulting from the coal mining directly underlying or near the TSF. Currently, there is coal mining underneath the

Winkelhaak and Leslie slimes dams, with proposed future coal mining underneath the Kinross slimes dam, shown in Figure 60.

The Kinross slimes dam is situated at the centre of the study area with Sasol future mining underneath it as seen in Figure 60. No subsidence is expected underneath the Kinross mine as seen in Figure 62 and Figure 63. This is a result of no high extraction coal mining directly underneath or near the Kinross slimes dam (Figure 63).

Subsidence is likely to the south-southwest of the Leslie slimes dam as high extraction coal mining will occur and it is expected that preferential pathways (fractures) linking the slimes dam with the underground coal mine working may be induced (Figure 64). This is only a assumption and further monitoring is required to confirm this.

Subsidence is most likely to the southeast of the Winkelhaak slimes dam, as high extraction coal mining will occur and it is expected that preferential pathways (fractures) linking the slimes dam with the underground coal mine working may be induced (Figure 66). This is only a assumption and further monitoring is required to confirm this.

There is thought to be an exploration linking the Winkelhaak slimes dam with the coal mining underneath the slimes dam. This borehole could not be confirmed as the coal mine is already flooded in this area.

The Ventersdorp Supergroup lavas appear to thin towards the south-southeast of the study area, with the exception of the southern boundary of the study area where the Ventersdorp Supergroup lava is either very thin or sub-outcrops against the Karoo Supergroup, as seen in Figure 67 and Figure 68. It was expected that groundwater interaction would occur here, but from field work done no groundwater interaction was found here.

Samples were collected from all water-bearing structures intersecting the gold mine and these are summarised in Table 7. It should be noted that these points are the only water-bearing structures found in the study and therefore the only known pathways connecting the Karoo aquifer with the Witwatersrand aquifer. There may be more structures in other parts of the mine but due to safety, inaccessibility and mining activities it was not possible to locate them.

- **H1** and **H4** - Water from faults intersecting the gold mine. The origin of this water is from the base of the Karoo aquifer where the Transvaal Supergroup (aquiclude) is absent and where the faults went through the Ventersdorp Supergroup (aquiclude) and into the Witwatersrand aquifer. Groundwater will move along these faults until they intersect the gold mine

workings. The position of the faults are at Evander No. 8 shaft, 11 level 1340 m below surface (Figure 42) and at Evander No. 8 shaft, 18 level 1830 m below surface. It unlikely that the coal mining will reach the area where these faults are (Figure 53) and therefore it is unlikely that the coal mine will have an impact on the gold mining through these specific faults (Table 7).

- **H2** - Water from dyke and exposed in the gold mine workings. The origin of this sample will be where fractures next to the dyke allowed for groundwater flow (Cook, 2003). These fractures may or may not be directly connected to surface (Cook, 2003) and therefore recharge may occur in the sub-surface at different depths through the influx of overlying aquifers or directly by surface precipitation from surface. The position of the fractures next to a dyke was encountered at Evander No. 8 shaft, Level 11, approximately 1340 m below surface, as shown in Figure 41. It is unlikely that the coal mining will reach the area where this dyke is encountered (Figure 53) and therefore it unlikely is that the coal mine will have an impact on the gold mining through this specific dyke (Table 7).
- **H3** - Water from an exploration borehole intersecting the gold mine workings. According to Middelbult Mine, Block 8 Expansion EMPR (2003), all gold mine exploration boreholes will be sealed off with a non-reactive material to prevent the drainage of groundwater from the coal mine to the gold mine. (Figure 53). It unlikely that the coal mining will reach this area where this borehole is situated, therefore coal mining will have no impact on the gold mining through this specific exploration borehole. The position of the exploration borehole is at No. 8 shaft, Level 15, 1620 m below surface (Table 7).
- **H5, H6, H7** and **H10** - Water dripping out of the mine roof, the origin of which is difficult to determine. The origin of these samples is thought to be flux from fissures/fractures and joints from overlying aquifers. The position of the samples can be seen in Table 7. All of these positions can be affected by coal mining except **H5** which is at Harmony No. 8 shaft and will remain unaffected by coal mining as no coal mining will occur around No. 8 shaft (Figure 53). **H6** and **H7** were taken near current coal mining activities and show a "fingerprint" that is characteristic of a Karoo aquifer affected by coal mining. Therefore the only current interaction between the coal mine and the gold mine is at No. 9 shaft, Level 1 (Figure 95).

9.1.1 Isotopes and hydro-chemistry conclusions

The 21 water samples were collected from different localities (Figure 71 and Figure 72) widely dispersed over the study area and covering a depth range of between 28 and 2152 m below surface. Three different types of sub-surface water were encountered in the study area and can be differentiated between.

9.1.1.1 Karoo aquifer origin samples and recharged by precipitation (KB1D, KB5D, WB1D, WB3D, WB5D, MHN47, MHR 45, MDBCasino and S1-S5

Samples from the shallow Karoo aquifer and those affected by coal mine activities (**KB1D, KB5D, WB1D, WB3D, WB5D, MHN47, MHR 45, MDBCasino** and **S1-S5**) are generally lower in Na- concentrations (Figure 81) and higher in SO_4 concentrations (Figure 83) than the deeper Witwatersrand aquifer samples. All have relative high concentrations of bicarbonate, suggesting they are recharged by precipitation or water in the shallow unconfined Karoo aquifer that freely reacts with the atmosphere. They all plot close to the local rainfall line (Figure 100) this also suggests that they have been affected in some way by precipitation directly or indirectly (mixing). They are relatively enriched in $\delta^{18}O$ and δD, suggesting they have had a relative short residence time in the sub-surface (Figure 103).

9.1.1.2 Witwatersrand samples recharged by influx from shallower Karoo aquifers (H1, H4, H6, H7)

Samples **H1, H4, H6** and **H7** are also regarded as Karoo aquifer origin samples based on **H1** and **H4** elevated Cl concentration shown in Figure 85 (ion-exchange), Na-SO_4 grouping with the shallower samples (**S1, S3, MHR45, WB5D** and **MDBCasino**) in the Piper diagram (

Figure 90), their isotopic signature showing their depleted $\delta^{18}O$ and δD (Figure 100), their unique Stiff diagram geometry (Figure 94) combined with the fact that they were taken from faults intersecting the gold mine workings linking the base of the Karoo aquifer with the Witwatersrand aquifer (Table 14).

H1 and **H4** are the samples most depleted in $\delta^{18}O$ and δD (Figure 100), as they were taken from faults. This suggests that reactions with rock minerals has taken place in the water as it travelled along the fault, depleting its $\delta^{18}O$ and δD composition (Figure 99).

H6 and **H7** are of Karoo aquifer origin based on their Stiff diagram (Figure 94) general geometry being the same as the coal mine samples (**S1-S5**) and their EDD plotting position in **Field 3** with the coal mine samples (**S1-S5**) which are expected to be found in high extraction coal mining. These samples have most probably undergone ion-exchange reactions in reducing conditions on the water's flow path through the Ecca shales. **H6** and **H7** are the samples taken closest to the No. 4L coal seam (Figure 95). **H6, H7** and **H10** are also the only samples that could have been affected by coal mining, as coal mining has not reached the area of the other underground gold mining samples (Figure 74).

9.1.1.3 Witwatersrand aquifer water recharged by influx from shallower Karoo aquifer with a long residence time and that may have mixed with connate water or paleo-meteoric water (H2, H3, H5, H10)

Sample **H2** (next to dyke), **H3** (exploration borehole), **H5** (out of stope) and **H10** (out of mine roof) all show depleted $\delta^{18}O$ and δD (Figure 100). They have relative high Na- concentrations (Figure 81) and low SO_4 concentrations (Figure 83) compared to the Karoo aquifer samples, but have lower in Na- concentration compared to the **H1** and **H4** samples (from faults), believed to be water from the base of the Karoo aquifer. They (**H2, H3, H5** and **H10**) all plot within **Field 9** of the EDD, which is very old, stagnant or paleo-meteoric water that has reached the end of the geohydrological cycle or water that has moved a long time and/or distance though the sub-surface and has undergone significant ion-exchange. **H3**'s bicarbonate concentrations are a mixture of precipitation and flux of confined aquifer water. **H2, H5,** and **H10** represent a flux of confined aquifer water as they were taken from fractures intersecting the gold mine workings. Their lower bicarbonate concentrations compared to **H3** are attributed to the reverse of Equation 14 in a closed system (confined aquifer) where there is no CO_2 present, resulting in the slow loss of HCO_3^- (Freeze & Cherry, 1979). This indicates that they are recharged by the shallower Karoo aquifer but that they have had a long residence time in the sub-surface.

9.1.1.4 Groundwater interaction between the Karoo aquifer and the Witwatersrand aquifer based on hydro-chemical interpretations

There is interaction between the aquifers, as seen in samples **H1 H3 H4 H6** and **H7**, through preferred pathways such as faults and fractures. Important is that **H1, H3** and **H4** interaction is occurring without the influence of the coal mine as coal mining has not reached the areas where these samples were taken.

H6, H7 and **H10** were taken near current coal mining activities. Only **H6** and **H7** show a "fingerprint" that is characteristic of a Karoo aquifer affected by coal mining. Therefore the only current interaction between the coal mine and the gold mine is at No. 9 shaft, Level 1 (Figure 95) and not all preferential pathways bearing water from the Karoo aquifer have been affected by coal mining.

9.1.2 Summary of possible interaction areas

Based on the mining activities, geology, hydrogeology, hydro-chemical and isotope interpretations in this study, the following can be stated. Groundwater interaction will possibly

occur between the shallower coal mine and the deeper gold mine through preferential pathways made by the coal mine in the areas listed below:

- The south-southeast corner of the Winkelhaak slimes dam, due to high extraction coal mining;
- The south-southwest corner of the Leslie slimes dam, due to high extraction coal mining;
- South-southwest of Harmony Evander's No. 9 shaft, Level 1, as seen in samples **H6** and **H7**. Although the current interaction is minimal as the water dripping out of the roof is less than one litre a day it may increase as future coal mining extends to a much larger area around the shaft and the coal mine fills up with water;

Interaction occurs in the central part of the study area near Harmony Evander's No. 8 shaft without the presence of coal mining, through faults, fractures next to dykes and exploration boreholes intersecting the gold mine workings.

Thus the coal mine is not the only contributor to the interaction between the mines, as naturally occurring structures allow for influx from the Karoo aquifer into the gold mine workings in the Witwatersrand aquifer. There is no future coal mining envisaged around No. 8 shaft and therefore the potential for groundwater in the Karoo aquifer affected by coal mining to interact with gold mine around the No. 8 shaft is very low.

The coal mine will in future cover most of the gold mining area except for the central part around Harmony Evander No. 8 and No. 7, it is expected that groundwater affected by the coal mining in the Karoo aquifer will only move along naturally occurring structures that links the two mines, from the base of the Karoo aquifer into the gold mine. This can only occur when structures that links the Karoo aquifer with Witwatersrand aquifer is encountered, which was found seldom in this study.

The possible interaction can therefore directly link to the number of structures that are water-bearing in the study area as well as the area covered by coal-mining activities. From the field work done in the underground gold mine, the number of structures that are water-bearing is the exception rather than the norm. Therefore the potential for groundwater interaction from future coal mining into the gold mine will be low as the Karoo aquifer is very poorly connected to the Witwatersrand aquifer based on:

- Frequency of water-bearing structures encountered within the study area;
- Travel time of the Karoo aquifer water to reach the Witwatersrand aquifer;

- Water level in the Karoo aquifer remains relatively constant;
- Rate of inflow in the gold mine remains relatively constant;
- Recharge in the gold mine is estimated at 0.5 %, which is less than 1-7 % of that in the coal mine;
- Water-bearing structures encountered within the study area have low water volumes;
- Prevention of interaction measures of each individual mine.

9.1.3 Expected impact of coal mine on the water quantity and quality within the study area

The amount of groundwater from surface into the coal is 1-3 % of annual recharge (Vermeulen & Usher, 2006). A higher proportion of infiltration of 5-7 % may occur in areas where the natural permeability is increased, such as the increased fracturing associated with high extraction mining.

The rate of recharge if subsidence occurs under the gold mine slimes dams may therefore be regarded as 5-7 % if preferential pathways are created with a direct link to the slimes dams. The quality of this water will be poor as the ARD has been extensive in the slimes dams.

Recharge of the deep aquifer occurs from the shallow aquifer through permeable fracture systems, faults and exploration boreholes that link the two aquifers. Induced fracturing associated with mining can extend from the deep aquifer up to the surface, and provides a relatively direct and highly permeable recharge route.

Groundwater draining into the mine workings will initially be of a good quality. The pH will be alkaline due to the presence of bicarbonate species. However, once the groundwater reaches the mine, the material that it comes into contact with will influence its quality.

The following sequence of chemical reactions is assumed to occur during the operational phase:

- The water seeping into the coal mine will generally be of good quality, except for suspended solids present. Most, if not all of the water resulting from operations, will be used during the operational phase. Isolated areas of water may be present, and will drain to the lowest point of the mine.
- The water present will be alkaline, but the Total Dissolved Solids/EC content will increase due to the contact with the coal floor/pillars.

- Groundwater will continue to percolate through the roof downward to the saturated areas. This will lead to the mixing of initially alkaline to neutral groundwater with relatively stagnant, alkaline groundwater on the mined horizon.
- The water liberated in the stratigraphical units above pillar extraction panels, as well as the water seeping into the mine, will generally be of good quality, but contain suspended solids, in the form of sediment and carbonaceous material, e.g. shale and coal.
- Very little, if any, pyrite oxidation will take place in this saturated zone. The quality of this groundwater will initially remain constant, providing that water is not continuously pumped out of this zone.
- Pyrite oxidation will commence in the unsaturated areas of the mined void (if any), as well as in the unsaturated zones of the goaf. The rate of oxidation will vary considerably, depending on the rate of ingress of groundwater (the residence time), the rate of ingress of oxygen and the contact areas available for oxidation.
- This initial acidification will be neutralised by the natural buffering capacity in the overlying rock. This will take place for many years, until all the neutralising potential is depleted. Isolated areas of buffering depletion might take place quickly, but regional acidification in the total goaf area will not occur for many years.
- Groundwater will percolate through the unsaturated goaf areas downward to the saturated mined void. This will lead to the mixing of initially alkaline to neutral groundwater with relative stagnant, alkaline groundwater on the mined horizon.
- Isolated areas of buffering depletion will take place. This will lead to the formation of acidic conditions in the goaf area, with low pH groundwater that will percolate downwards to the saturated zones.

The following sequence of chemical reactions is most likely to occur post-closure of the coal mine:

- Pyrite oxidation on the mined horizons will be extensive due to the slow flooding during the post-closure phase.
- Initial acidification will be neutralised by the natural buffering capacity in the coal seam, as well as from groundwater flooding the sections. This will take place over many years, until all the neutralising potential is depleted.
- Poor quality groundwater will be present in the mine horizon when total flooding is completed.

9.1.4 Expected impact of gold mine on the water quantity and quality within the study area

The impact will consist of two aspects:

- The impact of deep level mining on the groundwater within the workings;
- The impact of gold mining and related activities on the Karoo aquifer.

Recharge into to the gold mine will be less than 1 % of annual precipitation.

Another aspect to consider is the effect that coal mining will have on the groundwater encountered within the gold mining area, as it is expected that groundwater which originates from the Karoo aquifer and is affected by coal mining could travel through preferential flow paths from the Karoo aquifer downward to the gold mining which affects the Witwatersrand aquifer.

Deep level gold mining operations will result in a degree of contamination of groundwater within the Witwatersrand aquifer. Most of the groundwater encountered within this aquifer during operational gold mining operations will be pumped to surface (Winkelhaak Mine EMPR, 1988).

Groundwater draining into the mine workings will be of varying quality as it will travel for a considerable distance within the subsurface to reach the gold mining activities. Sulphate-rich minerals will give rise to a low pH (depending on oxygen and buffering capacity of the carbonate minerals) while carbonate-rich minerals will give rise to a higher pH.

The following sequence of chemical reactions will occur during the operational phase:

- The water seeping into the gold mine will generally be of varying quality, except for suspended solids present, which are expected to be at high levels due to the considerable distance travelled. Most, if not all of the water will be pumped to surface during the operational phase. Isolated areas of water may be present, however, and will drain to the lowest point of the mine.
- Pyrite oxidation will commence in the mined void. The rate of oxidation will vary considerably, depending on the rate of ingress of groundwater (the residence time), the amount of oxygen available and the amount of sulphate-rich minerals that react with the groundwater.

The following sequence of chemical reactions is most likely to occur post-closure of the gold mine:

- Pyrite oxidation on the mined horizons will be extensive due to the slow flooding during the post-closure phase.

- Poor quality groundwater will be present in the mine horizon when total flooding is completed.

9.1.5 Current conceptual model for decant in Sasol coal mining operations under operational (pumping) conditions

For groundwater affected by the coal mining activities and left to fill the mining voids to decant, it will have to overcome more than four bars of pressure, which is unlikely. As the piezometric level from the mine and the water level in the fractured zone combine, the excess water will seep out as water that is unaffected by underground coal mining activities. The average thickness of the overburden above the No. 4L coal seam of the Middelbult Block 8 area is approximately 90 m (refer Karoo Supergroup, Figure 22) while the average thickness of the overburden covering the Sasol Secunda mining complex is more than 100 m thick.

9.1.6 Conceptual model for decant in Harmony Evander gold mining operations post-closure (no-pumping)

After the mining voids have flooded with water, the piezometric level of the artificial gold mine aquifer will rise with the storage coefficient value of the artificial gold mine aquifer (not the specific yield) as conditions in the artificial mine aquifer have changed from an unconfined aquifer to a confined aquifer. The influx of water from the overlying aquifers into the mine aquifer will decrease as the Witwatersrand piezometric level approaches the Karoo aquifers water level in the gold mine shafts shown in Figure 110. The lowest point of the coal seam floor is at 1450 m.a.m.s.l once the water level in the shafts reaches this elevation the Witwatersrand aquifer's piezometric level and the Karoo aquifer's water level will become one. As the piezometric level from the gold mine and the water level in the Karoo aquifer combine the excess water will seep out as water that is unaffected by underground gold mining activities (Vermeulen & Dennis, 2009). For groundwater affected by the gold mining activities and left to fill the mining voids to decant it will have to overcome the same four bar of pressure as the coal mine artificial aquifer , which is unlikely.

9.1.7 Time for gold mine workings' voids to flood

If the current inflow rate for the total Harmony gold mine is taken as 3 454 790 m^3 (Table 15) the time for Harmony Evander gold mine workings to flood to the coal seam floor will be ***406 years***. The piezometric level of the artificial gold mine aquifer will rise with the storage coefficient value of the artificial gold mine aquifer (not the specific yield). The inflow of water from the overlying aquifers into the mine aquifer will decrease as the piezometric level in the shafts rises,

decreasing the gradient and thereby decreasing the inflow rate (Equation 18). The inflow of water in the shafts will be a high in the beginning but will decrease over time, as shown in Figure 113 and Figure 114.

Therefore, the time for the water level to reach the coal seam is estimated at 406 years if current pumping conditions are ceased at an inflow rate of 3 454 790 m^3.

In general, a conservative approach was taken during this investigation. It is recommended that the system be monitored and re-calibrated as further monitoring data are collected.

9.1.8 Limitations of this study

There were some limitations in this study and are listed below:

- Some of the old mining areas such as No. 1 shaft and No. 6 shaft are inaccessible as they have been decommissioned making them unsafe to investigate for groundwater interaction;
- Some of Middelbult Mining's area mostly to the south of the interaction area has already been flooded with water making them inaccessible for investigation;
- Water level data from the decommissioned shafts are relatively old and is not constantly measured, therefore water level data were heavily relied on from previous reports;
- The positions of exploration boreholes are difficult to determine as they are not marked on surface;
- The fact that no one has marked were water-bearing structures are encountered or if they were sufficiently plugged;

9.2 Recommendations

The two mines have specific regulations in place to prevent groundwater interaction between the mines. These regulations are listed below and in their respective Environmental Management Programmes. It is of utmost importance that both mines comply with these regulations to prevent any groundwater interaction between the two mines.

- The minimum distance that high extraction coal mining activities will take place from the perimeter of the gold mine slimes dams is given as 300 m (Block 8 Expansion EMPR, 2003).
- No mining activities will take place directly underneath the gold mine tailings storage facilities (Block 8 Expansion EMPR, 2003).
- Coal mining activities will keep a barrier pillar of 50 to 100 m from vertical gold mine shafts. (Block 8 Expansion EMPR, 2003). By keeping a barrier pillar of 50 to 100 m from the shafts there will be no influx of water from the coal mine into the gold mine shafts as the barrier will act as an impermeable layer restricting groundwater flow.
- All gold mine exploration boreholes when intersected by the coal mine will be sealed off with a non-reactive material to prevent the drainage of poor quality, low pH groundwater from the coal mine to the gold mine (Block 8 Expansion EMPR, 2003).
- The gold mine shafts will be sealed using design and methods specified by a competent professional Civil Engineer (Leslie Mine EMPR, 1994). This would significantly decrease the ability of the shafts as possible recharge sources as well as preferential pathways linking the two mines.
- The water levels in the decommissioned gold mine shafts should be measured bi-annually to establish the exact final water level of the Witwatersrand aquifer. This data can then be used in a numerical model to confirm the findings in this report.
- Influxes encountered during the intersection of water-bearing structures in both underground mines can usually be plugged (grouted), or the influx water can be pumped away and dealt with as part of the mine water balance.
- The rate of influx where faults, fractures and exploration boreholes or any other water-bearing structure intersecting the gold mine workings should be measured to establish the exact volumes of groundwater flowing in the gold mine through structures. This data can then be used in a numerical model to confirm the findings in this report.
- The position of the exploration borehole intersecting the gold mine workings at No. 8 shaft 15 level should be located on surface. The borehole should then be sampled for hydro-

chemical, stable environmental isotopes at surface and underground where it intersects the gold mine workings. This should be done to determine the rate of flow from surface to the gold mine workings. The borehole should be sealed if the coal mine intersects it.

- All drainage in the floor of the coal mine should be investigated and where possible sealed. This will restrict vertical movement of water into the underlying formation and hence the Witwatersrand aquifer.
- Design long-term water management schemes taking cognisance of neighbouring mining activities.
- Design the mine layouts to retain as much of the mine water as possible in the underground workings whilst mining.
- Flood mine workings (cease pumping) as soon as possible after closure to limit oxidation reactions within both mines.
- Water balances should be done in a more dynamic manner, clearly identifying the source water.
- The area around number No. 9 shaft should be monitored as interaction is occurring there.
- The areas around Leslie and Winkelhaak slimes dam should be monitored as possible interaction from the gold mine slimes dam could affect the water quality in the Karoo aquifer.

References

Appelo, C.A.J., Postma, D. (2005). "Geochemistry, Groundwater and Pollution." (2nd edition). A.A. Balkema Publishers, Rotterdam, Netherlands.

Asano, Y., Uchida, T., Ohte, N. (2002). "Residence times and flow paths of water in steep unchannelled catchments." Tanakami, Japan. Journal of Hydrology. p 261, 173-192.

Bredenkamp, D.B., Van Der Westhuizen C., Wiegmans F.E., Kuhn C.M. (1986). "Groundwater Supply Potential of Dolomite compartments west of Krugersdorp, South Africa." Technical Report No. GH 3440, Directorate of Geohydrology, Department of Water Affairs.

Clark, I.D., Fritz, P. (1997). "Environmental isotopes in hydrogeology," Lewis Publishers, New York, USA. p. 328-329.

Cook, P.G. (2003). "A guide to regional groundwater flow in fractured rock aquifers." CSIRO, Land and Water, Glen Osmond, SA, Australia. p 1-10, 14-23.

Criss, R.E., Davisson, M.L. (1996). "Isotopic imaging of surface water/groundwater interactions, Sacremento Valley." California. Journal of Hydrology, Vol 178. p. 205-222 .

Deer, W.A., Howie, R.A. Zussman, J. (1992). "Rock forming minerals, Single Chain Silicates." Longman, Volume 2A London. p 696.

Drever, J.I. (1997). "The geochemistry of natural waters, Surface and Groundwater Environments." Third edition, Prentice Hall, New Jersey.

Du Preez, M., Dennis, R., G.J. van Tonder. (2007). "Experimental Measurements of Specific Storativity by the Determination of Rock Elastic Parameters." Institute for Groundwater Studies, University of the Free State.

Eby, G.N. (2004). "Principles of Environmental Geochemistry." Thomson Brooks/Cole, Pacific Grove, CA.

Falcon, R.M.S. (1986). A brief review of the origin, formation and distribution of coal in Southern Africa. In: Mineral deposits of Southern Africa, I & II, Ahaeusser, C.R. and Maske, S. (eds.) Geological Society of South Africa, Johannesburg. p. 1879-1899.

Freeze, R.A., Cherry, J.A. (1979). "Groundwater." Prentice-Hall, Inc. Englewood Cliffs, New Jersey. p. 39 - 44, 47-49, 114-139.

Fritz, P., Fontes, J., C.H., Elsevier, A. (1980). "Handbook of Environmental Isotope Geochemistry, Volume 1, The Terrestrial Environment." New York. USA. p. 21-29, 283-321, 473-495.

Gat, J.R. Carmi, I. (1970). "Evolution of the isotopic composition of atmospheric waters in the Mediterranean Sea area." J. Geophys. Res 75:3039-48.

Gat, J.R. (1996). "Oxygen and hydrogen isotopes in the hydrologic cycle." Unpublished paper, Department of Environmental Sciences and Energy Research, Weizmann Institute of Science, 76100 Rehovot, Israel.

Grobbelaar, R. (2001). "Quantification and management of intermine flow in the western Witbank Coalfield: Implication for mine water volumes and quality." Unpublished M.Sc thesis, Institute for Groundwater Studies, University of the Free State.

[GCS] Groundwater Consulting Services. (2002). "Harmony gold mining company Evander operations water quality status report." Project nr 2002-11-338.

[GCS] Groundwater Consulting Services. (1998). "Evander goldmines geohydrological investigation final report, Johnstone, A.C. and Jansen H.C.

Harmony/Sasol Working Group (2005). Interaction between Gold and Coal mining. A Minism W analysis. Ref no. ERE 8-27/2005.

Harmony Evander Gold Mining Servitudes (2008). Excel sheet from Harmony Evander's Geological Department.

Harmony Gold Mining Company (1988). "Winkelhaak Mines Limited, Environmental Management Programme Report."

Harmony Gold Mining Company (1994). "Leslie Gold Mines Limited, Environmental Management Programme Report."

Harmony Gold Mining Company (1994). "Kinross Mines Limited, Environmental Management Programme Report."

Havenga, A. (2002). The long-term impact of intermine flow from Collieries in the Mpumalanga Coalfields." Unpublished M.Sc thesis, Institute for Groundwater Studies, University of the Free State.

Hem, H.D. (1985). "Study and interpretation of the Chemical Characteristics of Natural Waters." United States Geological Survey - Supply Paper, no. 2254.

Hodgson F.D.I., Krantz R.M. (1995). "Investigation into the groundwater quality deterioration in the Olifants River catchment above the Loskop dam with specialised investigation into the Witbank dam sub-catchment." Institute for Groundwater Studies, University of the Free State.

Hodgson, F.D.I., Grobbelaar, R. (1998). "Investigation into long-term water quantity and quality trends at Ermelo Colliery." Confidential Report to Ingwe S.A.

Jasper Muller Associates cc. Van der Berg, J. (2002). "Compilation of geology and groundwater inputs for the Middelbult block 8 EMPR - SASOL coal volume I and II - text and appendices." Report prepared for Sasol Mining (Pty) Limited.

Johnson, M.R., Anahaeusser, C.R., Thomas, R.J. (2006). "The Geology of South Africa, Council for Geoscience." Pretoria, RSA, p 155-208.

Kruseman, G.P., N.A. De Ridder (1994). "Analysis and Evaluation of Pumping Test Data." 2nd Edition. Wageningen, Netherlands, ILRI Publication No. 47.

Lippmann, J. Stute, M. Torgesen, T. Moser, D.P. Hall, J. Lihung, L. Borcsik, M. Bellamy, R.E.S. Onstott, T.C. (2003). "Dating ultra-deep mine waters with noble gases and ^{36}Cl, Witwatersrand Basin, South Africa." Geochimica et Cosmochimica Acta. Vol.67, Issue (23). p. 4597-4619.

McKnight Geotechnical Consulting, C. Oliver, D. De Bruyn, I. (2002). "Evander mine poplar gold project, Mpumalanga, A review of the geological structural model and assessment of possible groundwater ingress for mining of Kimberley Reef." Internal Report prepared for Rison Groundwater Consulting.

Middelbult Mine: Block 8 Addendum Volume 1. (2003). "Environmental Management Programme Report for the Middelbult Mine: Block 8 Expansion." Prepared for Sasol Mining (Pty) Limited. Oryx Environmental. nr.OE63.

Midgley, D.C., Pitman W.V., Middleton B.J. (1994). "Surface water resources of South Africa" 1990. WRC Report No. 298/1/94. Water Research Commission, Pretoria.

Mulholland, G. (1982). "Poplar mine limited. The Potential ingress of water into the proposed underground workings." Gencor Mines Geological Department. Bulletin No. 2462.

Onstott, T.C., Lin, Davidson, M, Mislowack, B. Borcsik M. Hall, J. (2006). "The Origin and Age of Biogeochemical Trends in Deep Fracture Water of the Witwatersrand Basin, South Africa." Department of Geosciences, Princeton University, Princeton, New Jersey, USA.

Phillips, F.M. (2009). "Chlorine-36 dating of Old Groundwater." New Mexico Institute of Mining and Technology. Socorro, NM, USA.

Piper, A. M. (1944). "A graphic procedure in the geo-chemical interpretation of water analyses." Am. Geophys. Union Trans., 25. p. 914-923.

Pritchard-Davies, E.W.D. (1962). Bulletin No. 77. "Sub- Karoo water table." Addenda 1-7.

Rison Groundwater Consulting, M. (2002) "Harmony Gold Mining Limited - Evander operations: Geohydrological assessment of the potential risk of groundwater inflow into the Rolspruit Project."

Rison Groundwater Consulting. (2003). "Harmony Gold Mining Limited - Evander operations: Geohydrological assessment of the potential risk of groundwater inflow into the Poplar Project."

Rison Groundwater Consulting, M. (2007). "Harmony Gold Mining Limited - Evander operations: Geohydrological assessment of the groundwater table in Evander no. 6 shaft."

Saayman, I.C. Scott, D.F. Prinsloo, F.W. Moses, G. Weaver, J.M.C. Talma, S. (2003) "Evaluation of the application of natural isotopes in the identification of the dominant stream flow characheteristics".

Schwartz., F.W. Zhang, H. (2003). "Fundamentals of Groundwater." Ohio State University. p. 42-130.

Snyman, J.P. (1998) Coal. "The mineral resources of South Africa." Eds Wilson, M.G.C and Anhaeusser , C.R. p. 136-161.

South African Weather Services (www.weathersa.co.za).

Talma, A.S., Weaver, J.M.C. (2003). "Evaluation of groundwater flow patterns in fractured rock aquifers using CFCs and Isotopes." Water Research Commission Report No. 1009/1/03, South Africa.

Tweedie, E.B. (1986). "The Evander Goldfield". In: Mineral Deposits of Southern Africa 1. Anhaeusser, C.R. & Maske, S. (eds). Geological Society of South Africa, Johannesburg, South Africa. p. 705-730.

Unesco (1973). "Ground-water studies. An international guide for research and practice." In Brown, R.H., Konoplyantsev, A.A, Ineson, J. and Kovalevsky, V.S. (eds). Nuclear techniques in ground-water hydrology. Chapter 10.

USGS. (2004) "Arsenic, Nitrate, and Chloride in Groundwater." Oakland County, Michigan, USA.

Usher, B.H., Cruywagen, L-M., de Necker E., Hodgson, F.D.I. (2001). "On-site and Laboratory Investigations of Spoil in Opencast Collieries and the Development of Acid Base Accounting procedures." Final report to the Water Research Commission; Report no 2001.

Verhagen, B.Th., Geyh, M.A., Fröhlich, K. and Wirth, K. (1991). "Isotope hydrological methods for the quantitative evaluation of groundwater resources in arid and semi-arid areas." Research Report, Fed. Ministry for Econ. Coop. of the Fed, Republic of Germany.

Verhagen, B.Th. (1997). "Use of environmental isotopes in the characterisation of the Table Mountain Sandstone Aquifer, South Africa." Progress Report to the International Atomic Energy Agency, Research Contract 8983/RO/Regular Budget Fund.

Verhagen, B.Th. (2000). "Environmental isotope hydrology: Principles and application to the geohydrology of the Karoo Basin." Karoo Aquifer Handbook, WRC, in preparation.

Verhagen, B.Th., Butler, M.J. (2004). "Isotope hydrology-An African Experience." Geoscience Africa , Extended Abstracts, Vol. 2. Geological Society of South Africa, Johannesburg. p. 671-672.

Vermeulen, P.D., Usher, B.H. (2006). "Sulphate generation in South African Underground and Opencast Collieries." Environmental Geology 49 (4): 552-569, February 2006.

Vermeulen, P.D., Usher, B.H. (2006.) "Recharge in South African underground collieries." Journal of Institute of Mining and Metallurgy 106: 771-788, November 2006.

Vermeulen, P.D., Dennis I. (2009). "Numerical Decant Models for Sasol Mining Collieries, Secunda." Institute for Groundwater Studies. University of the Free State.

Vermeulen, P.D. (2010). "The assessment of mine rebound and decanting in deeper coal mines." Proceedings - Mine Water and Innovative Thinking. International Mine Water Association. Nova Scotia, Canada. p. 511-515.

Weaver, J.M.C., Talma A.S., Cavé L.C (1999). "Geochemistry and Isotopes for Resource Evaluation in the Fractured Rock Aquifers of the Table Mountain Group. Report No. 481/1/99, Water Research Commission, Pretoria.

Yechieli, Y., Wood, W.W. (2002). "Hydrogeological processes in saline systems: playas sabkhas and saline lakes." Earth Science Reviews, 58, pp. 343-365.

Groundwater interaction between a deep coal mine and a deeper lying gold mine

Abstract

After the closure of mines, it is expected that water in the mined-out areas will flow along preferred pathways and accumulate in lower-lying areas (Grobbelaar, 2001). Over time, these man-made voids will fill up with water and hydraulic gradients will be exerted on peripheral areas within mines, resulting in groundwater flow between mines and possibly surface. This flow is referred to as intermine flow (Grobbelaar, 2001). Due to the potential long-term impact of intermine flow in terms of water quantities and qualities, the Department of Water Affairs and Forestry regards intermine flow as one of the most important challenges in the mining industry.

Hydro-chemical and stable environmental isotope sampling were used to determine the interaction between the Karoo aquifer and the Witwatersrand aquifer. Comparison between the results showed that there is interaction between the Karoo and Witwatersrand aquifer, both where coal mining is present and where coal mining is not present.

As the coal mine in future will cover most of the gold mining area except for the central part of the study area, it is expected that groundwater affected by the coal mining in the Karoo aquifer will move along naturally occurring structures from the base of the Karoo aquifer into the gold mine workings if preferential pathways are encountered. This interaction can directly link to the number of structures that are water-bearing in the study area and are covered by coal mining activities. From the field work done in the underground gold mine, the number of structures that are water-bearing are the exception rather than the norm. Therefore the potential for groundwater interaction from future coal mining into the gold mine will be low.

Based on current inflow rates, the gold mine workings will take approximately 406 years to flood and reach the bottom of the coal mine workings. It is highly unlikely that this flooding will decant onto the surface through the coal mine, as the shallowest coal mine workings are at 39 m below surface in the study area. In the unlikely event of decanting, polluted water originating from the mining cavities will seep out as normal unpolluted springs at low points.

Appendices

Appendix A: Hydro-chemical Results

SiteName	DateTimeMeas	pH	EC	Ca	Mg	Na	K	PAlk	MAlk	F	Cl	NO2(N)	Br	NO3(N)
K1D	2010/03/01 12:00	7.41	189	228.53	156.90	122.23	4.09	0	345	0.1881	834.0	-0.1	4.4398	0.0196
K5D	2010/03/01 12:00	7.21	383	263.74	230.81	184.02	4.99	0	229	0.2952	1060.0	-0.1	5.8736	0.0273
W1 D	2010/03/01 12:00	7.78	89.1	27.51	16.63	137.90	4.18	0	297	0.3529	89.0	-0.01	0.4403	0.0676
WB 3 D	2010/03/01 12:00	7.26	500	402.26	326.19	139.74	38.26	0	325	0.2241	1190.0	-0.1	5.543	0.0541
WB 5 D	2010/03/01 12:00	8.16	172	46.67	42.48	247.54	6.46	0	253	0.2014	250.4	-0.1	1.288	0.0148
S5	2010/03/01 12:00	8.11	56.2	24.57	7.83	91.34	9.11	0	271	1.0095	24.8	0.0132	0.1096	0.0753
S4	2010/03/01 12:00	7.97	188	9.65	3.73	421.07	2.97	0	715	4.4182	190.3	0.287	0.5367	0.1473
MDBCASINO	2010/03/01 12:00	6.82	336	132.98	39.09	594.57	6.21	0	561	7.2704	217.6	-0.1	0.6127	0.039
S1	2010/03/01 12:00	7.6	529	334.08	166.44	729.04	9.78	0	258	1.2374	162.3	-0.1	0.2575	0.2489
S3	2010/03/01 12:00	7.85	265	148.40	84.07	265.35	6.80	0	331	0.2556	585.0	0.1085	2.574	0.0856
MHN47	2010/03/01 12:00	7.55	156	55.29	26.06	257.61	4.20	0	539	1.1082	60.6	-0.1	0.4362	3.0489
S2	2010/03/01 12:00	8.54	272	2.73	1.82	690.65	2.66		1376	9.9881	141.1	-0.1	0.5596	0.0481
MHR45	2010/03/01 12:00	6.33	449	246.91	68.87	739.77	11.13	0	266	1.1537	158.7	-0.1	0.3978	0.024
H6	2010/03/01 12:00	8.68	196	8.06	5.29	438.08	2.29		757	8.9569	176.0	-0.01	1.1557	0.7427
H7	2010/03/01 12:00	8.63	148	3.70	0.10	370.00	2.12		572	8.8198	168.2	-0.1	1.0097	0.1052
H10	2010/03/01 12:00	8.04	198	34.59	3.17	382.07	2.53	0	209	5.4121	456.1	-0.1	1.5611	0.0249
H1	2010/03/01 12:00	6.75	488	135.11	0.91	816.13	3.76	0	25	2.837	1595.0	-0.1	7.5205	0.0457
H2	2010/03/01 12:00	8.8	130	2.81	0.36	250.22	1.67		107	9.3553	323.9	-0.1	0.7323	0.0393
H3	2010/03/01 12:00	8.26	177	7.99	3.49	347.17	1.80	0	244	8.494	358.1	-0.1	1.2966	0.1383
H4	2010/03/01 12:00	6.7	472	211.09	3.11	717.23	5.18	0	8.85	2.3909	1612.0	-0.1	7.477	0.0533
H5	2010/03/01 12:00	8.04	169	6.20	0.60	342.20	1.67	0	252	8.3895	362.4	-0.1	1.5202	0.0462

PO4	SO4	Al	Fe	Mn	CA Hard.	Mg Hard.	Tot. Hard.	Ag	Al	As	Ba	Be	Cd	Co	Cr	Cu	Fe
-1	58.818	0.028	0.039	1.039	571.3	643.3	1214.6	<0.010	0.010	<0.006	0.631	<0.001	<0.001	0.230	<0.006	0.016	0.027
-1	420.6812	0.022	0.019	0.004	659.3	946.3	1605.7	<0.010	0.005	<0.006	0.060	<0.001	<0.001	0.308	<0.006	0.006	0.010
-0.1	53.5297	0.018	0.020	0.066	68.8	68.2	137.0	<0.010	0.004	<0.006	0.101	<0.001	<0.001	0.014	<0.006	0.003	0.013
-1	921	0.040	0.030	0.017	1005.6	1337.4	2343.0	<0.010	0.008	<0.006	0.033	<0.001	<0.001	0.366	<0.006	0.013	0.014
-1	247.0905	0.021	0.016	0.005	116.7	174.2	290.9	<0.010	0.012	<0.006	0.071	<0.001	<0.001	0.008	<0.006	0.005	0.012
-0.1	5.317	0.016	0.036	0.006	61.4	32.1	93.5	<0.010	0.003	<0.006	0.425	<0.001	<0.001	<0.005	<0.006	0.002	0.030
-1	45.56	0.101	0.029	0.004	24.1	15.3	39.4	<0.010	0.013	<0.006	0.374	<0.001	<0.001	<0.005	<0.006	0.003	0.024
-1	1024	0.027	0.072	1.004	332.4	160.3	492.7	<0.010	0.010	<0.006	0.052	<0.001	<0.001	<0.005	<0.006	0.003	0.048
-1	2759	0.050	0.037	2.093	835.2	682.4	1517.6	<0.010	0.013	<0.006	0.015	<0.001	<0.001	0.024	<0.006	0.004	0.025
-1	213.3041	0.021	0.027	0.123	371.0	344.7	715.7	<0.010	0.004	<0.006	0.133	<0.001	<0.001	<0.005	<0.006	0.005	0.020
0.2542	200.6636	0.024	0.020	0.426	138.2	106.8	245.1	<0.010	0.013	<0.006	0.089	<0.001	<0.001	<0.005	<0.006	0.003	0.017
-1	4.3192	0.015	0.051	0.004	6.8	7.5	14.3	<0.010	0.005	<0.006	0.399	<0.001	<0.001	<0.005	<0.006	0.003	0.011
-1	2066	0.023	8.735	2.740	617.3	282.4	899.7	<0.010	0.007	<0.006	0.057	<0.001	<0.001	<0.005	<0.006	0.002	6.188
-0.1	44.4517	0.017	0.018	0.003	20.1	21.7	41.8	<0.010	0.010	<0.006	0.066	<0.001	<0.001	<0.005	<0.006	0.005	0.018
-1	54.1747	0.018	0.178	0.017	9.3	0.4	9.7	<0.010	0.001	<0.006	0.013	<0.001	<0.001	<0.005	<0.006	0.002	0.036
-1	121.7786	0.017	0.014	0.004	86.5	13.0	99.5	<0.010	0.005	0.018	0.036	<0.001	<0.001	<0.005	<0.006	0.003	0.010
-1	14.1217	0.023	0.032	0.009	337.8	3.7	341.5	<0.010	0.008	<0.006	1.182	<0.001	<0.001	<0.005	<0.006	0.003	0.010
-1	4.0017	0.017	0.016	0.004	7.0	1.5	8.5	<0.010	0.003	0.015	0.001	<0.001	<0.001	<0.005	<0.006	0.000	0.003
-1	67.456	0.700	0.024	0.045	20.0	14.3	34.3	<0.010	0.537	<0.006	0.020	<0.001	<0.001	0.101	<0.006	0.008	0.023
-1	14.9831	0.020	0.014	0.021	527.7	12.8	540.5	<0.010	0.003	<0.006	1.375	<0.001	<0.001	<0.005	<0.006	0.004	0.012
-1	12.968	0.022	0.012	0.004	15.5	2.5	18.0	<0.010	0.013	0.088	0.023	<0.001	0.003	<0.005	<0.006	0.004	0.015

Mn	Mo	Ni	Pb	Sb	Se	V	Zn
0.937	<0.003	<0.010	<0.006	<0.006	0.020	<0.006	0.017
0.002	<0.003	<0.010	<0.006	<0.006	0.014	<0.006	0.015
0.074	<0.003	<0.010	<0.006	<0.006	0.016	<0.006	0.005
0.014	<0.003	<0.010	0.006	0.006	0.016	0.017	0.009
0.002	<0.003	<0.010	<0.006	<0.006	0.013	<0.006	0.007
0.003	<0.003	<0.010	<0.006	<0.006	0.013	<0.006	0.004
0.002	<0.003	0.019	<0.006	<0.006	0.021	<0.006	0.005
0.843	<0.003	<0.010	<0.006	<0.006	0.024	<0.006	0.007
1.507	<0.003	0.028	<0.006	<0.006	0.010	<0.006	0.069
0.135	0.017	<0.010	<0.006	<0.006	0.010	<0.006	0.017
0.422	0.004	<0.010	<0.006	<0.006	0.023	<0.006	0.008
0.002	<0.003	<0.010	<0.006	<0.006	0.028	<0.006	0.004
1.707	<0.003	<0.010	<0.006	<0.006	0.012	<0.006	0.011
0.001	0.005	<0.010	<0.006	<0.006	0.034	<0.006	0.005
0.003	0.003	<0.010	<0.006	<0.006	0.025	<0.006	0.002
0.001	0.018	<0.010	<0.006	<0.006	0.012	<0.006	0.005
0.008	<0.003	<0.010	0.006	0.006	<0.006	<0.006	0.012
0.000	<0.003	<0.010	<0.006	<0.006	<0.006	<0.006	0.002
0.054	0.003	0.409	<0.006	<0.006	0.010	<0.006	0.026
0.024	<0.003	<0.010	<0.006	<0.006	<0.006	<0.006	0.011
0.001	0.003	0.010	<0.006	<0.006	0.013	<0.006	0.007

Appendix B: Isotope Results

Sample No.	Sample Name	δ^2H Reportable Value (permil)	δ^2H Standard Deviation (permil)	$\delta^{18}O$ Reportable Value (permil)	$\delta^{18}O$ Standard Deviation (permil)	Analysis Date
1	H1	-25.86	0.63	-5.97	0.20	08-03-2010
2	H2	-26.82	1.01	-5.36	0.21	08-03-2010
3	H3	-26.72	1.23	-5.30	0.21	08-03-2010
4	H4	-28.26	0.99	-6.37	0.26	08-03-2010
5	H5	-26.08	1.30	-4.99	0.19	08-03-2010
6	H6	-26.03	0.92	-4.49	0.08	08-03-2010
7	H7	-9.67	1.39	-3.29	0.09	08-03-2010
8	H10	-15.82	1.18	-3.35	0.26	08-03-2010
9	S1	-10.43	1.38	-2.35	0.27	08-03-2010
10	S2	-28.31	0.14	-4.85	0.07	08-03-2010
11	S3	-13.78	0.96	-2.96	0.09	08-03-2010
12	S4	-21.11	0.77	-4.41	0.18	08-03-2010
13	S5	-19.85	0.76	-4.46	0.17	08-03-2010
14	KB1D	-24.78	1.33	-5.12	0.26	08-03-2010
15	KB5D	-22.81	1.11	-4.70	0.18	08-03-2010
16	WB1D	-21.73	1.27	-4.27	0.22	08-03-2010
17	WB3D	-13.57	1.04	-3.36	0.11	08-03-2010
18	WB5D	-25.52	1.69	-5.11	0.04	08-03-2010
19	MHN47	-14.36	1.50	-3.35	0.17	08-03-2010
20	MHR45	-9.72	1.10	-2.52	0.14	08-03-2010
21	MDB Casino	-24.68	0.69	-4.57	0.28	08-03-2010
22	Rain water	3.53	1.51	-1.95	0.25	08-03-2010

LGR DT-100 Accuracy of standards preparation

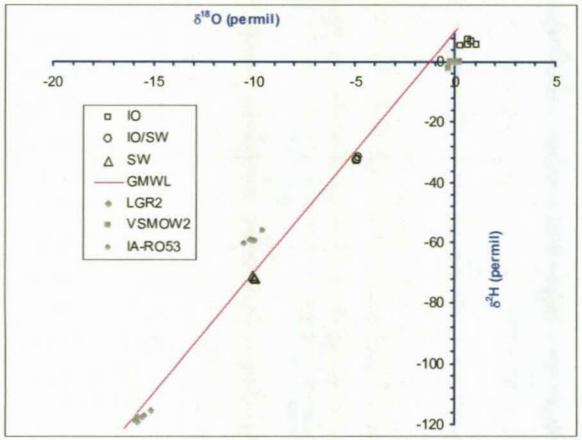

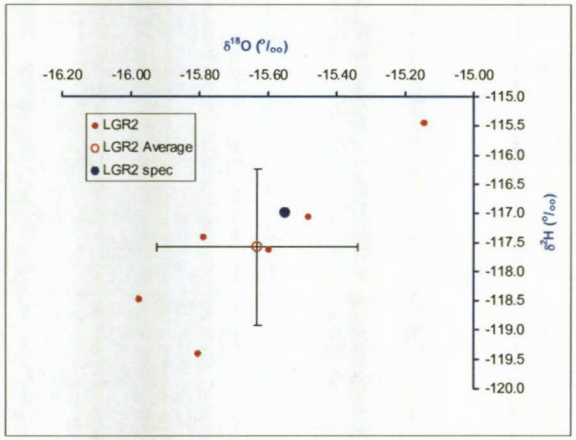

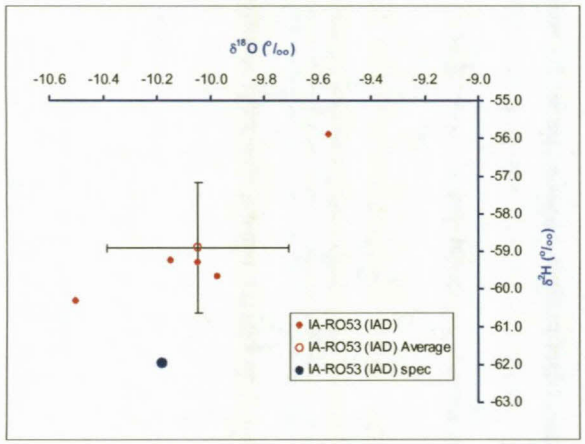

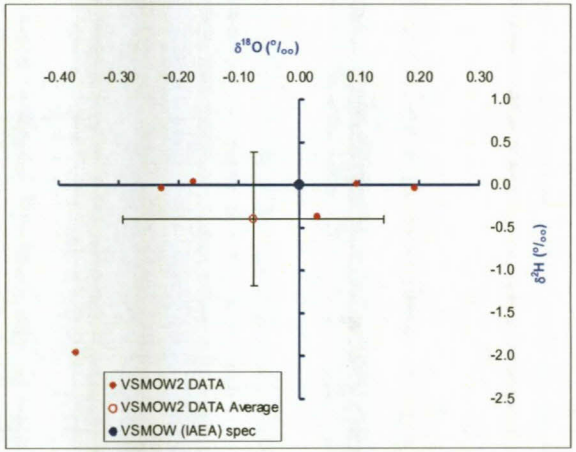

SBEEH STANDARD	Calibrated δ^2H (°/oo)	Current run δ^2H (°/oo)	Std Dev Current run δ^2H (°/oo)	Calibrated ^{18}O(°/oo)	Current run $\delta^{18}O$ (°/oo)	Std Dev Current run $\delta^{18}O$ (°/oo)
IO	6.33	6.30	0.35	0.68	0.68	0.14
IO/SW	-32.21	-32.28	0.40	-4.88	-4.61	0.11
SW	-71.56	-71.35	0.11	-10.02	-10.01	0.19

Appendix C: Harmony Gold mining data

Harmony Gold Mining Company																	
EVANDER GOLD MINE: WATER BALANCE DATA																	
Rainfall Average (Weather Bureau)			134.0	94.0	78.0	46.0	19.0	7.0	8.0	10.0	25.0	78.0	128.0	120.0	**747.0**	**62.3**	
Evaporation Average (Weather Bureau)			179.8	151.1	147.8	111.1	94.8	79.2	89.0	132.0	167.0	186.6	167.6	195.9	**1701.9**	**141.8**	
		Month	**Jan-09**	**Feb-09**	**Mar-09**	**Apr-09**	**May-09**	**Jun-09**	**Jul-09**	**Aug-09**	**Sep-09**	**Oct-09**	**Nov-09**	**Dec-09**	**Total year**	**Ave/ mth**	
Winkelhaak Shafts Complex																	
Rainfall			364.1	157.7	91.8	4	33.6	28.5	0.3	20.8	12.5	117.7	195.2	141.7	1167.9	154.4	mm
Total Shaft areas (45 ha)			163.845	70.965	41.31	1.8	15.12	12.825	0.135	9.36	5.625	52.965	87.84	63.765	525.6	69.5	Ml
Tons treated			32,061	29,003	23,000	21,419	30,359	28,317	24,581	15,581	25,735	28,482	31,206	18,413	308,157	26,371	Tons
Vent Shaft Water																	
Down cast water in air			18.8	19.5	17.9	20.727	17.5	18.102	17.89	17.362	17.98	18.648	19.254	20.54	224.2	19.2	Ml
Up cast water water in air			41.576	42.7	41.85	41.5	41.5	37.158	36.3	35.283	35.35	34.916	36.523	36.673	461.3	41.9	Ml
Excess water in air			22.776	23.2	23.95	20.773	24	19.056	18.41	17.921	17.37	16.268	17.269	16.133	237.1	22.7	Ml
IN																	
No 2 Shaft Fissure water			95.000	98.000	89.000	106.000	75.000	96.000	108.000	73.000	113.000	68.000	105.000	105.000	1131.000	97.0	Ml
No 2 Shaft Sludge			3.600	3.900	3.300	2.900	4.100	3.700	3.400	3.100	3.800	2.900	2.400	2.400	39.500	3.4	Ml
Rainfall	Tailings Dam		899.860	410.020	238.680	10.400	87.360	74.100	0.780	54.080	32.500	306.020	507.520	368.420	2989.740	389.7	Ml
	L/Emergency dam		30.457	18.293	8.078	0.352	2.957	2.508	0.026	1.830	1.100	10.358	17.178	12.470	105.607	14.3	Ml
	Plant area		21.804	9.935	5.783	0.252	2.117	1.796	0.019	1.310	0.788	7.415	12.298	8.927	72.444	9.4	Ml
Rainfall runoff Emergency catchment			25.335	5.772	6.720	0.293	2.460	2.086	0.022	0.761	0.000	8.616	14.289	10.372	76.726	9.5	Ml

Water from Kinross Met. Plant to TFC			74.277	75.918	78.769	88.287	97.219	92.750	91.324	97.497	0.000	58.668	61.428	59.409	875.546	79.3	Ml
Water from Kinross Kariba dam			0.000	0.000	0.000	0.000	0.000	0.000	0.000	0.000	0.000	0.000	0.000	0.000	0.000	0.0	Ml
Moister from rock hoisted			1.924	1.740	1.380	1.285	1.822	1.699	1.475	0.935	1.544	1.709	1.872	1.105	18.490	1.6	Ml
		Total	1152.257	623.578	431.710	209.769	273.035	274.639	205.046	232.513	152.732	463.686	721.985	568.103	5309.053	604.3	Ml
OUT																	
Water to Kinross Met plant			90.22	80.519	88.838	64.322	83.087	73.4	64.398	36.778	60.236	80.456	86.929	79.357	888.540	81.0	Ml
Evaporation	Tailings Dam		547.204	322.752	159.243	66.599	124.178	109.689	63.996	104.865	20.914	244.195	368.959	292.689	2425.283	273.9	Ml
	L/Emergency dam		14.216	7.43	12.924	10.793	7.629	5.914	3.464	7.986	12.531	11.996	13.207	11.548	119.638	11.3	Ml
L/Emergency Dam to Leeuwpan			167.876	63.596	109.071	18.449	20.966	27.58	15.157	66.312	0	41.031	84.005	54.36	668.403	113.5	Ml
Water Spillage into W/haak spruit			5.5	3.5	0	0	0	0	0	0	0	0	0	0	9.000	2.3	Ml
Change in Emergency Dam level			35	0	-33.6	20	-18.2	8	30.4	-28.9	49.3	-23.4	-1.8	1.8	38.600	5.4	Ml
Slime dam intersitual water			292.241	145.781	95.235	29.606	55.374	50.055	27.631	45.473	9.75	109.406	170.684	128.349	1159.585	140.7	Ml
		Total	1152.257	623.578	431.711	209.769	273.034	274.638	205.046	232.514	152.731	463.684	721.984	568.103	5309.049	604.3	Ml
Kinross Mine Complex																	
Rainfall			303.6	188.9	98.8	3	25	27	0.3	22.7	9.5	100.4	163.9	155.3	1098.4	148.6	mm
Total Shaft areas (16 ha)			48.576	30.224	15.808	0.48	4	4.32	0.048	3.632	1.5	16.064	26.224	24.848	175.7	23.8	Ml
Tons Treated			56,939	62,997	67,000	72,081	77,141	78,683	81,919	88,911	82,265	77,518	65	80,387	825,906	64,754	Tons
Vent Shaft Water																	
Down cast water in air			22.475	23.4	22.2	21.9	22.89	22.473	20.056	17.386	15.241	24.498	26.678	27.787	267.0	22.5	Ml
Up cast water water in air			41.976	40.6	41.54	41.8	41.7	45.29	37.883	37.991	39.114	90.915	92.716	94.41	645.9	41.5	Ml
			19.501	17.2	19.34	19.9	18.81	22.817	17.827	20.605	23.873	66.417	66.038	66.623	379.0	19.0	Ml
IN																	
No 7 Shaft Fissure water			123.71	84.962	105.875	124.333	120.209	105.929	119.464	109.613	108.889	106.518	47.221	62.001	1218.724	104.8	Ml
No 8 Shaft Fissure water			84	84	87	80	84	84	87	85	85	68	72.21	90.87	991.080	83.8	Ml
No 7 Shaft Sludge from U/g			7.21	5.117	6.103	5.916	5.943	11.406	3.818	4.275	7.114	8.046	4.948	5.333	75.229	6.1	Ml

Rand Water			7.7	5.258	6.899	6.202	5.938	5.316	5.771	4.849	5.156	7.669	8.035	4.341	73.134	6.5	Ml
Rainfall	Tailings Dam		569.857	354.565	185.445	5.631	46.925	50.679	0.563	42.608	17.832	188.451	307.64	291.498	2061.694	278.9	Ml
	Plant area		18.823	11.712	6.126	0.186	1.55	1.674	0.019	1.407	0.589	6.225	10.162	9.629	68.102	9.2	Ml
	Kariba Dam		32.182	20.023	10.473	0.318	2.65	2.862	0.032	2.406	1.007	10.642	17.373	16.462	116.430	15.7	Ml
	Toe dam		12.144	7.556	3.952	0.12	1	1.08	0.012	0.908	0.067	4.016	6.556	6.212	43.623	5.9	Ml
Rainfall runoff	Kariba Dam catchment		2.131	1.326	0.694	0.021	0.176	0.19	0.002	0.08	0.067	0.705	1.151	1.09	7.633	1.0	Ml
	Toe Dam catchment		100.522	13.601	7.114	0.216	1.8	1.944	0.022	4.903	0.38	7.229	4.72	4.473	146.924	30.4	Ml
Sludge/water from Winkelhaak Met plant			90.22	80.519	88.838	64.322	83.087	73.4	64.398	36.778	60.236	80.456	86.929	79.357	888.540	81.0	Ml
Water return from Grootspruit (KM 4)			10	20	12	40	35	48	70	60	40	45	44	45	469.000	20.5	Ml
Moister from rock hoisted			3.416	3.78	4.02	4.325	4.628	4.721	4.915	5.335	4.936	4.651	3.92	4.823	53.470	3.9	Ml
		Total	1061.915	692.419	524.539	331.590	392.906	391.201	356.016	358.162	331.273	537.608	614.865	621.089	6213.583	652.6	Ml
OUT																	
To Winkelhaak Tailings dam			74.277	75.918	78.769	88.287	97.219	92.750	91.324	97.497	0.000	58.668	61.428	59.409	875.546	79.3	Ml
To Crushers			4.000	4.000	4.000	4.000	4.000	4.000	4.000	4.000	4.000	4.000	4.000	4.000	48.000	4.0	Ml
Evaporation	Tailings Dam		404.437	210.597	57.187	48.940	61.038	70.381	10.226	13.789	131.110	132.202	79.905	175.732	1395.544	180.3	Ml
	Kariba Dam		16.914	11.076	13.641	11.085	9.189	7.276	4.157	5.526	8.544	10.906	14.811	17.885	131.010	13.2	Ml
	Toe Dam		6.462	4.180	4.905	4.183	3.468	2.317	2.771	3.684	5.696	5.453	5.589	6.749	55.457	4.9	Ml
Kariba pumped to Leeuwpan			273.951	234.112	306.586	194.958	210.244	177.194	241.048	226.545	141.737	254.455	315.716	279.311	2855.857	252.4	Ml
Change in Dam levels			0.000	0.000	0.660	-32.760	-14.600	14.780	-9.800	-14.400	3.800	14.500	53.460	1.880	17.520	-8.0	Ml
Water spillage into Grootspruit			158.000	71.500	11.200	0.000	0.000	0.000	0.000	0.000	0.000	0.000	0.000	0.000	240.700	60.2	Ml
Water to Winkelhaak Emergency dam.			0	0	0	0	0	0	0	0	0	0	0	0	0.000	0.0	Ml
Slime dam intersitual water			123.875	81.035	47.592	12.898	22.348	22.502	12.289	21.521	37.002	57.424	79.956	76.122	594.564	66.4	Ml
			1061.916	692.418	524.540	331.591	392.906	391.200	356.015	358.162	331.889	537.608	614.865	621.088	6214.198	652.6	Ml
Leslie Mine Complex																	

Rainfall			237.7	127	99.8	1.8	26.3	50	3.2	19.3	9.8	87.3	117.5	130.5	910.200	116.6	mm
Total Shaft areas (3 ha)			7.131	3.81	2.994	0.054	0.789	1.5	0.096	0.579	0.294	2.619	3.525	3.915	27.306	3.5	Ml
IN																	
Water returned from Grootspruit (BM 13)			9.000	5.300	2.100	5.400	3.000	6.500	4.350	3.402	2.179	14.760	14.395	8.300	78.686	5.5	Ml
Rainfall	Tailings Dam		701.215	374.650	294.410	5.310	77.585	147.500	9.440	56.935	28.910	257.535	346.625	384.975	2685.090	343.9	Ml
	Kariba Dam		30.426	16.256	12.774	0.230	3.366	6.400	0.410	2.470	1.254	11.174	15.040	16.704	116.504	14.9	Ml
Rainfall runoff Kariba Catchment area			4.176	2.231	1.753	0.032	0.462	0.879	0.056	0.145	0.172	1.534	2.064	2.293	15.797	2.0	Ml
Irrigation water (Rand water)			0.000	0.000	0.000	0.000	0.000	0.000	0.000	0.000	0.000	0.000	0.000	0.000	0.000	0.0	Ml
			744.817	398.437	311.037	10.972	84.413	161.279	14.256	62.952	32.515	285.003	378.124	412.272	2896.077	366.3	Ml
OUT																	
Evaporation	Tailings Dam		490.708	262.218	205.329	3.696	54.003	103.093	6.593	39.634	20.117	179.473	242.636	269.306	1876.806	240.5	Ml
	Kariba Dam		10.985	7.895	9.986	8.34	5.895	4.376	4.711	5.799	7.006	9.27	9.501	11.473	95.237	9.3	Ml
Kariba pumped to Leeuwpan			0	0	0	0	0	0	0	0	0	0	0	0	0.000	0.0	Ml
Water Spillage from Kariba into Grootspruit			0	0	0	0	0	0	0	0	0	0	0	0	0.000	0.0	Ml
Slime dam intersitual water			210.365	112.395	88.323	1.593	23.276	44.25	2.832	17.081	8.673	77.261	103.988	115.493	805.530	103.2	Ml
Change in Kariba Dam level			32.76	15.93	7.4	-2.657	1.24	9.56	0.12	0.24	-3.28	19	22	16	118.313	13.4	Ml
			744.818	398.438	311.038	10.972	84.414	161.279	14.256	62.754	32.516	285.004	378.125	412.272	2895.886	366.3	Ml
Leeuwpan																	
Dam Area			647	645	645	643	642	643	641	639	635.5	639	639	638	7696.500	645.0	ha
Rainfall (measured)			301.7	35.7	110	4.2	24.6	28.6	0.5	22	11.3	115.9	112.9	135.4	902.800	112.9	mm
Evaporation (measured)			197	129	151.4	129.1	90.3	71.5	81.5	113.7	178	168.3	172.5	208.3	1690.600	151.6	mm
Evaporation Factor			0.82	0.96	0.98	0.7	0.93	0.74	0.87	0.98	0.65	0.82	0.87	0.84	10.160	0.9	
IN																	
Mine Water			441.827	297.708	415.657	213.407	231.210	204.774	256.205	292.857	141.737	295.486	399.721	333.671	3524.260	342.1	Ml
Rainfall			1951.999	230.265	709.5	27.006	159.858	183.898	3.205	140.58	71.812	740.601	721.431	866.56	5806.715	729.7	Ml

Run-off			203.805	17.415	70.62	0	15.985	18.361	0	0	0	100.96	93.933	110.72	631.799	73.0	Ml
			2597.631	545.388	1195.777	240.413	407.053	407.033	259.410	433.437	213.549	1137.047	1215.085	1310.951	9962.774	1144.8	Ml
Runoff from 1070 ha catchment (%)			6.0	4.0	6.0	0.0	6.0	6	0	0	0	8	7	7	50.000	4.0	%
OUT																	
Evaporation			1045.164	798.768	959.999	581.079	536.145	340.211	454.501	712.012	678.714	881.858	958.979	1119.821	9067.251	846.3	Ml
Spill + Release			0	0	0	0	0	0	0	0	0	0	0	0	0.000	0.0	Ml
			1045.164	798.768	959.999	581.079	536.145	340.211	454.501	712.012	678.714	881.858	958.979	1119.821	9067.251	846.3	Ml
Total balance																	
Total in			5556.620	2259.822	2463.063	792.744	1157.407	1234.152	834.728	1087.064	730.069	2423.344	2930.059	2912.415	24381.487	2768.1	Ml
Total out			4004.155	2513.202	2227.288	1133.411	1286.499	1167.328	1029.818	1365.442	1195.850	2168.154	2673.953	2721.284	23486.384	2469.5	Ml
Imbalance			-1552.465	-253.380	235.775	-340.667	-129.092	-66.824	-195.090	-278.378	-465.781	255.190	256.106	191.131	895.103	298.5	Ml
Imbalance equals on Leeuwpan			239.9	-39.3	36.6	-53.0	-20.1	10.4	-30	-43.6	-73	40	40	30	137.202	11.4	mm
Actual change in water level (mm)			240	-40	10	-50	-20	10	-30	-50	-70	40	40	30	110.000	40.0	mm
Actual change in water level (Ml)			1552.8	-258	64.5	-321.5	-128.4	64.3	-192.3	-319.5	-444.85	255.6	255.6	191.4	719.650	259.5	Ml
% imbalance			100	98	366	106	100.5	103.9	101.5	87.1	104.7	99.8	100.2	99.9			

EVANDER GOLD MINES PRODUCTION STATS (up till 30th April 2010)											
		Winkelhaak Mine			**Kinross Mine**		**Leslie Mine**			**Bracken Mine**	
	Mined	Tons milled		Mined	Tons milled	Mined	Tons milled		Mined	Tons milled	
Fin Year	m²	000	Fin Year	m²	000	m²	000	Fin Year	m²	000	
1958/86	12112878	49442	1968/85	7471807	28500	8234150	28200	1963/84	6489338	20912	
1987	548120	2204	1986	541761	2155	290285	1382	1985	267115	1003	
1988	584211	2162	1987	453868	1920	310764	1415	1986	264867	954	
1989	524672	2015	1988	507749	2057	307874	1409	1987	227664	915	
1990	526558	2106	1989	475436	2106	298048	1370	1988	224920	842	
1991	436389	1925	1990	444989	2043	298427	1383	1989	184859	687	
1992	448167	1898	1991	431836	1918	212014	1039	1990	143458	530	
1993	426818	1756	1992	412882	1899	149616	578	1991	108372	388	
*1994	267219	1161	1993	423980	1892	122014	418	1992	49223	185	
1995	345230	1442	*1994	315277	1382	114203	404	❁1993	5245	31	
1996	351002	1479	1995	381467	1672	119515	397	*1994	-	-	
1997	250275	1315	1996	370640	1598	99198	306	Total	7965061	26447	
1998	92400	688	1997	355179	1648	117438	403				
1999	43992	221	1998	267517	1334	117565	424	❁ Underground production ceased in March 1993 . Because			
2000	86581	438	1999	258015	1261	144777	474	of lack of detail one can assume 600 - 700 Kg came from plant			
2001	92676	606	2000	271754	1221	91054	388	clean up .			
2002	106616	692	2001	280795	1313	86131	469				
2003	113548	669	2002	261851	1267	72099	293				
2004	75374	644	2003	201462	1109	41651	196				
2005	98230	493	2004	208358	1145	35076	138				
2006	60476	338	2005	81487	1042	31463	139				
2007	57287	323	2006	201102	939	36063	183				
2008	58289	324	2007	195384	1111	4413	26				
2009	48811	306	2008	170871	956	11333838	41434				
‡ 2010	23795	146	2009	130491	776						
Total	17779614	74793	Δ 2010	89652	540						
			Total	152056	64804						

				10								
				m²	Tons '000							
	TOTAL UNDERGROUND (incl Bracken plant c/u)			**522841 23**	**207478**							